Compte rendu de la

DIXIÈME RENCONTRE
DE MORIOND

Méribel-lès-Allues (France) 2-14 Mars 1975

VOL. II

CHARME, COULEUR ET LES $\mathcal{Y}$

J. TRAN THANH VAN

SOUS LE HAUT PATRONAGE DE

- INSTITUT NATIONAL DE PHYSIQUE NUCLÉAIRE ET DE PHYSIQUE DES PARTICULES
- LABORATOIRE DE L'ACCÉLÉRATEUR LINÉAIRE
- LABORATOIRE DE PHYSIQUE THÉORIQUE ET HAUTES ÉNERGIES
- LABORATOIRE DE PHYSIQUE THÉORIQUE ET PARTICULES ÉLÉMENTAIRES

PUBLICATION SUBVENTIONNÉE PAR LE CNRS

La deuxième session de la dixième Rencontre de Moriond sur Charme, Couleur et les $\mathcal{F}$
était organisée par

J. Trân Thanh Vân

avec la précieuse collaboration de

M. Gourdin

et L. Montanet

Secrétariat permanent :
Rencontre de Moriond
Laboratoire de Physique Théorique et Particules Élémentaires
Bâtiment 211 - Université de Paris-Sud
91405 ORSAY (France)
Tél. 928.59.87

Proceedings of the

TENTH RENCONTRE DE MORIOND

Méribel-lès-Allues (France) March 2-14, 1975

VOL. II

CHARM, COLOR AND THE $\mathcal{J}$

edited by

J. TRAN THANH VAN

SPONSORED BY

- INSTITUT NATIONAL DE PHYSIQUE NUCLÉAIRE ET DE PHYSIQUE DES PARTICULES
- LABORATOIRE DE L'ACCÉLÉRATEUR LINÉAIRE
- LABORATOIRE DE PHYSIQUE THÉORIQUE ET HAUTES ÉNERGIES
- LABORATOIRE DE PHYSIQUE THÉORIQUE ET PARTICULES ÉLÉMENTAIRES

AND BY THE CNRS FOR PUBLICATION

The Second Session or the Tenth Rencontre de Moriond on
Charm, Color and the $\mathcal{Y}$
was organized by

J. Trân Thanh Vân

with the active collaboration of

M. Gourdin
and L. Montanet

Permanent Secrétariat :
Rencontre de Moriond
Laboratoire de Physique Théorique et Particules Élémentaires
Bâtiment 211 - Université de Paris-Sud
91405 ORSAY (France)
Tél. 928.59.87

AVANT - PROPOS

La Rencontre de Moriond qui s'est tenue du 2 au 14 mars 1975 à Méribel-les-Allues (Savoie), est la dixième d'une série commencée en 1966.

La première Rencontre a eu lieu à Moriond dans des chalets savoyards où les physiciens, expérimentateurs et théoriciens, partageaient non seulement leurs préoccupations scientifiques, mais aussi les tâches culinaires et les travaux ménagers. Elle regroupait principalement les physiciens français travaillant dans les interactions électromagnétiques. Au cours des Rencontres suivantes venait s'ajouter à la session sur les interactions électromagnétiques une session sur les interactions fortes à hautes énergies.

Le but principal de ces Rencontres est d'une part, de faire le point sur les récents développements de la physique contemporaine, et d'autre part, de promouvoir une collaboration effective entre expérimentateurs et théoriciens dans le domaine des interactions électromagnétiques et des particules élémentaires. Par ailleurs, la durée relativement longue de la Rencontre et le faible nombre des participants doivent permettre à la fois une meilleure connaissance humaine entre les participants et une discussion approfondie et détaillée des communications présentées.

Ce souci de recherche et d'expérimentation de nouvelles formes de communication, de nouveaux terrains d'échange et de dialogues, qui depuis l'origine anime les Rencontres de Moriond, nous a amenés, il y a cinq ans, à susciter la création pour les biologistes de la première Rencontre de Méribel sur la Différenciation Cellulaire qui se tient en même temps et dans les mêmes locaux que la première session de la Rencontre de Moriond. Des séminaires communs ont été organisés afin d'étudier dans quelle mesure les méthodes d'analyse utilisées en physique pouvaient être appliquées à certains problèmes qui se posent en biologie. Cette année, M. le Professeur ZICHICHI a donné une Conférence sur la Physique des

des Hautes Energies et les méthodes expérimentales, et M. le Professeur VAN DER WALLE a présenté une méthode d'analyse des données dans la recherche sur le cancer. Ces conférences ainsi qu'une table ronde sur les problèmes actuels de la Biologie ont suscité de nombreuses discussions "informelles", animées et enrichissantes entre biologistes et physiciens. Ces échanges font espérer qu'un jour peut-être, les problèmes, pour le moment si complexes, posés en Biologie, donneront naissance à de nouvelles méthodes d'analyse ou à de nouveaux langages mathématiques.

La première session de la dixième Rencontre de Moriond (2-8 mars 1975) est consacrée aux interactions hadroniques à hautes énergies. A. CAPELLA, A. KRZYWICKI ainsi que B. et F. SCHREMPP m'ont aidé à l'élaboration de ce programme de la Rencontre.

La seconde session (8 au 14 mars 1975) est consacrée aux interactions leptoniques à hautes énergies et la coordination est assurée par M. GOURDIN et L. MONTANET. Une attention particulière a porté sur la découverte des nouvelles résonances étroites et sur leur interprétation.

Mmes Geneviève BEUCHEY et Marie-Thérèse PILLET, Mlles Marie-Paule COTTEN et Nicole RIBET ont dépensé beaucoup de temps et d'efforts pour la réussite de cette Rencontre. Au nom de tous les participants, nous les remercions, ainsi que M. et Mme RAIBERTI qui nous ont accueillis dans leur hôtel.

J. TRAN THANH VAN

FOREWORD

The Rencontre de Moriond held at Meribel-les-Allues (France) from March 2 to 14, 1975, was the tenth such meeting.

The first one was held in 1966 at Moriond in the French Alps. There, physicists - experimentalists as well as theoricians - not only shared their scientific preoccupations but also household chores. That meeting grouped essentially French physicists interested in electromagnetic interactions. At following meetings a session on high energy strong interactions was added to the electromagnetic one.

The main purpose of these meetings is to discuss recent developments of contemporary physics and to promote effective collaboration between experimentalists and theoriticians in the field of electromagnetic interactions and elementary particles. Besides, the length of the meeting coupled with the small number of participants favours better human relations as well as a more thorough and detailed discussion of the contributions.

This concern for research and experimentation of new channels of communication and dialogue which from the start animated the Moriond meetings, incited us, five years ago, to organize a simultaneous meeting of biologists on Cellular Differenciation at Meribel-les-Allues. Common seminars were organized to study to what extent analytical methods used in physics could be applied to some biological problems. This year, Professor ZICHICHI, gave an introductory talk to the High Energy Physics and the experimental methods and Professor VAN DER WALLE has presented a method of data analysis in the research on the cancer. These conferences as well as a round table discussion on the present problems of Biology gave rise to spirited and enriching discussions between biologists and physicists. They led us to hope that biological problems, at present so complex, may gave birth in the future to new analytical methods or new mathematical languages.

The first session of the tenth Rencontre de Moriond (March 2-8, 1975) is devoted to high energies hadronic interactions. A. CAPELLA, A. KRZYWICKI, Barbara and F. SCHREMPP have given me their help in setting the program of the Rencontre.

The second session (March 8-14, 1975) was devoted to high energies leptonic interactions and the coordination was assumed by M. GOURDIN and L. MONTANET. A particular attention was given on the discovery of the narrow resonances and their interpretation.

Mrs G. BEUCHEY and M.T. PILLET, Misses M.P. COTTEN and N. RIBET, all devoted much of their time and energy to the success of this meeting. On behalf of the participants I thank them as well as Mr. and Mrs. Raiberti who welcomed us in their hotel.

J. TRAN THANH VAN

PARTICIPANTS

Second session

ALTARELLI Guido	Istituto di Fisica, Università di Roma, Piazzale delle Scienze 5, 00100 Roma (Italie)
BARDACKI Korbut	Laboratoire de Physique Théorique, Ecole Normale Supérieure, 24 rue Lhomond, 75231 Paris Cedex 05 (France)
BARBIELLINI Giorgio	Laboratori Nazionali di Frascati, Casella Postale 70 - I-00044 Frascati (Roma)(Italie)
BECKER Ulrich	M.I.T. Laboratory for Nuclear Science, Cambridge, 02139 (U.S.A)
BREIDENBACH M	SLAC, Stanford University, Stanford, Ca 94305 (U.S.A)
CLOSE Francis	Division TH, CERN, 1211 Genève 23 (Suisse)
COLGLAZIER E. William	Th group, Rutherford Laboratory, Chilton, Didcot, OX11 OQX (England) and Institute for Advanced Study, Princeton, New Jersey (U.S.A)
COURAU André	Laboratoire de l'Accélérateur Linéaire, Bât. 200, Université de Paris-Sud, 91405 Orsay (France)
DAR Arnon	Physics Department, Technion Institute of Technology, Haifa (Israel)
DIAMANT-BERGER Alain	D.Ph.P.E./S.E.E., C.E.N. Saclay, B.P. 2, 91190 Gif sur Yvette (France)
DIAZ José	Grupo Altas Energias, J. Energia Nuclear, Ciudad Universitaria, Madrid-3 (Spain)
FARRAR Glennys	Caltech 452-48, Pasadena, CA 91125 (U.S.A)
GAILLARD Jean-Marc	Division NP, CERN, 1211 Genève 23 (Suisse)
GAILLARD Mary K.	Laboratoire de Physique Théorique et Particules Elémentaires, Bât. 211, Université de Paris-Sud 91405 Orsay (France)
GEFFEN Donald	Laboratoire de Physique Théorique et Particules Elémentaires, Bât. 211, Université de Paris-Sud 91405 Orsay (France)

GOURDIN Michel	Laboratoire de Physique Théorique et Hautes Energies Tour 16, Université de Paris-VI, 4 place Jussieu, 75230 Paris Cedex 05 (France)
HEUSCH Clemens	Institut für Physik, Max-Planck-Institut für Physik und Astrophysik, 8 Munchen 40 (Germany)
JAFFRE Michel	Laboratoire de l'Accélérateur Linéaire, Université de Paris-Sud, Bât. 200, 91405 Orsay (France)
KADYK John	Lawrence Berkeley Laboratory, Berkeley, CA 94720 (U.S.A)
KLUBERG Louis	Ecole Polytechnique, Laboratoire de Physique Nucléaire des Hautes Energies, 17 rue Descartes, 75230 Paris Cedex 05 (France)
KLUBERG-STERN Hannah	D.Ph.T. Orme des Merisiers, C.E.A., B.P. 2, 91190 Gif sur Yvette (France)
KRUSE Ulrich	Max Planck Institut für Physik und Astrophysics, Föhringer Ring 6, 8 Munchen 40 (Germany)
KUTI Julius	Central Research Institute for Physics, Hungarian Academy of Sciences, H-1525 Budapest P.F. 49, (Hungary)
LAPLANCHE Francis	Laboratoire de l'Accélérateur Linéaire, Université de Paris-Sud, Bât. 200, 91405 Orsay (France)
LAYSSAC Jacques	Laboratoire de Physique Mathématiques, Université des Sciences et Techniques du Languedoc, 34060 Montpellier Cedex (France)
LE YAOUANC Alain	Laboratoire de Physique Théorique et Hautes Energies, Bât. 211, Université de Paris-Sud, 91405 Orsay (France)
LLORET Antoine	Division TC.L. CERN, 1211 Genève 23 (Suisse)
LONDON Georges	L.P.N.H.E. Université de Paris-VI, Tour 32, 4 Place Jussieu, 75230 Paris Cedex 05 (France)
MENNESSIER Gérard	Laboratoire de Physique Théorique et Hautes Energies, Tour 16, Université de Paris-VI, 4 place Jussieu, 75230 Paris Cedex 05 (France)
MERRITT Franck	California Institute of Technology, Charles C. Lauritsen Laboratory of High Energy Physics, Pasadena, CA 91109 (U.S.A)
MONTANET Lucien	Division TC, CERN, 1211 Genève 23 (Suisse)
MUSSET Paul	Division TC, CERN, 1211 Genève 23 (Suisse)

NGUYEN-KHAC UNG	Laboratoire de Physique Nucléaire des Hautes Energies, Ecole Polytechnique, 17 rue Descartes, 75230 Paris Cedex 05 (France)
NUSSBAUM Mirko	Division NP, CERN, 1211 Genève 23 (Suisse)
NUYTS Jean	Faculté des Sciences, 19 avenue Maistriau, Université de Mons, 7000 Mons (Belgique)
ORITO Shuji	DESY, Notkestieg 1, 2 Hamburg 52 (Germany)
PASCAUD Christian	Laboratoire de l'Accélérateur Linéaire, Université de Paris-Sud, Bât. 200, 91405 Orsay (France)
PASCHOS Emmanuel	Department of Physics, Brookhaven National Lab. Upton, N.Y. 11973 (U.S.A)
PENSO Gianni	Istituto di Fisica, Università di Roma, Piazzale delle Scienze 5, 00100 Roma (Italie)
PEREZ-Y-JORBA Jean	Laboratoire de l'Accélérateur Linéaire, Université de Paris-Sud, Bât. 200, 91405 Orsay (France)
PHAM TRI NANG	Centre de Physique Théorique, Ecole Polytechnique, 17 rue Descartes, 75230 Paris Cedex 05 (France)
PICCOLO Marcello	Laboratori Nazionali di Frascati, Casella Postale 70, I-00044 Frascati (Roma)(Italie)
RAYNAL Jean-Claude	Laboratoire de Physique Théorique et Particules Elémentaires, Bât. 211, Université de Paris-Sud 91405 Orsay (France)
REMIDDI Ettore	Laboratoire de Physique Théorique, Ecole Normale Supérieure, 24 rue Lhomond, 75230 Paris Cedex 05 (France)
RENARD Fernand	Laboratoire de Physique Mathématique, Université des Sciences et Techniques du Languedoc, 34060 Montpellier Cedex (France)
SANNES Felix	Physics Department, Rutgers University, New Brunswick, N.J. 08903 (U.S.A)
SCHILDKNECHT Dieter	DESY, Notkestieg 1, 2 Hamburg 52 (Germany)
SCHILLING Klaus	Fachbereich 6, University of Wuppertal, 56 Wuppertal Hofkamp 82 (Germany)
TRAN THANH VAN Jean	Laboratoire de Physique Théorique et Particules Elémentaires, Bât. 211, Université de Paris-Sud 91405 Orsay (France)
TURLAY René	D.Ph.P.E., C.E.N. Saclay, B.P. 2, 91190 Gif sur Yvette (France)

VAN DE WALLE Remy	Physics Lab. University of Nijmegen, Toernooiveld Nijmegen (Netherlands)
VAN DONINCK Walter	Inter-University Institute for High Energies, (ULB-VUB) 50 Av. F.D. Roosevelt, 1050 Bruxelles (Belgique)
VENUS Walter	Rutherford Laboratory, Chilton, Didcot, Oxon , OX11 0QX (England)
VIALLET Claude	Laboratoire de Physique Théorique et Hautes Energies Tour 16, Université de Paris-VI, 4 place Jussieu 75230 Paris Cedex 05 (France)
WAHL Heinrich	Division TC, CERN, 1211 Genève 23 (Suisse)
WIIK Björn Havard	DESY, Notkestieg 1, 2 Hamburg 52 (Germany)
ZICCICHI Antonino	Division NP, CERN, 1211 Genève 23 (Suisse)

Secrétariat :

BEUCHEY Geneviève	D.Ph. P.E./S.E.E., CEN Saclay, B.P. 2, 91190 Gif sur Yvette (France)
COTTEN Marie-Paule	Laboratoire de l'Accélérateur Linéaire, Bât. 200, Université de Paris-Sud, 91405 Orsay (France)
PILLET Marie-Thérèse	Laboratoire de Physique Théorique et Particules Elémentaires, Bât. 211, Université de Paris-Sud, 91405 Orsay (France)
RIBET Nicole	Laboratoire de Physique Théorique et Hautes Energies, Université de Paris-VI, Tour 16, 4 place Jussieu, 75230 Paris Cedex 05 (France)

J. TRAN THANH VAN AND P. MUSSET

G. ALTARELLI AND U. BECKER

MRS. AND MR. U. KRUSE

M. NUSSBAUM AND J. KADYK

D. GEFFEN AND F. MERRITT

L. MONTANET AND J. DIAZ

M. BREIDENBACH, MRS. AND MR. SCHILLING

A. DIAMANT-BERGER, H. WAHL, R. TURLAY AND J.M. GAILLARD

CONTENTS

Second Session

INTRODUCTION

Il est hors de doute que le point central de la dixième Rencontre de Moriond est la découverte des nouvelles résonances étroites faites presque simultanément par plusieurs laboratoires américains et européens. Que nous soyons à la session des interactions fortes ou à celle des leptons, les nouvelles particules dominent toutes les discussions d'autant plus que c'était la première conférence Internationale à aborder ce sujet dans son ensemble.

L'an dernier, à la neuvième Rencontre de Moriond, H. Lynch a présenté les résultats obtenus à SLAC pour le rapport des sections efficaces d'annihilation e^+e^- en hadrons ou en $\mu^+\mu^-$, rapport qui croit avec l'énergie alors que dans l'approximation d'échange d'un photon on s'attend à ce qu'il reste constant. Nombreux sont les modèles théoriques : leptons lourds, courants neutres, vecteurs mésons, quarks colorés et/ou charmés etc..., pour tenter de rendre compte de ce phénomène. Cette découverte nous laisse espérer pour bientot comme nous l'avons écrit dans l'introduction des Comptes Rendus de la Neuvième Rencontre de Moriond, de nouveaux et surprenants résultats expérimentaux et un avenir excitant pour la Physique des Particules.

En Novembre dernier, l'annonce simultanée faite à Brookhaven et à SLAC sur la découverte d'une puis de deux nouvelles résonances très étroites ouvre une ère nouvelle pour la Physique des Particules. A cette Rencontre, nous avons réuni les représentants des différents laboratoires ayant pu produire ces nouvelles particules qu'on appelle J ou ψ ou encore $\mathcal{J}$. Ce sont : Ulrich Becker (BNL), Martin Breidenbach et John Kadyk (SLAC-Berkeley), Barbiellini, Penso et Piccolo (Frascati) et Orito-Wiik (Desy) ainsi que J. People (F.N.A.L). Les principaux résultats présentés sont les suivants :

1) les nombres quantiques de la particule 3.1 Gev sont
   - spin, parité et conjugaison de charge $J^{PC} = 1^{--}$
   - spin isotopique et parité G $I^G = 0^-$

2) la largeur totale est de 69 ± 15 Kev et le rapport de branchement en leptons èst de 1/14. Cette si petite largeur pour une si grande masse implique l'existence soit de nouvelles règles de sélection soit de nouvelles particules avec de nouveaux nombres quantiques.

3) il n'y a pas d'asymétrie de charge avant-arrière dans l'annihilation en leptons et cela implique la conservation de la parité dans cette interaction.

4) la deuxième résonance, de masse 3,7 Gev environ, a une largeur plus grande, de l'ordre de 250 Kev. Bien que le spin-parité n'a pas encore pu être déterminé, des évidences indirectes montrent que ses nombres quantiques sont les mêmes que cuex de la résonance 3,1 Gev. Par exemple, le fait que Ψ (3,7) se désintègre copieusement en Ψ (3,1) plus deux pions chargés montre qu'ils ont la même parité G, lë rapport de branchement de $\Psi_{3.1}\pi^+\pi^-$ / Ψ (3,1) + n'importe quoi est compatible avec un isopin 0. D'autre part, la distribution angulaire des leptons dans l'état final est compatible avec la désintégration d'une résonance de spin 1.

5) en faisant varier l'énergie des faisceaux d'électrons et de positrons, on trouve une bosse dans la section efficace totale d'annihilation vers 4,1 Gev. Cette structure est assez large (250-300 Mev) et la section efficace varie de 18 nb à 32 nb au maximum du pic pour redescendre à 15-18 nb.

6) la photoproduction de Ψ (3,1 Gev) a été observée à SLAC et à FNAL et les sections efficaces mesurées sont très faibles et de l'ordre de 10 nanobarns.

7) d'autres modes de désintégration de Ψ ont été trouvés comme $e^+e^- \rightarrow \Psi(3,1) \rightarrow p\bar{p}$ ou en $\eta\gamma$ etc...

Sur le plan théorique, plusieurs tentatives d'interprétation ont été proposées : bosons intermédiaires, charmes et/ou couleurs. Il est maintenant communément admis que l'hypothèse du boson intermédiaire est complétement écartée et qu'à la fois les charmes (M.K. Gaillard) et les couleurs (F. Close et D. Schildknecht) sont en difficulté pour certains points précis. En effet, si les couleurs permettent de comprendre facilement les taux de

désintégration leptoniques des nouvelles particules et la petitesse des largeurs hadroniques, on rencontre de grosses difficultés avec les désintégrations radiatives de Ψ (3,1 Gev) : expérimentalement la largeur de désintégration radiative est très faible ($\simeq$ kev) tandis que la prédiction théorique est de l'ordre du Mev. Par contre, si les charmes donnent une simple compréhension des différents taux de désintégration, spécialement celui de Ψ (3,7) $\rightarrow \Psi$ (3,1) + $\pi^+\pi^-$, on s'étonne toujours pourquoi, malgré les recherches de plus en plus poussées, on n'a pas encore découvert de mésons ou de baryons charmés.

M. Nussbaum a présenté les résultats préliminaires de la recherche des charmes aux ISR et Cl. Heusch a fait une revue détaillée des méthodes expérimentales de la recherche des charmes et des expériences en cours.

Dans les interactions faibles, un troisième événement de courant neutre (un à chaque Rencontre de Moriond depuis 1973 !) vient d'être observé et a été copieusement fêté par la collaboration. Ces trois évènements observés sont en accord avec le chiffre de 4 à 5 attendus si l'angle de mélange est de $\sin^2 \theta_W = 0.38$ comme cela a été obtenu dans les voies semi-leptoniques (Musset). F. Merritt a présenté les résultats des courants neutres de l'expérience Caltech-Fermilab et Nguyen Khac Ung la production des particules étranges ou charmés avec des faisceaux de neutrinos.

Sur le plan théorique, des revues ont été faites par E. Paschos sur les courants neutres semi-leptoniques, par G. Altarelli sur les désintégrations faibles des mésons charmés et par J. Kuti sur le confinement des quarks et la spectroscopie du charmonium. M. Gourdin a présenté des résultats concernant les formules de masse dans la symétrie SU(4), M. Teper et T. Inami ont discuté le caractère SU(4) du Pomeron en relation avec la production des nouvelles particules.

A la fin de cette excitante Dixième Rencontre de Moriond, il semble qu'une ère nouvelle s'ouvre à la Physique des Hautes Energies et nous espérons que l'an prochain la plupart des mystères mentionnés aura trouvé une explication satisfaisante.

J. TRAN THANH VAN

The focus of the Tenth Rencontre de Moriond was, without doubt, the discovery of the new narrow resonances, made simultaneously by several American and European laboratories. Whether at the session of Hadronic Interactions or Leptonic Interactions, the new particles were the leading theme of all discussions so that this meeting was the first International Conference to deal with this subject in its entirety.

Last year, at the Ninth Rencontre de Moriond, H. Lynch presented the SLAC results for the ratio of the annihilation cross-section of e^+e^- into hadrons to the cross section of e^+e^- into $\mu^+\mu^-$. Experimentally, this ratio increases with energy while theoretical models had predicted it to remain constant. Many new theoretical models have been proposed to explain this ; e.g. : heavy leptons, neutral currents, vector mesons, colored/charmed quarks etc ...

As we note in the Introduction to the IX Rencontre de Moriond, this discovery leads us to expect still more surprising experimental results and an exiting future for particle physics.

Last November, the simultaneaous announcement by Brookhaven and SLAC of the discovery of one and later two new very narrow resonances opened a new era to Particle Physics. At this meeting, we are privileged to have with us physicists from the different laboratories where the new particles, called J or Ψ or sometimes $\mathcal{Y}$, have been produced. They are : Ulrich Becker (BNL), Martin Breidenbach and John Kadyk (SLAC-Berkeley), Barbiellini, Penso and Piccolo (Frascati) and Orito-Wiik (Desy) and J. People (FNAL).

At the present time the main results are the following ones :

1) the quantum number of the 3.1 Gev particle are :

- spin, parity and charge conjugation $J^{PC} = 1^{--}$
- isospin and G parity $I^G = 0^-$

2) the total width is (69 ± 15) Kev and the leptonic branching ratio is 1/14. This very small width for such a high mass particle implies either new selection rules or new particles involving new quantum numbers.

3) there is no forward-backward charge asymetry in the leptonic annihilation and this implies parity conservation in this reaction.

4) the second resonance at 3.7 Gev has a bigger width of the order of 250 Kev. Although its spin parity has not been determined yet indirect evidence shows its quantum numbers are the same as those of the 3.1 resonance. For example the fact that Ψ (3.7) decays into Ψ (3.1) and two charged pions show that Ψ (3.7) and Ψ (3.1) have the same G parity. The branching ratio $\Psi(3.1) + \pi^+\pi^- / \Psi(3.1)$ + anything is compatible with I = 0. Finally the angular distribution of the leptons in the final state is compatible with the decay of a spin 1 particle.

5) by increasing the energy of the incident e^+ and e^- beams one sees an enhancement in the total annihilation cross section near 4.1 Gev. This structure is rather broad (250-300 Mev) and the cross section varies from 18 nb up to 32 nb at the peak maximum and then decreases again to 15-18 nb.

6) the photoproduction of Ψ (3.1) has been observed at SLAC and FNAL and the measured cross-sections are very small, of the order of 10 nb.

7) other decay modes of Ψ have been observed such as $e^+ e^- \rightarrow \Psi(3.1) \rightarrowtail p\,p$ or $\eta\,\gamma$ etc.

On the theoretical front, different interpretations of these new phenomena have been proposed : intermediate vector bosons charm and/or color. It is now commonly believed that the vector boson hypothesis is completely ruled out and that both the charm hypothesis (M. K. Gaillard) and the colour interpretation (F. Close and D. Schildknecht) are in trouble on some specific points. Indeed, if the color models have a natural explanation for the leptonic widths and the small hadronic widths, they, on the other hand cannot accomodate the narrow radiative decay width of Ψ (3.1) : experimentally, the radiative width is very small ($\simeq$ kev) whereas the theoretical predictions are in the Mev range. As for the charm interpretation they give a simple explanation of the partial decay width, in particular for $\Psi(3.7) \rightarrow \Psi(3.1) + \pi^+ \pi^-$, but then one wonders why the experiments which are becoming more and more refined, have not yet discovered any evidence for the existence of charmed mesons and baryons.

M. Nussbaum presented preliminary results on the search for charmed particles at ISR while Cl. Heusch gave a detailed review of the experimental methods used in the search for charm as well as of the present experiments.

In weak interactions, a third neutral current event (one at each Rencontre de Moriond since 1973 !) has just been observed and has been heartily celebrated by the collaboration. These 3 observed events are in agreement with 4 or 5 events expected if the mixed angle $\sin^2 \theta_W = 0.38$ as observed in semi-leptonic channels.(Musset). F. Merritt presented the Caltech-FNAL results on neutral currents and Nguyen Khac Ung talked about production of strange and charmed particles by neutrino beams.

On the theoretical side, review talks have been given on Neutral Currents in Semi-leptonic reactions (E. Paschos), on weak decays of charm particles (G. Altarelli) and on quark confinement and charmonium spectroscopy (J. Kuti). M. Gourdin presented results concerning mass formulae in SU(4), M. Teper and T. Inami discuted the SU(4) character of the Pomeron in relation with the prod uction of the new narrow resonances.

At the end of this exciting Tenth Rencontre de Moriond, it seems that a new era is opening to Hihg Energy Physics and we hope that next year we will return to Méribel with most of the puzzles completely solved.

J. TRAN THANH VAN

Discovery of J (3.1) in Lepton Production by Hadron Collisions

U. Becker
Massachusetts Institute of Technology
Cambridge, Mass., USA

Abstract: The discovery of the new long-lived state J (3.1) at Brookhaven National Laboratory is reported.

Résumé: La découverte du nouvel état de longue vie, nommé J (3.1), au Brookhaven National Laboratory est rapportée.

Introduction:

There have been many theoretical speculations[2] postulating the existence of long-lived neutral particles with large masses, $\gtrsim 10\ \mathrm{GeV}/c^2$, which for example, may play a role in weak interactions. Nevertheless, till 1974 no hint[3] for narrow resonances in the mass region 2-5 GeV/c^2 was brought to attention.

It may therefore be worthwhile to recall the original motivation for the experiment[1] to be described, which yielded the discovery of the J (3.1).

It is the logical continuation of previous work, done by the same group in photoproduction of vector mesons[4] and production with subsequent leptonic decay[5,6,7].

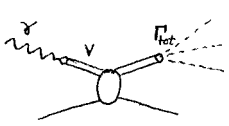

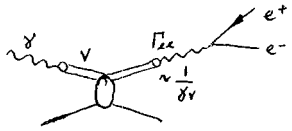

Comparison of the processes yields the branching ratios $\Gamma_{ee} / \Gamma_{tot} = BR$, and the coupling constants by: $\frac{\gamma_V^2}{4\pi} = \frac{\alpha^2}{12} \frac{m_V}{BR.\Gamma_{tot}}$

Accordingly measurements were done for ρ [5], φ [6], ω [7], and ρ' [3]. The coupling constants obtained this way agreed with those from storage ring measurements of $e^+e^- \to \rho\ (\omega, \varphi)$. Inserted in a specific prediction for amplitudes by the Vector Dominance Model [8], one finds for $t \to 0$ at 9.3 GeV:

$$\sqrt{\frac{d\sigma}{dt}(\gamma p \to \gamma p)} = \sqrt{\frac{\pi\alpha}{\gamma}}\sqrt{\frac{d\sigma}{dt}(\gamma p \to \rho^0 p)} + \sqrt{\frac{\pi\alpha}{\gamma\omega}}\sqrt{\frac{d\sigma}{dt}(\gamma p \to \omega p)} + \sqrt{\frac{\pi\alpha}{\gamma\phi}}\sqrt{\frac{d\sigma}{dt}(\gamma p \to \phi p)} + \ldots$$

$$.87 \pm .02 \overset{?}{=} .57 + .07 + .04 + .08(\rho') = .74 \pm .04 + ? \qquad (1)$$

The discrepancy here is puzzling in the view of many accurate predictions in photoproduction of vector mesons.
Most easily this may be attributed to more, unknown V-mesons, still missing in eq.(1).

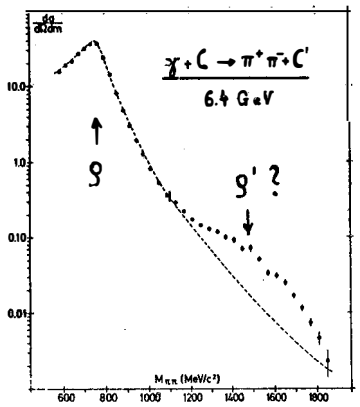

An attempted search[9] is seen in Fig. 2, however, the energy was too low to recognize the shoulder at 1.6 GeV by diffractive production as the new vector meson ρ' [3,8].

Fig. 2

Consequently, a new search for additional vector mesons was proposed at a machine with higher energy in the reaction:

$$p\ Be \rightarrow e^+e^- + X \qquad (2)$$

The alternating gradient synchroton at Brookhaven supplies incident protons of 28.5 GeV making a CMS energy of $E^* = 7.5$ GeV available.

The question arises, what other mechanisms could produce e^+e^- pairs in hadronic collisions.
In the parton model[10] one expects from parton-antiparton annihilation virtual photons with conseqent decay into e^+e^- (or $\mu^+\mu^-$). Taking this as the cross-channel reaction of inelastic e-p scattering and assuming a specific anti-parton distribution a "continuum" of e^+e^-, falling with the pair mass is predicted, roughly in agreement with early measurements[11].

To summarize the situation in summer 74:

Besides the general demand for vector mesons and the omnipresent suggestion of very heavy weak field quanta and leptons; there was - including symmetry schemes - no justification from theory to expect new particles in the mass region of $2 < m_{ee} < 5.5$ GeV/c^2, the range covered by the proposed experiment.

The discovery of the new

particle J (3.1) with long life time

came as a complete surprise - which conversely results in its importance. Since it was an "unguided" experimental discovery, we may pay due respect to the details of the experimental techniques used.

In particular, since a very small e^+e^- signal had to be defected in presence of a huge background of "normal" hadron production.

Detection apparatus at Brookhaven

The symmetrical double arm spectrometer for the detection of e^+e^- pairs is shown in Fig. 3. Essential for the design were the following considerations:

1) Hadron pairs like $\pi^+\pi^-$, K^+K^-, $p\bar{p}$... will dominate over e^+e^- pairs from virtual photon decay by roughly a factor.

$$\frac{\alpha^2}{m_{e\ell}} \cdot \text{Formfactor} \simeq 10^{-6}$$

Therefore many threshold Cerenkov counters are needed to achieve a rejection of better than 10^{-8} against all particles other than electron pairs.

2) Because the e^+e^- cross sections are small, high beam

intensities are necessary. Conversely the apparatus must be able to stand high hadron fluxes.

3) If the production has approximately similar characteristics to ρ and ω produced in pp collisions:

$$\frac{d\sigma}{dp_{\parallel}^{*}\, dp_{\perp}} \sim \frac{e^{-bp_{\perp}} e^{-cp_{\parallel}^{*}}}{E^{*}}$$

the maximal yield will occur for production of a particle with mass M at rest ($x = 0$) in the overall CMS. Then the

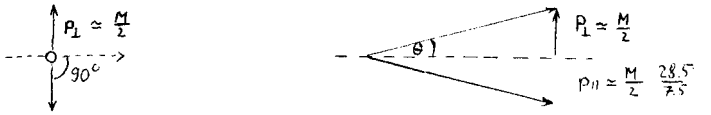

± 90° decay in the CMS appears as ± θ = arc tg $(\frac{1}{\gamma})$ = 14.6° in the lab. system for incident protons of 28.5 GeV. This is independent of the mass M of the particle produced! Therefore the spectrometer opening angle was chosen (to be) ± 14.6°.

The intense proton beam of up to $2 \cdot 10^{12}$ protons/sec. was focused by quadrupoles to a 4 x 6 mm image spot size on a 10 % interaction length target. This consisted of 9 beryllium pieces, equidistantly spaced over 60 cm.

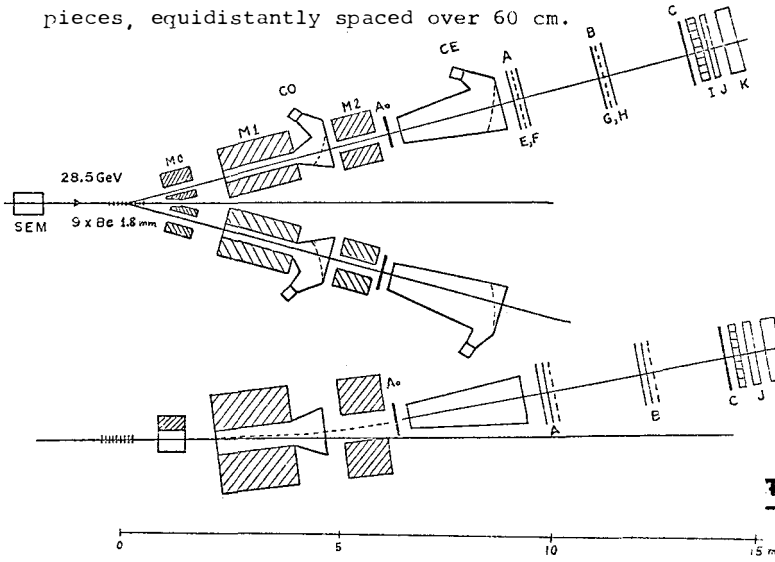

Fig 3a

Fig 3b


e±
e±
PARTICLE
POSITION
DETECTORS
CERENKOV
COUNTERS
MAGNETS
MAGNETS

The top view shows how at ± 14.6° created e^+e^- propagate through the dipole magnets M0, M1, M2, which do not deflect in this plane, allowing an unobstructed measurement of the opening angle and a re-extrapolation of the rays to the target. $e^\pm$ pass subsequently through the two threshold Cerenkov counters C_0 and C_E, identifying only e^+ and e^-. The proportional wire chambers A_0, A, B, C determine the coordinates accurately, having 8000 wires with 2 mm spacing. The conventional hodoscopes E, F and G, H are arrays of 8 horizontal and vertical elements defining the time more accurately. The I, J counters are hodoscopes, too, but made of leadglass-counters of 3 X_0 each, followed by 7 horizontal shower counters of 11 X_0. They identify by big pulse heights, which correspond to electron induced showers, the $e^+(e^-)$ again and enable in case of an event with two trajectories in one arm to find out the $e^+(e^-)$ track. Fig. 3c shows the apparatus before it was embedded in 10 000 t of shielding.

The following features of the system deserve special attention:

a) The momentum is determined by measuring the vertical deflection accurately with the wire chambers; see Fig. 3b. Since this is decoupled from the measurement of the opening angle a good mass resolution of 10 MeV is achieved.

b) To obtain a rejection of 10^{-8} or better, extreme care was given to the threshold Cerenkov counters C_0 and C_E. They are filled with 1 atm and 0.8 atm of hydrogen respectively; the gas having the least electrons to produce knock-on electrons with and thereby simulating wrong particles. The windows were kept thin for the same reason. Scintillation in hydrogen is little and in addition the counters were painted black inside

as to absorb that random light. The rejection of each counter was measured to be 10^{-3}. C_o is shown in Fig. 4a.

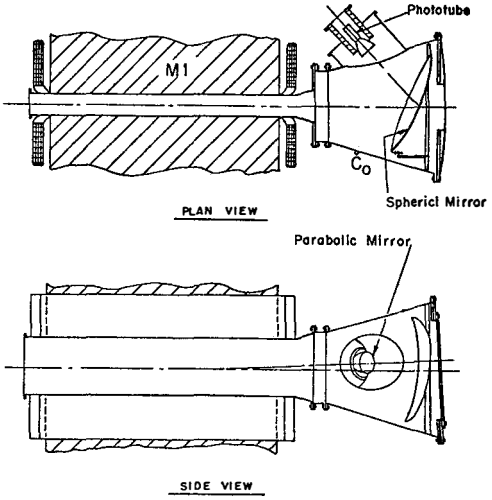

Fig 4 a

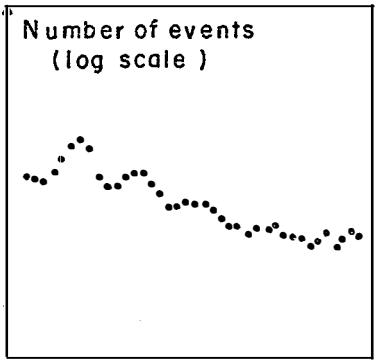

Fig 4 b

The Cerenkov light created yields about 40 photons, which are focused via a precision spherical mirror of only 3 mm thickness and a mirror parabola onto the photo cathode of a RCA 31 000 M multiplier. These are very new and special devices with excellent cathode efficiencies of about 25 %. Furthermore, due to an extremely high gain of the first dynode they have an excellent time resolution and can resolve single photo electrons. Fig. 4b gives a measurement with helium gas yielding only $\langle n \rangle \approx 2$ photo electrons on the average. This demonstrates how the estimated performance (inefficiency $e^{-\langle n \rangle}$ with $\langle n \rangle \approx 10$ for H_2) may be checked directly. The rejections are decoupled as far as possible by magnetic fields curling up δ-rays. The

system has a measured rejection of 10^{-10}.

c) The high beam intensity of 10^{12} protons/sec imposes special problems on the performance of the proportional chambers. The 20 MHz at chamber A_o made two $\pm 5^\circ$ planes necessary to decouple the dead time. The "aging" from such high radiation doses causes a severe problem, which was overcome by a special gas mixture of Argon and Methylal of 2°C only. Using specially sensitive amplifiers[13] the chambers work with standard 7 mm gap and 2 mm pitch at comfortably low voltages; see Fig. 5.

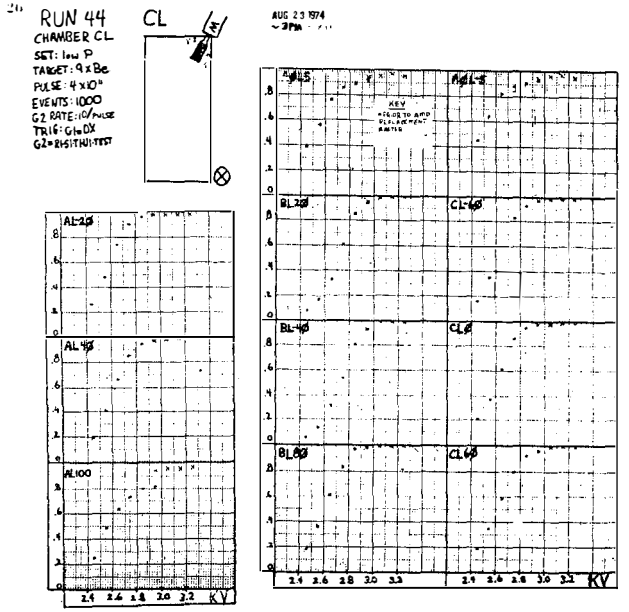

Fig. 5

Efficiency of all the wire planes as a function of the applied voltage.

Chambers A B C have 3 planes each rotated 120° relatively, each legal point fulfills the condition $\sum_{1}^{3}$ wires = const, an advantage in presence of neutron background. To reduce multi-track ambiguities the chambers are rotated 20° relatively to each other as shown in Fig. 6.

Configuration Of Wire Planes In Proportional Chambers

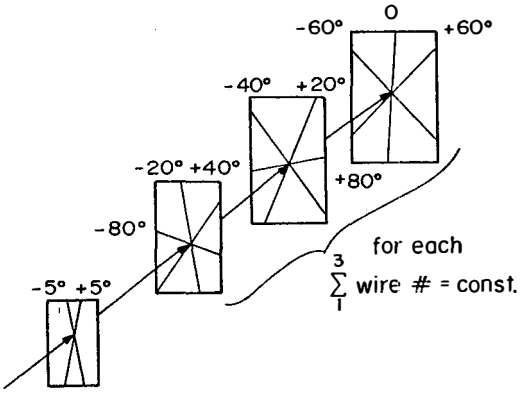

Fig. 6

Thus the proportional chambers locate each track within their accuracy of 2 mm, enabling in the non-bending plane (Fig. 3b) accurate measurement of the momentum. Together this yields mass-resolutions better than 20 MeV FWHM.

d) E, F and G, H are hodoscopes of standard scintillation material, subdividing each area in 64 fields by 8 horizontal and 8 vertical elements. Each of those is connected to a time of flight unit like the Cerenkov counters and by computer recorded event by event, to ensure the event is genuine, i.e. the time difference as between arms zero. Also this helps to

eliminate "wrong time" tracks. The time resolution for one counter is seen in Fig. 7a.

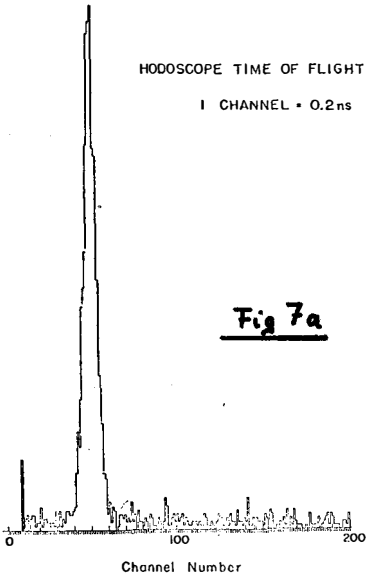

Fig 7a

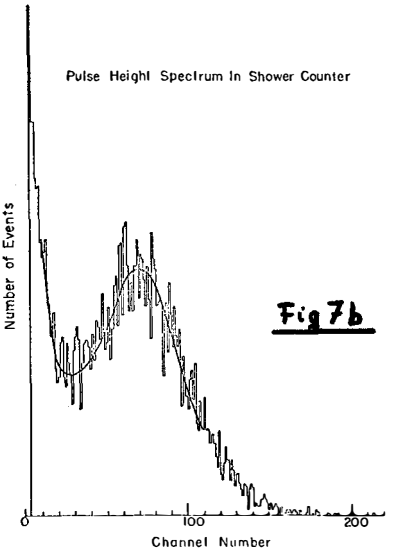

Fig 7b

e) Also all lead glass and shower counters had their pulse heights recorded for each event. One of these 78 spectra is displayed in Fig. 7b in response to triggered electrons. The small pulse heights are not admixtures of other particles, they are partial showers and disappear, when all counters in line with a trajectory are summed up.

f) Multiple scattering, photon conversion and bremsloss are kept small by minimizing the material in each spectrometer arm. The windows of the Cerenkov counters are only .12, the mirrors 3.0, and the hodoscopes 1.6 mm thick.

g) To reduce the photon and neutron contamination due to the intense beam, all counters and chambers are mounted such, that they do not "see" the target directly. Furthermore all apparatus was shielded by 10 000 tons of concrete.

h) A remaining source of background will be the Dalitz decay of $\pi^0 \to e^+e^-\gamma$ which occurs with ~ 1 %. Two π^0's may masquerade as e^+e^- pair, however, with a random distribution in time and space along the target! The e^+ and e^- from a single π^0 have a small opening angle and run in the same spectrometer arm. If then, say, e^+ has sufficient energy to pass all magnets of the spectrometer, the e^- momentum is likely to be small. A weak magnet will sweep it into a Cerenkov counter of pie shape as shown in Fig. 8a.

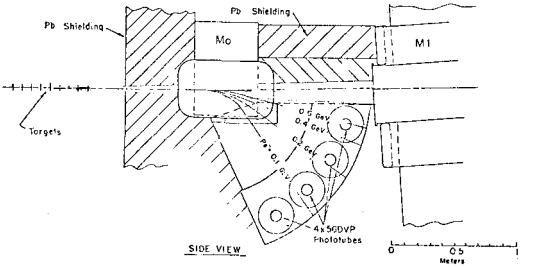

Fig 8a

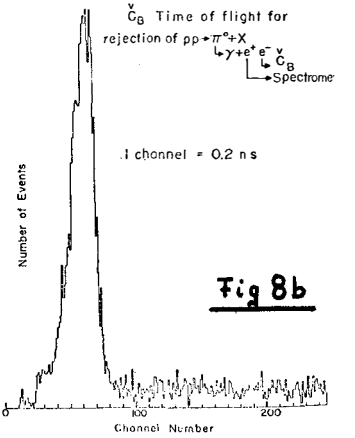

Fig 8b

90 % of the π^0 may be recognized by the fact that this counter responds at the same time as the Cerenkov counters in the

spectrometer, which is the case at about channel 60 ± 20 in Fig. 8b. Events of this type are easily vetoed, this is important at small pair masses in ee.

Conversely this can be used as to calibrate the (shower, etc.) counters in a spectrometer arm, in particular that Ce is efficient on a single e^- and not a pair.

The acceptance of this spectrometer in each arm is:

in the LS: $\theta \pm \Delta\theta = 14.6 \pm 1^\circ$ (CMS: $90 \pm 5^\circ$)

$\Delta\varphi = \pm 2^\circ$

$.6\, p_o \leq p_o \leq 1.8\, p_o$

where p_o is the principal axis momentum, which is set by the bending power of the dipole magnets. Thus the spectrometer has

1) a large mass acceptance, allowing to cover the entire region $1.5 < m_{ee} < 5.5$ GeV/c^2 in three overlapping settings.
2) a relatively small acceptance in $p_\perp$ for a produced resonance.
3) by design the acceptance is biggest at $x = \frac{p_\parallel}{p_\parallel^{max}} \simeq 0$

Data and Results

For data taking the entire apparatus got recalibrated to ensure no long term drift occurred in the time of flight of the 64 hodoscopes and 6 Cerenkov counters, as well as the pulse heights of the 78 leadglass and shower counters. The 22 planes of PWC were checked for 100 efficiency and tested at the same time (as) the read out of the 8000 wires.

As a safeguard half the data were taken at each magnet polarity setting of the spectrometer.

Fig. 9 shows the time of flight between the Cerenkov counters in the e^+ vs the e^- arm in the mass region 2.5 to 3.5 GeV/c^2. The solid line represents all events taken. Clearly at τ = 0ns a genuine signal is seen. Also a random background is noticed, which disappears as soon as a common vertex of the trajectories in the target is demanded (dotted line). This fits the description of π^0 background. Taking the sample from $3.0 < m_{ee} < 3.2$ GeV does not put a further restriction since this interval contains 90 % of the events anyway (see Fig. 11).

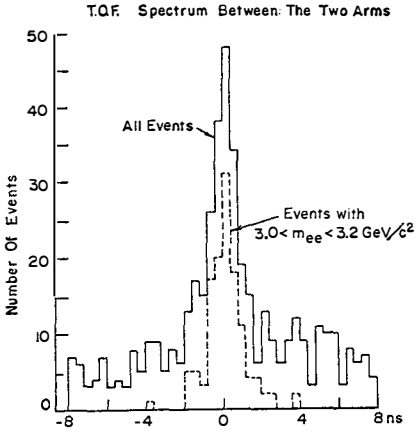

Fig. 9

Fig.10 shows the total energy-spectra from the lead glass and shower counters in each arm for the same sample of events. The high pulse heights proof that as $e^+(e^-)$ most of them with high momentum.

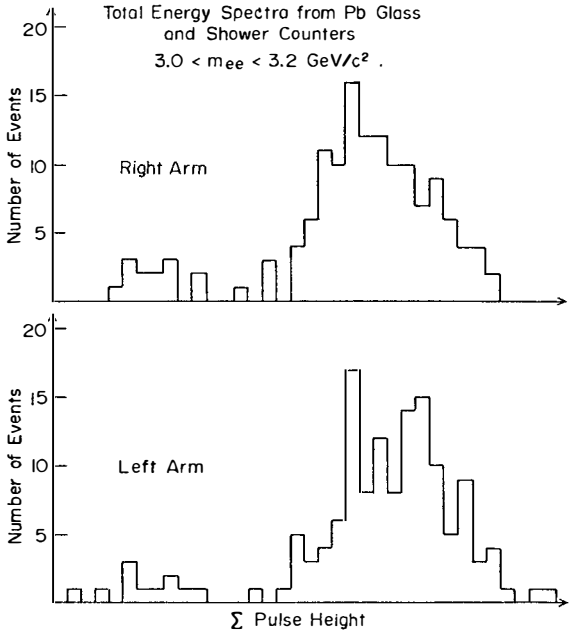

Fig 10

The first measurements were taken in August and are displayed in Fig. 11 as shaded area. Very pronounced a clear sharp enhancement is observed at

3.1 GeV, being the discovery of the J.

This was a total surprise, quite different from the expectations of a broad vector meson or an annihilation continuum. Therefore many checks were performed, to ensure it is a real particle:

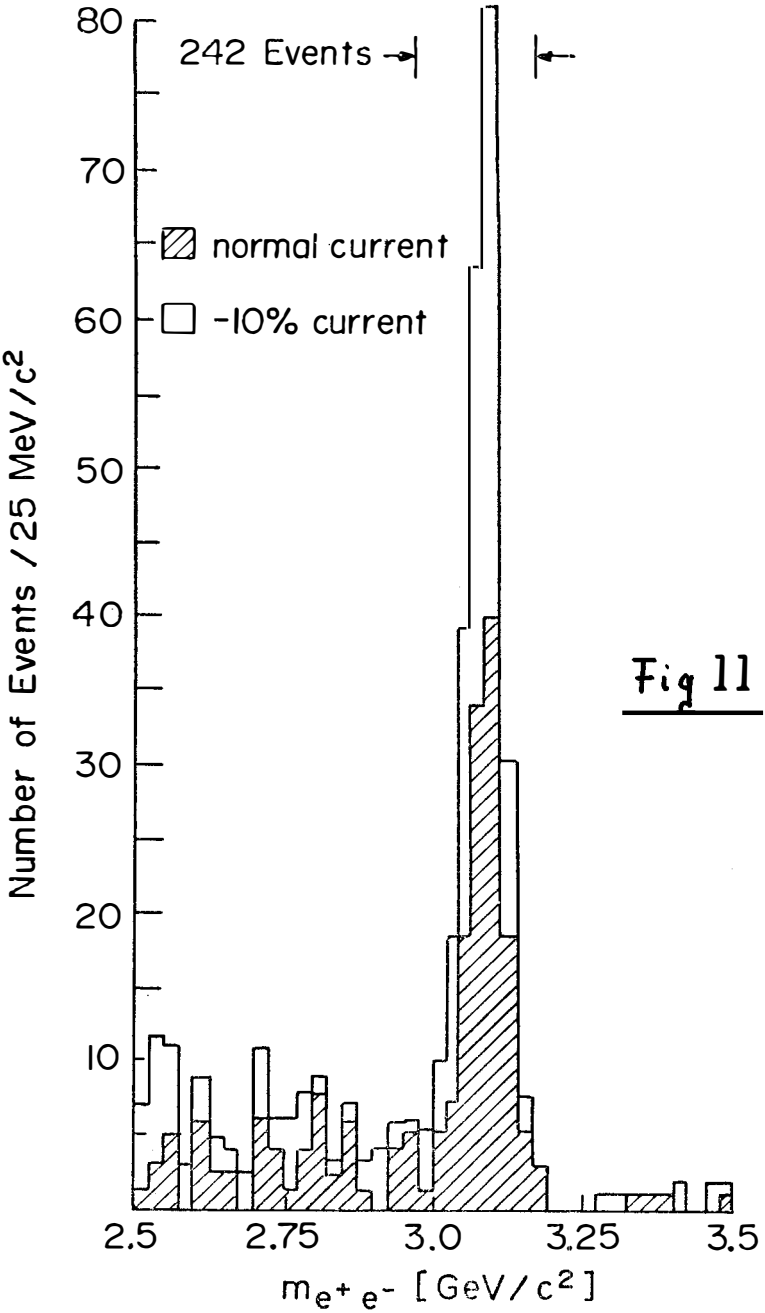
80
70
60
50
40
30
20
10
242 Events
normal current
-10% current
Number of Events /25 MeV/c²
2.5
2.75
3.0
3.25
3.5
m e+ e- [GeV/c²]

Fig 11

1) Decreasing magnet currents by 10 % shifts the acceptance as well as the spatial region of the trajectories, reconstructing to m_{ee} = 3.1 GeV. The peak remained fixed, see white area of Fig. 11.

2) Doubling the target enhanced the rate by a factor two and not four as background would behave.

3) Only events with 1.5" clearance to all magnet walls were considered, the yield corresponded to this reduced acceptance.

4) Changes in beam intensity, the high voltage of all shower counters, the reconstruction method, etc. revealed no way of similating this peak.

Assuming a production mechanism for J like

$$\frac{d^3\sigma}{dp_\perp^2\, dp_\parallel^*} = \frac{1}{E^*}\, e^{-6 p_\perp} \quad , \text{ independent of } p_\parallel^*$$

and an isotropic decay distribution, we obtain

$$\sigma(p\,Be \rightarrow J\,(3.1) + X) \simeq 10^{-34}\ cm^2/\text{nucleon}$$
$$\hookrightarrow e^+e^-$$

for 28.5 GeV incident protons.

We furthermore note how high the signal exceeds the "background". Since the observed width in Fig. 11 was the apparatus resolution, a partial analysis of the width has been attempted in Fig. 12, indicating the real width of J to be less than 5 MeV/c^2.

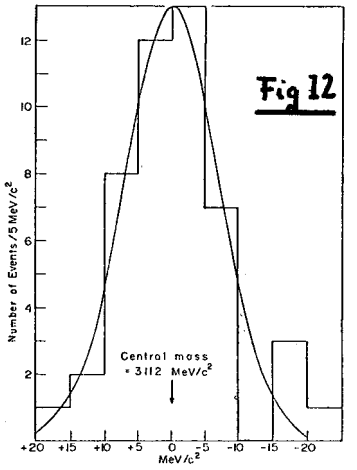

The width is even less than the energy resolution of the storage rings SPEAR[14] of 2 MeV[15], observing this particle, too. Presently[16], the calculated width is: $\Gamma_{ee} \simeq 5.2 \pm 1.2$ keV and the measured branding ratio

$$B_{ee} = \frac{\Gamma_{ee}}{\Gamma_{all}} = 7\ \%.$$

Fig. 13 below shows e^+e^- pairs in the region 3.2-4.0 GeV/c^2. The acceptance in this region is smooth, varying less than a factor two. All events are consistent with random coincidences. Therefore with 95 % confidence level no particle is produced and decaying into e^+e^- in this region with

$$\geq 1\ \% \text{ of } J$$

or, assuming the same production mechanism than J

$$\sigma \cdot B_{ee} \leq 10^{-36}\ \text{cm}^2/\text{nucleon}.$$

In particular this means, a low production cross section for the resonance[17] seen at 3.7 GeV/c^2. To exploit more details about the production mechanism an excitation measurement is planned at BNL, that is to measure the yield as function of the incident beam energy from 20 to 30 GeV.

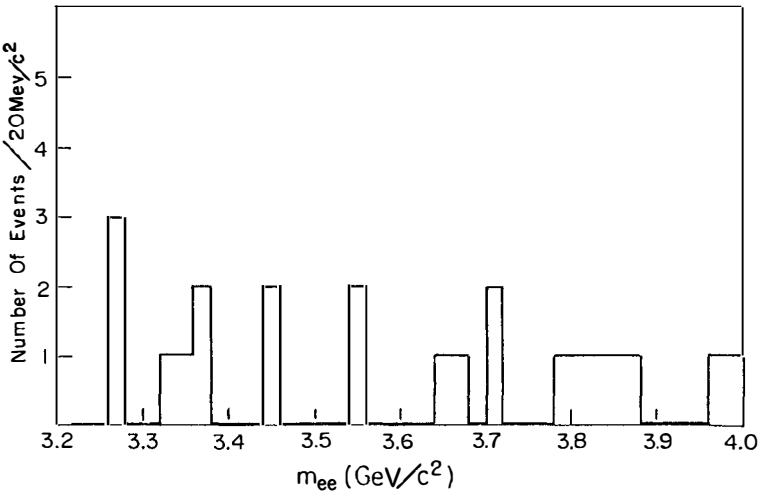

Results

J (3.1) was observed meanwhile in

a) hadron collisions: BNL-MIT[1], FNAL[18]

b) e^+e^- annihilation: SPEAR, Adone, DORIS, see Ref. 14,17)

c) Photoproduction: FNAL[18], SLAC I, II

All measurements are compatible with

$$m_J = 3.10 \pm .01 \text{ GeV/c}^2$$

The width is deduced from $\Gamma_{ee}^2/\Gamma_{tot} = \frac{m_J^2}{6\pi}\int \sigma_e(E)\,dE$

After radiative corrections, the measured $\Gamma_{ee}/\Gamma_{tot} \simeq 7$ % and $\int \sigma_e(E)dE \simeq 11.0$ μb·GeV yield [14,16]:

$$\Gamma_J = 72 \pm 20 \text{ keV}$$

Even though J is very heavy, it is not a baryon:

$$B = 0$$

since it decays into e^+e^-. It is conjectured to be a

$J^{PC} = 1^{--}$ state, because

$\Gamma_{ee} \simeq 5.2$ keV is a "typical" electromagnetic decay width of a vector meson, compared to 6.5 keV for ρ^0 and 1.4 for φ. The observation of $\Gamma_{ee} \simeq \Gamma_{\mu\mu}$ is in agreement with this assumption as well as preliminary measurements of decay angular distributions and interference effects with the calcul able $e^+e^- \to \mu^+\mu^-$ Q.E.D. amplitude. Also no sizeable $J \to 2\gamma$ decay[14] is observed, $\Gamma_{\gamma\gamma} < .4$ keV.

The question, is the

J = hadron? is more difficult, but the following indications exist! Imagine the measurement of Fig. 11 done with 2 MeV resolution. Then the J would be 200 times above the "normal electromagnetic background" indicating a relatively "strong" production, compared to a 10:1 enhancement in $e^+e^- \to e^+e^-$. Conversely this is noticed in the decay[16], too:

$$\frac{e^+e^- \to \text{hadrons}}{e^+e^- \to \mu^+\mu^-} = \begin{cases} 2.5 \text{ off resonance} \\ 12.5 \text{ at } 3.1 \text{ GeV.} \end{cases}$$

The mystery of the small width, however, remains. If this particle lives so long it s decay must be forbidden for a presently unknown reason.

The important question arises how big is the family of these new particles[19], in particular, are there charged J-type particles.

References

1) J.J. Aubert et al. Phys. Rev. Lett. 33, 1408 (1974)

2) T.D. Lee, Phys. Rev. Lett. 26, 801 (1971);
S. Weinberg, Phys. Rev. Lett. 19, 1264 (1967); Phys. Rev. Lett. 27, 1688 (1971); Phys. Rev. D5, 1412 (1972) and Phys. Rev. D5, 1962 (1972);
A. Salam, in Elementary Particle Theory, edited by N. Svartholm (Almquist and Farlag, Stockholm, 1968).

3) G. Barbarino et al., Lett. al Nuovo Cimento 3, 693 (1972).

4) J.G. Asbury et al., Phys. Rev. Lett. 19, 865 (1967);
H. Alvensleben et al., Phys. Rev. Lett. 24, 786 (1970);
H. Alvensleben et al., Phys. Rev. Lett. 28, 66 (1972);
K. Gottfried, 1971 International Symposium on Electron/Photon Interactions at High Energies, Cornell (1971); see references listed therein.

5) J.G. Asbury et al., Phys. Rev. Lett. 19, 869 (1967).

6) U. Becker et al., Phys. Rev. Lett. 21, 1504 (1968).

7) H. Alvensleben et al., Phys. Rev. Lett. 25, 1373 (1970);
P. Biggs et al., Phys. Rev. Lett. 24, 1197 (1970).

8) G. Wolf, DESY 72/61 (1972), report

9) H. Alvensleben et al., Phys. Rev. Lett. 26, 273 (1971)

10) S.D. Drell and T.M. Yan, Phys. Rev. Lett. 25, 316 (1970).

11) J.H. Christenson et al., Phys. Rev. Lett. 25, 1523 (1970).

12) V. Blobel et al., Phys. Rev. Lett. 48B, 73 (1974).

13) H. Cunitz, W. Sippach, J. Dieperink, Nucl. Instr. and Methods 91, 211 (1971)

It is a pleasure to appreciate the help of W. Cunitz and W. Sippach on the electronics for the proportional chambers, which turned out to be very essential for the success.

14) J.E. Augustin et al., Phys. Rev. Lett. 33, 1406 (1974).
C. Bacci et al., Phys. Rev. Lett. 33, 1408 (1974).
W. Braunschweig et al. Phys. Rev. Lett. 53B, 393 (1974).
15) D.R. Yennie, Phys. Rev. Lett. 34, 239 (1975).
16) G. Wolf, MIT Seminar, also Roy Schwitters.
Values include radiative corrections.
17) Seen in $e^+e^- \rightarrow$ 3.7
G.S. Abrams et at. Phys. Rev. Lett. 33, 1453 (1974).
L. Criegee et al. Phys. Rev. Lett. 53B, 489 (1975).
18) B. Knapp et al. see later in these proceedings.
19) H.T. Nieh, T.T. Wu, and C.N. Yang, Phys. Rev. Lett. 34, 49 (1975); A. de Rujula and S.L. Glashow, Phys. Rev. Lett. 34, 46 (1975); C.G. Callam, R.L. Kingsley, S.B. Treiman, F. Wilczek and A. Zee, Phys. Rev. Lett. 34, 52 (1975); J.J. Sakurai, Phys. Rev. Lett. 34, 56 (1975).
H.P. Duerr, Phys. Rev. Lett. 34, 422 (1975).

THE $\psi(3.1)$ AND THE SEARCH FOR OTHER NARROW RESONANCES OF SPEAR

Presented by M. Breidenbach
Stanford Linear Accelerator Center
Stanford University, Stanford, California 94305

J. E. Augustin, A. M. Boyarski, F. Bulos, J. T. Dakin,
G. J. Feldman, G. E. Fischer, D. Fryberger, G. Hanson,
B. Jean-Marie, R. R. Larsen, V. Lüth, H. Lynch, D. Lyon,
C. C. Morehouse, J. M. Paterson, M. L. Perl, B. Richter,
B. Rapidis, R. F. Schwitters, W. Tanenbaum, F. Vannucci

Stanford Linear Accelerator Center
Stanford University, Stanford, California 94305

and

G. S. Abrams, D. Briggs, W. Chinowsky, C. E. Friedberg, G. Goldhaber,
R. J. Hollebeek, J. A. Kadyk, A. Litke, B. Lulu, F. Pierre,
B. Sadoulet, G. H. Trilling, J. S. Whitaker, J. Wiss, J. E. Zipse

Lawrence Berkeley Laboratory
University of California, Berkeley, California 94720

ABSTRACT

A sharp peak at 3.095 ± 0.005 GeV is seen in the cross section for e^+e^- annihilation. The width is $\Gamma = 77 \pm 19$ KeV. Angular distributions and interference effects imply that the J^{PC} of the $\psi(3.1)$ is 1^{--}. A study of the exclusive final states suggests that the G-Parity is odd. With the exception of another sharp resonance at 3.7 GeV, the $\psi(3.7)$, no other comparable structure is seen for masses between 3.2 and 5.9 GeV.

On observe un pic tres étroit a 3.095 ± 0.005 GeV dans la section efficace d'annihilation e^+e^-. La largeur est $\Gamma = 77 \pm 19$ KeV. Les distributions angulaires ainsi que les effets d'interference conduisent a assigner 1^{--} pour les nombres quantiques du $\psi(3.1)$. Une etude des canaux exclusifs suggère une parité G=-1. Si l'on exepte l'autre resonance $\psi(3.7)$, aucune structure comparable a eté trouvé entre 3.2 GeV et 5.9 GeV.

In November 1974, two narrow resonances coupled to e^+e^- at masses of 3.1 and 3.7 GeV were discovered.[1,2,3,4] A search[5] for other narrow resonances was conducted between 3.2 and 5.9 GeV, and no others of comparable strength were found. However, some interesting structure[6] in the total hadronic cross section from e^+e^- annihilation (σ_T) has been found near 4.1 GeV. This talk will attempt to describe the present experimental situation; it should be realized that many of the results are preliminary and therefore are not to be considered as firm or final.

The storage ring SPEAR circulates one bunch of electrons and one bunch of positrons in a single magnetic guide field. The bunches collide alternately in two interaction regions. The beam energies may now be varied between about 1.3 GeV and 4 GeV. The energy distribution of electrons within a beam bunch is approximately Gaussian with a width that increases approximately quadratically with energy, and has a σ of about 1 MeV at a total energy ($E_{cm} = 2\ E_{beam}$) of $E_{cm} = 3$ GeV. The absolute energy calibration is based on measurements of the particle orbits and the magnetic guide fields and is known to about 0.1%. The bunch shapes are Gaussian with σ's in the transverse plane of approximately 0.1 cm and longitudinally a few cm. The luminosity is about 3×10^{29} cm^{-2} sec^{-1} at $E_{cm} = 3$ GeV.

The magnetic detector is shown schematically in Fig. 1. The magnetic field of 4 kilogauss is axial and within a volume about 3 meters in diameter by 3 meters long. The interaction region is surrounded by a stainless steel vacuum pipe 0.15 mm thick. Coaxial with the pipe are a pair of cylindrical plastic scintillation counters that form one element of the trigger system. Continuing radially outward are four sets of multiwire spark chambers. Each set consists of four "planes" of wires at $\pm 2^\circ$ and $\pm 4^\circ$ with respect to the beam axis. Thus, each set of chambers provides redundant azimuthal (resolution ≈ 0.5 mm) and longitudinal (resolution ≈ 1.2 cm) position information for each charged particle. Following the spark chambers are a set of 48 plastic scintillator trigger counters. These counters are used in the trigger

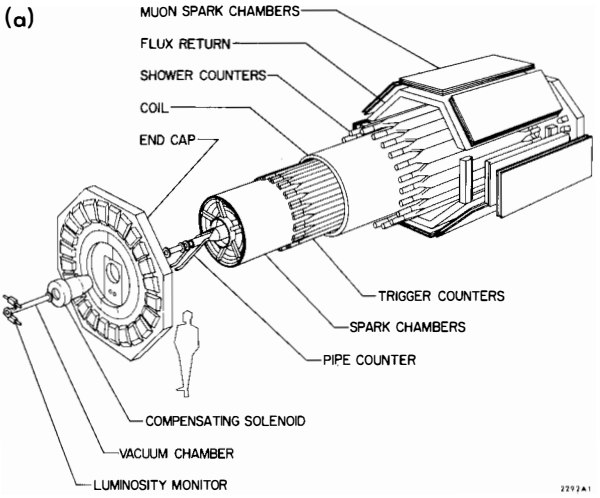

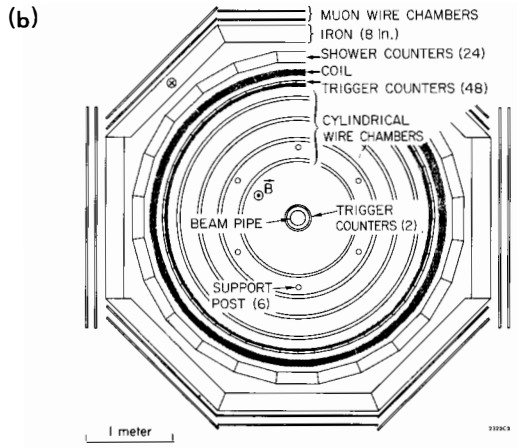

Fig. 1

(a) Telescoped view of detector; (b) end view of detector.

system and in a time-of-flight particle identification system with a resolution (σ) of about 0.5 nsec, allowing π/K separation up to about 0.6 GeV/c. Next comes the aluminum coil of the solenoid with a thickness of about 1 radiation length, followed by a layer of 24 lead-scintillator sandwich electron shower counters used to identify electrons. The next element is the iron return yoke of the magnet which also serves as a hadron filter for the final set of spark chambers which aid in muon identification.

The trigger requirement is two or more charged particles with transverse momenta greater than about 200 MeV/c. The complete detector system covers a solid angle of $0.65 \times 4\pi$. A hadronic event is defined to be one with 3 charged particles or two charged particles accolinear by 20° or more. The detector efficiency for hadronic events varies smoothly from 40% at $E_{cm} = 2.5$ GeV to 65% at 4.8 GeV. Backgrounds have been studied using separated beams and longitudinal (z) distributions of events. The background contribution to the resonances is very small, of order 0.01 to 0.1%, and is roughly 5% in the nonresonant region. Normally, cross sections are normalized by measuring Bhabha scattering in the magnetic detector. However, in the vicinity of the narrow resonances, the e^+e^- pair production cross section is strongly enhanced by photonic decays of the resonance. Hence, the luminosity is integrated by a set of small counters monitoring Bhabha scattering at small angles, (where the scattering is dominantly caused by space-like photons). The luminosity monitor is calibrated with the magnetic detector at a beam energy far from the resonances.

Figure 2 shows the total hadronic cross section versus E_{cm} in the region $E_{cm} = 3.1$ GeV. A sharp peak is seen at a mass of 3.095 ± 0.005 GeV. The peak cross section is rather large, approximately 2500 nb, and the observed width is about 2.5 MeV FWHM. The width is that expected from the convolution of a much narrower resonance shape, the inherent spectral resolution of the storage ring, and radiative corrections in the production of a virtual photon.

Figure 3a shows the cross section for production e^+e^- pairs; Figure 3b

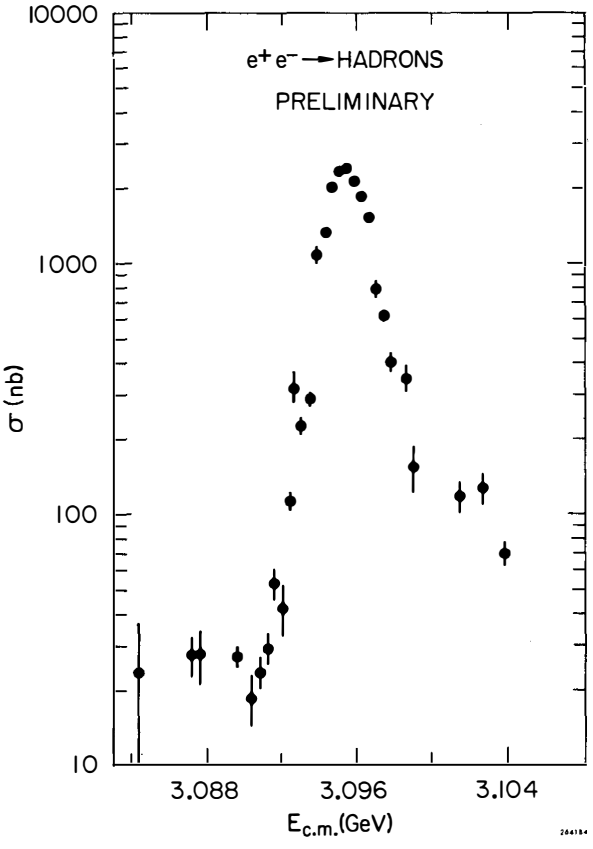

Fig. 2

Total cross section for hadron production vs. center-of-mass energy for ψ(3.1), corrected for detector acceptance.

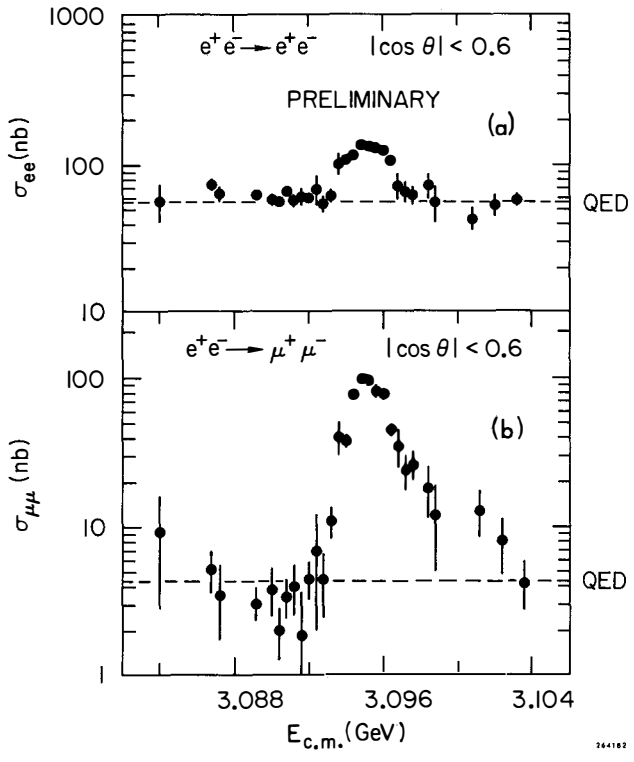

Fig. 3

Cross section for production of lepton pairs integrated over the range $|\cos\theta| \leq 0.6$ vs. center-of-mass energy; (a) electrons, (b) muons. No correction has been applied for the loss of events having $|\cos\theta| > 0.6$.

shows the cross section for $\mu^+\mu^-$ pairs. These data allow the determination of the total resonance width Γ and the width into electrons Γ_e and muons Γ_μ. The resonant cross section to any set of states f may be written

$$\sigma_f = \frac{(2J+1)\pi}{W^2} \frac{\Gamma_e \Gamma_f}{(M-W)^2 + \Gamma^2/4}$$

where J is the spin of the resonance, W is the center-of-mass energy, M is the resonance mass, and Γ_f is the width to the set of final states. If this expression is integrated, it may be compared to the integrated experimental cross section (after appropriate radiative corrections) without explicit dependence on the storage ring energy resolution. Thus:

$$\int \sigma_f(W)\, dw = \frac{(2J+1)\, 2\pi^2}{M^2} \frac{\Gamma_e \Gamma_f}{\Gamma} .$$

The integrated total hadronic cross section is $\int \sigma_h\, dw = 10.8 \pm 2.7$ nb GeV. Assuming that $\Gamma = \Gamma_h + \Gamma_\mu + \Gamma_e$ and that $\Gamma_\mu = \Gamma_e$ and that $J = 1$, $\Gamma = 77 \pm 19$ KeV and $\Gamma_e = 5.2 \pm 1.3$ KeV. The quoted errors are derived from the statistical errors combined in quadrature with the known systematic uncertainties, including hadron detection efficiency (10%), luminosity measurements (10%), and reproducability of the integral of the measured cross section (8%).

The analysis assumed $\Gamma_e = \Gamma_\mu$ (muon-electron universality) because the e-pair cross section has a large contribution from space-like momentum transfer QED processes. If the QED contributions are removed, then the ratio of the resonant μ to e cross sections is 0.99 ± 0.06. See Figures 4a and 4b.

The assumption that J=1 can be tested by examining the angular distribution of the produced μ's and e's. Figure 4a shows the angular distribution of the positron for e^+e^- production. The solid points are the measured data and the open points have the QED space-like contribution removed. Figure 4b shows the similar distribution for μ's. Both curves are for data in a E_{cm} interval of 1 MeV centered at the peak of the $\psi(3.1)$. A fit to the form $a + b \cos^2\theta$ yields a b/a ratio of 1.3 ± 0.2, thus suggesting that J=1. The expected value for J=1 is unity. The measured μ asymmetry at the resonance

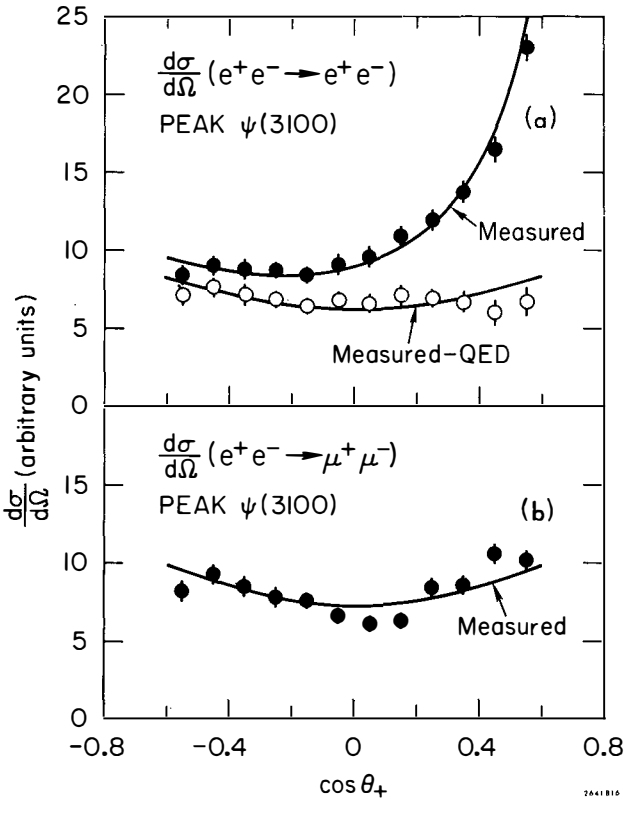

Fig. 4

Angular distribution of the positive particle for production of lepton pairs. The center-of-mass energy is within 1 MeV of the peak of the $\psi(3.1)$. (a) Electrons. The solid points are measured; the open points have the QED contribution removed. (b) Muons. The curves are the expected distribution for a spin 1 resonance.

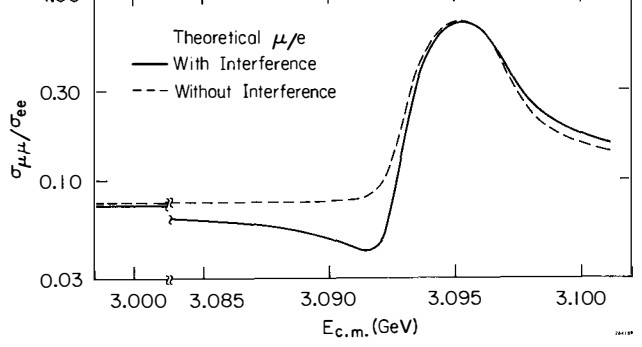

Fig. 5

Predictions for the ratio of μ-yield to e-yield for no interference and complete interference.

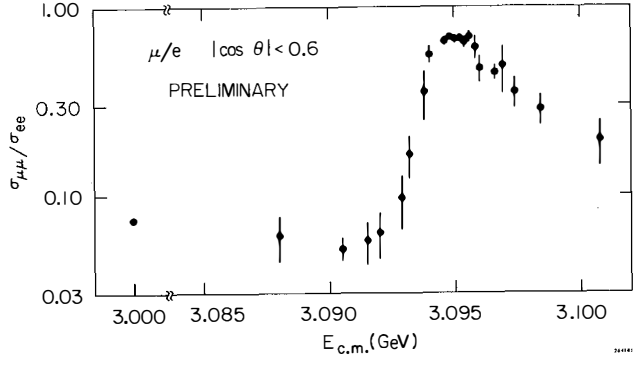

Fig. 6

Experimental data for the ratio of μ-yield to e-yield. The hypothesis of no interference can be excluded by having a confidence level of less than 0.15%.

peak (forward μ^+ - backward μ^+ divided by total) is 0.014 ± 0.02, implying that either vector or axial vector accounts for at least 97% of the total resonant amplitude (95% confidence).

The parity of the $\psi(3.1)$ may be determined by looking for an interference between the resonant and QED amplitudes in the $\mu^+\mu^-$ channel. This interference is manifested in the energy dependence of the $\mu^+\mu^-$ cross section which is integrated over an angular interval centered at 90°. The resonant 1^- amplitude will interfere with the QED contribution destructively below the peak and constructively above. A resonant 1^+ amplitude will not interfere. Figure 5 shows the prediction for the ratio $\sigma_{\mu\mu}$ to σ_{ee} as a function of energy with and without interference (corresponding to 1^- and 1^+ amplitudes). The effect above the peak is obscured by the radiative corrections. This choice of the $\sigma_{\mu\mu}$ to σ_{ee} ratio is made to minimize systematic errors. Figure 6 shows the data. For the 1^- hypothesis, the interference dip extends from about 14 to 4 MeV below the peak. In a 4 MeV interval in this region, 1360 $e^\pm$ pairs were observed; we expect 100 ± 10 $\mu^\pm$ for no interference and 71 ± 8 with interference. We observe 68 $\mu^\pm$ which is over 3 standard deviations from the prediction for no interference and quite compatible with the interference hypothesis. We believe that the $\psi(3.1)$ has the same quantum numbers, J^{PC}, as the photon.

Several exclusive decay modes of the $\psi(3.1)$ have been identified. One of the interesting questions is the determination of the G-Parity and isospin of the $\psi(3.1)$ from its multipion decay states. It is possible to calculate the missing mass distribution according to the hypothesis $n(\pi^+\pi^-) + X$. Mass squared distributions for the X for n=2 and n=3 are shown in Figs. 7 and 8. A large peak near a mass square of 0 is seen. The resolution is inadequate to distinguish a π° from a single photon. The cross section in the peak for the $2(\pi^+\pi^-) + X$ is about 90 nb, the $3(\pi^+\pi^-) + X$ channel is about 60 nb, and the $\pi^+\pi^-$ X channel is somewhat smaller. A hint that the X is indeed a π° is shown in Figure 9. Here the sample of presumed $\pi^+\pi^-\pi^+\pi^-\pi^\circ$ events are binned

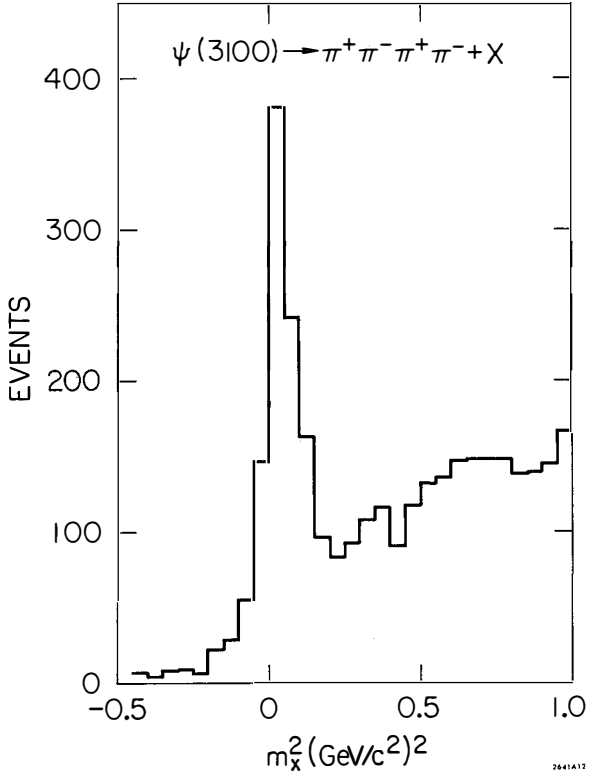

Fig. 7

Missing mass squared distribution for the hypothesis $\psi(3.1) \rightarrow \pi^+\pi^-\pi^+\pi^- + X$.

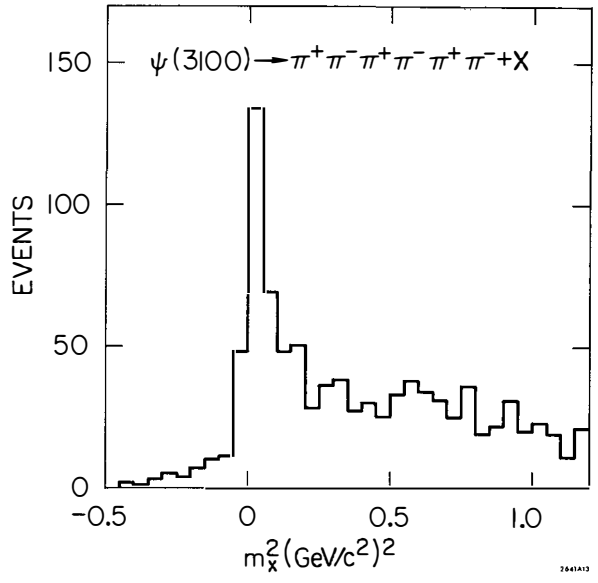

Fig. 8

Missing mass squared distribution for the hypothesis $\psi(3.1) \rightarrow \pi^+\pi^-\pi^+\pi^-\pi^+\pi^- + X$.

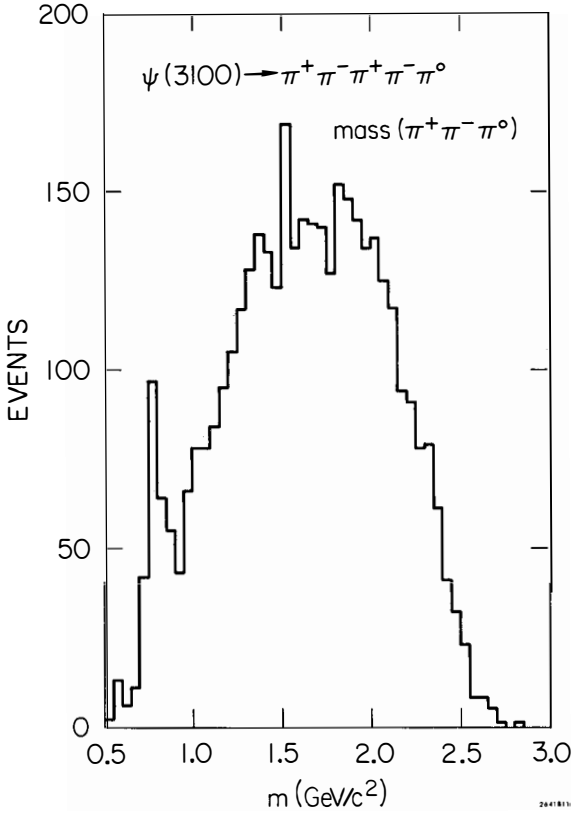

Fig. 9

Mass distribution of the $\pi^+\pi^-\pi^0$ combination in the decays $\psi(3.1) \rightarrow \pi^+\pi^-\pi^+\pi^-\pi^0$.

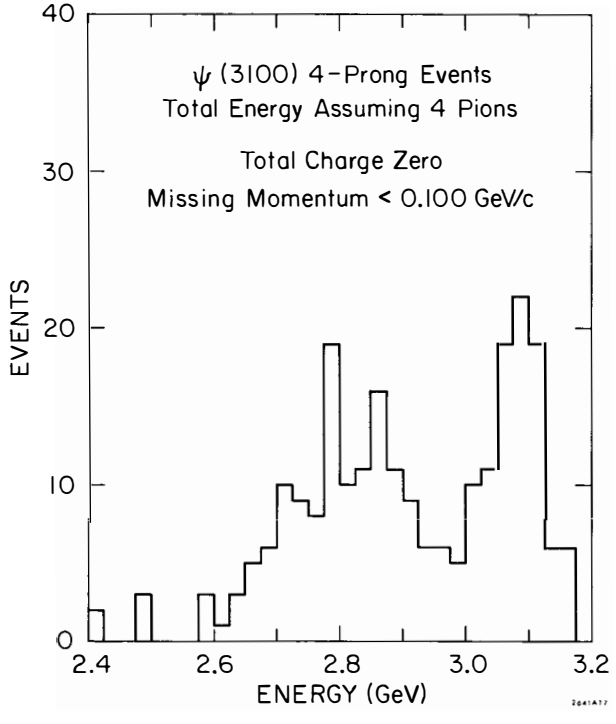

Fig. 10

Total energy distribution for 4-constraint fits to 4 charged particles assuming all are π's. The peak at 3.1 corresponds to this hypothesis, and the lower energy peak corresponds to $\pi^+\pi^-K^+K^-$ production.

in invariant mass intervals of the $\pi^+\pi^-\pi^o$ combination. A clean signal is seen at the mass of the ω.

Four constraint fits (measurement of all the particles of an event) have also been done. Figure 10 shows the total energy distribution of an event assuming a particle identification $\pi^+\pi^-\pi^+\pi^-$. The peak around 3.1 GeV indeed corresponds to this hypothesis. The peak at about 2.7 corresponds to $\pi^+\pi^-K^+K^-$, i.e., these events move to 3.1 GeV when appropriate particles are assigned kaon masses. States of $p\bar{p}$ and $\Lambda\bar{\Lambda}$ have been seen. The 4-C multipion status have a cross section consistent with that expected from the photonic decay of the $\psi(3.1)$ rather than a direct hadronic decay. If we take the $\psi(3.1) \rightarrow \mu^+\mu^-$ decay as a measure of the branching ratio for the ψ to decay via a virtual photon, we expect the cross section for any given exclusive final state to be enhanced by a factor of about 20 compared to its value just off resonance. The cross section for $2(\pi^+\pi^-)$ has been measured to be about 0.6 nb at W = 3.0 GeV; an enhancement by a factor of approximately 20 is observed. Conversely, an upper limit for the $2(\pi^+\pi^-) + \pi^o$ cross section off resonance is 0.6 nb; the observed resonant cross section is at least 150 times greater. The favored direct hadronic decay into states of odd numbers of π's would imply negative G-Parity and even isospin, probably 0.

Shortly after the discovery of the $\psi(3.1)$, SPEAR and the detector were modified to allow a sequential sweep in energy in steps of 1.8 MeV in E_{cm}. Measurements were made at each energy for several minutes, so that the expected hadron rate was about 2 per step. Realtime computation allowed an evaluation of the cross section within a few seconds of completion of an energy step. Using this technique, another narrow resonance was found at 3.7 GeV, and is named $\psi(3.7)$. After the discovery of the $\psi(3.7)$, the scanning process was continued up to a W of 5.9 GeV. The results are shown in Fig. 11. Only the $\psi(3.7)$ stands out clearly. The region below 3.2 GeV has not yet been finished. Upper limits on the resonance strength $\int \sigma_h dw$ for other narrow resonances are shown for various energy intervals in Table I. We hope to extend the range of the scan by a few GeV in the near future.

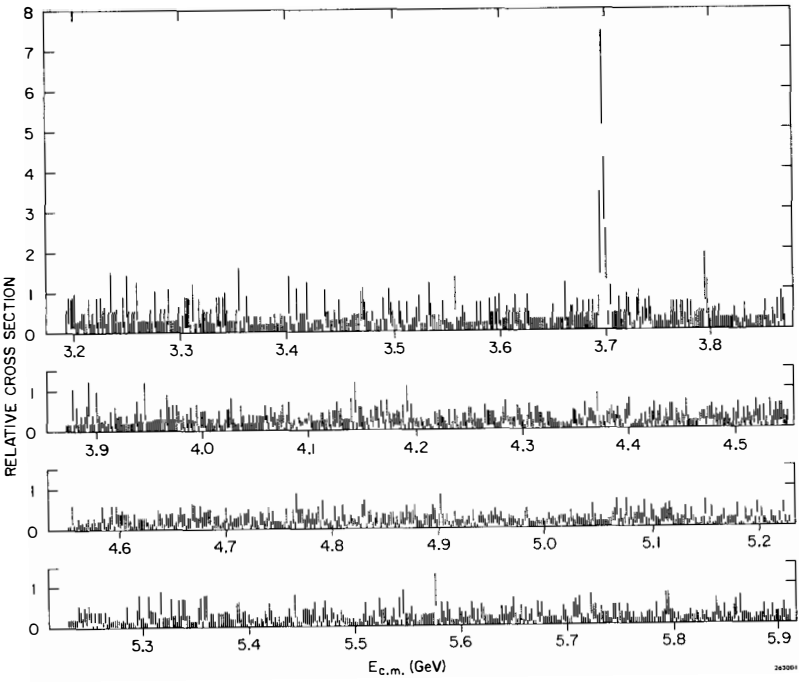

Fig. 11

Relative cross sections from the fine mesh energy scan. The $\psi(3.7)$ is clearly visible.

REFERENCES AND FOOTNOTES

1. J. J. Aubert et al., Phys. Rev. Letters 33, 1404 (1974).

2. J. E. Augustin et al., Phys. Rev. Letters 33, 1406 (1974).

3. C. Bacci et al., Phys. Rev. Letters 33, 1408 (1974).

4. G. S. Abrams et al., Phys. Rev. Letters 33, 1453 (1974).

5. A. M. Boyarski et al., "Search for Narrow Resonances in e^+e^- Annihilation in the Mass Region 3.2 to 5.9 GeV," submitted to Phys. Rev. Letters.

6. J. E. Augustin et al., "Total Cross Section for Hadron Production by e^+e^- Annihilation," submitted to Phys. Rev. Letters.

TABLE I

Upper limits at the 90% confidence level for the radiatively corrected integrated cross section of a possible resonance. The units are nb Mev.

Mass range (GeV)	Resonance width (FWHM in MeV) 0[a]	10	20
3.200 to 3.500	970	1750	2230
3.500 to 3.690	780	1090	1540
3.720 to 4.000	1470	1530	1860
4.000 to 4.400	620	1260	1860
4.400 to 4.900	580	1080	1310
4.900 to 5.400	780	1100	1720
5.400 to 5.900	800	1120	1470

[a]Width less than the mass resolution

SOME PROPERTIES OF THE $\psi(3.7)$ RESONANCE, AND FEATURES OF THE TOTAL HADRONIC CROSS SECTION IN e^+e^- ANNIHILATION FROM 2.4 GeV TO 5.0 GeV C.M. ENERGY

Presented by J. A. Kadyk
Lawrence Berkeley Laboratory
University of California, Berkeley, California 94720

G. S. Abrams, D. D. Briggs, W. Chinowsky, C. E. Friedberg,
G. Goldhaber, R. J. Hollebeek, A. Litke, B. A. Lulu, F. Pierre,
B. Sadoulet, G. H. Trilling, J. S. Whitaker, J. E. Wiss, J. E. Zipse

Lawrence Berkeley Laboratory and Department of Physics
University of California, Berkeley, California 94720

and

J.-E. Augustin, A. M. Boyarski, M. Breidenbach, F. Bulos, J.T. Dakin, G.J. Feldman
G. E. Fischer, D. Fryberger, G. Hanson, B. Jean-Marie, R. R. Larsen,
V. Luth, H. Lynch, D. Lyon, C. C. Morehouse, J. M. Paterson, M. L. Perl,
B. Richter, B. Rapidis, R. F. Schwitters, W. Tanenbaum, F. Vannucci

Stanford Linear Accelerator Center
Stanford University, Stanford, California 94305

ABSTRACT

An analysis of data at the $\psi(3.7)$ resonance gives a partial width to electrons, $\Gamma_e = 2.2 \pm 0.5$ keV, and limits on total width 200 keV $< \Gamma <$ 800 keV. The decay $\psi(3.7) \rightarrow \psi(3.1)\pi^+\pi^-$ is observed with a branching ratio 0.31 ± 0.04, and $\psi(3.7) \rightarrow \psi(3.1)$ + anything has a branching ratio of 0.54 ± 0.08. The ψ resonances appear to have the same G-parity.

An enhancement occurs in the total hadronic cross section at a c.m. energy of about 4.1 GeV, rising to about 32 nb from a level of 18 nb adjacent to peak, which is about 300 MeV wide. The integrated cross section for the peak is about 5.5 nb-GeV, comparable to that for the $\psi(3.7)$ and $\psi(3.1)$ resonances.

Une analyse des mesures expèrimentales sur la résonance $\psi(3.7)$ donne une largeur partielle pour la désintègration en une paire d'electrons, $\Gamma_e = 2.2 \pm 0.5$ keV, et des limites sur la largeur totale, 200 keV $< \Gamma <$ 800 keV. La désintegration $\psi(3.7) \rightarrow \psi(3.1)\pi^+\pi^-$ est observée avec un rapport d'embranchement de 0.31 ± 0.04, et $\psi(3.7) \rightarrow \psi(3.1)$ + n'importe quoi a un rapport d'embranchement de 0.54 ± 0.08. Les resonances ψ semblent avoir la même parité G.

Une hausse de la section efficace totale hadronique se produit à une énergie dans le centre de masse de 4.1 GeV. La section efficace monte de son niveau de 18 nb à des énergies avoisinantes jusqu'à 32 nb avec une largeur d'à peu près 300 MeV. L'intégrale de la section efficace pour cette structure est approximativement 5.5 nb-GeV, comparable à celles des résonances $\psi(3.7)$ et $\psi(3.1)$.

I. $\psi(3.7)$

Following the discovery of the $\psi(3.1)$, a systematic search was initiated to look for other very narrow resonances. The method of search has been described previously,[1] but can be briefly explained as an automatic ramping of the SPEAR beam energy by $\sim$ 1 MeV steps every few minutes, the data collected at each energy being processed on-line by the SLAC IBM 168 computer complex. By this means, the cross sections were immediately computed in very fine steps ($\Delta E_{cm} \sim 2$ MeV) although with large statistical errors. However, this technique was more than adequate in detecting narrow resonances as was proven by going back over the $\psi(3.1)$ resonance, which was seen clearly, and, much more importantly, by the discovery of the $\psi(3.7)$ soon after the search began[2] (see Fig. 1).* The sensitivity was such that resonances having σ_{had} at the peak greater than a few hundred nb would have been detected.

Shortly after observing the ψ', the shape of the peak was carefully mapped out as illustrated in Fig. 2, in order to obtain Γ_e by integration of the cross section, as was done for the ψ. The result after radiative corrections is:

$$\int \sigma_{had}\, dW = 3.7 \pm 0.9 \text{ nb-GeV} .$$

This is about a factor of 3 less than for the ψ. To obtain the width to the e^+e^- channel and the total width, it is necessary to know the branching ratio into e^+e^-, or into $\mu^+\mu^-$, if μ-e universality is assumed. First attempts to observe the leptonic modes were disappointing, only the slightest suggestion of any enhancement being visible. Soon it became clear that the situation was rather complex, since it was discovered that the ψ' decayed into the ψ part of the time,[2] and since the ψ subsequently decayed into leptons, that decay mode must be distinguished from those due to direct decay of the ψ'. We will return to discuss the ψ' cascade decay in a moment.

*Within this paper we will subsequently refer to the $\psi(3.7)$ as ψ' and $\psi(3.1)$ as ψ.

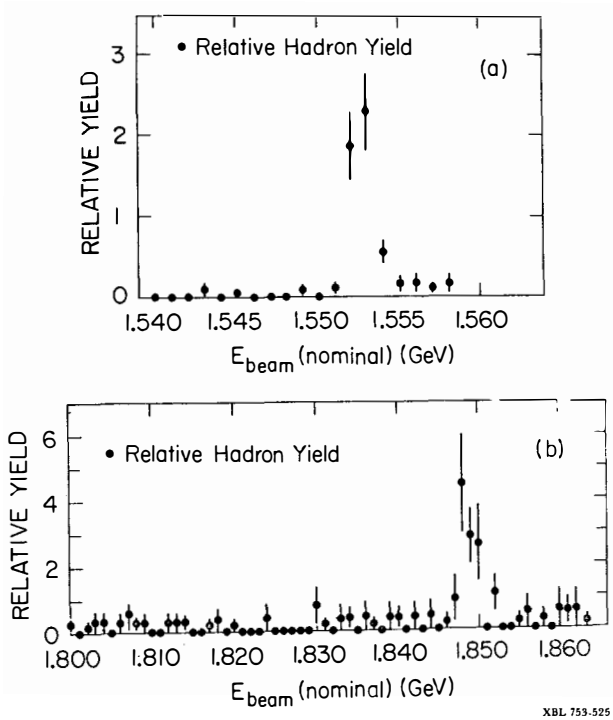

Fig. 1. Examples of data taken in the early scan or search mode, leading to the discovery of the $\psi(3.7)$. (a) Data taken in the vicinity of the $\psi(3.1)$ to confirm the sensitivity of the method, (b) data taken during the run in which the $\psi(3.7)$ was first found.

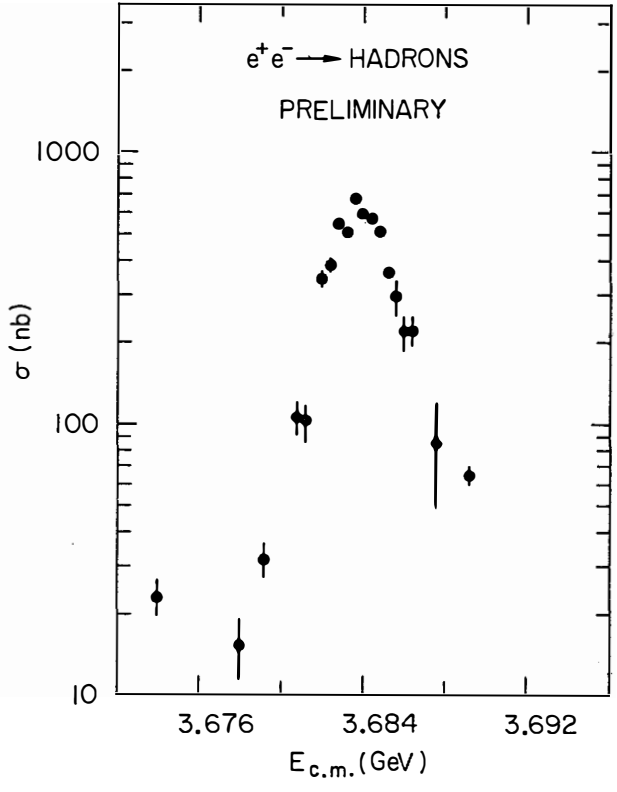

Fig. 2. The $\psi(3.7)$ resonance peak as defined by much higher luminosities per point. Some apparent fluctuations are due to a small current-dependency of the SPEAR beam energy width.

Although the e^+e^- decay mode of the ψ' was difficult to separate from the dominant t-channel Bhabha background, as well as from the ψ electron decay mode, the $\mu^+\mu^-$ mode was more easily isolated, as will be seen. Subtracting the QED background, the branching ratio to muons is found:

$$\frac{\Gamma(\psi' \rightarrow \mu^+\mu^-)}{\Gamma(\psi' \rightarrow \text{all})} \cong 0.005 \pm 0.003 \ .$$

If we assume μ-e universality and the spin assignment $J = 1$, then the widths are determined:

$$\Gamma_e(\psi') = 2.2 \pm 0.5 \text{ keV} \ ,$$

$$200 \text{ keV} < \Gamma(\psi') < 800 \text{ keV} \ .$$

The electron width determination is nearly independent of the lepton ratio, because the latter is so small, and the errors on Γ_e reflect just the uncertainty of $\int \sigma_{had} \, dW$. The large uncertainty in the limit on the total width comes about partly from the background subtraction, which is reflected in the $\mu^+\mu^-$ branching ratio, but also from the possible contribution due to interference with the QED amplitude. The presence or extent of the interference has not yet been investigated in detail experimentally. The expectation is to obtain a much more precise determination of these quantities when more data is collected. The position of the peak is known more accurately than originally, due to recalibration of a flip coil used to determine the SPEAR magnetic guide field. The new value is 3.684 ± 0.005 GeV. It should be noted that the ψ', although very narrow, seems to be markedly broader than the ψ.

Let us now examine in more detail the decay

$$\psi' \rightarrow \psi\pi^+\pi^- \ , \qquad (1)$$

the mode by which this cascade decay was discovered. From a sample of about 30,000 events, the missing mass distribution shown in Fig. 3 was obtained, showing conclusive evidence for decay (1). The branching ratio for decay by (1) was determined, after suitable efficiency corrections and background subtraction:

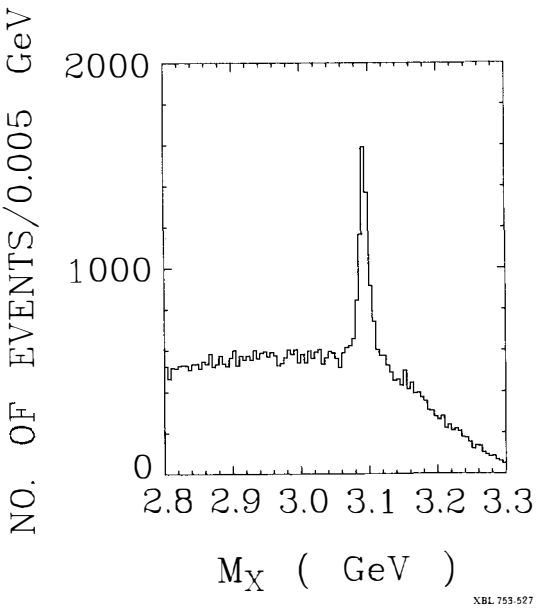

Fig. 3. Distribution of missing mass, M_X, opposite $\pi^+\pi^-$ in reaction (1). The peak corresponds to decays in which $X \equiv \psi(3.1)$.

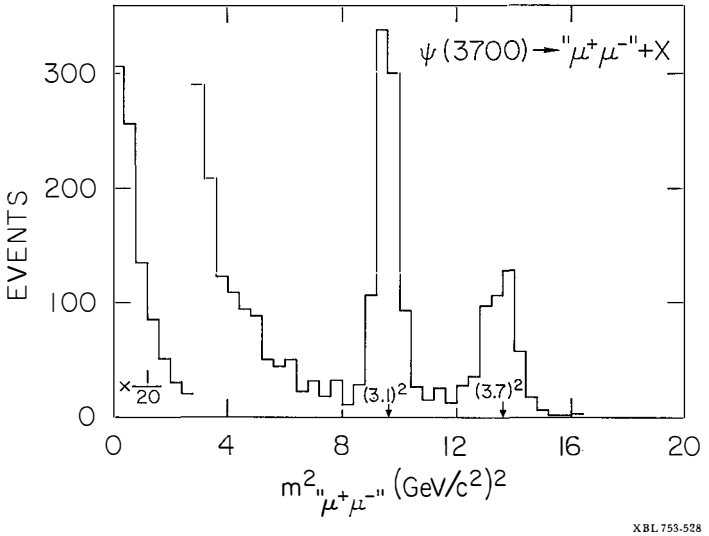

Fig. 4. Effective mass distribution of $\mu^+\mu^-$ arising from $\psi(3.7)$ decays. The muons pairs coming from $\psi(3.1)$ decay in the cascade decay (2) are well separated.

$$\frac{\Gamma(\psi' \rightarrow \psi\pi^+\pi^-)}{\Gamma(\psi' \rightarrow \text{all})} = 0.31 \pm 0.04 \ .$$

The branching ratio for the inclusive decay,

$$\psi' \rightarrow \psi + X \qquad (2)$$
$$\hookrightarrow \mu^+\mu^-$$

was also found, by isolating the muon pair decays of the ψ, and scaling by the known leptonic branching ratio of the ψ. Figure 4 shows the square of the effective $\mu^+\mu^-$ mass, and the events corresponding to ψ decay in (2) are clearly separated. Approximately 800 events correspond to reaction (2). Here, the highest momentum positive and negative particles have been chosen, and e^+e^- decays have been eliminated by requiring small pulses from the shower counters. The e^+e^- mode was not used for this purpose, due to the relatively large background from the radiative tail of the Bhabha scattering process. The result was:

$$\frac{\Gamma(\psi' \rightarrow \psi + \text{anything})}{\Gamma(\psi' \rightarrow \psi\pi^+\pi^-)} = 1.80 \pm 0.10 \ .$$

We expect the "anything" above to consist, at least partly, of $2\pi^o$, since $\pi^+\pi^-$ is observed (unless the pions are in an $I = 1$ state). The ratio above has the theoretical values 1.5, 1.0, and 3.0, for $\pi\pi$ isospin states of 0, 1, and 2, respectively (these become 1.52, 1.00, and 3.10 for uniform phase space when the $\pi^\pm/\pi^o$ mass difference is taken into account). Clearly isospin-zero is preferred, but the lack of good agreement may result from admixture of other final states.

Corresponding to the ratios presented above, there is the branching ratio of cascade decays to all ψ' decays:

$$\frac{\Gamma(\psi' \rightarrow \psi + \text{anything})}{\Gamma(\psi' \rightarrow \text{all})} = 0.54 \pm 0.08 \ .$$

It is of interest to look at the recoil mass against the ψ in reaction (2) as determined from the $\mu^+\mu^-$ decay, a relatively clean sample. As seen in Fig. 5, there is no peak at low mass indicating a decay of ψ' into a single low mass particle, such as a γ or π^o. The apparent absence of the single π^o cascade decay and the observed large branching ratio by two final

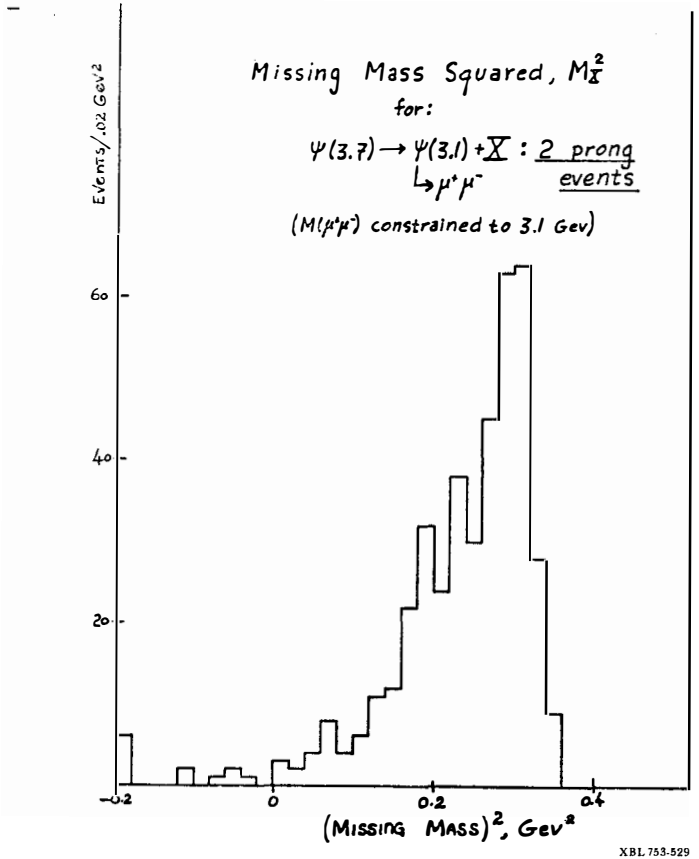

XBL 753-529

Fig. 5. Missing mass distribution for reaction (2). Note the absence of any peak at low mass.

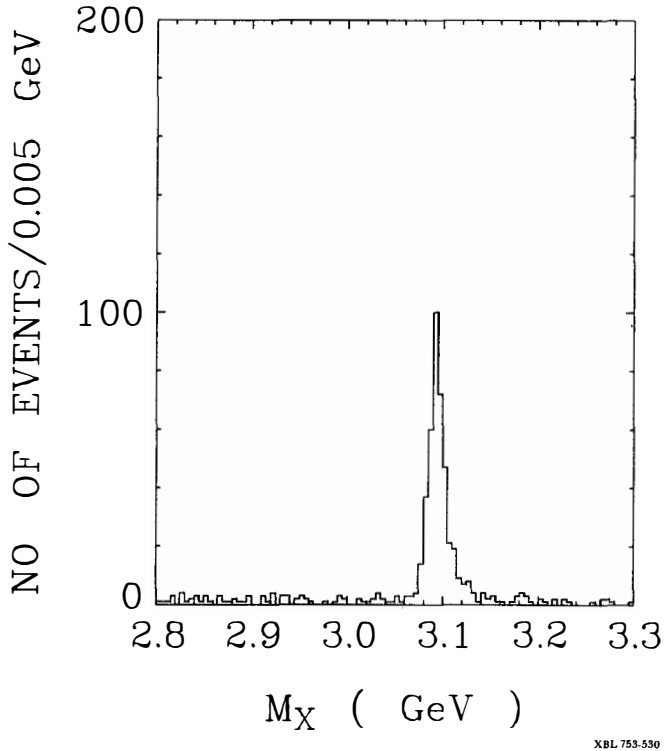

XBL 753-530

Fig. 6. Missing mass distribution similar to Fig. 3, but for the subset of events shown there which correspond to reaction (3) and in which the observed particles satisfy overall momentum-energy conservation, within measurement errors.

state pions in (1) indicates that the ψ and ψ' have the same G parity, and that G parity is, to a good approximation at least, preserved in the decay process.

A study was also made of the exclusive channel:

$$\psi' \rightarrow \psi\pi^+\pi^- \qquad (3)$$
$$\hookrightarrow \mu^+\mu^- \text{ or } e^+e^- \ .$$

Here, a selection of the ψ leptonic modes was made, and rather loose cuts imposed by energy-momentum conservation to insure that no particles were unobserved in the 4-prong event. Figure 6 shows the very clean sample which results, a subset of Fig. 3. The ratio between these samples in in good agreement with the known leptonic decay branching ratio of the ψ, which is about 14%. This sample, consisting of about 350 events, was used to study the final state distributions. That the decay (1) occurs predominantly through S wave is supported by the observed angular distribution for the 2π system, which is consistent with isotropy, and the distribution of leptons from ψ decay, which is consistent with $1 + \cos^2\theta$ (as well as with isotropy). Furthermore, the ψ angular distribution seems consistent with isotropy.

However, the $M(\pi^+\pi^-)$ plot (shown in Fig. 7) shows a rather strong suppression of low mass states, and this is not due to instrumental effects investigated thus far. In particular, it is not caused by a trigger bias against the low-momentum pions, since the analysis required the trigger to be satisfied by the ψ decay leptons alone. The inclusion of final state S-wave interaction does not appear to be sufficient to explain the observed distribution. Although the isotropic angular distribution suggests S-wave, higher angular momentum states cannot be excluded, and the interpretation of this mass distribution is still open at this time.

The present data sample and results of analysis of the ψ' is summarized in Table I. The principal conclusions which may be drawn at present, are that the $\psi(3.7)$ resembles the $\psi(3.1)$ in being a very narrow resonance for such a large mass, and it has comparable coupling to the e^+e^- state. However, it decays with a large branching ratio into the ψ, at a rate that

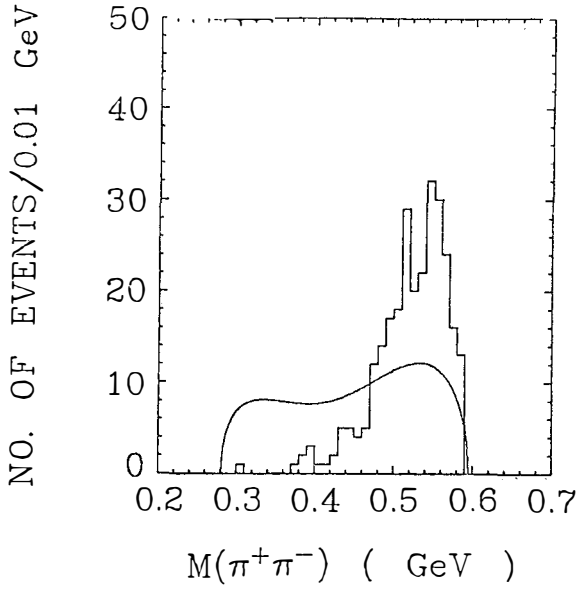

XBL 753-531

Fig. 7. Effective mass distribution of the $\pi^+\pi^-$ pair from reaction (3). The curve represents the prediction for uniform phase space corrected for detector acceptance.

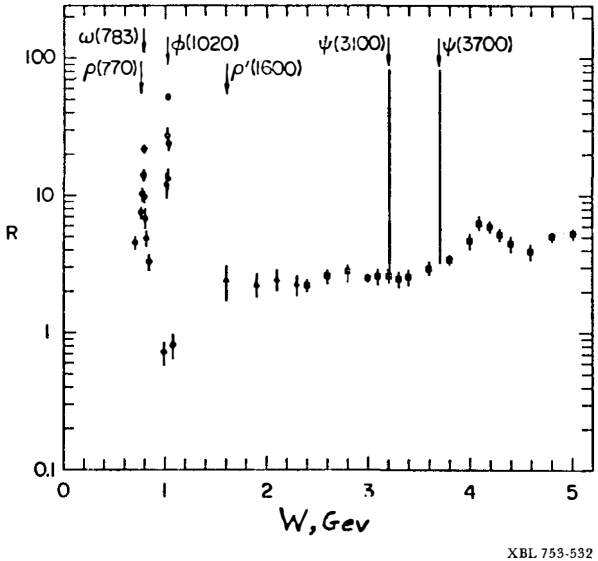

XBL 753-532

Fig. 8. Log plot of $R = \frac{\sigma_{total}(hadrons)}{\sigma_{QED}(\mu^+\mu^-)}$ vs total c.m. energy.

appears to be much less strongly suppressed than the direct decay into the more usual hadron final states. That this cascade decays via two pions, but not one pion, indicates that the ψ and ψ' have the same G quantum number, which appears to be odd as determined from analysis of ψ decays. The relative rates of decay of $\psi' \rightarrow \psi$ plus charged pions or undetected particles (neutrals) in the cascade decay seems to prefer an $I = 0$ final pion state, though this is an inference needing direct confirmation.

II. THE TOTAL CROSS SECTION AND THE ENHANCEMENT AT 4.1 GeV

Leaving aside now the very sharp ψ resonance peaks which are the most spectacular features of the SPEAR data, we should take a careful look into the "foothills" of the cross-section plot.[3]

First of all, let us look in Fig. 8 at the energy dependence of $R = \frac{\sigma_{tot}(\text{hadrons})}{\sigma_{QED}(\mu^+\mu^-)}$ on a log scale. This shows clearly the beautiful work done several years ago at Orsay in studies of the ρ, ω and φ, and the "average" values from Frascati at intermediate energies, where the overabundant production of hadrons first became evident. Following at higher energies are current SPEAR results showing the generally smooth behavior of R, relatively flat to about 3.6 GeV, then an enhancement whose exact nature is not yet clear, and finally at the highest energy values observed perhaps a leveling off of R. The "bump" appears much more striking on a linear scale in Fig. 9, where there is shown both R and σ_{total}. The measured values are generally spaced 0.2 GeV in $W(=\sqrt{s})$, the c.m. energy, although some data with finer resolution, 0.1 GeV, exists in the regions of the $\psi(3.1)$ and the 4.1 enhancement.

The prior descriptions of the sharp resonances did not discuss very much about backgrounds, corrections and other analysis details since the signal was so large as to render some of these corrections unnecessary (the non-annihilation background in the ψ region is at most about 0.1%). However, at the more civilized cross sections of 20-30 nb, the corrections are not negligible, and perhaps should be mentioned again briefly to present a

complete picture. The trigger requires at least two charged tracks within the $0.65(4\pi)$ sensitive solid angle coverage, where the efficiency for each track is well above 90% for high momentum tracks, but drops rapidly for momenta below 200 MeV/c. As described in the earlier paper, a hadron event was defined as having ≥ 3 tracks, or two tracks acoplanar by more than 20° with small pulse height (not electrons). These observed efficiencies and acceptances are incorporated in a Monte-Carlo program used to compute the average efficiencies per event as a function of number of charged particles. From these the true multiplicities were derived through a set of simultaneous equations, and the average detection efficiency, $\bar{\epsilon}$, also determined. It should be noted that these determinations use a model by which the Monte-Carlo events are generated, but the form of the model does not enter directly into the determination of $\bar{\epsilon}$. That $\bar{\epsilon}$ is quite insensitive to the model was verified by using three quite different models (including a jet model) which predicted values for $\bar{\epsilon}$ differing by only $\pm$ 5%.

Background due to beam gas interactions was determined from the longitudinal distributions of reconstructed vertices, which peak strongly in the interaction region. The subtraction for this background was $< 8\%$ at all energies. The contamination from photon-photon processes was measured using small-angle electron tagging counters (20 mrad), and was appreciable only in the two-prong events, varying between 8% and 3% from highest to lowest energies. For ≥ 3 prongs, this type of contamination was $2 \pm 2\%$.

The radiative tails due to the $\psi(3.1)$ and $\psi(3.7)$ were removed, and then the resulting cross-section values corrected for the nonresonant radiative effects.

The normalization for σ_{total} was the sample of Bhabha events collected concurrently, the validity of QED having been previously established in this energy range (except, of course, for the resonances).[5]

Aside from these corrections, an estimated point-to-point systematic uncertainty of 8% has been combined quadratically. Additional slowly varying systematic variations not included might exist at the 10%- 15% level, as

well as an uncertainty in absolute normalization of about 10%.

The principal structure seen in Fig. 9 is the peak at about 4.1 GeV, having a width of 250 - 300 MeV, and rising from a level of $\sim$ 18 nb outside the peak to $\sim$ 32 nb at the top. The integrated total cross section corresponding to the peak is about 5.5 nb-GeV, a value comparable to that of the ψ and ψ'. At present there is very little data available in the region of the 4.1 GeV enhancement, because cross sections in this region are relatively small, and no large amount of running has been done at this energy. Therefore, there are at the moment no significant results on decay modes from the peak region. However, a large amount of data does exist just below the peak at 3.8 GeV, and also above the peak at 4.8 GeV. Studies of this energy region are presently in progress, and no results are yet available. It is, of course, of great importance to understand this enhancement, whether as a resonance or a threshold effect, and particularly its possible relationship to the two ψ particles and the rise in R beginning at 3.6 GeV.

Table I. Preliminary Determination of Parameters of $\psi(3.7)$ Resonance.

Quantity	Value	Comment
Mass	3684 ± 5 MeV	
$\int \sigma_{had}\, dW$	3.7 ± 0.9 μb-MeV	
Partial decay width to ee pairs, Γ_e	2.2 ± 0.5 keV	Spin J = 1 assumed
Full width, Γ	200 keV $< \Gamma <$ 800 keV	

Major Decay Modes	Branching Ratio
$\psi(3.7) \rightarrow \psi(3.1)\pi^+\pi^-$	0.31 ± 0.04
$\psi(3.7) \rightarrow \psi(3.1)$ + anything	1.80 ± 0.10

G-Parity: Inferred to be the same as $\psi(3.1)$ due to above decay to $\psi(3.1)\pi\pi$, and apparent absence of $\psi(3.1)\pi$ mode. No determinations yet from direct (i.e., non-cascade) decays.

Spin: Inferred to be 1^-, due to production via e^+e^- annihilation. No determination yet from interference with QED amplitude.

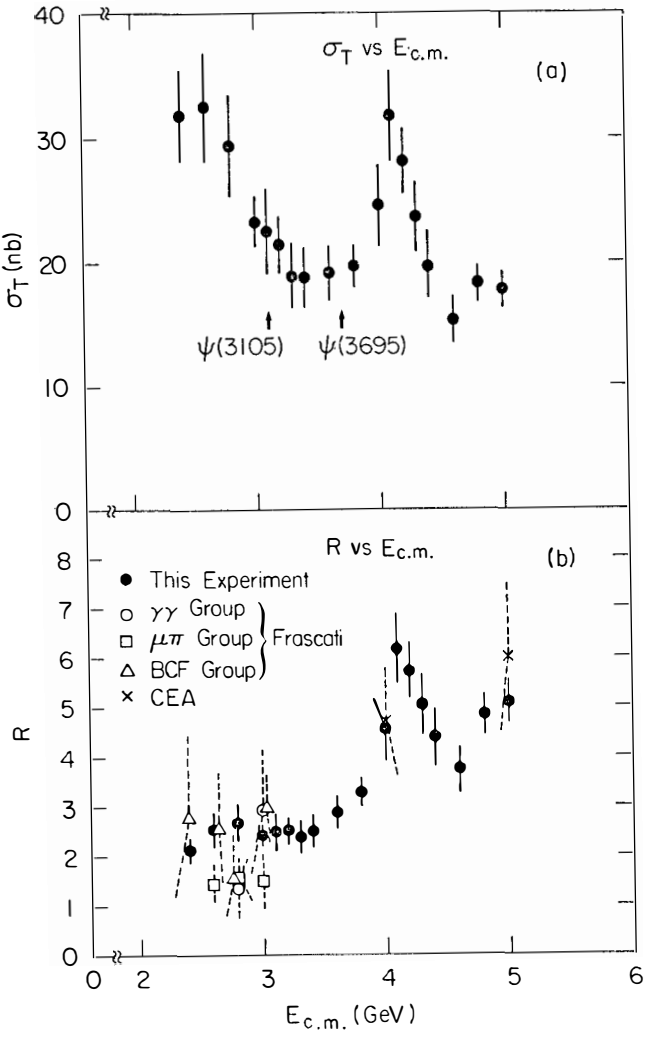

XBL 753-533

Fig. 9. (a) The total hadronic cross section, σ_T, vs c.m. energy, W. (b) $R = \sigma_T/\sigma_{QED}(\mu^+\mu^-)$ vs W. Corrections have been made for the radiative tails of the $\psi(3.7)$ and $\psi(3.1)$ resonances.

REFERENCES

1. A. M. Boyarski et al., Search for Narrow Resonances in e^+e^- Annihilation in the Mass Region 3.2 to 5.9 GeV, SLAC-PUB-1523 and LBL-3632, January 1975, submitted to Phys. Rev. Letters. Also, see previous talk by M. Breidenbach.
2. G. S. Abrams et al., Discovery of a Second Narrow Resonance in e^+e^- Annihilation, Phys. Rev. Letters 33, 1453 (1974).
3. G. S. Abrams et al., Observation of the Decay Modes $\psi(3.7) \rightarrow \psi(3.1)$ + Anything and $\psi(3.7) \rightarrow \psi(3.1)\pi^+\pi^-$, LBL-3369, March 1975, to be submitted for publication.
4. J.-E. Augustin et al., Total Cross Section for Hadron Production by Electron-Positron Annihilation Between 2.4 GeV and 5.0 GeV Center-of-Mass Energy, SLAC-PUB-1520 and LBL-3621, January 1975, submitted to Phys. Rev. Letters.
5. J.-E. Augustin et al., Phys. Rev. Letters 34, 233 (1975); B. L. Beron et al., Phys. Rev. Letters 33, 663 (1974).

Provisional Properties of the Ψ (3100) and Ψ (3700)

(March 9, 1975)

Quantity	Value	Comments
	Ψ (3100)	
Mass m	3095 ± 5 MeV/c^2	
Full width Γ	77 ± 20 KeV	
Partial width to electron pairs, Γ_e	5.2 ± 1.3 KeV	
Resonance strength $\int \sigma_h \, dE$	10.8 ± 2.7 nb - GeV	
Spin, parity, charge conjugation	$J^{PC} = 1^{--}$	This assignment is based on lepton pair angular distributions at resonance and a three standard deviation interference effect with electrodynamic lepton pair production.
Isotopic spin, G-parity	$I^G = (0)^-$	Based on relative abundance of states with even and odd numbers of pions on and slightly below resonance, and decay to $p\bar{p}$ and $\Lambda\bar{\Lambda}$.
	Ψ (3700)	
Mass	3864 ± 5 MeV/c^2	
Full width Γ	200 KeV $< \Gamma <$ 800 KeV	
Partial width to electron pairs, Γ_e	2.2 ± 0.5 KeV	Spin is assumed to be $J = 1$ for this determination
Resonance strength $\int \sigma_h \, dE$	3.7 ± 0.9 nb - GeV	Area of hadronic peak

Major decay mode :

$$\Psi(3700) \rightarrow \Psi(3100) + \pi^+ \pi^-$$

Branching ratios :

$$\frac{\Gamma(\Psi(3700) \rightarrow \Psi(3100) + \pi^+ \pi^-}{\Gamma(\Psi(3700) \rightarrow \text{all})} = 0.31 \pm 0.04$$

$$\frac{\Gamma(\Psi(3700) \rightarrow \Psi(3100) + \text{anything})}{\Gamma(\Psi(3700) \rightarrow \text{all})} = 0.54 \pm 0.08$$

$$\frac{\Gamma(\Psi(3700) \rightarrow \Psi(3100) + \text{anything})}{\Gamma(\Psi(3700) \rightarrow \Psi(3100) + \pi^+ \pi^-} = 1.80 \pm 0.90$$

THE EXPERIMENTAL PROGRAM AT DORIS AND A FIRST LOOK AT THE NEW RESONANCES

B.H.Wiik
Deutsches Elektronen-Synchrotron DESY
Notkestieg 1, 2 Hamburg 52, BD

Abstract: The present status of the DESY e^+e^- colliding ring DORIS and the experimental program is presented. Also the first preliminary results using the Double Arm Spectrometer (DASP) to investigate the properties of the new resonances will be given.

Résumé : La situation actuelle de l'anneau de collision DORIS e^+e^- de DESY et le programme expérimental sont présentés. On donne aussi les premiers résultats préliminaires du Spectromètre à deux bras sur les propriétés des nouvelles résonances.

THE EXPERIMENTAL PROGRAM AT DORIS AND A FIRST LOOK AT THE NEW RESONANCES

Electrons and positrons were injected and stored in the DESY colliding ring DORIS for the first time just before Christmas 1973. After less than a year of machine development the main parts of two large experiments - DASP and PLUTO - were installed and at the end of 1974 the first data on the narrow resonances at 3.1 GeV and 3.7 GeV became available. Early in February after collecting several ten thousands of events at these resonances PLUTO was replaced by the experiment of the DESY-Heidelberg-group.

In this talk I'll describe the present status of the accelerator and the experimental program. Also the first - rather preliminary results - using the Double Arm Spectrometer (DASP) will be given.

DORIS

Electrons and positrons from a 400 MeV linear accelerator are injected into the 7.5 GeV synchrotron and here accelerated to the proper energy for transfer to DORIS. DORIS is in the shape of an race track with two nearly independent rings stacked one above the other. The beams cross in the vertical plane in the middle of the two long straight sections. There is a twofold advantage in employing two rings instead of one:

Firstly, besides electron - positron also electron - electron or electron - proton collisions can be studied. Secondly, since the beams are separated except in the two interaction regions, many bunches can be used, in principle making it possible to reach very high luminosities.

Note, however, that the high circulating currents inherent to this scheme might cause severe background problems.

Although in principle CMS energies as high as 7 GeV can be reached with the present accelerator, all the data so far have been collected for energies between 3 GeV and 4.2 GeV. Upgrading the present magnet power supplies and installing all the available r.f. power in one ring, will make it possible to reach a CMS energy of 10 GeV. This is scheduled for 1976.

With the present optics the measured specific luminosity around 4 GeV can be written as $10^{31}\ I^2$ ($A^{-2}cm^{-2}sec^{-1}$) with the circulating current I measured in Amperes. This is in good agreement with the value of $1.2 \cdot 10^{31}$ ($A^{-2}sec^{-1}cm^{-2}$) predicted from the current optics. So far a luminosity of $10^{30}\ cm^{-2}sec^{-1}$ has been reached with stored currents of 0.3 - 0.4 Ampere in each beam. However, at these high currents, the energy spread in the

beam increases due to coherent synchrotron oscillations. These oscillations can be damped for currents less than 0.2 - 0.25 Ampere by a second r.f. transmitter turned slightly off the resonance frequency. Hence during the data taking at the 3.1 GeV and 3.7 GeV resonances, where a good mass resolution is imperative, the currents were limited to less than 0.25 Ampere corresponding to a maximum luminosity of 0.6×10^{30} $cm^{-2} sec^{-1}$.

Another important parameter is the size of the interaction volume. Due to the finite crossing angle and the high r.f. frequency used, the interaction "point" is around 2-3 cm long. The transverse dimensions are less than 0.6 mm.

The main parameters of DORIS are summarized in Table I.

Table I

Max.Energy:	7 GeV (9 GeV in the fall of 1975) (10 GeV during 1976)
Average Circulating current:	0.200 - 0.400 Ampere
Number of Bunches:	1 - 480
Average Luminosity:	$1 - 3 \times 10^{29}$ cm^{-2} sec^{-1}
Beam lifetime:	> 5 hrs
Gas pressure:	$1 - 5 \times 10^{-9}$ torr (depending on the current)
Interaction volume:	
along the beam	2 - 3 cm
transverse to the beam	< 0.6 mm

THE DETECTORS

So far data have been collected using three rather complementary detectors. The construction and the properties of these detectors will be discussed next.

PLUTO

PLUTO, the DESY 4π detector, is shown in Fig. 1 viewed along the beam direction. The main component of the detector is a superconducting solenoid 1.15 m long and 1.4 m in diameter. The magnetic field is parallel to the beam axis; the field strength is 2 Tesla. The magnetic field volume is filled with proportional chambers divided into an inner and outer part by a set of 24 plastic counters located at a radius of 20 cm. The inner detector covers a solid angle of 94%, the outer detector 88% of 4π. In the

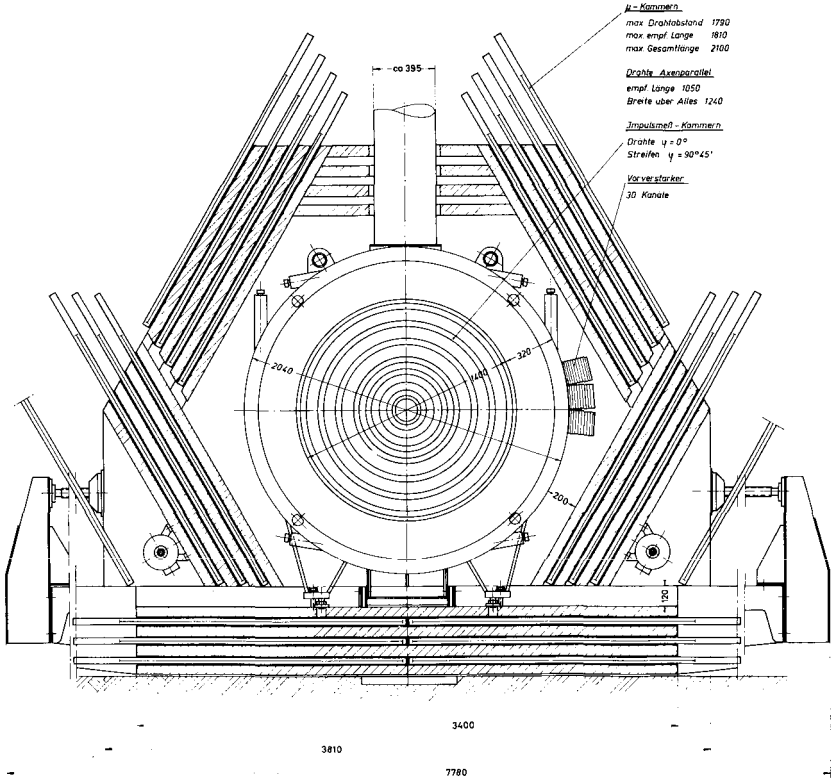

Fig.1

PLUTO viewed along the beam axis

outer detector 10 chambers are foreseen, each having one plane of wires parallel to the beam direction. Also the signals induced on the high voltage electrodes are read out. The high voltage electrodes consist of strips, 16 mm wide, with dip angles of $\pm$ 45° with respect to the signal wires. At a radius of 37.5 cm, a lead cylinder 0.35 of a radiation length thick is inserted. Between the beam tube and the scintillation counter 4 proportional chambers with only ϕ read out are mounted. The fast signals from the proportional chambers are fed to a hard wired dataprocessor, which reconstructs the tracks emerging from the interaction point. This makes it feasible to trigger the system on well defined tracks and reject beam-gas and cosmic ray events on line.

In the iron return yoke of the solenoid two layers of proportional tube chambers for identifying muons can be inserted. These chambers cover production angles between 73° and 107° with essentially 2π in azimuth.

For these first measurements the detector was completely installed except for the plastic counters and a few of the proportional chambers.

THE DESY-HEIDELBERG-DETECTOR

The basic layout of the apparatus used by the DESY-Heidelberg group is shown in Fig. 2. The apparatus has a cylindrical inner part surrounding the beam pipe made out of two sets of scintillation counters and three drift chambers. Each drift chamber has one signal plane which determines the azimuthal coordinate to an accuracy (σ) of 0.1 mm. This corresponds to an angular resolution of 4 mrad in ϕ. The axial coordinate is fixed by the signal induced on the cathode strips. The resulting resolution in θ is 20-30 mrad. In front of the last drift chamber is a cylinder-shaped container, which can be filled with 2 radiation lengths of mercury. The inner detector covers production angles between 30° and 150° for all azimuthal angles. To the right and left of the inner detector NaI and lead glass counters, 6.1 and 7.6 of a radiation length thick respectively, cover 25% of 4π. The counters are followed by iron plates 60 cm thick and drift chambers to separate muons from hadrons and electrons. Above and below the beam pipe the outer detector covers more than 25% of 4π. It is made of lead glass counters and iron absorbers.

This set up has a good on line rejection of background events and is capable of separating hadrons, electrons and muons over a large solid angle. Another strong virtue of the detector is the excellent energy resolution for photons down to a few hundred MeV. The measured energy resolution is

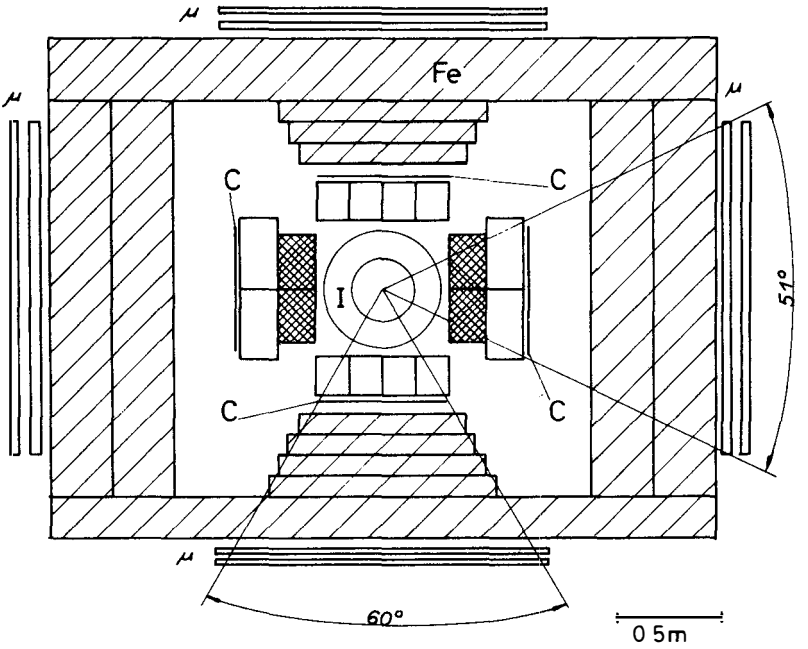

▩ - NAJ - Crystal

▭ - Lead glass counters

C - Anti Cosmic counters

μ - Chambers

I - Inner detector

2 - Scintillator hodoscopes

3 - Driftchambers with cathode reade out

1 - Hg-Converter 2 X_0 thick

Fig. 2

The DESY-Heidelberg detector viewed along the beam axis

on the order of 15% (FWHM) at an incident energy of 500 MeV decreasing to 10% at 1 GeV.

DASP

A schematic drawing of DASP viewed along the beam direction is shown in Fig. 3. The main component of the detector is two large H-magnets, positioned symmetric with respect to the interaction point and spaced 2.1 m apart.

The geometric acceptance of the magnet is from 48° to 132° in production angle and $\pm 9^{\circ}$ in azimuth resulting in a solid angle of 2 x 0.45 sterad for both magnets. The acceptance for a charged particle is smaller than the value listed above and depends on the momentum, the field strength and last detector plane required. The maximum field strength is 1.1 Tesla, the integrated field length 1.8 Tm.

A charged particle emerging from the interaction point traverses the following detectors before reaching the magnet gap: a scintillation counter adjacent to the beam pipe, a second scintillation counter which starts the time of flight measurement, two proportional chambers (3 planes in each chamber, 2 mm wire spacing) a third scintillation counter used for triggering and a wire spark chamber with magnetostrictive readout (2 planes, 1 mm wire spacing).

The momentum of a charged particle is determined from the measurement of one space point on the trajectory in front of the magnet and the knowledge of the trajectory of the particle behind the magnet. The trajectory behind the magnet is measured by 6 wire spark chambers (each has 2 signal planes, 1 mm wire spacing, 5.6 by 1.7 m^2 sensitive area). At the present a resolution of $\pm$ 1.4% is reached for a particle with 1.5 GeV/c momentum and with the magnet at 2/3 of its full excitation.

The particles are identified using time of flight, shower and range information:

The time of flight counters are mounted behind the spark chambers at an average distance of 4.7 m from the interaction point. The measured time of flight resolution is 0.5 nsec FWHM averaged over the 31 elements in one arm. This makes it feasible to separate pions and kaons for momenta less than 1.8 GeV/c, and kaons and protons for momenta less than 3 GeV/c, by time of flight alone. The hadrons and muons are separated from the electrons by the pulse height in the shower counters. These counters are

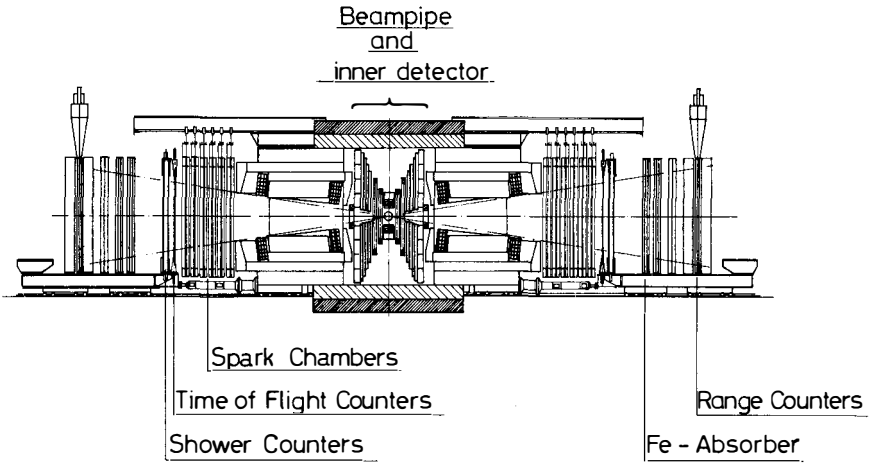

Fig. 3

DASP viewed along the beam direction

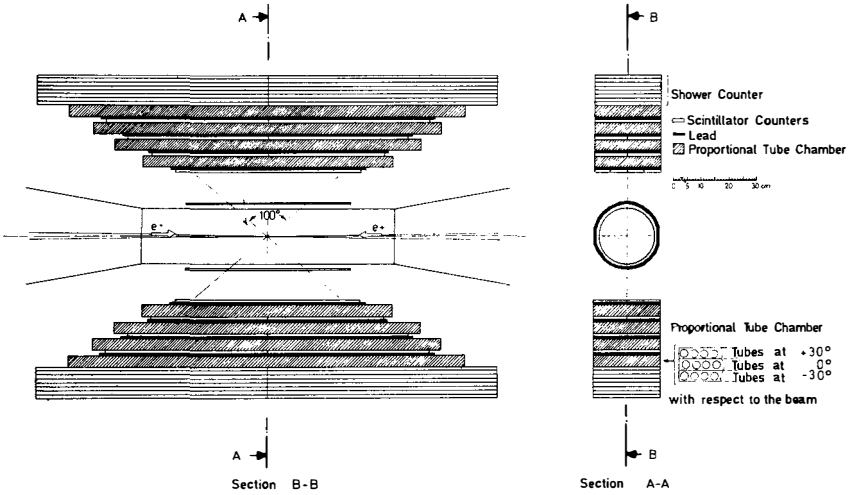

Fig. 4

Part of the inner detector used in the first experiments

made of alternating sheets of lead and scintillator, a total of 6.2 radiation lengths thick. For an incident particle with a momentum of 1.5 GeV/c the cut in the shower pulse height can be made such that 80% of the pions but only 10^{-3} of the electrons have pulse heights below the cut, that is, an electron rejection in the pion signal of 10^{-3} in one arm.

The muons are positively identified by their range. The absorbers in the range telescope are made of iron a total of 90 cm thick, subdivided into plates of different thickness in order to allow for an optimal pion/muon separation at a given momentum. After each plate sufficient space for either a scintillation counter hodoscope or a spark chamber is provided. The data were taken with one wall of scintillators at a depth of 70 cm in the iron.

The inner detector, made out of proportional chambers, scintillation counters, proportional tube chambers, and shower counters, is located in the free space between the magnets. This part of the detector - when completed - will cover 85% of 4π and is well suited for a measurement of the direction and energy of photons and also the direction, and in some cases, the energy of charged particles. For these first measurements, only the part mounted above and below the beams pipe and the four proportional chambers adjacent to the beam pipe were installed. During the course of the experiment the large shower counters attached to the magnet were also installed.

The part of the detector used in the first experiment is shown in more detail in Fig. 4. With this detector, events with production angles between 35° and 145° are accepted in a total solid angle of 1.4 sterad. The basic unit is made of a scintillation counter hodoscope, a sheet of lead 5 mm thick, and a proportional tube chamber. Each chamber has three layers of brass tubes, 10 mm in diameter and with 0.25 mm wall thickness, oriented at 0° and $\pm 30^{\circ}$ with respect to the beam axis. The measured efficiency for detecting one charged particle is 95% per plane, a value consistent with the geometric efficiency. A particle emitted in the direction of this detector first traverses one of the 22 scintillation counters surrounding the beam pipe, then four of the units just described, and finally a lead-scintillator shower counter eight radiation lengths thick. The rest of the inner detector, constructed like the part just described, will be completed during the summer of 1975.

EXPERIMENTAL RESULTS

Soon after the initial discovery [1] of the new resonances at BNL and SLAC an effort to confirm these results were made at DORIS. DASP searched in the twobody and inclusive channels and PLUTO in the total cross section. After a brief search the resonances were found [2] at the masses and with the widths listed below:

3.1 GeV state: $M = 3090$ MeV

$\sigma_w = 0.96 \pm 0.15$ MeV

3.7 GeV state: $M = 3680$ MeV

$\sigma_w = 1.04 \pm 0.15$ MeV

The measured widths are all consistent with the values expected from the energy spread in the beams alone and are hence only upper limits to the real widths of the particles. The masses were determined from the nominal energy of the colliding electrons and positrons. These values are uncertain a few MeV due to errors in the magnetic field measurements and to uncertainty in the position of the orbit in the accelerator.

After this initial search, the main emphasis at DORIS has been on investigating these resonances in more detail. Some preliminary results of these measurements using DASP [3] will be discussed below.

$e^+e^- \to e^+e^-$

In Fig. 5 the dependence on the total energy of the yield of e^+e^- scatters between 40° and 140° is plotted. A peak centered at 3090 GeV is clearly seen. The angular distributions (summed over θ and $\pi-\theta$) are plotted in Fig. 6 for energies outside and inside the peak. The absolute cross sections in Figs. 5 and 6 have been determined by fitting the distribution outside the peak to the nonresonant Bhabha scattering differential cross section corrected for bremsstrahlung and higher order radiative effects [4]. Since the energy spread in the beams is much larger than the natural width of the resonance the interference with nonresonant scattering will effectively cancel for energies close to the peak. The angular distribution for the decay of the 3.1 particle into e^+e^- pairs is thus obtained by subtracting the theoretical Bhabha scattering cross section from the angular distribution neasured in the peak. A fit of the form $1 + b\cos^2\theta$ gives $b = 1.1 \pm 0.6$ in agreement with $b = 1$ as expected for a spin 1 particle decaying into lepton pairs.

Assuming a $1 + \cos^2\theta$ distribution and integrating over the resonance we obtain:

$$\int \sigma(E)\, dE = (965 \pm 141)\ \text{nb} - \text{MeV}.$$

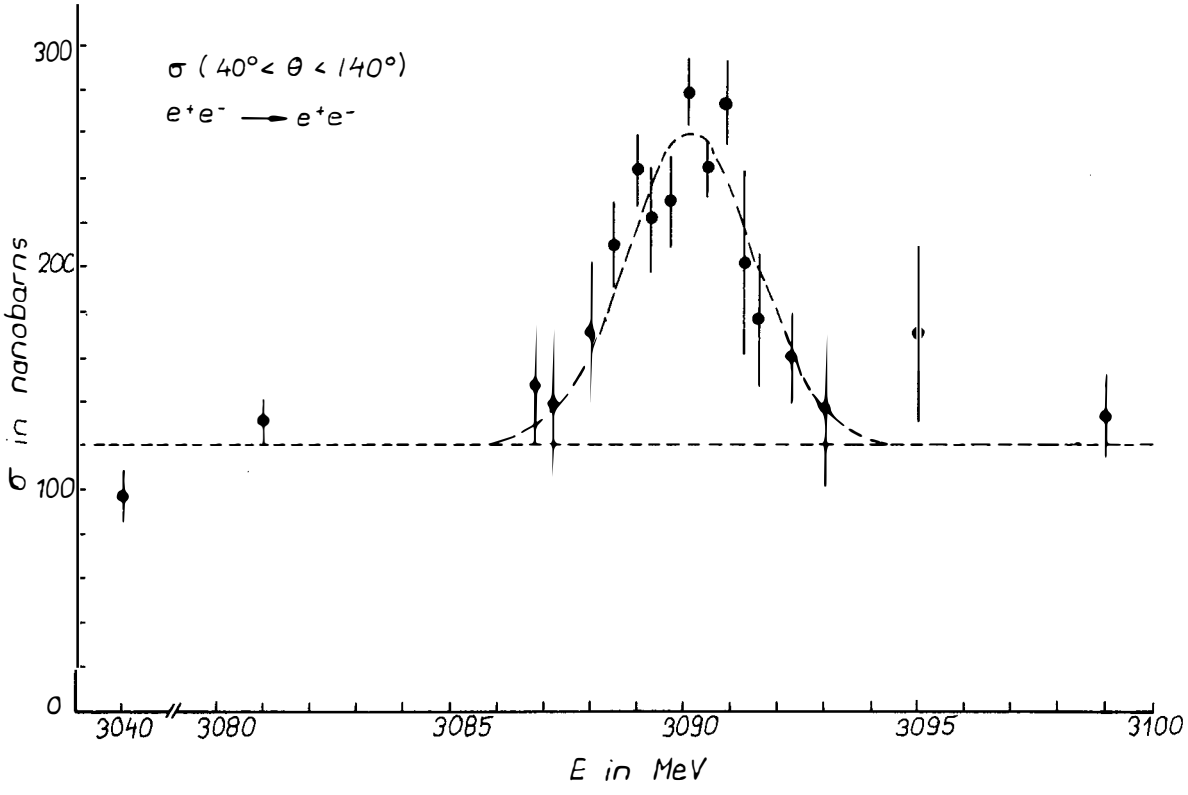

Fig.5

The observed e^+e^- scattering cross section for $40^\circ < \theta < 140^\circ$ plotted against the total energy. The dashed lines show the best fit Gaussian plus nonresonant background

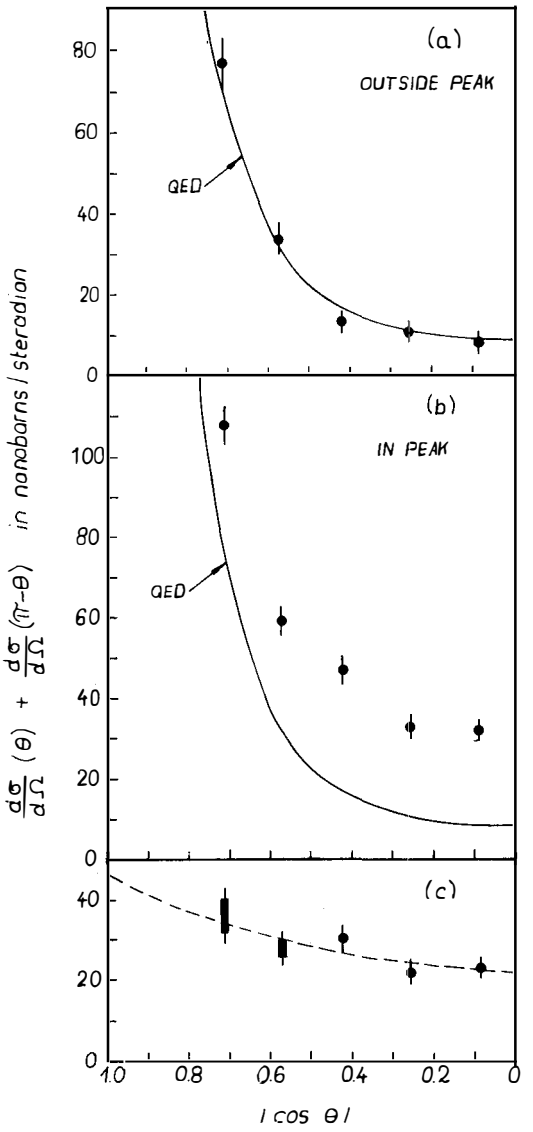

Fig.6

a) Angular distribution of the e^+e^- scatters for energies outside the peak

b) Angular distribution of the e^+e^- scatters for energies in the peak ($3089 \leq E \leq 3091$ MeV) The solid line is the nonresonant Bhabha scattering cross section

c) Angular distribution of the e^+e^- from the decay of the resonance. The dashed line is a best fit to the form $1 + \cos^2\theta$.

This value has been corrected for radiative effects according to the prescription given by Yennie [5]. The cross section integral can be related to the mass and decay widths of the resonance:

$$\int \sigma(E)\, dE = \frac{6^2}{m^2} \cdot \frac{\Gamma_{ee}^2}{\Gamma_{tot}} .$$

Using the value for the integral listed above:

$$\frac{\Gamma_{ee}^2}{\Gamma_{tot}} = (0.41 \pm 0.06) \text{ keV}$$

LIMITS DERIVED FROM $e^+e^- \to \gamma\gamma$

The cross section for observing two collinear or nearly collinear photons has been measured using the inner detector for CMS energies around the 3.1 GeV and 3.7 GeV resonances. A measurement at the 3.1 GeV resonance, based on fewer than a half of the present events has already been published [6]. The selection criteria used to extract $\gamma\gamma$ events and the various corrections to the data are discussed in that publication.

Collinear photons are produced in the two photon annihilation $e^+e^- \to \gamma\gamma$. The cross section for this reaction can be computed from QED and decrease smoothly as $1/E^2$ with increasing energy. Superimposed on this smoothly decreasing cross section there might be a peak due to any of the following reactions:

1) $e^+e^- \to$ resonance $\to \gamma\gamma$

This decay is strictly forbidden for a spin 1 state. It is allowed for all other values of the spin provided C is even or not converved.

2) $e^+e^- \to$ resonance $\to \pi^0 \gamma$

In this case there will always be two photons collinear to within an angle m_π/E. If the second photon from the π^0-decay is not detected the event will look like a two photon event.

3) $e^+e^- \to$ resonance $\to X\,\gamma$, $X \to \gamma\gamma$

The resonance decays with the emission of a single photon into a heavy particle X which in turn decays into two photons. If the mass m_x is close to that of the resonances (3.1 GeV or 3.7 GeV) X will be produced nearly at rest and the two photons will be nearly collinear.

The measured cross section for collinear photons at CMS energies around the 3.1 GeV resonance is shown in Fig. 7a, and for all photon pairs in

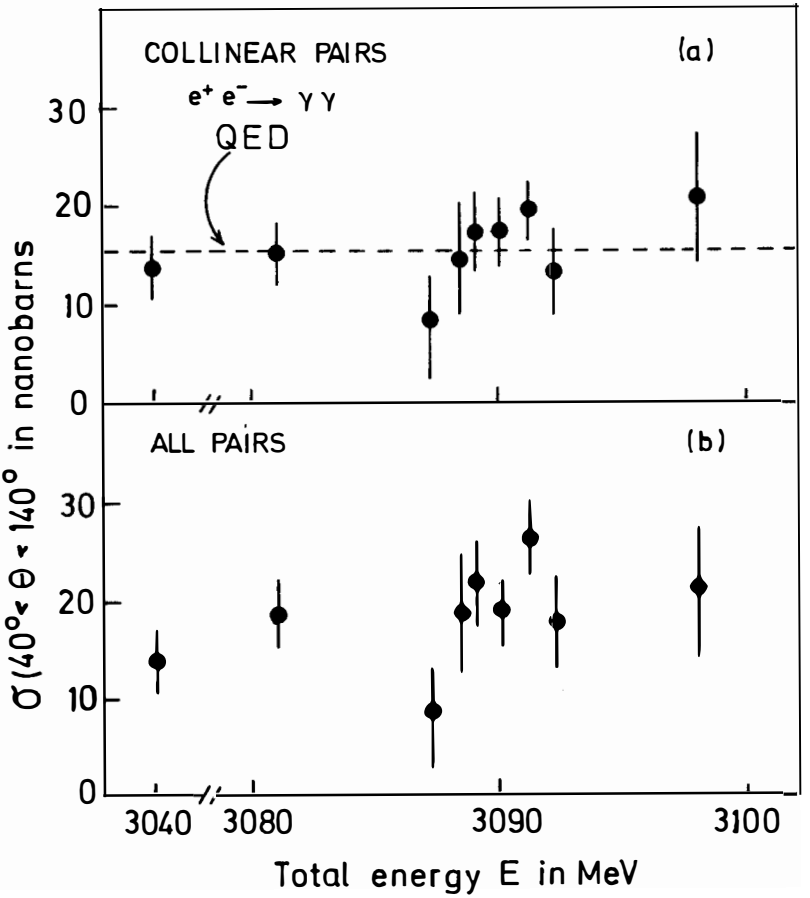

Fig 7

The observed cross section for $e^+e^- \to \gamma\gamma$ as a function of the CMS energy around 3.1 GeV:

a) collinear photons

b) without the collinearity requirement

Fig. 7b.

The cross section for the collinear pairs is consistent with the theoretical cross section obtained from QED including radiative corrections [7]. Fitting the data with a nonresonant background plus a Gaussian peak with mass and width as observed in the e^+e^- scattering data, an upper limit (90% confidence) is derived for the decay of the resonance into two photons:

$$\int \sigma_{\gamma\gamma}(E)\, dE < 34 \text{ nb} - \text{MeV}.$$

Using the measured value of Γ_{ee}^2/Γ we find:

$$\Gamma_{\gamma\gamma} / \Gamma_{ee} < 0.035.$$

From a similar fit to all photon pairs, without a cut in the collinearity angle, limits on

$$3.1 \to \pi^o\gamma \quad \text{and} \quad 3.1 \to X\gamma \quad \text{(with } X \to \gamma\gamma\text{)}$$

are set.

We find:

$$\int \sigma_{\pi^o\gamma}(E)\, dE < 121 \text{ nb} \cdot \text{MeV}$$

or

$$\Gamma_{\pi^o\gamma} / \Gamma_{ee} < 0.13.$$

Since the detection efficiency for $X \to \gamma\gamma$ decreases with decreasing mass m_x of X, the search for X is only sensitive for m_x between 2.6 GeV and 3.1 GeV. Ih this range we find:

$$\left(\frac{\Gamma_{3.1 \to X\gamma}}{\Gamma_{ee}}\right)\left(\frac{\Gamma_{X \to \gamma\gamma}}{\Gamma_{X \to \text{all}}}\right) < 0.13 - 0.24.$$

The measured cross section for CMS energies around the 3.7 GeV resonance is shown for collinear photons in Fig. 8a, and for all photon pairs in Fig. 8b. No clear peak is seen at the mass of the resonance and the collinear photons are well fit by QED alone.

From the collinear photons, the limit on the two photon decay of the 3.7 GeV resonance can derived. We find:

$$\int \sigma_{\gamma\gamma}(E)\, dE < 32 \text{ nb} - \text{MeV}.$$

From a fit to all the photon pairs, without a cut in the collinearity angle, the limit on $3.7 \to \pi^o\gamma$ is found:

$$\int \sigma_{\pi^o\gamma}(E)\, dE < 76 \text{ nb} - \text{MeV}.$$

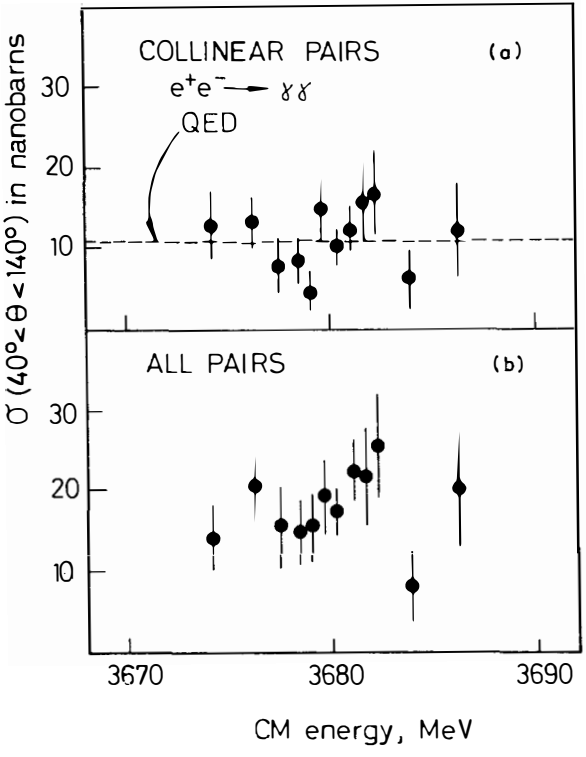

Fig. 8

The observed cross section for $e^+e^- \to \gamma\gamma$ as a function of the CMS energy around 3.7 GeV:

a) collinear photons

b) without the collinearity requirements

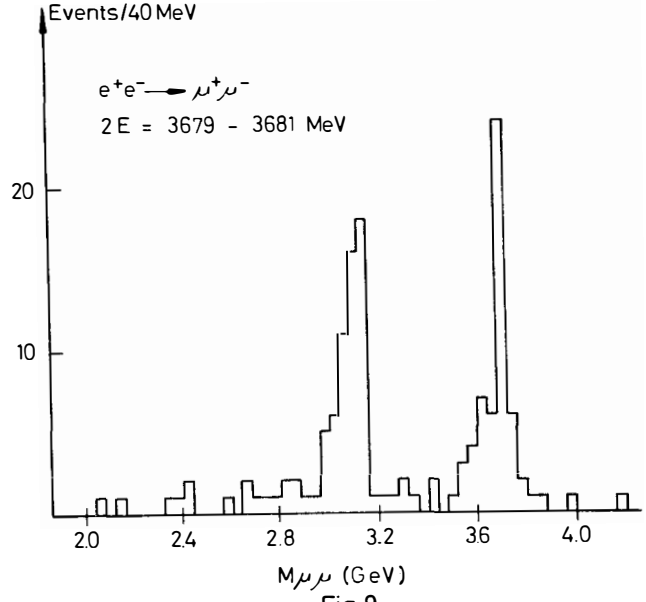

Fig. 9

The yield of muon pairs, produced at the 3.7 GeV resonance, is plotted as a function of the pair mass.

The limit on $3.7 \to X\gamma$ ($\to \gamma\gamma$) varies between 76 nb - MeV and 152 nb - MeV for 3.1 GeV < M < 3.7 GeV.

$e^+e^- \to$ resonance $\to \eta\gamma$

Using the inner detector the decay of the resonances into $\eta\gamma$ has been investigated using the 2γ decay mode of the η. Demanding an all neutral final state with exactly 3 coplanar photons eliminated the much more abundant beam-gas, cosmic ray and multihadron events. Note that the kinematic is completely determined by a measurement of the direction of the three photons. In particular, possible π^0 and η' events are excluded using the opening angle and invariant mass of the secondary photons.

At the 3.1 GeV resonance 3 events are found. This allow us to put the limit 0.1 keV < $\Gamma_{\eta\gamma}$ < 2.0 keV for the decay $3.1 \to \eta\gamma$.

A search for $3.7 \to \eta\gamma$ failed to yield any events. The 90% confidence limit for this decay is:

$$\Gamma_{ee} \cdot \frac{\Gamma_{\eta\gamma}}{\Gamma} < 0.025 \text{ keV}.$$

$e^+e^- \to \mu^+\mu^-$

Muon pair production has been investigated for CMS energies around the 3.1 GeV resonance with the magnetic part of the spectrometer. The muon pairs were identified using the following criteria:

1) The geometrical reconstruction required one track of opposite charge in each spectrometer arm collinear to within 0.15 rad.
2) The production vertex was within $\pm$ 5 cm of the nominal interaction point. These criteria selected pair events. To positively identify the muons it was required that:
3) At least one range counter had fired.

Further cuts on time of flight, track momenta and vertex positions were not needed since the distribution of events along the beam direction proved that the background from cosmic rays and beam gas interactions were already negligible. A study of events where the range counters on both, on one or on neither side fired revealed that the contamination due to hadron pairs was also completely negligible.

Since a full account of this experiment can be found in the literatur [8] let me just list the main results:

1) The angular distribution of the muons for $|\cos\theta| \leq 0.6$ is consistent with $1 + \cos^2\theta$ as expected for a spin one particle decaying into two leptons.
2) Within the errors no forward - backward asymmetry is observed, the experimental number is:

$$\frac{F - B}{F + B} = 0.01 \pm 0.11$$

3) Assuming a $1 + \cos^2\theta$ angular distribution we find

$$\int \sigma_{\mu\mu}(E)\, dE = (1240 \pm 230)\ \text{nb} - \text{MeV}.$$

This leads to

$$\frac{\Gamma_{\mu\mu} \cdot \Gamma_{ee}}{\Gamma_{tot}} = (0.51 \pm 0.09)\ \text{keV}$$

consistent with the value found for $\Gamma_{ee}^2 / \Gamma_{tot}$.

$e^+e^- \rightarrow h^+h^-$

The good particle identification properties of DASP makes it possible to measure the cross sections for pion and kaon pairproduction. To select these events and to separate them from the muon and electron pairs, the following criteria were used:

1) Pairs selected using criteria 1 and 2 of the section above
2) Momentum of the track should be within $\pm$ 50 MeV of the nominal momentum.
3) Pulseheight in the shower counters should be less than 4 times the most probable value for a minimum ionizing particle.
4) No range counter fired.

At the 3.1 GeV resonance no events that satisfied the criteria above were found. The 90% confidence limits are:

$$\Gamma_{\pi^+\pi^-} / \Gamma_{\mu^+\mu^-} < 0.004$$

$$\Gamma_{K^+K^-} / \Gamma_{\mu^+\mu^-} < 0.008$$

The reaction $e^+e^- \to p\bar{p}$ was identified using the same criteria except:

1) The momentum of the track should be between 1140 MeV/c and 1260 MeV/c.
2) No cut on the pulseheight in the shower counter for the negative track was made.

We find 15 $p\bar{p}$ pairs which satisfy these criteria. To evaluate the branching ratio, however, the angular distribution must be known. Since this is not the case, we list the width for three possible angular distributions:

$$\Gamma_{p\bar{p}} / \Gamma_{\mu^+\mu^-} = (0.034 \pm 0.007) \text{ assuming } 1 + \cos^2\theta$$
$$= (0.023 \pm 0.006) \text{ assuming constant}$$
$$= (0.016 \pm 0.004) \text{ assuming } \sin^2\theta$$

$e^+e^- \to 3.7 \to 3.1\ X$

In Fig. 9 the yield of muon pairs produced at the 3.7 GeV resonance is plotted as a function of the effective mass of the pair. Centered at 3.7 GeV a peak resulting from the direct decay of the 3.7 GeV resonance is seen. Superimposed on its radiative tail there is a second peak at 3.1 GeV. This peak results from the charakteristic muon decay of the 3.1 GeV resonance and clearly demonstrates the decay mode $3.7 \to 3.1 + X$. The possible decay modes X are: $\pi^+\pi^-$, $\pi^o\pi^o$, η, $2\pi^+\pi^-$, $2\pi^o\pi^o$, $\gamma_1\gamma_2$ (via an intermediate state P_c). To investigate the cascade decay, events were selected for which the magnetic part of the detector showed a $\mu^+\mu^-$ pair with an effective mass between 2.9 and 3.2 GeV. 67 events were found. For these events, the missing mass recoiling against the $\mu^+\mu^-$ pair was computed from the known muon momenta assuming that all were due to the decay of the 3.1 GeV resonance. Finally the inner detector was examined for evidence of photons or charged particles.

The result of this search can be summarized as follows:

1) No candidates for $2\pi^+\pi^-$ or $2\pi^o\pi^o$ were found.

2) The two photons from the chain decay $3.7 \to P_c\ \gamma_1 \to (3.1\gamma_2)\ \gamma_1$ are nearly uncorrelated. A sizable fraction of these decays will therefore have an effective mass below $2m_\pi$ as determined from the momentum of the muon pairs. No such events have been found, leading to an upper limit (90%) for the decay via an intermediate state P_c.

$$\frac{3.7 \to P_c\ \gamma_1 \to (3.1\ \gamma_2)\gamma_1}{3.7 \to 3.1 \cdot \text{all}} < 0.13.$$

3) The decay $3.7 \to 3.1\ \pi^+\pi^-$ is clearly seen. The branching ratio is found to be

$$\frac{3.7 \to 3.1\ \pi^+\pi^-}{3.7 \to 3.1\ \text{all}} = 0.58 \pm 0.15$$

This value is in good agreement with 0.54 ± 0.06 measured [10] at SPEAR.

4) The $\pi^o\pi^o$ decay mode is established by the observation of events with masses m_x between $2m_\pi$ and the mass of the η, where photons, but no charged particles are seen in the inner detector.
The ratio

$$\frac{3.7 \to 3.1\ \pi^o\pi^o}{3.7 \to 3.1\ \pi^+\pi^-}$$

will be 1/2, 0 or 2 for the isospin of the pion pair 0, 1 or 2 respectively. The ratio found is consistent with I = 0.

5) There is also evidence for the decay $3.7 \to 3.1\ \eta$. This is based on the observation of events at the mass of the η where photons and charged particles are seen in the inner detector. This observation is supported by events of the type $3.7 \to 3.1\ \gamma\gamma$ with the effective mass of the $\gamma\gamma$-pair near the mass of the η.

References

1) J.J.Aubert et al.
Phys.Rev.Letters 33 (1974) 1404

J.E.Augustin et al.
Phys.Rev.Letters 33 (1974) 1406

2) DASP Collaboration
Phys.Lett. 53B (1974) 393

L.Criegee et al.
Phys.Lett 53B (1974) 489

3) The following Institutions and physicists are involved in the DASP-collaboration:
W.Braunschweig, C.L.Jordan, U.Martyn, H.G.Sander, D.Schmitz, W.Sturm, and W.Wallraff - I.Physikalisches Institut der RWTH Aachen,

K.Berkelman, D.Cords, R.Felst, E.Gadermann, G.Grindhammer, H.Hultschig, P.Joos, W.Koch, U.Kötz, H.Krehbiel, D.Kreinick, J.Ludwig, K.-H.Mess, K.C.Moffeit, D.Notz, G.Poelz, K.Sauerberg, P.Schmüser, G.Vogel, B.H.Wiik, and G.Wolf - Deutsches Elektronen-Synchrotron DESY and II. Institut für Experimentalphysik der Universität Hamburg, Hamburg,

G.Buschhorn, R.Kotthaus, U.E.Kruse, H.Lierl, H.Oberlack, S.Orito, K.Pretzl, and M.Schliwa - Max-Planck-Institut für Physik und Astrophysik, München,

T.Suda, Y.Totsuka, and S.Yamada, University of Tokyo, Tokyo.

4) F.A.Berends, K.F.Gaemers, and R.Gastmans
Nucl.Phys. B68 (1974) 541

5) D.R.Yennie
Phys.Rev.Letters 34 (1975) 239

6) DASP Collaboration
Phys.Lett. 53B (1975), 491

7) F.A.Berends and R.Gastmans,
Nucl.Phys. B61 (1973) 414

8) DASP Collaboration - to be published in Phys.Lett.

9) G.S.Abrams et al.
LBL - 3669, SLAC-PUB-1556

STATUS REPORT ON ψ (3.1 GeV) RESONANCE FROM ADONE

presented by

G. Penso

Istituto di Fisica dell'Università di Roma and Istituto Nazionale di Fisica Nucleare, Sezione di Roma (Italy)

and

M. Piccolo

Laboratori Nazionali di Frascati del CNEN, Frascati (Italy)

ABSTRACT

The present status of the Adone results on the ψ (3.1 GeV) resonance is reported. Channels $e^+e^- \rightarrow$ multihadrons, e^+e^-, $\mu^+\mu^-, \pi^0\gamma, \eta\gamma, \gamma\gamma$ have been studied. Preliminary results are reported on a search for possible narrow resonance at lower energies.

RÉSUMÉ

Les résultats sur la résonance ψ(3.1 GeV) obtenus jusqu'à présent à Frascati sont passés en revue. Les réactions $e^+e^- \rightarrow$ $\rightarrow$ multihadrons, e^+e^-, $\mu^+\mu^-$, $\pi^0\gamma, \eta\gamma, \gamma\gamma$, ont été étudiées. Les résultats préliminaires sur la recherche d'éventuelles résonances étroites à plus basse énergie sont rapportés.

$B\bar{B}$ group

G. Barbiellini and G. Nicoletti
Laboratori Nazionali di Frascati del CNEN - Frascati (Roma)

G. Barbarino, M. Castellano, F. Cevenini, G. Di Giugno, S. Patricelli, P. Parascandolo, E. Sassi, L. Tortora, G. Troise, U. Troya and S. Vitale
Istituto di Fisica dell'Università - Napoli
Istituto Nazionale di Fisica Nucleare - Sezione di Napoli

C. Bemporad, M. Calvetti, F. Costantini and P. Lariccia
Istituto di Fisica dell'Università - Pisa
Istituto Nazionale di Fisica Nucleare - Sezione di Pisa

R. Biancastelli
Istituto Superiore di Sanità - Roma
Istituto Nazionale di Fisica Nucleare - Sezione Sanità di Roma

$\gamma\gamma$ group

C. Bacci, G. Penso, B. Stella
Istituto di Fisica dell'Università - Roma
Istituto Nazionale di Fisica Nucleare - Sezione di Roma

R. Baldini-Celio, M. Bernardini, M. Bozzo(x), G. Capon, R. Del Fabbro, M. Grilli, E. Iarocci, L.H. Jones(+), C. Mencuccini, G.P. Murtas, M. Spinetti and V. Valente
Laboratori Nazionali di Frascati del CNEN - Frascati (Roma)

MEA group

B. Esposito, F. Felicetti, I. Peruzzi, M. Piccolo and F. Ronga
Laboratori Nazionali di Frascati del CNEN - Frascati (Roma)

G.T. Zorn(o)
Department of Physics, University of Maryland - College Park, Md.

B. Bartoli, A. Nigro, and F. Vanoli
Istituto di Fisica dell'Università - Napoli
Istituto Nazionale di Fisica Nucleare - Sezione di Napoli

D. Bisello, M. Nigro
Istituto di Fisica dell'Università - Padova
Istituto Nazionale di Fisica Nucleare - Sezione di Padova

A. Marini, P. Monacelli, L. Paoluzi, G. Piano Mortari, F. Sebastiani and L. Trasatti
Istituto di Fisica dell'Università - Roma
Istituto Nazionale di Fisica Nucleare - Sezione di Roma

(x) - From Istituto Nazionale di Fisica Nucleare, Sezione di Genova.
(+) - Now at Department of Physics and Atronomy, University of Maryland.
(o) - Supported by U.S.A.E.C.

STATUS REPORT ON ψ (3.1 GeV) RESONANCE FROM ADONE

The more recent results obtained at Adone are reported[1÷4]; they concern the study of the newly discovered ψ (3.1 GeV) particle and a first search for possible other new particles with lower mass.

We should begin by reminding the main parameters of Adone since the machine characteristics play an important role in many problems concerning the observation of this new kind of particle.

The energy range covered by Adone is $W = 2E = \sqrt{s} = 1.1 \div 3.0$ GeV. The machine group allowed experimentalists to work 100 MeV above the maximum design energy, in order to reach the ψ mass.

The luminosity, at maximum energy is $\sim 0.3\ \mu b^{-1}\ sec^{-1}$, measured by small angle (~ 70 mrad) Bhabha scattering, by single bremsstrahlung and by double bremsstrahlung.

The beams lifetime is typically 8 hours. Each beam consists of three bunches which cross in six regions of the machine: two of them are occupied by R.F. cavities, four are available for experiments.

The collision is an "head on" one and the source longitudinal density is gaussian-like with full width at half maximum of $(47 \pm 5)E^{3/2}$ cm (E in GeV). The radial and vertical dimensions of the source are 1 mm and 0.1 mm respectively (at 3.1 GeV).

The total c.m. energy spread Γ_W(FWHM) of the machine depends on the energy itself according to

$$\Gamma_W(\text{MeV}) \simeq .31\ W^2\ (\text{GeV}).$$

The reliability of the energy setting is of the order of 0.3 MeV. Recent calibration of Adone magnetic field, give for the ψ mass the value 3103 ± 6 MeV.

EXPERIMENTAL APPARATA -

Actually three of the four experimental crossing regions are occupied by the experimental set-up of:

i) $B\bar{B}$ group (Frascati, Napoli, Pisa collaboration)
ii) $\gamma\gamma$ group (Frascati, Roma collaboration)
iii) MEA group (Frascati, Napoli, Padova, Roma collaboration)

i) $B\bar{B}$ experiment. - The set up of the baryon-antibaryon group (Fig. 1) consists[2] of two symmetrical telescopes (six counters each).

Informations on the detected particles come from pulse height and timing analysis on the phototube signals.

Cosmic rays rejection is achieved hardware (time of flight between S_1 and S_2).

The collinearity of detected particles and the source point are determined by using measurement of the impact point on S_1 and S_2.

Electron identification is achieved by pulse height analysis on S_3.

The material between S_2 and S_3 is about 3.5 r.l. thick.

The angular region covered by this set up is : $\theta = 44^o \div \div 136^o$; $\Delta\varphi = 40^o$.

ii) $\gamma\gamma$ experiment. - This set up (Fig. 2) consists[3] of two kinematical spark chambers (KSC), two shower detectors (SD) sandwiches of spark chambers, plastic scintillators and lead converters, and two thick plate spark chambers (sandwiches of spark chambers and iron plates) (ISC). Two circular digitized side telescopes (ST) (magnetostrictive chambers and scintillation counters) complete the system. The total solid angle covered by the set up is for a point-like source $0.5 \times 4\pi$ sterad for the optical detection system and $0.15 \times 4\pi$ sterad for the side telescopes. The polar angle θ accepted by the set up ranges from 20^o to 160^o. The apparatus can be triggered by different configurations e.g.: two or more charged particles, at least one in the upper part and one in the lower part, or only photons in the upper and lower part of the apparatus. This last trigger is particularly suitable to look at the neutral decays of $\psi(3.1)$ particle. Time of flight technique is used for cosmic rays rejection. In this way the cosmic rays rate is lowered by a factor $\sim 10^3$.

iii) MEA experiment. - This set up[4] (Fig. 3) is a magnetic detector. The magnetic field is produced by a large (2 meters diameter, 2 meters length) solenoid, with Al coil: the axis is perpendicular to e^+e^- direction; the zero integral value of the magnetic field along the beam path is obtained by means of two compensator magnets. The maximum field available is 4.5 KG, but actually the running field was 2 KG. In this working condition the momentum resolution is $\sim$ 10% for 1 GeV/c particles.

A set of multiwire proportional chambers (MWPC) are placed above and below the crossing region. These chambers have wires parallel to the direction of the beam and are used both in the trigger system and in off-line reconstruction of the events.

A system of narrow and wide gap optical spark chambers is used to measure the emission angle and the momentum of the particles. The wide gaps are cylindrical and coaxial with the solenoid; the electrodes are made of wire in order to reduce multiple scattering and to simplify the optical system. In fact in this way a single photografic camera

can give the reconstruction of the events in space.

A scintillation counter system ($S_1 \div S_4$, $S'_1 \div S'_3$) is used for triggering. The trigger request is at least one particle with a minimum energy of 130 MeV (if pion) in the upper part ($S_1 S_2 S_3 S_4$) and one particle of 110 MeV (if pion) in the lower part ($S'_1 S'_2 S'_3$). To reduce machine background, events with all particles at small angle with respect to the beam are rejected. The solid angle covered by the set up for point-like source is $\Delta\Omega_m = 0.4 \times 4\pi$ sterad ($40^o \leq \theta \leq 140^o$) for momentum analysis; $\Delta\Omega_i = 0.27 \times 4\pi$ sterad for particles identification (chambers C_3 C'_3). The effect of the extended source is to lower $\Delta\Omega_m$ to $\sim 0.09 \times 4\pi$ sterad at 3.1 GeV.

Cosmic rays background is rejected by time of flight measurement, by requiring correct timing with bunch-bunch collision and by requesting that radial position of the source lies within $\pm$ 5 cm from the beam line (fast logic of MWPC). With such requirements the cosmic ray rate is reduced by a factor $\sim 10^4$.

EXPERIMENTAL RESULTS -

The reactions we are studing around 3.1 GeV are:

(1) $e^+e^- \rightarrow$ many hadrons ($\gamma\gamma$, MEA)

(2) $e^+e^- \rightarrow e^+e^-$ ($B\bar{B}$, $\gamma\gamma$, MEA)

(3) $e^+e^- \rightarrow \mu^+\mu^-$ ($B\bar{B}$, $\gamma\gamma$, MEA)

(4) $e^+e^- \rightarrow$ neutrals ($\gamma\gamma$)

Reaction (1) has also been studied in the total c.m. energy range 1.9 $\div$ $\div$ 3.1 GeV in fine steps.

The identification criteria for the various channels are:

Channel 1 - 2 non collinear tracks or more than two tracks, coming from interaction region and having correct timing with beam--beam interaction (MEA).
- 2 tracks (one in each part of the apparatus) plus anything. ($\gamma\gamma$)

Channel 2 - 2 collinear tracks with proper: timing with the beam; source position; time of flight in both side of the apparata; furthermore:
- showering in the external spark chamber. (MEA).
- showering in the shower detector ($\gamma\gamma$)
- ionizing $\geq$ 2 times minimum after 3.5 r.l. ($B\bar{B}$).

Channel 3 - The $\mu^+\mu^-$ events have to satisfy the same collinearity requirements as the e^+e^- events and are caracterized by:
- absence of e.m. showers ($B\bar{B}$, $\gamma\gamma$, MEA)
- absence of nuclear interactions in thick plates spark chamber ($\gamma\gamma$, MEA)
- correct momentum within $\pm$ 20% (MEA).

The $B\bar{B}$ set up cannot at present, distinguish between $\mu^+\mu^-$ pairs and hadrons pairs.

Channel 4 - No charged particle should be present but only photons coming from interaction region, having correct timing with the beam-beam interaction and showering in the shower detector ($\gamma\gamma$).

To extract from experimental data the resonance parameters, e.g. the width Γ_i, in this case ($\Gamma_i \ll \Delta W$ = c.m. energy spread of the machine) the simplest procedure is to integrate the resonant cross-section over ΔW ; one obtains for $J^P = 1^-$:

$$\int_{\Delta W} \sigma(e^+e^- \longrightarrow \text{had})dW = \frac{6\pi^2}{M_\psi^2} \frac{\Gamma_{e^+e^-}\Gamma_{had}}{\Gamma_{tot}} \tag{5}$$

$$\int_{\Delta W} \left[\sigma(e^+e^- \longrightarrow e^+e^-) - \sigma(e^+e^- \longrightarrow e^+e^-)_{QED}\right] dW =$$

$$= \frac{6\pi^2}{M_\psi^2} \frac{\Gamma^2_{e^+e^-}}{\Gamma_{tot}} \tag{6}$$

$$\int_{\Delta W} \left[\sigma(e^+e^- \longrightarrow \mu^+\mu^-) - \sigma(e^+e^- \longrightarrow \mu^+\mu^-)_{QED}\right] dW =$$

$$= \frac{6\pi^2}{M_\psi^2} \frac{\Gamma_{e^+e^-}\Gamma_{\mu^+\mu^-}}{\Gamma_{tot}} \tag{7}$$

In expression (6) and (7), we have assumed that the interference term, integrated over the machine resolution is negligible.

The above integrals do not depend on the machine resolution.

To deduce the width from the experimental data, radiative corrections have to be taken into account.

$e^+e^- \rightarrow$ many hadrons. -

In Fig. 4 is reported the experimental total cross section for $e^+e^- \rightarrow$ many hadrons ($\gamma\gamma$ experiment), together with the theoretical curve calculated by taking into account radiative corrections[5] and machine energy spread.

The experimental results for multihadronic channel are:

$$\int_{\Delta W} \sigma(e^+e^- \rightarrow \text{had})\, dW = \begin{cases} (6.7 \pm 2.4) \text{ nb x GeV}(\gamma\gamma) \\ (7.0 \pm 1.8) \text{ nb x GeV (MEA)} \end{cases}$$

Here and in the following, the quoted errors include also uncertainties on detection efficiencies, and on luminosity measurement.

This corresponds to (without radiative corrections):

$$\frac{\Gamma_{e^+e^-}\,\Gamma_{had}}{\Gamma_{tot}} = \begin{cases} (2.8 \pm 0.9) \text{ KeV}(\gamma\gamma) \\ (2.9 \pm 0.7) \text{ KeV (MEA)} \end{cases}$$

Applying radiative corrections[5] we obtain

$$\frac{\Gamma_{e^+e^-}\,\Gamma_{had}}{\Gamma_{tot}} = \begin{cases} (3.8 \pm 1.3) \text{ KeV}(\gamma\gamma) \\ (4.1 \pm 1.1) \text{ KeV (MEA)} \end{cases}$$

In Fig. 5 are shown the charged, neutral and total multiplicity distributions of the detected multihadron events as obtained by $\gamma\gamma$ experiment.

The average charged multiplicity observed in the MEA set up is $\langle N_c \rangle = 3.3 \pm 0.3$; lower limits for high multiplicity channels turn out to be:

$$\frac{N_{\geqslant 6}}{N} \geqslant (0.13 \pm 0.02) \text{ (MEA)}$$

$$\frac{N_{\geqslant 8}}{N} \geqslant (0.02 \pm 0.01) \text{ (MEA)}$$

where $N_{\geqslant 6}$, $N_{\geqslant 8}$ and N are respectively the number of events with at least 6 or 8 charged particles, and the total number of events.

$e^+e^- \rightarrow e^+e^-$.-

For the channel $e^+e^- \rightarrow e^+e^-$ the resonance contribution is of the same order of magnitude as the QED.

In Fig. 6 is reported the excitation curve for the reaction $e^+e^- \rightarrow e^+e^-$ ($B\bar{B}$ experiment).

In Fig. 7 the measured angular distribution is reported for the $B\bar{B}$ and MEA experiments.

From the integral (6) one obtains (without radiative corrections):

$$\frac{\Gamma^2_{e^+e^-}}{\Gamma_{tot}} = \begin{cases} (0.23 \pm 0.09)\,\text{KeV}\,(B\bar{B}) \\ (0.36 \pm 0.12)\,\text{KeV}\,(\gamma\gamma) \\ (0.21 \pm 0.07)\,\text{KeV})\,(\text{MEA}) \end{cases}$$

The above MEA value has been derived from back scattering ($\theta \geq 90^o$) events for which QED background is lower.

After radiative corrections[5] have been applied these values become (not yet calculated for MEA results)

$$\frac{\Gamma^2_{e^+e^-}}{\Gamma_{tot}} = \begin{cases} (0.34 \pm 0.14)\,\text{KeV}\,(B\bar{B}) \\ (0.65 \pm 0.22)\,\text{KeV}\,(\gamma\gamma) \end{cases}$$

$e^+e^- \rightarrow \mu^+\mu^-$.-

In this channel the QED background is very small. In Fig. 8 the excitation curve for reaction $e^+e^- \rightarrow \mu^+\mu^-$ is reported (MEA experiment). From the integral (7) one obtains (without radiative corrections):

$$\frac{\Gamma_{e^+e^-}\,\Gamma_{\mu^+\mu^-}}{\Gamma_{tot}} = \begin{cases} (0.21 \pm 0.07)\,(B\bar{B}) \\ (0.26 \pm 0.09)\,(\gamma\gamma) \\ (0.24 \pm 0.04)\,(\text{MEA}) \end{cases}$$

By applying radiative correction:

$$\frac{\Gamma_{e^+e^-}\,\Gamma_{\mu^+\mu^-}}{\Gamma_{tot}} = 0.31 \pm 0.09 \quad (B\bar{B})$$

The radiative corrections have not been yet calculated for $\gamma\gamma$ and MEA results. It is important to notice that, within the experimental errors, $\Gamma_{e^+e^-} \simeq \Gamma_{\mu^+\mu^-}$ as expected from the μ-e universality.

$\mu^+\mu^-$ angular distribution (MEA experiment):

A possible forward-backward asymmetry in the $\mu^+\mu^-$ angular distribution has been investigated[6] by the MEA experiment; the asymmetry is defined by

$$\Sigma = \frac{N_F - N_B}{N_F + N_B}$$

where N_F is the number of the events in which the angle θ between e^+ and μ^+ directions is less than 85^o, while N_B is the number of events in which θ is greater than 95^o.

The measured Σ values averaged on the energy interval $3100.5 \div 3105.5$ is consistent with zero: namely

$$\Sigma = \frac{49-53}{49+53} = -0.04 \pm 0.1$$

If further analysis is performed looking at the energy dependence of the asymmetry we find:

$$3100.5 \leqslant W \leqslant 3102.5\ ; \quad \Sigma = \frac{32-16}{32+16} = 0.33 \pm 0.14$$

$$3103.5 \leqslant W \leqslant 3105.5\ ; \quad \Sigma = \frac{12-28}{12+28} = -0.40 \pm 0.14$$

The errors are statistical only.

This result is quite difficult to explain; if it is not a statistical fluctuation, the energy spread of the machine should average any energy dependent asymmetry due to such a narrow resonance.

It is important to outline that, in the 1^- hypothesis, radiative corrections would generate[5] a forward-backward asymmetry in the angular distribution of the $\mu^+\mu^-$ pair of the order of + 5%.

Tests are in progress to check MEA apparatus symmetry: inversion of the magnetic field and of beam's direction.

$e^+e^- \rightarrow$ photons. -

The production of only photons at energies around the ψ (3,1 GeV) resonance has been studied by the $\gamma\gamma$ group, whose apparatus is particularly suitable for photon detection.

A sketch of the counters and converters arrangement in the shower detector SD is shown in Fig. 9.

A photon is defined by the coincidence $\bar{V}\cdot[(1\cdot2\cdot3)+(2\cdot3\cdot4)]$ The trigger efficiency is $\sim$ 75% for photon energies $E_\gamma \geq$ 500 MeV. Full tracking efficiency is reached in the shower detector for photon energies $E_\gamma \geq$ 200 MeV.

Experimental results. -

With this set-up three channels have been studied up to now[7]:

(8) $e^+e^- \rightarrow \gamma\gamma$

(9) $e^+e^- \rightarrow \pi^o\gamma$, $\pi^o \rightarrow \gamma\gamma$

(10) $e^+e^- \rightarrow \eta\gamma$, $\eta \rightarrow \gamma\gamma$

In order to detect these reactions at least two photons are required one in the upper part and one in the lower part of the apparatus and no charged particles should be present either in the main telescopes or in the side telescopes.

A total luminosity of 19 nb^{-1} was collected at energies ranging from 3090 to 3110 MeV; 41 events were detected with two photons coplanar within $\pm 5^o$ with the beam line. The collinearity distribution of these events is reported in Fig. 10. No three photons events were detected at the resonance energy.

A MonteCarlo calculation shows that for the reactions (9) and (10) the three photons configuration is favoured by a factor of $\sim 2 \div 3$ with respect to the two photons configuration. More precisely the efficiencies for detection of $\pi^o\gamma$ and $\eta\gamma$ reaction in 2γ or 3γ configuration are:

$\varepsilon_{2\gamma}(\pi^o\gamma) = (1.9 \pm 0.06)\%$ $\quad \varepsilon_{3\gamma}(\pi^o\gamma) = (5.7 \pm 0.1)\%$

$\varepsilon_{2\gamma}(\eta\gamma) = (2.9 \pm 0.1)\%$ $\quad \varepsilon_{3\gamma}(\eta\gamma) = (4.8 \pm 0.1)\%$

Therefore the absence of three photon events allows to give the following upper limits for the cross sections for reaction (9) and (10), integrated over the energy spread of the machine, at the resonance energy

$$\int_{\Delta W} \sigma_{\pi^o\gamma}(w)dw < 27 \text{ nb} \cdot \text{MeV} \quad (90\% \text{ c.l.})$$

$$\int_{\Delta W} \sigma_{\eta\gamma}(w)dw < 89 \text{ nb} \cdot \text{MeV} \quad (90\% \text{ c.l.})$$

Radiative corrections have not yet been taken into account. In calculating the $\sigma_{\eta\gamma}$ upper limits the $\eta \to \gamma\gamma$ branching ratio has been used:

$$(\ \eta \to \gamma\gamma\ )/(\ \eta \to \text{all modes}) = 0.38$$

The above results correspond to the following upper limits for the partial width.

$$\frac{\Gamma_{\pi^0\gamma}}{\Gamma_{had}} < 0.5\% \quad (90\%\ \text{c.l.})$$

$$\frac{\Gamma_{\eta\gamma}}{\Gamma_{had}} < 1.6\% \quad (90\%\ \text{c.l.})$$

From these results it follows that the contribution from reaction (9) and (10) to the 41 two-photons events, is negligible. In order to study reaction (8) only 39 events out of the 41, have been selected by requiring the collinearity of the two photons within $\pm 15^o$.

The excitation curve of these events is reported in Fig. 11. Within the present statistics no clear evidence appears for the existence of a peak in the cross section for reaction (8), at an energy corresponding to the mass of the ψ . An estimate of a possible enhancement of the cross section for reaction (8) around 3103 MeV is given by the ratio:

$$r = \frac{\gamma\gamma \text{ yield } (3100 \leq W \leq 3106)}{\gamma\gamma \text{ yield } (W < 3100;\ W > 3106)} = 1.6 \pm 0.6$$

Search for new resonances with masses below 3.1 GeV. -

Possible new resonances in the mass region 1.9 to 3.1 GeV are being searched for. The preliminary results from $\gamma\gamma$ group are now reported. Up to now, the following mass intervals have been explored: 1915 ÷ 2045 MeV and 2205 ÷ 2544 in steps of 1 MeV; and 2966 ÷ 3090 in steps of 2 MeV. The energy spread Γ_W (FWHM) of the total c.m. energy (W) of the beams depends on the energy itself, according to $\Gamma_W(\text{MeV}) \simeq 0.31\ W^2(\text{GeV})$. In the explored range of mass, Γ_W varies from 1.1 MeV to 3.0 MeV. Therefore the 1 or 2 MeV steps allow to detect also possible very narrow resonances.

Experimental results. -

For each energy value, the following luminosities were accumulated: 0.12 nb^{-1} for $1915 \leq W \leq 2045$ MeV; 0.066 nb^{-1} for $2205 \leq W \leq 2544$ MeV; 0.18 nb^{-1} for $2966 \leq W \leq 3090$ MeV. The multihadrons yield was recorded as a function of energy. The results are shown in Fig.12.

For comparison, the ψ (3.1 GeV) peak is reported on the same scale as the other experimental points. No statistically significant structures other than the ψ (3.1 GeV) seems to appear. In the multihadron channel an upper limit on experimental cross section of about 400 nb (90% c.l.) can be given for possible new narrow resonances.

The same conclusion can be deduced from the MEA data, although their statistics is lower by a factor $\sim$ 2. Work is in progress to increase the statistics and to complete the energy interval covered by Adone storage ring.

REFERENCES. -

(1) - Phys. Rev. Letters 33, 1404, 1406, 1408 (1974)

(2) - $B\bar{B}$ group, Lett. Nuovo Cimento 11, 718 (1974).

(3) - $\gamma\gamma$ group, Lett. Nuovo Cimento 11, 711 (1974).

(4) - MEA group, Lett. Nuovo Cimento 11, 705 (1974).

(5) - M. Greco, G. Pancheri-Srivastava and Y. Srivastava, Frascati Report LNF - 75/9 (P); submitted to Phys. Letters.

(6) - MEA group, Frascati Report LNF-74/64 (1974).

(7) - $\gamma\gamma$ group, Lett. Nuovo Cimento 12, 269 (1975).

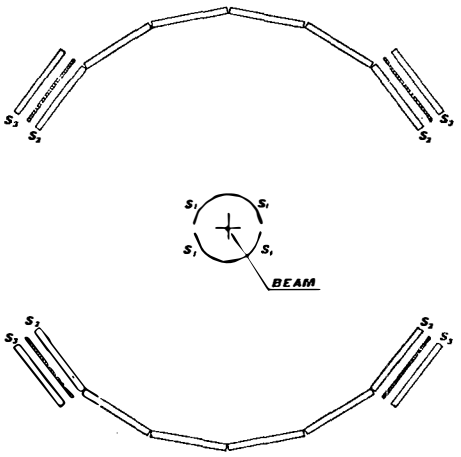

FIG. 1 - Experimental set-up of the $B\bar{B}$ experiment. S_1, S_2 and S_3 are scintillation counters.

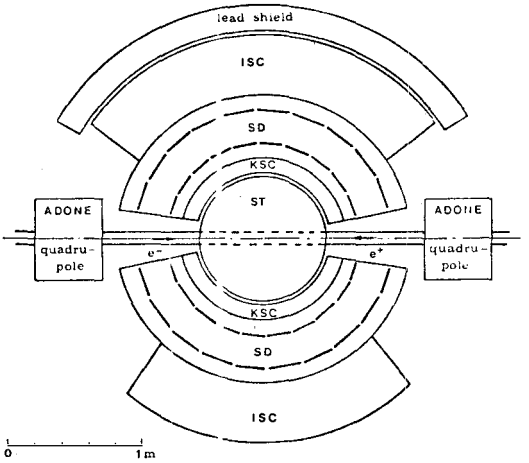

FIG. 2 - Experimental set-up of the $\gamma\gamma$ experiment.

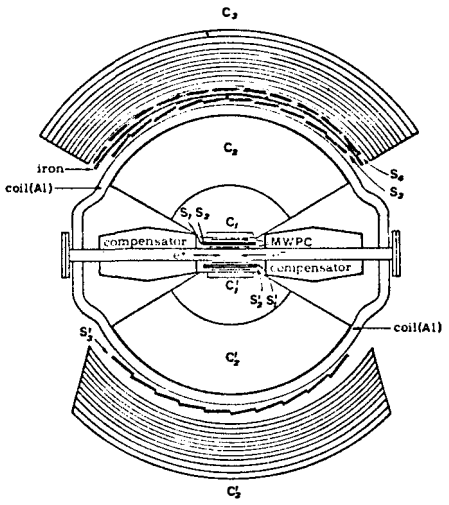

FIG. 3 - Experimental set-up of the MEA experiment. $S_1 \div S_4$, $S'_1 \div S'_3$ are scintillator counters.

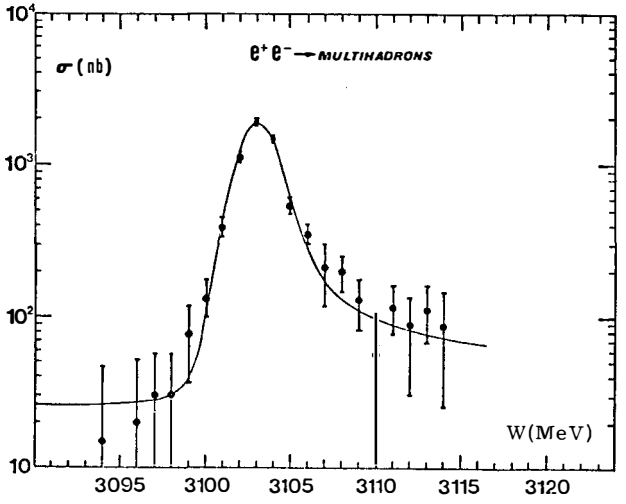

FIG. 4 - $e^+e^- \longrightarrow$ many hadrons total cross section ($\gamma\gamma$ experiment). The solid line is a fit of the experimental points with the radiative corrections formula of ref. (5), plus a constant background. The beam energy spread has been folded in. The errors are statistical only.

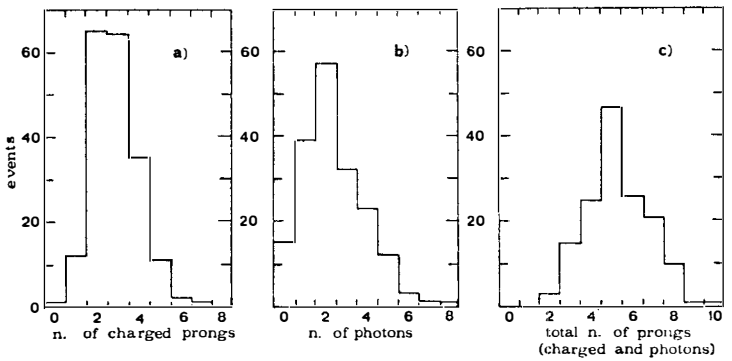

FIG. 5 - Multihadrons events multiplicities in the $\gamma\gamma$ experiment set-up. a) Charged prong multiplicity; b) Photon multiplicity; c) Total (charged + photons) multiplicity.

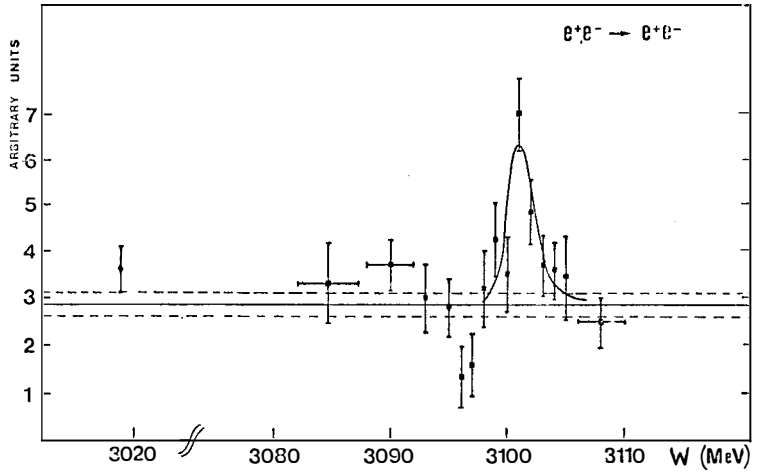

FIG. 6 - Excitation curve for $e^+e^- \rightarrow e^+e^-$ ($B\bar{B}$ experiment). The solid line is the average Bhabha level, measured outside the resonance. The dotted lines represent an estimate of uncertainties on this level. The errors are only statistical.

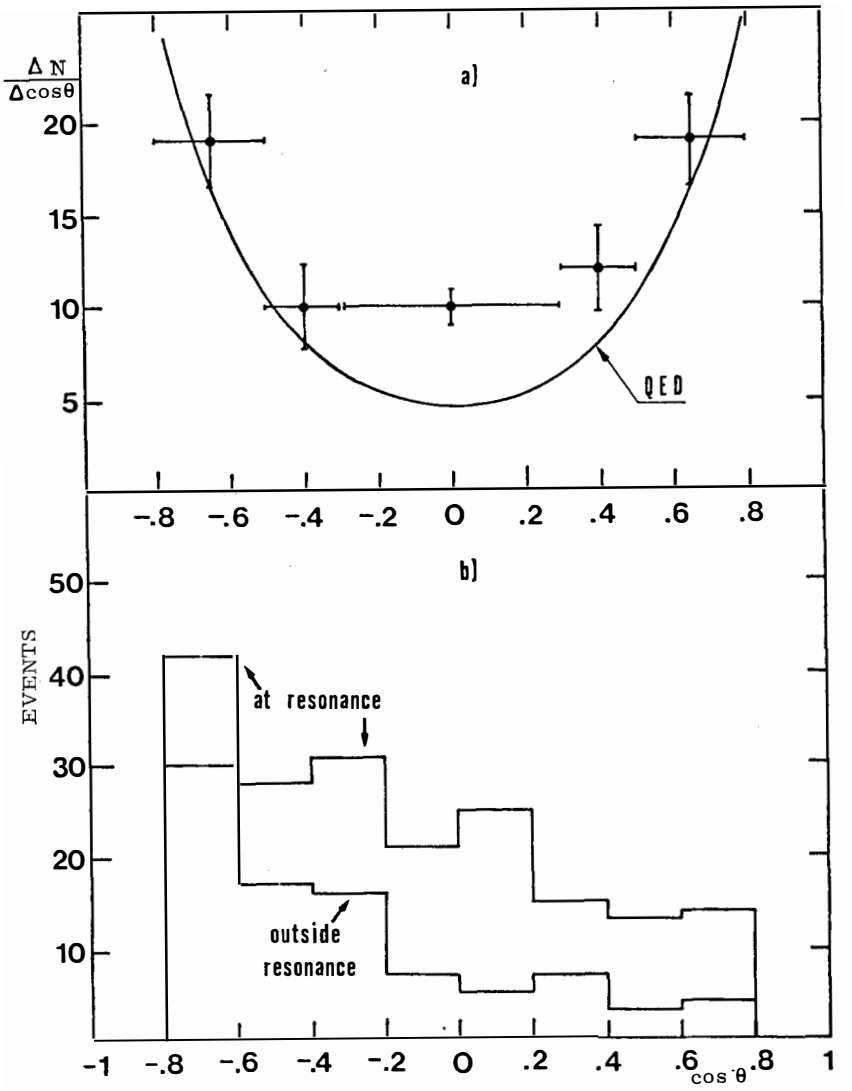

FIG. 7 - $e^+e^- \rightarrow e^+e^-$ Angular distribution: a) from the $B\bar{B}$ experiment. The solid line is the QED prediction. b) From the MEA experiment, inside and outside the resonance. The errors are statistical only.

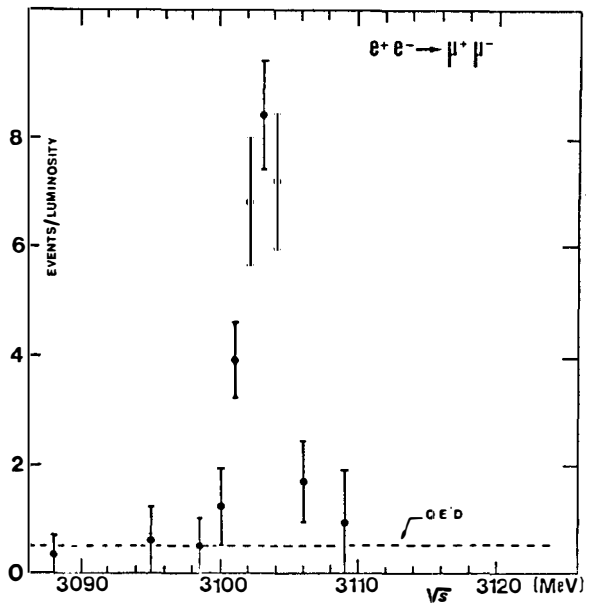

FIG. 8 - $e^+e^- \longrightarrow \mu^+\mu^-$ excitation curve from MEA experiment. The errors are statistical only.

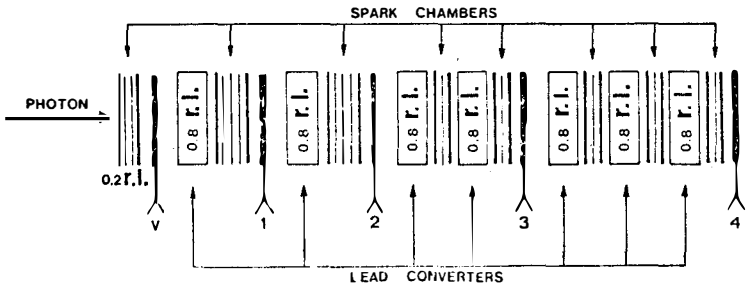

FIG. 9 - A sketch of one of the two main telescopes (SD) of the $\gamma\gamma$ apparatus. V, 1, 2, 3 and 4 are scintillation counters.

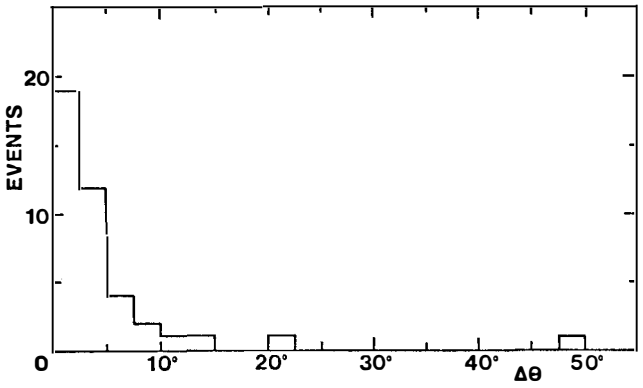

FIG. 10 - Collinearity distribution for two-photon events coplanar with the beam ($\gamma\gamma$ experiment).

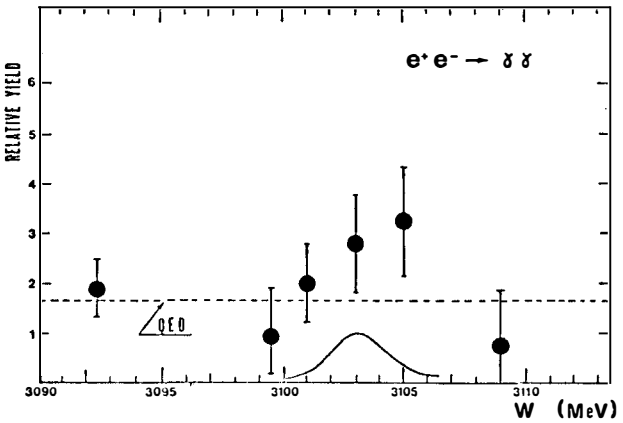

FIG. 11 - Relative yield for the production of collinear photon pairs as a function of the total c.m. energy. ($\gamma\gamma$ experiment) The horizontal dashed line represents the $e^+e^- \longrightarrow \gamma\gamma$ level as deduced by averaging the first and last point. The position and the shape of the ψ (3.1 GeV) resonance is shown.

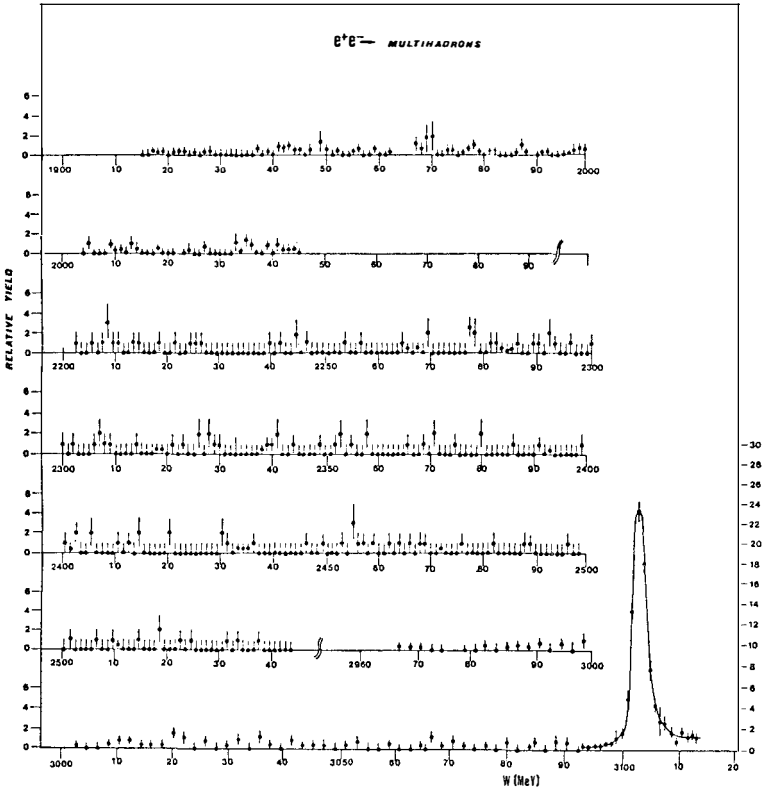

FIG. 12 - Multihadron relative yield ($\gamma\gamma$ experiment) as a function of total c.m. energy W. The $\psi(3.1$ GeV) is reported for comparison, on the same scale as the other points.

CHARMLESS COLOURFUL MODELS OF THE NEW MESONS

F.E. CLOSE
CERN, Geneva

J. WEYERS
CERN, Geneva
Université de Louvain, Belgium

Abstract : It is shown that a strongly broken colour model is compatible with the present data on the new particles. Experimental consequences of the model are pointed out.

Résumé : On montre qu'un modèle de couleur fortement brisée est compatible avec les données actuelles sur les nouvelles particules. On donne des conséquences expérimentales du modèle.

This is a progress report on attempts to investigate the simplest varieties of theories which contain a new non-additive quantum number and can be formulated consistent with the known facts on the new particles [1]. We present our current understanding of such schemes in the hope that at least it may stimulate others to consider possibilities beyond the familiar charm [2] and colour [3] models which are discussed elsewhere in these proceedings [4].

I. THE CHARGE OPERATOR

If one wishes to formulate a unified theory of weak and electromagnetic interactions that has no anomalies when couplings including hadronic degrees of freedom are introduced, then it is necessary that [5]

$$\sum_i e_i = \sum_{\text{leptons}} e_i + \sum_{\text{hadrons}} e_i = 0$$

where e_i are the charges of the fundamental fields in the theory.
If one does not introduce heavy leptons then there are two types of possible theories.

(i) charged leptons in the fundamental multiplet(s) are $e^- \mu^-$

Hence the hadronic quarks must have total charge +2. This is the "charm like" solution ; the quarks are p,n,λ, p' with the usual charges and come in three colours RYB.

(ii) charged leptons in the fundamental multiplet(s) are $e^- \mu^+$

Hence the hadronic quarks have total charge zero. This is satisfied by the familiar p,n,λ (with or without colour). If one introduces new quarks one requires

$$\sum_{\substack{\text{new} \\ \text{quarks}}} e_i = 0 \qquad (2)$$

It is theories of this type that we are investigating.

The simplest realisation is two triplets of p,n,λ - male and female, known as the sex model. This model leads to some frustration and appears to be unsatisfactory. We then proceed to a three triplet model which is consistent with present data and leads to some spectacular predictions like the supression of the cascades (4.1) → (3.1, 3.7)+X and the (possible) existence of doubly (or even triply) charged meson states.

II. TWO TRIPLET (SEX) MODEL

2.a. The basic idea

Two triplets of quarks $(pn\lambda)_M$ and $(pn\lambda)_F$ form the basic representation of $SU(3)_M \oplus SU(3)_F$. The hadrons known before November 1974 are male states (singlets under $SU(3)_F$) made from the $(pn\lambda)_M$ quarks. A female universe - states built from $(pn\lambda)_F$ - exists in parallel with the familiar male world.

The photon connects the two worlds and is postulated to transform as $\gamma = \gamma_M + \gamma_F = (8_M, 1_F) + (1_M, 8_F)$. In addition to $(\rho\omega\phi)_M$ states which couple directly to γ_M there exist $(\rho\omega\phi)_F$ states which couple directly to γ_F. The (J,ψ) mesons are assigned to these female states.

2.b. Problems

Assigning 3.1 and 3.7 to the ϕ_F and ω_F states seems to fit nicely with the observed leptonic widths. However where is the predicted ρ_F state ? Naïvely one expects $f^2_{\rho_F\gamma} \simeq 9\, f^2_{\omega\gamma}$ and although one can play with arbitrary mass factors it seems difficult to avoid the predictions that $\Gamma^{e^+e^-}_{\rho F} \gtrsim$ 15-20 keV ! The failure to observe this state is serious and makes a two triplet model unsatisfactory.

However it is worthwhile to point out that as far as weak interactions are concerned a two-triplet model leads to interesting possibilities which we now elaborate since they may be taken one in more complicated theories.

2.c. Weak interactions

There are basically two ways of proceeding from the requirement that strangeness changing neutral currents are supressed.

(i) The charm analogue

Two "Cabibbo triplets" $(pn_c\lambda_c)_M$, $(pn_c\lambda_c)_F$ generate the charge raising weak current

$$W^+ \simeq (\bar{p}n_c + \bar{p}'\lambda_c) + (\bar{p}'n'_c + \bar{p}\lambda'_c) \qquad (3)$$

where the primes denote the females, unprimed the males.
W^- follows immediately and then the neutral current will have structure given by $W_3 \sim [W^+, W^-]$.

Since the weak interactions connect the M and F worlds then, to eliminate parity violating effects in strong interactions (to order α), the Weinberg-Nanopoulos [6] theorem suggests that the gluons couple symmetrically to M and F worlds. $SU(3)_M \oplus SU(3)_F$ becomes SU(6) and this latter model has already been suggested in the literature [7].

(ii) No charm because no Cabibbo

We begin with two triplets $(pn\lambda)_{1,3}$ each degenerate in mass at 300 MeV and 2 GeV respectively. The electromagnetic current is written

$$\gamma\omega \left(\frac{2}{3} p\bar{p} - \frac{1}{3} n\bar{n} - \frac{1}{3} \lambda\bar{\lambda} \right)_1 + \left(\frac{2}{3} p\bar{p} - \frac{1}{3} n\bar{n} - \frac{1}{3} \lambda\bar{\lambda} \right)_3 \qquad (4)$$

$$\equiv \left[(I=1)_z + \frac{1}{\sqrt{3}} (I=0) \right]_1 + \left[(V=1)_z + \frac{1}{\sqrt{3}} (V=0) \right]_3 \qquad (5)$$

(compare the figure 1)

The charged weak currents are an I spin rotation in world 1 and V spin rotation in world 3.

$$W_1^{\pm} = I^{\pm} \; ; \; W_3^{\pm} = V^{\pm}$$

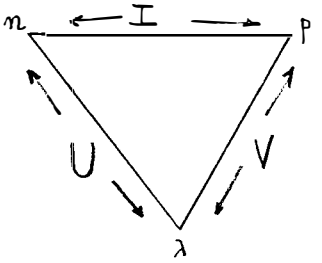

Gauge theories are built in worlds 1 and 3 so that

$$W_1^z = I^z \; ; \; W_3^z = V^z .$$

The medium strong interaction mixes states containing λ quarks in worlds 1 and 3 yielding the M and F worlds

$$\begin{aligned} (I^{\pm})_M &= (I^{\pm})_1 \\ (K^{\pm})_M &= (K^{\pm})_3 \sin\theta + (K^{\pm})_1 \cos\theta \\ (K^{\pm})_F &= (K^{\pm})_3 \cos\theta - (K^{\pm})_1 \sin\theta \end{aligned} \qquad (6)$$

The observed medium strong splitting of the M world and the ≃ 2 GeV separation of the quarks in worlds 1 and 3 generate the magnitude of θ . Using masses (as against mass squared) then $\theta \simeq \theta_c$! Hence

$$(W^{\pm})_M = g_1 I^{\pm} + g_3 V^{\pm} \sin\theta \quad , \quad \theta \simeq \theta_c \qquad (7)$$

where $g_{1,3}$ are the coupling strengths of the $W_{1,3}$ bosons.

These ideas (Viz, that nature utilises two axes associated with two sets of mesons rather than one axis with a Cabibbo rotation) have essentially been anticpated by Schwinger [6]. His picture has $g_1 = g_3$ and differs from the Cabibbo current only by 0.97 : 1 in $I^{\pm}$.

With our two couplings we obtain

$$(W^{\pm})_M = g_3 \left[\frac{g_1}{g_3} I^{\pm} + V^{\pm} \sin\theta \right]$$

then

$$\frac{g_1}{g_3} = \frac{m_{W_1}}{m_{W_3}} = 0.97.$$

Unifying with electromagnetism one finds typically $m_{W_3} \simeq 65$ GeV and $m_{W_1} \simeq 63$ GeV.

It is not clear whether such schemes can be shown to be fully sound. However they deserve further examination since they have some motivation now that new states have been found, and are of interest as a "non charm" approach to the weak interaction neutral current problem.

III. A THREE TRIPLET MODEL [9]

3.a. The basic idea

As in many colour schemes we assume the fundamental hadron symmetry to be SU(3) x $SU(3)_c$ and the photon to transform as (8,1) + (1,8). However, (and this possibility seems to have been overlooked in previous models) we postulate that $SU(3)_c$ is strongly broken down to $SU(2)_c \times U(1)_c$ ("colour isospin" and hypercharge"), hence ordinary mesons are not expected to transform as colour singlets anymore.

Explicitly we consider three triplets labelled ΛNP with N,P an isocolour doublet and Λ an isocolour singlet. The charges of the p,n,λ quarks are

	P	n	λ
Λ	z	z-1	z-1
N	z'	z'-1	z'-1
P	z"	z"-1	z"-1

(9)

The constraint that there be no anomalies becomes

$$z + z' + z'' = 2 \qquad (10)$$

and so the "average charge" of p,n,λ quarks will be

$$\langle e_p \rangle = 2/3 \qquad \langle e_{n,\lambda} \rangle = -1/3 \qquad (11)$$

under $SU(3)_c$ we consider states

$$V(\Lambda\bar{\Lambda}), \quad \chi \left(\frac{N\bar{N} + p\bar{p}}{\sqrt{2}} \right), \quad \psi \left(\frac{N\bar{N} - p\bar{p}}{\sqrt{2}} \right) \qquad (12)$$

the states V, χ having $I^c=0$ while ψ has $I^c=1$. Physical $I^c=0$ states could be arbitrary mixtures of V and χ ; however we shall argue, and support this claim later, that the physical mesons are to a good approximation the V and χ described above.

Each of these families contains three vector mesons which we shall label ρ_V, ω_V, ϕ_V etc...
The familiar vector mesons $\rho_V(770)$ $\omega_V(780)$ $\phi_V(1020)$ are thus isocolour singlets. All three couple directly to the photon and their leptonic widths are consistent with the familiar choice $z = 2/3$. Similarly the $\rho_\chi \omega_\chi \phi_\chi$ $I^C=0$ states all couple directly to the photon and the ratios of their various leptonic widths will be similar to that of the $\rho_V\omega_V\phi_V$. This already prevents one from assigning the 3.1 and 3.7 GeV states to $I^C=0$ since one would have the embarrasing failure to see a ρ-like state with $\Gamma^{e^+e^-} \sim 20$ keV.

The couplings of the photon to the $I^C=1$ ψ states are

$$\rho_{\psi\gamma} = 0 \qquad \omega_{\psi\gamma} = \sqrt{2}\,\phi_{\psi\gamma} \sim z' - z'' \tag{13}$$

The $I^C=1$ phenomenology is now perfect for the 3.1 and 3.7 identification as $\omega_\psi(3.1)$, $\phi_\psi(3.7)$. The isocolour conservation will forbid the strong decay of the ψ states into ordinary mesons and so one already has some hope of understanding the narrow widths.

3.b. Spectroscopy

Our model predicts 81 vector mesons, eight of which couple to the photon, namely

$$\Lambda\bar{\Lambda}\,\rho_V\omega_V\phi_V \text{ with } I^C=0 \text{ and } I=1,0 \tag{14}$$

$$\frac{N\bar{N} - p\bar{p}}{\sqrt{2}} \qquad \omega_\psi\,\phi_\psi \qquad \text{with } I^C=1 \text{ and } I=0 \tag{15}$$

$$\frac{N\bar{N} + p\bar{p}}{\sqrt{2}} \qquad \rho_\chi\omega_\chi\phi_\chi \qquad \text{with } I^C=0 \text{ and } I=1,0 \tag{16}$$

We would identify the $\chi(4.1)$ with ρ_χ or perhaps a mixture of ρ_χ and ω_χ. In the latter case, using the masses

$$\frac{\phi_V - \omega_V}{\phi_V + \omega_V} \sim 12\,\% \quad \text{and} \quad \frac{\phi_\psi - \omega_\psi}{\phi_\psi + \omega_\psi} \sim 9\% \text{ as a guide one predicts}$$

the ϕ_χ to lie around 5 GeV.

For baryons our scheme leads to several possibilities the simplest of which is that baryons are colour singlets i.e.

$$B \sim PN\Lambda.$$

Note that the "average charges" of pnλ quarks being 2/3, -1/3, -1/3 has the consequence that all baryon charges will be sensible whatever z z' z"

may be so long as their sum is 2.

The simplest (but by no means unique) choice for the quark charges compatible with these assumptions and which avoids fractionally charged meson states is then [10]

$$z = 2/3 \qquad z' = -1/3 \qquad z'' = 5/3 \tag{17}$$

(note that $z' \neq z''$ which is forced by eq. (13) and $\omega_{\psi\gamma} \neq 0$).

The most naive mass formulae would then lead us to predict, in this version of the model, that an isocolour doublet ($I^C=1/2$, $p\bar{\Lambda}$) family exists around 2 GeV. The (ordinary) SU(3) nonets which correspond to it will contain a doubly charged state ($p p \bar{n} \bar{\Lambda}$).

3.c. Widths and decay modes of the new particles

Isocolour conservation forbids the strong decay of the ψ states (3.1 and 3.7) into ordinary mesons.

The only "legal quark diagram" for the decay of $\psi(3.1)$ and $\psi(3.7)$ into conventional hadrons is the following.

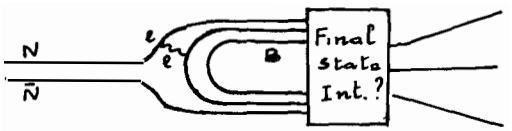

(ordinary hadrons)

and hence of order α^2 for the widths (and of course there will be $\psi \to \gamma \to$ hadrons which is already $O(\alpha^2)$). Consequently one might anticipate that the $\bar{B}/\pi$ ratio will be larger within the peaks than outside.

With the assignments given in our model there is no legal diagram of order e which does not violate Zweigs rule. (We thus avoid a difficulty of conventional colour models where the ordinary mesons are $\frac{\Lambda\bar{\Lambda} + p\bar{p} + N\bar{N}}{\sqrt{3}}$ so that order e diagrams exist are yield rates which are estimated to be of order MeV and hence too large). By the usual arguments we do expect some violation of Zweig's rule but we have no reliable estimate for it.

For the $\chi(4.1)$ on the other hand, strong decays into $B\bar{B}$ states (virtual or real) are allowed and hence our model predicts an "ordinary" width for the 4.1 resonance(s).

Finally, the decay $\psi(3.7) \to \psi(3.1) + 2\pi$ is an ordinary strong decay supressed by (the ordinary SU(3)) Zweig's rule.

Although not completely satisfactory, the phenomenology of the new states based on our model is in remarkable qualitative agreement with the experimental facts. We summarise some of the as yet untested predictions of our model for the new particles.

(i) If the $\chi(4.1)$ is a mixture of ω_χ and ρ_χ we predict yet another state around 5 GeV with $\Gamma^{e^+e^-} \lesssim 2$ KeV and hence probably only visible in topological (in particular, strange particle) rather than total hadronic cross section.

(ii) An important decay mode of $\chi(4.1)$ should be in $B\bar{B}$ (or related) channels. In particular, by isocolour conservation the $\chi(4.1)$ should <u>not</u> significantly cascade into the $\psi(3.1, 3.7)$. More precisely cascading into the ψ states is allowed in first order in electromagnetism and hence could account for a few MeV <u>at most</u> of the total width of the 4.1.

(iii) If the isocolour doublet states predicted by our model have indeed a mass of $\simeq$ 2 GeV, a significant fraction of the 4.1 width could be due to decays into a pair of these states. If this is the case, narrow structures could be seen in <u>doubly-charged</u> channels. It is worth pointing out that our model does predict the existence of such states but depending upon the complications one is willing to accept in the mass formulae, their masses can be almost anything (unfortunately). To the extent that isocolour is exact then <u>triply charged</u> states should exist around 3 to 4 GeV.

(iv) Some of the states predicted by our model should be seen in $\bar{p}p$ annihilation. More detailed predictions will be presented elsewhere. Of particular interest is the state ρ_ψ which does not couple to the photon and which a naïve mass formula would put at $\simeq$ 3.1 GeV. With the usual caveats about the mass formula this state can probably be seen [*] in the decay $\phi_\psi(3.7) \to \rho_\psi(\simeq 3.1) + \pi_v$.

v) Coloured pseudoscalars should also exist but their masses cannot be predicted at this stage.

vi) With the simplest charge assignment for the quarks which, we repeat, is by no means unique, our model predicts that R will continue to rise and that its asymptotic value is 8.

---

[*] In conventional colour models one expects around 600 keV for this mode width which is much too large to be accomodated. For us the colour Zweig rule supresses it due to the $V(\Lambda\bar{\Lambda})$ state assignment.

3d Outlook

Colour models of the new states are traditionally beset by three problems.

1) Radiative widths such as $\psi,\psi' \to \pi\gamma$, are expected to be of the order of MeV ; $\psi' \to \rho(3.05)\pi$ is expected to be of the order of 600 keV. All of these estimates are too large to be accomodated by the known data.

2) One expects, on the basis of the parton model, that the structure functions in deep inelastic electro-production should exhibit a sizeable enhancement at colour threshold. No evidence for such an enhancement exists.

3) The data on the $\psi(3.1)$ suggests that G parity is conserved in the decay-typically a strong interaction selection rule and not obvious for an electromagnetic process.

In our model the first problem is immediately solved- the colour breaking with the associated assignment of ordinary mesons to $\Lambda\bar{\Lambda}$ colour states, supresses all of these decays by the (colour) Zweig rule. It is this feature which distinguishes this from previous (unbroken) colour models and enables the widths to be in accord with data.

The parton model, with the present model's quark charges, would suggest that at $x \simeq 0$ a fourfold increase takes place in νW_2 as one crosses colour threshold. Such a prediction, however, has implicitly assumed that all dynamics that are independent of quark charges are identical in PNΛ sectors. That this may well not be the case is suggested by the fact $\sigma(\psi p) \sim \frac{1}{25}\sigma(pp)$. Incorporating this in the νW_2 calculation in the lowest possible way yields for the increase

$$\frac{\nu W_2 \text{ (above)}}{\nu W_2 \text{ (below)}} = 1 + \frac{9\,\sigma(\psi p)}{\sigma(v_p) + 2\sigma(\chi p)} \quad \begin{array}{l} \sigma_\psi = \sigma_V = \sigma_\chi \rightarrow \quad 400\ \% \text{ (as in parton model)} \\ \sigma_\psi << \sigma_V, \sigma_\chi \rightarrow \quad 10\ \% \end{array}$$

and the rise at colour threshold could be very small.

Furthermore since the "average" quark charges are $\frac{2}{3}, -\frac{1}{3}, -\frac{1}{3}$ the parton sum rules for electroproduction remain untouched in our model.

We have no simple answer to the third problem. Clearly, given the freedom in the various form factors at the photon-quark vertices, there is no fundamental reason why G = - final states could not dominate over G = +. Whether or not this can be achieved with reasonable dynamical assumptions remains to be seen.

Finally, concerning the weak interaction, the possibilities mentioned in Section 2 can of course be taken over (with variations) in the three triplet model. The main problem here seems to be that we have too much freedom.

REFERENCES

1) See e.g. the talks by M. Breidenbach and B. Wiik in these proceedings.

2) Y. Hara, Phys. Rev. 134 B 701 (1964)
J.D. Bjorken and S.L. Glashow, Phys. Letters 11, 255 (1964)
S.L. Glashow, J. Iliopoulos and L. Maiani, Phys. Rev. D2, 1285 (1970)

3) M.Y. Han and Y. Nambu, Phys. Rev. 139 B, 1006 (1969)

4) See the talks of M. Gourdin, M.K. Gaillard, M. Altarelli and D. Schildknecht in these Proceedings
See also e.g. F.J. Gilman SLAC-PUB (Feb. 1975) and ref. (9)

5) S.L. Adler Brandeis Lectures 1970

6) S. Weinberg, Phys. Rev. Letters 31, 494 (1973)
D.V. Nanopoulos, Nuovo Cimento Letters 8, 873 (1973)

7) R.M. Barnett, Phys. Rev. Letters 34, 41 (1975) and Harvard report (February 1975)

8) J. Schwinger, Phys. Rev. D8, 960 (1973)

9) Three triplet models are reviewed by D.W. Greenberg Invited talk at Orbis Scientiae II (January 1975)

10) We are indebted to Dr. H. Osborn for informing us that such quarks have already appeared in the literature
T. Tati, Prog. Theor. Phys. 35, 126 (1966) ; 35, 973 (1966)
See Y. Nambu and M. Han, Phys. Rev. D10, 674 (1974)

COLOR AND THE NEW PARTICLES. A BRIEF REVIEW.

D. Schildknecht
Deutsches Elektronen-Synchrotron DESY,
Hamburg, Germany

Abstract : The possibility of interpreting the new particles as colored ω and ϕ mesons is discussed in the light of the experimental information available on widths and decay modes.

Résumé : Nous discutons de la possibilité d'interpréter les nouvelles particules comme des mesons colorés ω et ϕ à la lumière des données expérimentales existantes concernant les largeurs et les modes de désintégration.

COLOR AND THE NEW PARTICLES
A BRIEF REVIEW

1. Introduction

The experimental facts on the new particles[1] have been thoroughly reported on by the experimentalists at this meeting. The experimental data on production in hadron interactions, e^+e^- annihilation and photoproduction strongly suggest that the new particles are hadronic vector states. In Table 1 I only show masses and total and leptonic widths Γ and Γ_e of the new particles and refer to the experimental talks[2] for detailed information on the decay modes, which have been observed so far.

	Mass [GeV]	Γ [keV]	Γ_e [keV]
$J(3,1) \equiv \psi(3,1)$	3.095 ±0.004	69 ±15	4.8 ±0.6
$\psi(3,7)$	3.684 ±0.0005	$200 \leq \Gamma \leq 800$	2.2 ±0.5
$\psi(4,1)$	~4.1	~250 to 300 MeV	~4

Table 1

Because of the narrow widths of the new particles an interpretation seems most natural, which somehow introduces a new hadronic degree of freedom. Starting from the SU(3) classification of hadronic states in the language of the quark model, we have the following alternatives:

(1) We can extend the symmetry group according to $SU(3) \to SU(n)$ $(n \geq 4)$, specifically $SU(4)$[3], i.e. we add at least one new quark to the p, n, λ, triplet p, n, $\lambda \to$ p, n, λ, c. The charmed quark (antiquark) c $(\bar{c})$ carries the charm quantum number $C = +1$ (-1), while the p, n, λ quarks have $C = 0$. The new particles are interpreted as $c\bar{c}$ states in close analogy to $\phi = \lambda\bar{\lambda}$. The narrow widths are related to a suppression of their decays via Zweig's rule as in the case of $\phi \to 3\pi$. The charm option is being discussed by other speakers[4] at this meeting, and I will not go into it any further.

(2) We extend the SU(3) symmetry group of the hadrons via $SU(3) \to SU(3) \times G$ with an appropriately chosen group G. In the quark model language this possibility corresponds to attributing to the p, n, λ quarks an additional internal degree of freedom, "color", $p,n,\lambda \to p_i, n_i, \lambda_i$, where the "color index" i runs over e.g. three values i = 1, 2, 3. The ordinary hadrons are usually assumed to correspond to the singlet representation of G. The higher dimensional irreducible representations of G are supposed to be filled by particles of higher masses. Each ordinary hadron within an SU(3) multiplet will then have higher mass partners with the same SU(3) quantum numbers, the number of additional multiplets and the number of states within each multiplet being, of course, dependent on the group G and the representation chosen for the fundamental constituents. In order to accommodate the new particles, J(3.1) and ψ(3.7), which couple directly to the photon, the electromagnetic current in such a scheme clearly has to have a piece, which does not transform according to the singlet representation of G. Consequently, the charges assigned to the constituents, e. g. the three quark triplets, in such a scheme will have to depend on the color degree of freedom.

Historically, a color degree of freedom (with three colors) for the basic quarks has first been introduced[5] in order to have an antisymmetric ground state wave function for the baryons classified according to the 56 representation in SU(6) with symmetric SU(6) and space parts of the wave function. For the purpose of obtaining Fermi statistics for the quarks, and also the approximately correct ($s \lesssim 9$ GeV^2) values of

$$R = \sigma_{e^+e^- \to h} / \sigma_{\mu^+\mu^-} \cong 2 \qquad (1)$$

and of the $\pi^o \to 2\gamma$ width, the color degree of freedom need not be excited. One may thus assume that all observable hadrons are color singlet states, and likewise that the current operator and the charges of the quarks do not contain any additional color non singlet pieces. Such models[5,6]

thus clearly work with three triplets of quarks, which have identical third integral charges, and do not allow for additional color non singlet hadrons coupled directly to the photon.

The kind of color model which could be relevant for a description of the new particles, i. e. a model, in which the photon has an additional color non singlet component and the charges of the three triplets of quarks are different, has first been given by Han and Nambu[7]. The group G in this model is identified with an SU(3) group, i. e. the underlying symmetry is $SU(3) \times SU(3)^{color}$. In a model[8] worked out by Govorkov the $SU(3)^{color}$ group is replaced by the discrete permutation group S_3. This model has much in common with the Han Nambu model, but predicts a much smaller number of additional non singlet hadron states; in particular it does not require doubly charged mesons. Tati[9] replaces $SU(3)^c$ by $SO(3)^c$ as color group. In what follows, we will concentrate on models based on $SU(3) \times SU(3)^c$.

2. Models Based on $SU(3) \times SU(3)^c$

2.1. The Spectrum of States and the Electromagnetic Current in the $SU(3) \times SU(3)^c$ Model

The fundamental building blocks of hadronic matter, the quarks p_i, n_i, λ_i (i = 1, 2, 3), are described[7,10] by the (3,3) or $(3,3^*)$ representation of $SU(3) \times SU(3)^c$. The group SU(3) transforms p, n and λ, while $SU(3)^c$ acts on the color index i = 1, 2, 3. The ordinary hadrons are usually classified[11] as singlets with respect to $SU(3)^c$, i. e. we have e. g. for vector mesons

$$\rho^+ = \frac{1}{\sqrt{3}} (p_1 \bar{n}_1 + p_2 \bar{n}_2 + p_3 \bar{n}_3) \equiv (\rho^+, \omega_1),$$
$$\phi = \frac{1}{\sqrt{3}} (\lambda_1 \bar{\lambda}_1 + \lambda_2 \bar{\lambda}_2 + \lambda_3 \bar{\lambda}_3) \equiv (\phi, \omega_1) \quad \text{etc.} \tag{2}$$

Here we have introduced the notation $(\rho^+,\omega_1) \equiv (\rho^+, 1^c)$ to be used subsequently. ω_1 specifies the $SU(3)^c$ singlet character of the vector meson ρ^+ in distinction to the color octet states to be discussed subsequently. The usual particle names are thus used to indicate the color quantum numbers (e. g. color isospin and color hypercharge) of the particle in question. Instead of writing down the $q\bar{q}$ decomposition (2) of the states explicitly we will equivalently use a matrix notation in the $SU(3) \times SU(3)^c$ space by writing for e. g. the ϕ meson

$$(\phi,\omega_1) \equiv \begin{pmatrix} 0 & & \\ & 0 & \\ & & 1 \end{pmatrix} \times \begin{pmatrix} 1 & & \\ & 1 & \\ & & 1 \end{pmatrix} . \tag{3}$$

In addition to the color singlet (1^c) mesons the model predicts color octet (8^c) states. Each ordinary (1^c) meson with fixed SU(3) quantum numbers thus has an octet of colored partners with the same SU(3) (isospin and hypercharge), but different color quantum numbers. In particular, one will have the additional vector mesons

$$(\phi,8^c), \quad (\rho,8^c), \quad (\omega,8^c), \quad (K^*,8^c),$$

where 8^c runs through the $SU(3)^c$ octet. With ideal singlet octet mixing in ordinary SU(3) (i.e. $\phi = \lambda\bar{\lambda}$), which mixing will be assumed later on, we have e. g. for the ϕ meson the color neutral 8^c states

$$\begin{aligned} (\phi,\omega_8) &= -\frac{1}{\sqrt{6}} (\lambda_1 \bar{\lambda}_1 + \lambda_2 \bar{\lambda}_2 - 2\,\lambda_3 \bar{\lambda}_3) \\ (\phi,\rho^o) &= -\frac{1}{\sqrt{2}} (\lambda_1 \bar{\lambda}_1 - \lambda_2 \bar{\lambda}_2) \end{aligned} \tag{4}$$

and six more, which correspond to the six other members of the color octet.

The electric charge of the quarks in the Han Nambu model is additively composed of a color independent part Q^{GMZ} identical with the Gell-Mann Zweig charges of the usual quarks, and a color dependent part Q^c, the color charge

$$Q = Q^{GMZ} + Q^c$$
$$Q^{GMZ} = \begin{pmatrix} 2/3 & & \\ & -1/3 & \\ & & -1/3 \end{pmatrix} \times \begin{pmatrix} 1 & & \\ & 1 & \\ & & 1 \end{pmatrix} . \tag{5}$$

Q^c is restricted[7,12] by the obvious requirement that the charges of the ordinary (1^c) mesons and baryons come out correctly. Indeed, the charge of e. g. the $\rho^+ \equiv (\rho^+, \omega_1)$,

$$(\rho^+, \omega_1) = \frac{1}{\sqrt{3}} (p_1 \bar{n}_1 + p_2 \bar{n}_2 + p_3 \bar{n}_3) \tag{6}$$

is given by

$$Q^{\rho^+} = Q^{GMZ}(p_i) - Q^{GMZ}(n_i) + Q^c(p_i) - Q^c(n_i) \tag{7}$$
$$= 1 + Q^c(p_i) - Q^c(n_i),$$

and thus Q^c has to fulfill the condition

$$Q^c(p_i) = Q^c(n_i) = Q^c(\lambda_i), \quad i = 1, 2, 3, \tag{8}$$

where the generalisation to the λ quark is obtained by also looking at the charge of the $K^{*+} = \frac{1}{\sqrt{3}} (p_1 \bar{\lambda}_1 + p_2 \bar{\lambda}_2 + p_3 \bar{\lambda}_3)$. The color charge from (8) thus has to be a singlet in ordinary SU(3).

The charges of the ordinary (1^c) baryons yield an additional restriction on Q^c. In fact, in order to obtain the correct charge for the proton $p \sim \sum \varepsilon_{ijk} p_i p_j n_k$ we must have

$$Q^c(p_1) + Q^c(p_2) + Q^c(n_3) = 0 . \tag{9}$$

With (8), p and n in (9) may be replaced by arbitrary combinations of p, n, λ and thus we have

$$Q^c = \begin{pmatrix} 1 & & \\ & 1 & \\ & & 1 \end{pmatrix} \times \begin{pmatrix} a_1 & & \\ & a_2 & \\ & & a_3 \end{pmatrix} \quad \text{with} \quad \sum a_i = 0, \tag{10}$$

i. e. the matrix acting on the color indices has to be traceless.

Thus from the requirement that the charges of the ordinary mesons and baryons (classified as singlets under $SU(3)^c$) come out correctly, the color piece of the electromagnetic current has to transform as a singlet under $SU(3)$ and an octet under $SU(3)^c$,

$$J_\mu = J_\mu^{GMZ}(8,1^c) + J_\mu^c(1,8^c). \tag{11}$$

Assuming moreover that the photon conserves color, i. e. forbidding transitions such as $\gamma p_1 \to p_2$, the 8^c part must transform as the color neutral member of the octet; the matrix in (10) must be diagonal (and traceless). Requiring also integral charges for the quarks, we finally obtain

$$Q^c = 1 \times \frac{1}{3}\begin{pmatrix} -2 & & \\ & 1 & \\ & & 1 \end{pmatrix}, \tag{12}$$

or permutations thereof

$$Q^c = 1 \times \frac{1}{3}\begin{pmatrix} 1 & & \\ & 1 & \\ & & -2 \end{pmatrix}, \quad Q^c = 1 \times \frac{1}{3}\begin{pmatrix} 1 & & \\ & -2 & \\ & & 1 \end{pmatrix}, \tag{13}$$

which choices are equivalent, as long as no direction in color space is a preferred one. Clearly, as soon as color symmetry is broken by medium strong interactions, which then define a preferred direction in color, the choices (12) and (13) correspond to different physics. As only the relative directions of the photon and a possible symmetry breaking by medium stronginteractions are important, we will use[13] (12) in what follows without loss of generality, and will consider different choices of breaking color symmetry by medium strong interactions. The basic quarks then correspond to the $(3,3^*)$ representation, and the color charge is described by the U^c spin scalar U^c,

$$Q = \frac{1}{3}\left\{\begin{pmatrix} 2 & & \\ & -1 & \\ & & -1 \end{pmatrix} \times \begin{pmatrix} 1 & & \\ & 1 & \\ & & 1 \end{pmatrix} + \begin{pmatrix} 1 & & \\ & 1 & \\ & & 1 \end{pmatrix} \times \begin{pmatrix} -2 & & \\ & 1 & \\ & & 1 \end{pmatrix}\right\} \tag{14}$$

$$= U \times 1 + 1 \times U^c .$$

The modified Gell-Mann Nishijima formula reads

$$Q = I_3 + \frac{1}{2} Y + I_3^c + \frac{1}{2} Y^c, \tag{15}$$

and clearly implies the existence of doubly charged meson states. The quantum numbers of the (integrally charged) Han Nambu quarks are given in Table 2.

	I_3	Y	I_3^c	Y^c	Q^{GMZ}	Q^c	Q
p_1	1/2	1/3	-1/2	-1/3	2/3	-2/3	0
n_1	-1/2	1/3	-1/2	-1/3	-1/3	-2/3	-1
λ_1	0	-2/3	-1/2	-2/3	-1/3	-2/3	-1
p_2	1/2	1/3	1/2	-1/3	2/3	1/3	1
n_2	-1/2	1/3	1/2	-1/3	-1/3	1/3	0
λ_2	0	-2/3	1/2	-1/3	-1/3	1/3	0
p_3	1/2	1/3	0	2/3	2/3	1/3	1
n_3	-1/2	1/3	0	2/3	-1/3	1/3	0
λ_3	0	-2/3	0	2/3	-1/3	1/3	0

Table 2

The peculiar third integral Gell-Mann Zweig charges in such a scheme appear as average charges of the quarks and antiquarks, respectively, in the color singlet states. The ρ^+ for example,

$$(\rho^+, \omega_1) = \frac{1}{\sqrt{3}} (p_1 \bar{n}_1 + p_2 \bar{n}_2 + p_3 \bar{n}_3),$$

spends one third of the time in the color 1, 2, and 3 states, the average quark and antiquark charges being 2/3 and -1/3 respectively.

2.2. Number of Vector Mesons Coupled to the Photon.

Assignment of the New Particles

From the form of the electromagnetic current (11) and (14), we now can discuss the number of vector mesons coupled directly to the photon and their coupling strengths, turning to an assignment of the new particles to colored vector mesons subsequently. In my discussion I will largely follow the work by M. Krammer, F. Steiner and myself[14]. Surveys of possible interpretations of the J and ψ including the color interpretation have been given in reference 15. Color interpretations have also been discussed in the papers listed in references 16,17.

As the color singlet (1^c) part of the electromagnetic current transforms as the U spin scalar component of an SU(3) octet, with no breaking of SU(3) by strong interactions we would have one 1^c vector meson only (the U spin = 0 component of the octet) coupled to the photon. Actually, because of symmetry breaking by the medium strong interaction, we expect two, and due to singlet octet mixing there are even three 1^c vector mesons coupled to the photon, the well known ρ^o, ω and ϕ. Schematically the situation for the 1^c states may be presented as follows:

$$1^c : \quad (\omega_8^{U=0}, \omega_1) \begin{cases} (\rho^o, \omega_1) \\ (\omega_8, \omega_1) \end{cases} \begin{cases} (\omega, \omega_1) \\ (\phi, \omega_1) \end{cases} \tag{16}$$

Next, let us look at the color octet (8^c) part of the electromagnetic current . As this part transforms as a singlet under SU(3), a priori, colored versions of the SU(3) singlet state, ω_1, only should be coupled directly to the photon. Within the quark model it seems natural, however, to assume ideal singlet octet mixing in SU(3) also for the color octet vector mesons. Then colored versions of ω and ϕ, consisting of non-strange and strange quarks respectively, should couple to the photon. (Colored ρ^o mesons cannot couple directly.) As the color octet part of the

electromagnetic current has been assumed to transform as a color U spin scalar, a maximum number of two additional colored ω and ϕ mesons may be expected. They correspond to the two $I_3^c = 0$, $Y^c = 0$ members of the color octet:

$$8^c : \quad (\omega_1, \rho_\omega^o) \begin{cases} (\omega, \rho_\omega^o) \\ (\phi, \rho_\omega^o) \end{cases} \tag{17}$$

Whether there are actually two colored ω and two colored ϕ mesons coupled to the photon, or whether the two states are degenerate, depends upon symmetry breaking in $SU(3)^c$.

In fact, if $SU(3)^c$ symmetry is exact except for electromagnetism, then the eigenstates of the mass matrix are Q^c, U^c multiplets within the color octet. The photon couples to the $Q^c = 0$, $U^c = 0$ member of the octet only:

$$8^c : \quad (\omega_1, \omega_8(U^c = 0)) \begin{cases} (\omega, \omega_8(U^c = 0)) \\ (\phi, \omega_8(U^c = 0)) \end{cases}$$

The relativ vector meson photon couplings $1/\gamma_V$ appearing in the matrix element

$$\langle 0 | J_\mu(0) | V \rangle = \frac{m_V}{2\,\gamma_V}\,\varepsilon_\mu \qquad \text{are then obtained} \tag{18}$$

from the $SU(3) \times SU(3)^c$ wave functions of the particles and the quark charges in Table 2. From

$$(\omega, \omega_8(U^c{=}0)) = \frac{1}{\sqrt{12}} (-2\, p_1 \bar{p}_1 + p_2 \bar{p}_2 + p_3 \bar{p}_3 - 2\, n_1 \bar{n}_1 + n_2 \bar{n}_2 + n_3 \bar{n}_3), \tag{19}$$

and

$$(\phi,\omega_8(U^c=0)) = \frac{1}{\sqrt{6}}(-2\,\lambda_1\,\bar{\lambda}_1 + \lambda_2\,\bar{\lambda}_2 + \lambda_3\,\bar{\lambda}_3)\,,$$

we obtain

$$\gamma^{-2}_{(\omega,\omega_8)} : \gamma^{-2}_{(\phi,\omega_8)} = 2 : 1\,. \tag{20}$$

Combined with the well known relation for color singlets we have

$$\gamma_\rho^{-2} : \gamma_\omega^{-2} : \gamma_\phi^{-2} : \gamma^{-2}_{(\omega,\omega_8)} : \gamma^{-2}_{(\phi,\omega_8)} = 9 : 1 : 2 : 8 : 4\,. \tag{21}$$

The coupling of the $U^c = 1$ states may clearly be explicitly checked to be zero from the decomposition

$$\begin{aligned}(\omega,\rho(U^c=1)) &= \frac{1}{2}(p_2\,\bar{p}_2 - p_3\,\bar{p}_3 + n_2\,\bar{n}_2 - n_3\,\bar{n}_3),\\ (\phi,\rho(U^c=1)) &= \frac{1}{2}(\lambda_2\,\bar{\lambda}_2 - \lambda_3\,\bar{\lambda}_3)\,.\end{aligned} \tag{22}$$

When deriving the ratios for the photon couplings, $SU(3) \times SU(3)^c$ symmetry of the dynamical part (the configuration space wave function in a quark model approach) of the matrix element (18) has of course been assumed. The 9 : 1 : 2 ratio for $\gamma_\rho^{-2} : \gamma_\omega^{-2} : \gamma_\phi^{-2}$ is empirically valid within experimental errors. There may be stronger symmetry breaking, however, when comparing color singlet with color octet couplings. The conclusions on the ratios (21) of the coupling constants and on the number of states coupled to the photon directly remains unchanged, if there is breaking of color symmetry by medium strong interactions, as long as the breaking is in the direction of the photon.

<u>If $SU(3)^c$ is broken by medium strong interactions in a direction different from the photon direction</u>, i. e. if the color octet breaks up into Y^c, I^c multiplets (whereas the photon transforms as a U^c spin scalar), then diagonalisation of the mass matrix leads to $\omega_8^c(I^c=0)$ and $\rho_o^c(I^c=1)$ states both coupled to the photon. The states

$$(\omega,\omega_8(I^c=0)),\quad (\omega,\rho^o(I^c=1)) \tag{23}$$

and

$$(\phi, \omega_8(I^c=0)), \quad (\phi, \rho^o(I^c=1)) \tag{24}$$

are simply obtained by cyclic permutation $123 \to 312$ from the $U^c = 0, 1$ states given in (19) and (22). The relative couplings for the four vector mesons are given in Table 3 (case B) together with the couplings (21) obtained for the case discussed before.

		Case A		Case B	
	ω_1^c	$\omega_8^c(U^c=0)$	$\rho^c(U^c=1)$	$\omega_8^c(I^c=0)$	$\rho^c(I^c=1)$
ρ^o	$\frac{3}{\sqrt{6}}$	0	0	0	0
ω	$\frac{1}{\sqrt{6}}$	$\frac{2\sqrt{2}}{\sqrt{6}}$	0	$\frac{-\sqrt{2}}{\sqrt{6}}$	$\frac{-\sqrt{6}}{\sqrt{6}}$
ϕ	$\frac{\sqrt{2}}{\sqrt{6}}$	$\frac{-2}{\sqrt{6}}$	0	$\frac{1}{\sqrt{6}}$	$\frac{\sqrt{3}}{\sqrt{6}}$

Table 3

The experimental observation of only two narrow states then suggests case A to be realized in nature and to make the assignment (Krammer, Schildknecht, Steiner[14] and Bars and Peccei[16])

$$\begin{aligned} J(3.1) &\equiv (\omega, \omega_8(U^c=0)), \\ \psi(3.7) &\equiv (\phi, \omega_8(U^c=0)) . \end{aligned} \tag{25}$$

The broader state at 4.1 GeV is then interpreted[14] as a recurrence (radial excitation) of the one at 3.1 GeV.

Alternatively, one may assume case B, strong breaking of $SU(3)^c$ symmetry in a direction different from the photon direction. In such a case it is tempting to identify (e. g. Stech[16])

$$
\begin{aligned}
J(3.1) &\equiv (\omega, \rho^o(I_c=1)), \\
\psi(3.7) &\equiv (\phi, \rho^o(I_c=1)), \\
J(4.1) &\quad (\omega, \omega_8(I_c=0)),
\end{aligned}
\tag{26}
$$

while evidence for the fourth state to be expected around 4.8 GeV is still missing. The above assignment seems to be preferable to (e. g. Sanda and Terazawa[16])

$$
\begin{aligned}
J(3.1) &\equiv (\omega, \rho^o(I_c=1)), \\
\psi(3.7) &\equiv (\omega, \omega_8(I_c=0)), \\
J(4.1) &\equiv (\phi, \rho^o(I_c=1)),
\end{aligned}
\tag{27}
$$

as a strong color isospin breaking must be invoked in (27) to allow for the observed cascade decay $\psi(3.7) \to J(3.1) + \pi\pi$, while otherwise $SU(3)^c$ should not be too badly broken, because of the narrow width of $J(3.1)$.

3. Experimental Consequences, Difficulties of the Color Interpretation

Let us now come to a discussion of consequences and experimental tests of the interpretation of the new particles as color excitations. We will concentrate on the assignment (25) corresponding to unbroken color symmetry or breaking of color symmetry in the photon direction. The main features of the color interpretation may be seen within this assignment[14].

3.1. $J(3.1)$ and $\psi(3.7)$ as Colored ω and ϕ

Photon Couplings: With the assignment (25)

$$
\begin{aligned}
J(3.1) &\equiv (\omega, \omega_8(U^c=0)) \\
\psi(3.7) &\equiv (\phi, \omega_8(U^c=0))
\end{aligned}
$$

the photon couplings should be in the ratio 2 : 1. Experimentally we have from Table 1 ($\Gamma_e = \alpha^2 \pi m_V/3 \gamma_V^2$)

$$\gamma_J^{-2} : \gamma_\psi^{-2} = 2.6 \pm 0.6 , \tag{28}$$

which is compatible with the prediction.

Additional States Predicted. Within the quark model, from the assignment (25) we may immediately obtain a naive estimate of the masses of the colored partners of ω and ϕ, namely $(\rho,\omega_8(U^C=0))$ and $(K^*,\omega_8(U^C=0))$. If the mass differences between the particles within the vector meson nonet are attributed to mass differences between nonstrange and strange quarks ($m_n = m_p \equiv m$; $m_\lambda = m + \Delta$), with ideal mixing we have

$$m_\rho^2 = m_\omega^2 , \tag{29}$$

and from

$$\begin{aligned} m_\phi^2 &= (m_\omega + 2\Delta)^2 \cong m_\omega^2 + 4\, m_\omega\, \Delta , \\ m_{K^*}^2 &= (m_\omega + \Delta)^2 \cong m_\omega^2 + 2\, m_\omega\, \Delta , \end{aligned} \tag{30}$$

also the relation

$$2\, m_{K^*}^2 = m_\phi^2 + m_\rho^2 . \tag{31}$$

Both, (29) and (31), as is well known, are fulfilled within a few percent for ordinary (1^C) vector mesons. Relations (29) and (31) should likewise hold for the color octet, and one predicts from the masses of J(3.1) and ψ(3.7) the masses of the colored ρ and K^* mesons to be

$$\begin{aligned} m[(\rho,\omega_8(U^C=0))] &= 3.1 \text{ GeV}, \\ m[(K^*,\omega_8(U^C=0))] &= 3.4 \text{ GeV}. \end{aligned} \tag{32}$$

As Δ is fixed by the masses of the color singlet states, consistency of the scheme requires the mass splittings of 1^C and 8^C mesons to be related by

$$m^2_{(\phi,\omega_8)} - m^2_{(\omega,\omega_8)} = (m^2_\phi - m^2_\omega)\frac{m_{(\omega,\omega_8)}}{m_\omega} \qquad (33)$$

which yields $m(\phi,\omega_8) = 3.41$ GeV instead of the experimental value of 3.7 GeV, if the mass of $J(3.1)$ is used as input. These naive estimates of the masses are thus not quantitatively consistent. Nevertheless, (32) may still be used as a reasonable guide; with the colored ϕ lying at 3.4 GeV, instead of at 3.7 GeV, the K^* mass would have shifted to about 3.3 GeV.

Each one of the color neutral vector mesons should be accompanied by other partners from the color octet. With no symmetry breaking in a direction different from the photon direction, there will be degeneracy between states of equal color charge. If mass splitting is due to electromagnetism only, it may be on the 1 % or 2 % level, i. e. 30 or 60 MeV. Non-neutral members of color octets would be weakly decaying long living states, some of them with ordinary and color electromagnetic charge, i. e. doubly charged.

Besides colored vector mesons, the color interpretation would require colored pseudoscalars in roughly the same mass range, and many further meson states[17] besides colored baryons, etc. We are not going into further discussions of the complete spectroscopy.

Hadronic Decays. Invariance of the interaction under the color group requires color conservation,

$$8^c \not\to 1^c + 1^c,$$

i. e. the decay of the colored vector mesons into ordinary hadrons is forbidden. This is the color interpretation of the narrow widths of $J(3.1)$ and $\Psi(3.7)$. The transition

$$8^c \to 8^c + 8^c$$

is allowed by color symmetry, but forbidden by sphase space, if 8^c states are assumed to be in the vicinity of 3 GeV. The transition

$$8^c \rightarrow 8^c + 1^c$$

requires closer inspection. For $\underline{J(3.1) \equiv (\omega,\omega_8)}$, the decays corresponding to $\omega \rightarrow 3\pi$, namely

$$\begin{aligned} J(3.1) \rightarrow\ & (\pi^o,\omega_8)\ \pi^+\ \pi^-, \\ & (\pi,\omega_8)\ \rho, \\ & (\rho,\omega_8)\ \pi, \end{aligned} \tag{34}$$

are again prohibited because of lack of phase space. The narrow width of J(3.1) yields lower limits for the colored pseudoscalars.

For the $\underline{\psi(3.7) \equiv (\phi,\omega_8)}$, we expect the decays .

$$\begin{aligned} \psi(3.7) \equiv (\phi,\omega_8) &\rightarrow (\omega,\omega_8) + \begin{cases} \pi^+\ \pi^- \\ \pi^o\ \pi^o \\ \eta \end{cases} \\ &\equiv J(3.1) + \begin{cases} \pi^+\ \pi^- \\ \pi^o\ \pi^o \\ \eta \end{cases} \end{aligned} \tag{35}$$

which are the observed cascade decays, the evidence for which has been thoroughly discussed in the experimental talks[2]. These decays are suppressed by Zweig's rule[18], much in analogy to $\phi \rightarrow \rho^o\ \pi$.

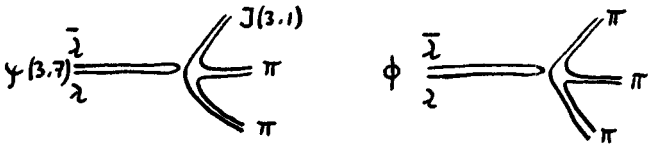

The decay

$$\psi(3.7) \equiv (\phi,\omega_8) \to (\rho^{\pm},\omega_8)\,\pi^{\mp} \tag{36}$$

is also suppressed by Zweig's rule, but from the above estimate (32) of the mass of the colored ρ is a rather crucial test of the model, as it seems hard to shift the (ρ,ω_8) mass to beyond the threshold of about 3.5 GeV. If (32) is correct, the decay should give a clean monoenergetic pion signal, as the colored ρ should be a narrow state. If its mass lies above 3.1 GeV, the colored ρ is expected to be broader, however, since cascade decay according to $(\rho,\omega_8) \to (\omega,\omega_8)\,\pi \equiv J(3.1)\,\pi$ becomes possible. The process would then contribute to the cascade $\psi(3.7) \to J(3.1) + \pi^+\,\pi^-$. To my knowledge, definite upper limits on reaction (36) have not been given as yet. Also by Zweig's rule suppressed are the modes

$$\begin{aligned} \psi(3.7) \to\ & (\pi^o,\omega_8)\,\rho, \\ & (\pi^o,\omega_8)\,\pi^+\,\pi^-, \end{aligned} \tag{37}$$

which, if nonexistent, put a lower limit on masses of colored pseudoscalars. The decays

$$\begin{aligned} \psi(3.7) \to\ & (K^{\pm},\omega_8)\,K^{\mp} \\ & (\eta,\omega_8)\,\omega \to (\eta,\omega_8)\,\pi^+\,\pi^-\,\pi^o \end{aligned} \tag{38}$$

are neither forbidden by color conservation nor inhibited by Zweig's rule and thus yield definite lower limits for the colored pseudoscalars, namely $m(K,\omega_8) \gtrsim 3.2$ GeV and $m(\eta,\omega_8) \gtrsim 3.2$ GeV.

Radiative Decays. Among the transitions $8^c \to 8^c + 1^c$ are the radiative decays, in which the 8^c vector mesons lose their color by radiating off a 8^c photon. These decays constitute the

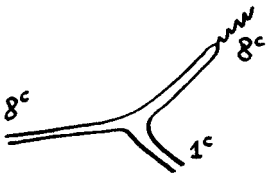

big problem of the color interpretation, as naive estimates indicate a width of these decays, which is orders of magnitude larger than the measured one. In fact, by simply starting from the measured width of $\omega \to \pi^o\gamma$, $\Gamma_{\omega\pi^o\gamma} = 0.9$ MeV and taking into account the enormous phase space available for $J(3.1) \to \eta\gamma$ according to

$$\Gamma = \alpha\, g^2\, p^3_{C.M.}/3, \tag{39}$$

one obtains $\Gamma_{J\to\eta\gamma} \sim 15$ MeV. Implicitly it has been assumed in this argument that the coupling $g_{8^c8^c1^c}$ between two 8^c and a 1^c state appearing in the J(3.1) decay is of the same magnitude as the color singlet coupling, $g_{1^c1^c1^c}$, of relevance for the ω decay. In the paper[14] by Krammer, Steiner and myself it has been argued that there may be a strong suppression $g_{8^c8^c1^c} \ll g_{1^c1^c1^c}$. Evidence for such a suppression effect has been given[14] by analysing the 8^c photon contribution to the $\eta \to \gamma\gamma$ decay within a vector dominance framework. From the measured $\eta \to \gamma\gamma$ and $\pi^o \to \gamma\gamma$ width, we concluded that in fact a strong suppression of the $V(8^c)V(8^c)$ $PS(1^c)$ couplings compared with the $V(1^c)V(1^c)PS(1^c)$ couplings should be expected.

Quite apart from the (as yet not convincingly solved) problem[19] of the absolute magnitude of the (radiative) widths, it is a firm prediction of the color scheme that the radiative decays $J, \psi \to \gamma +$ hadrons should be dominant. At this meeting we have heard that the DASP group at DESY has identified events for the reaction $J(3.1) \to \eta\,\gamma$ giving limits of $0.1\ \text{keV} < \Gamma_{\eta\gamma} < 2.0\ \text{keV}$. The decay width for this transition is quite small, but it may be considered a positive point for color that it does exist. The prominent radiative decays may actually be multibody decays, such as

$$J \to \pi^+\pi^-\gamma,\quad \pi^+\pi^-\pi^+\pi^-\gamma,\quad \pi^+\pi^-\pi^+\pi^-\pi^+\pi^-\gamma. \tag{41}$$

As we have heard from the SPEAR group[2], there is actually a considerable fraction of events of the type

$$J(3.1) \to \pi^+\pi^-\pi^+\pi^- X_{\text{neutral}},\quad \pi^+\pi^-\pi^+\pi^-\pi^+\pi^- X_{\text{neutral}}, \tag{42}$$

where the system X has not been directly observed, its mass being consistent with zero (i. e. the photon mass) and the π^o mass. Assuming that X is a π^o, a peak at the ω mass has been found, which shows that the missing neutral system X cannot always be a photon. Further conclusions cannot be drawn at the moment, except for the rather obvious remark: If the major decay mode of the J(3.1) is an odd number of pions (i. e. of the type of the color forbidden decay $8^c \to 1^c + 1^c$), while the color allowed decay into γ + hadrons constitutes a negligible fraction, then there is no reason to keep the color interpretation any longer. Conversely, if the radiative decays are dominant after all, the color interpretation may well be on the right track, and we may look for an explanation of the small absolute value of the total (radiative) width with increased confidence in the model. Let me also remind you of the fact that the so called "energy crisis" i. e. an appreciable increase[20] of the neutral to charged energy ratio in the region around 3.8 GeV, where R seems to rise, is still present, and colored photons would still be an attractive resolution.

Recurrences of J(3.1), ψ(3.7). Via "new duality"[21], recurrences of J(3.1) and ψ(3.7), i.e. of the colored ω and ϕ respectively, may be predicted as follows. First of all, for color singlet vector mesons, by requiring scaling of $\sigma_{e^+e^- \to \text{hadrons}}$ (i.e. constancy of R) with the

scale being set by the low lying leading vector mesons, we simply have[21,22]

$$R(1^c) = \sum_{\rho^o,\omega,\phi} R_V = \frac{3\pi}{4} \sum_V \frac{1}{(\gamma_V^2/4\pi)} \cdot \cdot \frac{m_V^2}{\Delta m_V^2} \Theta\left(s - (m_V^2 - \frac{\Delta m_V^2}{2})\right) . \tag{43}$$

With a Veneziano type mass spectrum[23], $m_n^2 = m_\rho^2(1 + 2n)$, $n = 0, 1, \ldots$, and the measured values of the ρ^o, ω, ϕ photon couplings, one obtains $R \cong 2.5$ from (43) which is in agreement with experiment below about 3 GeV, where effects due to the production of J and ψ start to set in. This value of $R \cong 2.5$ roughly coincides with the value obtained from the squares of the color singlet parts of the quark charges, $R = \sum (Q^{GMZ})^2 = 2$. Thus in ref. 14, we have speculated that consistency between R obtained via "new duality" and the squares of the quark charges should also hold for the production of colored vector states, i. e.

$$R(8^c) = R_J + R_\psi = 2.$$

Inserting masses and photon couplings for J and ψ, a level spacing $\Delta m_V^2(8^c) = 6.8$ GeV^2 is obtained, which is dramatically different from the level spacing of ordinary vector mesons. The masses of the recurrences and the leptonic widths thus predicted are listed in Table 4. The state at about 4.1 GeV and its leptonic width nicely fit into the scheme and have actually been predicted[14] prior to the confirming data. If our conjecture of the 4.1 GeV state being a recurrence of the one at 3.1 GeV is correct, we expect a strong cascade decay of $J'(4.1) \to J(3.1)$. No evidence for the required recurrence of the colored ϕ has been reported so far. Figure 1 shows how the asymptotic value of R interpolates the low lying resonances which separately set the scale for each particular kind of hadronic matter coupled to the photon.

n		mass [GeV]	e^+e^- width [keV]
0	$J(3.1) \equiv (\omega, \omega_8^c)$	3.105 (input)	4.8 ±0.6 (input)
1	J'	4.05	3.7
2	J"	4.8	3.1
0	$\psi(3.7) \equiv (\phi, \omega_8^c)$	3.7 (input)	2.2 ±0.5 (input)
1	ψ'	4.5	1.8
2	ψ''	5.2	1.6

Table 4

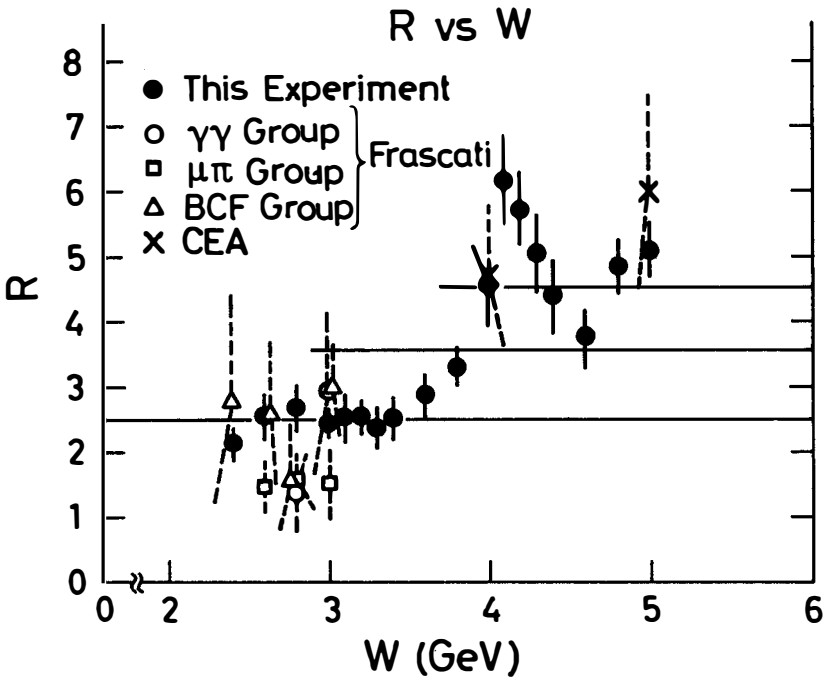

Fig. 1 The contributions to R dual to ρ, ω, φ and to J(3.1) and ψ(3.7). Compare ref. 2 for data.

4. Summarizing Conclusions

I have concentrated on color and the new particles and could not comment on deep inelastic scattering and weak interactions in this brief review[24]. Let me summarize the main points, which have been made. The ratios of the leptonic widths of the new particles (including the 4.1 GeV state) can be nicely accommodated within the color scheme, and likewise, suppressing the hadronic widths via color conservation and the cascade decay via Zweig's rule, does not pose serious problems. The extreme narrowness of the total widths, i. e. the strong suppression of the radiative decays (assuming the color interpretation to be correct) constitutes a big problem. Nevertheless, I think it would be premature to give up the color model, as long as the most firm prediction of the model, dominance of the radiative decay modes, does not seem to be ruled out. It is satisfying that the color scheme may be readily disproved by just looking at the J(3.1) decays: If the color forbidden ($J(3.1) \to$ hadron, e. g. many pions) turns out to be allowed in nature, while the color allowed ($J(3.1) \to$ hadrons + γ) is forbidden, there will be no reason to keep the scheme any longer.

Acknowledgement

I would like to thank my collegues in Hamburg for extensive useful discussions, especially M. Krammer and F. Steiner.

References and Footnotes

1) J.J. Aubert et al., Phys. Rev. Letters 33, 1404 (1974).
J.-E. Augustin et al., Phys. Rev. Letters 33, 1406 (1974).

2) Compare the contributions by M. Breidenbach, J.A. Kadyk and B. Wiik, these proceedings.

3) J.D. Bjorken and S. Glashow, Phys. Letters 11, 255 (1964).
Z. Maki, Progr. Theoret. Phys. 31, 331 (1964).
Y. Hara, Phys. Rev. 134, B701 (1964).

4) M.K. Gaillard, M. Gourdin, J. Kuti, these proceedings.

5) O.W. Greenberg, Phys. Rev. Letters 13, 598 (1964).
O.W. Greenberg and D. Zwanziger, Phys. Rev. 150, 1177 (1966).

6) M. Gell-Mann, Acta Physica Austriaca Supp. 9, 733 (1972).
W.A. Bardeen, H. Fritzsch and M. Gell-Mann, in Scale and Conformal Symmetry in Hadron Physics, ed. R. Gatto (Wiley, New York, 1973) p.139.

7) M.Y. Han and Y. Nambu, Phys. Rev. 139, B1006 (1965).
Y. Nambu and M.Y. Han, Phys. Rev. 10D, 674 (1974).

8) A.B. Govorkov, JINR P2-5871, Dubna 1971.
S.B. Gerasimov and A.B. Govorkov, Dubna preprint E2-8472 (1974).
See also N.N. Bogolubov et al., JINR P-2141, Dubna 1965.
A. Tavkhelidze, Proc. of the Seminar on High Energy Physics and Elementary Particles, Trieste, 1965 (IAEA, Vienna, 1965), p. 763.

9) T. Tati, Prog. Theoret. Phys. 35, 126 (1966) and 35, 973 (1966).

10) N. Cabibbo, L. Maiani and G. Preparata, Phys. Lett. 25B, 132 (1967).
See also J.C. Pati and C.H. Woo, Phys. Rev. D3, 1173 (1971).

11) See however F.E. Close and J. Weyers, UCL-IPT-75/06, Louvain preprint and these proceedings. These authors do not classify the ordinary hadrons as color singlets.

12) H.J. Lipkin, Physics Reports 8c, 173 (1973).

13) This is in contrast to the convention adopted by Krammer, Steiner and myself in reference 14, where we fixed the direction of $SU(3)^C$ symmetry breaking by medium strong interactions (I^C,Y^C base) and changed the photon direction ($U^C = 0$ and $I^C = 0$ models).

14) M. Krammer, D. Schildknecht and F. Steiner, DESY 74/64 (1974).
Phys. Rev. to be published.

15) H. Harari, SLAC-PUB-1514 (1974).
CERN Boson Theory Workshop, CERN TH.1964 (1974).
I. Bars et al., SLAC-PUB-1522 (1975).

16) I. Bars and R.D. Peccei, Phys. Rev. Letters 34, 985 (1975),Stanford preprint, ITP-484.
A.I. Sanda and H. Terazawa, Rockefeller University preprint COO-2232B-70.
B. Stech, preprint Heidelberg 1974.
N. Marinescu and B. Stech, HD-THEP-75-4.
W. Alles, Bologna preprint, 1974.
T.C. Yang, University of Maryland, 75-052 (1975).
B.G. Kenny, D.C. Peaslee and L.J. Tassie, Phys. Rev. Letters 34, 429 (1975).
S.B. Gerasimov and A.G. Govorkov, Dubna E2-8656.
S.Y. Tsai, Nihon University preprint.
S. Hori, T. Suzuki, A. Wakasa, E. Yamada, Kanazawa University preprint.

17) S. Kitakado and T.F. Walsh, DESY 75/02 (1975).

18) G. Zweig, in Symmetries in Elementary Particle Physics (Academic Press) New York 1969, p. 192.

19) Further comments on the problem of the radiative width may be found in references 15 and 16.

20) B. Richter, Proc. of the Internat. Conf. on High Energy and Elementary Particle Physics, London, 1974, p. IV-37.

21) A. Bramon, E. Etim and M. Greco, Phys. Letters 41B, 609 (1972).
J.J. Sakurai, Phys. Letters 46B, 207 (1973).
M. Böhm, H. Joos and M. Krammer, Acta Physica Austriaca 38, 123 (1973).

22) D. Schildknecht and F. Steiner, Phys. Letters 56B, 36 (1975).

23) The level spacing $\Delta m^2 = 2\, m_\rho^2$ requires the existence of a $\rho'(1250)$ meson. See e. g. M. Conversi et al., Phys. Letters 52B, 493 (1974) for the empirical evidence for its existence.

24) While the written version of this talk was completed, I obtained the recent excellent review by O.W. Greenberg on the color scheme (University of Maryland, report No. 75-064), to which I refer for additional information.

CHARM

Mary K. Gaillard
CERN, Geneva, Switzerland

and

Laboratoire de Physique théorique et Particules élémentaires
Orsay, France

Abstract : The expected properties of charmed particles are briefly reviewed and discussed in the light of recent data, with emphasis on the properties of the newly observed resonances.

Résumé : La phénoménologie du charme est rapidement passée en revue. L'interprétation des nouvelles résonances dans le cadre du charme est discutée, ainsi que d'autres observations expérimentales récentes.

1. INTRODUCTION

Before discussing the more phenomenological aspects of charmed particles, I shall give a flash review of the underlying theory.

When the quantum number dubbed "charm" by Bjørken and Glashow was first introduced[1], one of the motivations was lepton-hadron symmetry. With the addition of a fourth quark, the left-handed components of quarks and leptons form four doublets:

$$\begin{pmatrix}\nu_e\\ e\end{pmatrix}_L , \quad \begin{pmatrix}\nu_\mu\\ \mu\end{pmatrix}_L , \quad \begin{pmatrix}p\\ n_c\end{pmatrix}_L , \quad \begin{pmatrix}c\\ \lambda_c\end{pmatrix}_L \tag{1}$$

which characterize their weak couplings. Here c is a "charmed" quark and

$$n_c = n \cos\theta_c + \lambda \sin\theta_c , \quad \lambda_c = \lambda \cos\theta_c - n \sin\theta_c ,$$

(where θ_c is the Cabibbo angle) are the eigenstates of "weak isospin" (as opposed to n and λ which are eigenstates of strong interactions). For fractionally charged quarks, leptons and quarks are distinguished by their "weak hypercharge", related to electric charge by

$$Y^W = Q - I_3^W .$$

Right-handed fermions are scalars under weak isospin with hypercharge $Y^W = Q$. According to the Weinberg-Salam model[2], the weak and electromagnetic interactions arise through the coupling of fermions to weak isospin and hypercharge gauge bosons:

$$\mathcal{L}_{weak} = g\left(\sum_i \psi_L^i \frac{\vec{\tau}}{2} \psi_L^i\right) \cdot \vec{W} + g'\left(\sum_i \psi^i Y^W \psi^i\right) B . \tag{2}$$

The theory is renormalizable if

a) all particles are massless (bosons must be massless to ensure local gauge invariance, and fermion masses would break weak isospin which acts only on the left-handed components of the fields), and

b) all interactions are invariant under weak hypercharge and isospin gauge transformations.

In practice these requirements are badly broken; however, renormalizability remains if the symmetry is broken only through couplings to Higgs scalars. In the simplest model one introduces only one Higgs scalar field $\phi = \begin{pmatrix} \phi^+ \\ \phi_0 \end{pmatrix}$ which is a "weak isodoublet", and its Hermitian conjugate. Its couplings to fermions must be invariant:

$$\mathcal{H}_{\phi f} = g_{ij}\bar{\psi}^i_R(\phi^\dagger \psi^j_L) + g'_{ij}\bar{\psi}^i_R\left[\phi^T(-i\tau_2)\psi^j_L\right] + \text{h.c.} \qquad (3)$$

and the observed symmetry breaking must occur only through a non-vanishing expectation value of the neutral component of the Higgs field:

$$\langle\phi_0\rangle_0 = \langle\bar{\phi}_0\rangle_0 = \lambda \neq 0 \ . \qquad (4)$$

Redefining the field so that $\phi' = \phi - \lambda$ has no vacuum expectation value, one generates an effective (non-diagonal) mass term in the Lagrangian:

$$\mathcal{L}_{\phi f} \to \mathcal{L}_{\phi' f} + \lambda g_{ij}\bar{\psi}^i_R(\psi^j_L)_2 + g'_{ij}\bar{\psi}^i_R(\psi^j_L)_1\Big] + \text{h.c.}$$

Similarly, a mass term for vector bosons is generated through their couplings to the Higgs scalars. Since the Higgs couplings as well as the symmetry breaking conserves charge, the mass matrices generated by the Higgs mechanism mix only charge-degenerate fields. Thus W_3 and B will mix, yielding one massless state coupled to the electromagnetic charge:

$$A = \cos\theta_w B + \sin\theta_w W_3 \ ,$$

and a massive vector boson:

$$Z^0 = \cos\theta_w W_3 - \sin\theta_w B \ .$$

The lepton mixing is not observable if the neutrinos are both massless (i.e. degenerate); ν_e is by definition the state which couples to the electron. For the quarks there is one observable mixing angle which by convention is the Cabibbo angle describing the n,λ mixing.

The important point here is that the mixing conserves the weak quantum numbers, I_3^W and Y^W. Since the neutral currents are diagonal and couple to these quantum numbers, under which n_c and λ_c are degenerate, these currents

are invariant under Cabibbo mixing:

$$J^0 \sim \bar{n}_c n_c + \bar{\lambda}_c \lambda_c = \bar{n}n + \bar{\lambda}\lambda \ .$$

Thus no strangeness-changing neutral currents are induced. Moreover, in the limit of p, c mass degeneracy, no effective $\lambda \leftrightarrow n$ transition can be induced in any order[3]. In order to understand the observed suppression of $K_L \to \mu^+\mu^-$, $K \to \pi\nu\bar{\nu}$, etc., it is sufficient that the p, c mass splitting be small on a mass scale determined by the weak interactions:

$$m_c - m_p << (m_W \sin^2 \theta) = 38 \text{ GeV} \ .$$

Indeed, the observed non-suppression of $K_L \to \gamma\gamma$ requires that the c, p degeneracy be badly broken on a hadronic mass scale[4].

As stated above, renormalizability of the theory requires that strong interactions (except for mass terms) be invariant under weak isospin and hypercharge. Together with parity and "strong" isospin conservation, this constraint implies invariance under chiral SU(4) $\otimes$ SU(4). Further restrictions arise from the non-observation of parity and strangeness-violating effects of order α. Such effects have been shown to be absent[5] provided that strong couplings also occur through a gauge-invariant coupling of quarks to vector bosons, and that the gauge group of strong interactions commutes with the gauge group of weak interactions. One possibility is that the strong gauge group is "colour SU(3)" (colour being the additional degree of freedom for quarks which allows fermi-statistics for quarks, a correct prediction for the π^0 decay rate, etc.). In this case the strong interactions are "asymptotically free" [6] -- providing, for example, an understanding of the observed scaling in deep inelastic lepton production. It is this theory that we shall adopt whenever strong interactions are relevant.

2. CHARM SPECTROSCOPY AND THE NEW RESONANCES

The postulate of a fourth quark, together with the requirement of SU(4) invariant couplings, leads us to anticipate bound states involving charmed quarks; these states should complete the observed hadron multiplets to form irreducible representations[7,8] of SU(4). For example, along with the meson nonets, there will be the SU(3) representations:

$$\bar{3}: \quad (c\bar{p}),\ (c\bar{n}),\ (c\bar{\lambda}) \equiv \begin{cases} D^+ ,\ D^0 ,\ F^+ & (0^-) \\ D^{+*},\ D^{0*},\ F^{+*} & (1^-) \end{cases} , \tag{5}$$

the conjugate representation 3, and an SU(3) singlet $\bar{c}c$ which may mix with the other I = Y = 0 states. Together these multiplets form an SU(4) 16-plet ($15 \oplus 1$) for each spin-parity. Similarly the baryon octet is extended to an SU(4) 20-plet, with the additional states listed in Table 1. The $(3/2)^+$ baryon states form a different 20-plet, i.e. with different SU(3) structure, containing the known decouplet.

The mass scale for charmed particles is *a priori* unknown -- apart from the remark made above that the symmetry should be "badly", but "not too

Table 1

Charmed $(1/2)^+$ baryon states

Provisional nomenclature	I	S	SU(3) representation	C
C_0^+	0	0	$\bar{3}$	1
$A^+,\ A^0$	1/2	-1		
$C_1^{++},\ C_1^+,\ C_1^0$	1	0	6	
$S^+,\ S^0$	1/2	-1		
T^0	0	-2		
$X_p^{++},\ X_n^+$	1/2	0	3	2
X_λ^+	0	-1		

badly", broken. However, the form of the symmetry breaking is known -- owing to the requirement that it should arise only from mass terms:

$$\mathcal{L}_{strong} = \mathcal{L}_{SU(4)\otimes SU(4)} + m_0\bar{q}q + m_8\bar{q}\lambda_8 q + m_{15}\bar{q}\lambda_{15}q \ . \qquad (6)$$

A perturbative treatment of a badly broken symmetry cannot be expected to be reliable. However, given that perturbative mass formulae work surprisingly well for broken SU(3), they might be valid at least as a first rough approximation for charmed particle masses. In this approximation it is sufficient to know the mass of one charmed quark bound state in order to determine the others (up to ambiguities as to whether quadratic or linear mass formulae should be used). The reason for this is that, for a given representation of SU(4), the matrix elements of the operator $\bar{q}\lambda_{15}q$, which breaks SU(4) only, is related to the matrix elements of $\bar{q}\lambda_8 q$, which breaks SU(3). The only unknown is the relative scale of the symmetry breaking: m_{15}/m_8. This parameter is independent of the SU(4) representation.

Before discussing the interpretation of the newly discovered resonances[9] in the framework of charm, one further element of theoretical input is needed, namely "Zweig's rule" [10]. This is the statement that a diagram involving the annihilation of two quarks into a quarkless intermediate state (Fig. 1a) is "forbidden", whereas the connected diagram of Fig. 1b is

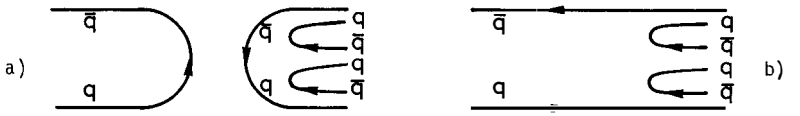

Fig. 1 Quark diagrams which are forbidden (a) and allowed (b) by Zweig's rule.

"allowed". While the theoretical justifications for this rule are not compelling, it does seem to work to an accuracy of 5-10% in amplitude, as in the suppression of $\phi \to 3\pi$ and ϕ production from non-strange particles.

Now let us examine the properties of the new resonances in the light of the above ideas. One anticipated new state is an isoscalar vector meson,

expected to be a nearly pure $\bar{c}c$ bound state. We shall identify the resonance at 3.1 GeV with this state, and those at 3.7 and 4.15 GeV with its radial excitations (or a possible D-wave state). We call these objects ϕ_c, ϕ_c', and ϕ_c'', respectively. Using as input $m_{\phi_c} = 3.1$ GeV, the masses of the lowest-lying 0^- and 1^- charmed states [Eq. (5)] are expected to have masses in the range 2.2-2.4 GeV.

The hadronic decays

$$\phi_c \to h \ , \quad \phi_c' \to h$$

are therefore forbidden by Zweig's rule. However, the observed hadronic widths are in fact much narrower than anticipated; in terms of effective couplings,

$$\frac{g^2(\phi_c \to h)}{g^2(\phi \to 3\pi)} \sim 1/50 \ .$$

Of the various explanations proposed for this extra suppression, one rather attractive idea[11,12] is related to asymptotic freedom. From charge conjugation and colour conservation, quark annihilation in the 1^- state requires the exchange of three gluons; the gluon coupling decreases as the exchanged mass increases (i.e. tends asymptotically to zero), thus explaining the suppression of the ϕ_c coupling relative to the ϕ coupling.

The cascade decay

$$\phi_c' \to \phi_c + \pi\pi$$

is also forbidden by Zweig's rule (Fig. 2). However since the exchanged quarkless state has C = +1, the suppression is expected to be less strong.

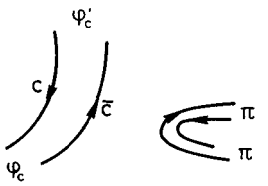

Fig. 2 Quark diagram for the decay $\phi_c' \to \phi_c \pi\pi$.

In Regge language this is because pomeron exchange is possible; in gluon language it is because only two gluons need be exchanged, so the amplitude is of lower order in the effectively small gluon coupling constant. In terms of effective couplings we have

$$\frac{g^2(\phi_c' \to \phi_c \pi\pi}{g^2(\rho' \to \rho\pi\pi)} \gtrsim (0.5 - 3) \times 10^{-2}$$

(the branching ratio for $\rho' \to \rho\pi\pi$ is not known), to be compared with the C = -1 suppression factor (at a comparable mass of the exchanged gluon system):

$$\frac{g^2(\phi \to \rho\pi)}{g^2(\omega \to \rho\pi)} \sim 3 \times 10^{-3} .$$

The radiative decays

$$\phi_c \to h\gamma$$

are also forbidden by Zweig's rule (Fig. 3a), unless the final-state hadron contains a $\bar{c}c$ component (Fig. 3b). The small width of the ϕ_c can be under-

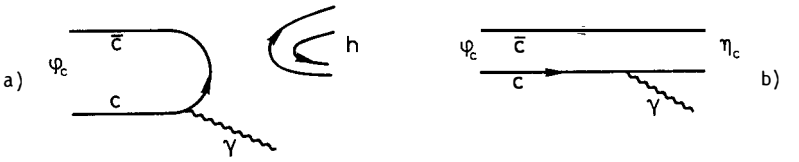

Fig. 3 Radiative decay diagrams which are forbidden (a) and allowed (b) by Zweig's rule.

stood only if no pseudoscalar state with a mass less than $\sim$ 3 GeV contains an appreciable component of $\bar{c}c$. This in fact is not what was anticipated from a simple perturbative treatment of the symmetry-breaking Lagrangian, Eq. (6). Rather, one finds[8,13] that, if the $\eta'(958)$ is a 0^- $\bar{q}q$ bound state, it should contain $\sim$ 25% $\bar{c}c$, and another state, η_c, with $\sim$ 75% $\bar{c}c$ is predicted at $m_{\eta_c} \simeq 2.7$ GeV.

The effective mass Lagrangian for mesons, derived from Eq. (6), may be written in the form[8]

$$\mathcal{L}_{eff} = m\ \mathrm{Tr}\ \pi^2 + \alpha\ \mathrm{Tr}\ \pi\Delta\pi + m_0(\mathrm{Tr}\ \pi)^2 + \beta\ \mathrm{Tr}\ \pi\ \mathrm{Tr}\ \Delta\pi\ , \qquad (7)$$

where π is the 4×4 matrix representation of the meson 16-plet, Δ is the quark mass matrix, and the other parameters are related to the reduced matrix elements of the operators in Eq. (6). In the quark model the first two terms in Eq. (7) represent the quark masses plus an exchange potential (Fig. 4a); the last two terms represent an annihilation potential (Fig. 4b)

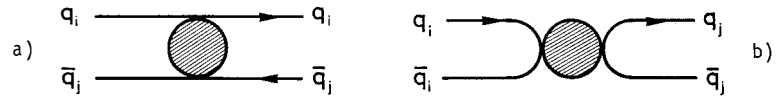

Fig. 4 Exchange potential (a) and annihilation potential (b) contributing to the meson mass matrix.

and in fact are forbidden by Zweig's rule. It is this annihilation potential which gives a departure from ideal mixing. If the gluon picture[11] discussed above is correct, the fact that ideal mixing is better for vector mesons than for pseudoscalars can be understood because

a) 1^- annihilation involves three-gluon exchange and 0^- annihilation involves two-gluon exchange;

b) vector mesons are more massive and therefore the effective gluon coupling in the annihilation channel is weaker.

Furthermore, the fact that the annihilation diagram varies with external mass means that the naïve perturbative treatment is not valid for these terms; the parameters m_0 and β cannot be treated as constants in Eq. (7). We find instead that the η_c should also be nearly pure $\bar{c}c$ with a mass $m_{\eta_c} \sim 3$ GeV, and that the $\bar{c}c$ contribution to $\eta'(958)$ is small. On the other hand, the exchange potential of Fig. 4a does not depend sensitively on the external mass, so large symmetry-breaking effects need not be present for the first two terms in Eq. (7).

There is also the possibility that the E(1420) rather than the $\eta'(958)$ is the 16th 0^- state; in this case a straightforward application of the naïve mass formulae[13,14] gives a nearly pure $\eta_c \simeq (\bar{c}c)_{0^-}$ at a mass of about 3 GeV.

The large width of $\phi_c''(4.15)$ remains to be discussed. Using the experimental limits in the partial width for the cascade decay of ϕ_c', one expects at most a total width of 10 MeV from cascade decays of the ϕ_c'':

$$\phi_c'' \to \phi_c + \pi\pi,\ K\bar{K},\ \eta',\ \eta\ .$$

The observed width of 250-300 GeV can be understood*) only if the ϕ_c'' is above threshold for decays into charmed particles:

$$\phi_c'' \to \begin{cases} D\bar{D}\ ,\ F\bar{F} \\ D^*\bar{D}^*,\ F^*\bar{F}^* \\ D^*\bar{D}\ ,\ \ldots\ . \end{cases}$$

Probably all the states of Eq. (5) must fall in the mass range

$$1.85\ \text{GeV} < m_{0^-},\ m_{1^-} \lesssim 1.9\text{-}2\ \text{GeV}\ ,$$

where the lower limit is imposed by the narrow width of $\phi'(3.7)$. This range is somewhat lower than the anticipated range of 2.2-2.4 GeV, but considering the large symmetry breaking [$m_{1S}/m_8 \sim 20$ in Eq. (6)], this can hardly be considered a difficulty. In this context, the discussion of Gourdin[14] is also relevant.

The production of ϕ_c by nucleons has been observed at Brookhaven (Aubert et al., Ref. 9):

$$\sigma(p + N \to \phi_c + X) \sim 10^{-33} - 10^{-32}\ \text{cm}^2\ ,\quad E_p \simeq 30\ \text{GeV}\ ,$$

and at FermiLab[15]:

$$\sigma(n + N \to \phi_c + X) \sim 10^{-31}\ \text{cm}^2\ ,\quad E_n \simeq 250\ \text{GeV}\ .$$

*) However, it has been remarked by John Ellis[12] that if the ϕ_c'' were less than ideally mixed -- by as little as 10% -- its width could be understood in terms of decays into ordinary hadrons.

Are these cross-sections compatible with the charm interpretation? As discussed in Ref. 14, since the ϕ_c is detected through its leptonic decay mode in these experiments, a comparison with the non-resonant background both at SLAC and BNL allows one to conclude that the hadronic production cross-section and decay width are compatible in the sense that the same mechanism is involved: here interpreted as a direct, albeit suppressed, strong coupling of the ϕ_c to hadrons. Then why is the cross-section at FermiLab at least an order of magnitude larger? Firstly, the production cross-sections for massive objects generally rise with energy (the di-lepton background is expected to rise[14] from BNL to FermiLab energies by a factor of 20-300). Secondly, the FermiLab energy is above threshold for the inclusive process:

$$N + N \rightarrow \phi_c + \text{charm} + \text{anti-charm} + X$$

which has a threshold energy of about 40 GeV, and which is not forbidden by Zweig's rule (see Fig. 5).

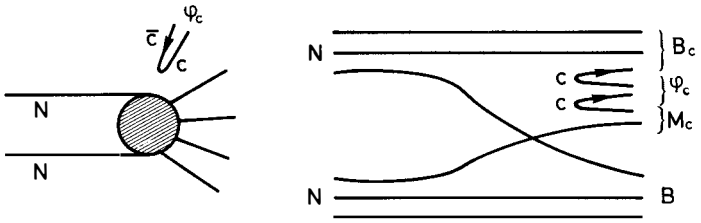

Fig. 5 Forbidden production (a) of ϕ_c, and an example of an allowed production process (b).

Photoproduction of the ϕ_c allows a determination of the $\phi_c N$ total cross-section via the optical theorem if vector meson dominance is assumed (Fig. 6). The extracted values are

$$\sigma(\phi_c N) \simeq 0.4 \text{ mb}, \quad E_\gamma = 11, 18 \text{ GeV} \quad [\text{Gillman},^{16})]$$

$$\sigma(\phi_c N) \simeq 1 \text{ mb}, \quad E_\gamma = 100 \text{ GeV} \quad [\text{Knapp et al.}^{17})] .$$

These values are to be compared with[18]

$$\sigma(\rho N) \simeq 26 \text{ mb}$$

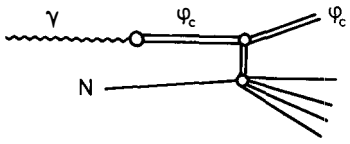

Fig. 6 Vector meson dominance mechanism for photoproduction of ϕ_c.

Symmetry breaking apparently suppresses the ϕ_c cross-section considerably more than the ϕ cross-section relative to the ρ, but the orders of magnitude are not unreasonable. In Ref. 17 it is found that the $\phi_c N$ cross-section is largely inelastic. Presumably the important inelastic channels involve charm production, so the total ϕ_c cross-section should not be compared with $\sigma(\rho N)$ and $\sigma(\phi N)$ except well above charm threshold. However, it is surprising that there is no apparent rise between 11 and 18 GeV.

3. DECAYS OF CHARMED PARTICLES

The theory of weak decays will be discussed in detail by Alterelli[19]. Here we outline the results needed for our subsequent discussion.

The dominant transitions for a truly decaying charmed quark are:

$$c \to \lambda + \ell^+ \nu \ , \quad \text{ampl.} \sim \cos\theta_c \sim 1 \ ,$$
$$c \to \lambda + \bar{p}n \ , \quad \text{ampl.} \sim \cos^2\theta_c \sim 1 \ .$$

The non-leptonic and leptonic decays are *a priori* comparable. However, the situation is similar for a freely decaying strange quark:

$$\lambda \to p + \ell^- \bar{\nu} \sim \sin\theta_c \ ,$$
$$\lambda \to p + \bar{n}p \sim \cos\theta_c \sin\theta_c \sim \sin\theta_c \ ,$$

but we know from experiment that the non-leptonic mode is effectively enhanced by a factor $\sim (\sin\theta_c)^{-1}$. This can be understood qualitatively if we compare the diagrams (Fig. 7) contributing to free quark decay -- which necessarily involve low-momentum W^+ exchange -- with contributions which can arise when strong interactions (gluon exchange) are taken into account

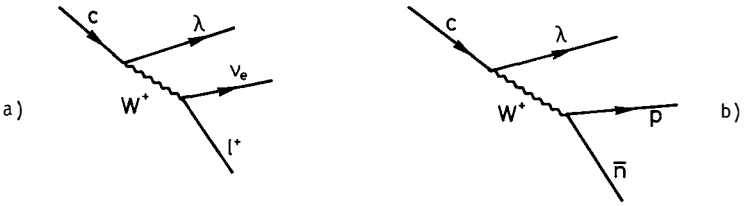

Fig. 7 Leptonic (a) and non-leptonic (b) decays of a free quark.

(Fig. 8). For leptonic decays the momentum carried by the W^+ necessarily remains equal to the di-lepton mass, i.e. small. But for non-leptonic transitions, loop diagrams of the type illustrated in Fig. 8b are dominated by large-momentum W's, so that the suppression due to the W propagator may be attenuated [in the theory considered here, m_W^{-2} is replaced by m_W^{-2} ln $(m_W/1\ \text{GeV})^2$].

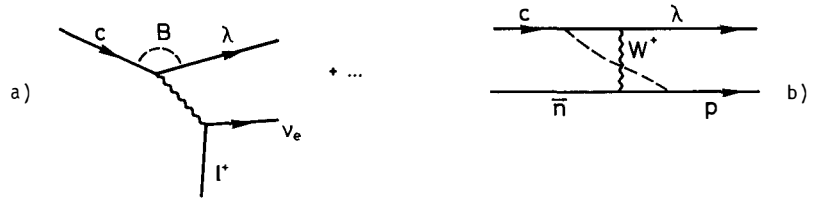

Fig. 8 Strong interaction corrections to (a) leptonic and (b) non-leptonic decays; B is a gluon field.

In asymptotically free theories, the leading corrections due to gluon exchange can be calculated. What one finds is that[20] to order m_W^{-2} a non-local V-A current-current interaction may be replaced by an effective local V-A current-current interaction -- just as in the free quark case or for μ decay -- but with the difference that the effective Fermi coupling is modified and depends on the internal symmetry structure of the current-current product:

$$\mathcal{H}_{\text{eff}} = \frac{G_F}{\sqrt{2}} \times C \times J_\mu J_\mu \times \text{appropriate Cabibbo factor.}$$

For C > 1, the effective interaction is enhanced relative to the free quark case, and for C < 1 it is suppressed. One finds for the theory outlined in Section 1 that the suppression or enhancement depends on the symmetry of the current-current product under the interchange of SU(4) quantum numbers of two quark or two antiquark fields. Explicitly:

$$C > 1 \text{ for } J_\mu J_\mu \sim \begin{cases} \lambda p(\bar{p}\bar{n} - \bar{n}\bar{p}) & (\Delta I = \tfrac{1}{2}) \\ cn(\bar{p}\bar{\lambda} - \bar{\lambda}\bar{p}) & (\Delta V = 0) \\ cn(\bar{p}\bar{n} - \bar{n}\bar{p}) & (\Delta I = \tfrac{1}{2}) , \end{cases}$$

$$C < 1 \text{ for } J_\mu J_\mu \sim \begin{cases} \lambda p(\bar{p}\bar{n} + \bar{n}\bar{p}) & (\Delta I = \tfrac{1}{2}, \tfrac{3}{2}) \\ cn(\bar{p}\bar{\lambda} + \bar{\lambda}\bar{p}) & (\Delta V = 1) \\ cn(\bar{p}\bar{n} + \bar{n}\bar{p}) & (\Delta I = \tfrac{1}{2}) . \end{cases}$$

In analogy with the enhancement of the $\Delta I = \frac{1}{2}$ rule for the usual strangeness changing decays, we obtain an enhancement of the V-spin conserving part[8,21] of the dominant (i.e. strangeness changing) amplitudes for charmed particle decay. The enhancement factor is universal; we take it to be empirically $\sim (\sin\theta_c)^{-1}$. In Table 2 we list the hierarchy of decays according to their strength and their selection rules. Approximate selection rules (i.e. those arising from dynamical enhancement) are indicated in parentheses.

If the vector mesons are higher in mass than their pseudoscalar counterparts as expected (although a small violation of the mass formulae could invert the spacing), they will decay electromagnetically or strongly depending on whether phase space is available for pion emission. In any case they are expected to be narrow ($\Gamma \sim$ MeV) as the level spacing is probably small. From isospin conservation $F^* \to F\pi$ is forbidden; thus the F^* decay will be predominantly electromagnetic:

$$F^* \to F\gamma ,$$

unless phase space is available for 2π emission:

$$F^* \to F\pi\pi .$$

Table 2

Decays of charmed particles

	Selection rules	Amplitude strength	Examples
Non-Leptonic	$\Delta S = \Delta C$ $\Delta I = 1$ $(\Delta V = 0)$	$G_F \cot \theta_c$	$D^0 \to K^- \pi^+$, $\bar{K}2\pi$ $D^+ \to \bar{K}2\pi$ $(D^+ \not\to \bar{K}^0\pi^+)$ $F^+ \to \eta\pi^+$, $K^+K_{S,L}$, 3π $F^+ \to \pi^+\pi^0$
	$\Delta S = 0$ $(\Delta I = 1/2)$	G_F	$D^0 \to \pi^+\pi^-$, $\pi^0\pi^0$ $D^+ \to \eta\pi^+$, 3π $(D^+ \not\to \pi^+\pi^0)$ $F^+ \to K^+\pi^0$, $K^+\eta$
Leptonic	$\Delta S = \Delta C = \Delta Q$ $\Delta I = 0$	G_F	$D^0 \to K^-\ell^+\nu$ $D^+ \to \bar{K}^0\ell^+\nu$ $F^+ \to \eta\ell^+\nu$
	$\Delta C = \Delta Q$, $\Delta S = 0$ $\Delta I = 1/2$	$G_F \sin \theta_c$	$D \to \pi\ell\nu$ $F^+ \to K^0\ell^+\nu$

Similarly

$$D^* \to D\gamma \ ,$$

or possibly

$$D^* \to D\pi \ .$$

For baryons the predictions vary drastically depending on whether quadratic or linear mass formulae are used[22] (see Table 3). In the first case, the $\bar{3}$ states will be stable against strong decay and will appear as narrow resonances in channels[8,21] with S = -1, -2 and Q = 0, 1, 2. (The C = +2 representation 3 will also be stable and will cascade decay similarly to the Ξ^-, Ω^-.) In the latter case, however, no charmed baryon will be stable against strong cascade decays with charmed meson emission. These states

Table 3

Charmed baryon masses

SU(3) representation	Lowest mass (GeV)	
	Quadratic formulae	Linear formulae
$\bar{3}$	2.7	4.5
6	3	6
3	4.1	9

will appear as broad resonances in many-body channels and will probably be very difficult to detect. In either case the 6 can cascade to the $\bar{3}$ through pion emission.

4. INDIRECT EVIDENCE FOR CHARMED PARTICLE PRODUCTION

Anomalous phenomena such as scaling violations and direct lepton production may constitute evidence for the production of new particles.

In deep inelastic leptoproduction, no dramatic effect is expected. This is because the electromagnetic current is diagonal in quarks (i.e. partons), and the $\bar{c}c$ component of the current can be excited only if charmed partons are present in the nucleon. If they are present at all, their contribution is expected to be concentrated at small x ($x \lesssim 0.1$). Explicitly, as charm threshold is crossed, one expects an increase in the cross-section[12]:

$$\frac{\Delta\sigma}{\sigma} = \frac{4/9(c + \bar{c})}{4/9(p + \bar{p}) + 1/9(n + \bar{n} + \lambda + \bar{\lambda})} \to 0 \quad \text{for } x > 0.1 \ ,$$

where c, p, etc., represent parton distribution functions. Apparently such a behaviour is compatible with the data from FermiLab[23].

In ν reactions, charmed particle production is expected and is calculable. Elastic baryon production

$$\nu + n \rightarrow C^{+}\mu^{-}$$

$$\nu + p \rightarrow C^{++}\mu^{-}$$

can be directly related[8,24] to

$$\nu + n \rightarrow p + \mu^{-}$$

by SU(4), and the estimate should be correct at least as to order of magnitude. A typical event of this type would be characterized by an S = -1 final state with possibly a di-lepton. However, the cross-section is proportional to $\sin^2 \theta_c$. A more favourable process might be that of diffractive production[8] of the F^* (Fig. 9) for which the cross-section is

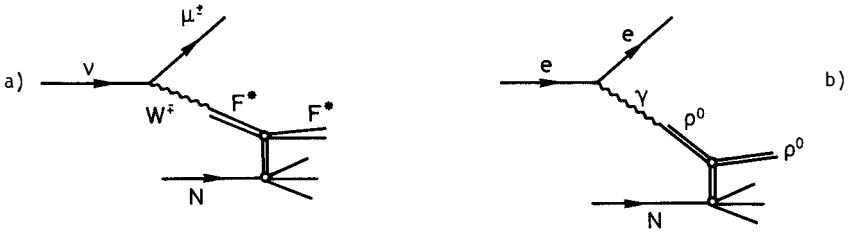

Fig. 9 Diffractive leptoproduction of (a) the F^* and (b) the ρ^0.

$\sim \cos^2 \theta_c$, and which should be similar to electroproduction of the ρ^0, apart from the difference in the W and γ propagators. A signature for the process would be an odd number of photons in the final state, for example:

$$F^{*\pm} \rightarrow F^{\pm}\gamma$$
$$\hookrightarrow \eta\pi^{\pm}$$
$$\hookrightarrow \gamma\gamma \ .$$

Apart from the detection of specific final states, the parton model allows estimates of inclusive charm production sufficiently above

threshold[8,25]. The basic process is illustrated in Fig. 10. The total cross-section is proportional to the structure function of the target parton:

$$d\sigma \sim \sum_q d\sigma(\nu q \to c\mu)\ F_q(x) \sim \begin{cases} \sin^2\theta_c & q = n,\ \bar{n} \\ \cos^2\theta_c & q = \lambda,\ \bar{\lambda} \end{cases} .$$

Parton structure functions may be estimated from a comparison of electroproduction and neutrino data. The λ and $\bar{\lambda}$ parton content is in fact compatible with zero. Nevertheless, if we assume

$$\int F_\lambda(x) = \int F_{\bar{\lambda}}(x) \simeq 0.5\ \left(\int F_n(x) + \int F_p(x)\right) ,$$

also compatible with the data, we predict a 5% contribution of charm production to the total ν cross-section and a 15% contribution to $\sigma_{\bar{\nu}}$ from the $\lambda \to c$ transition. Since both production and decay satisfy $\Delta S = \Delta C$, the overall process will be predominantly strangeness conserving, and events appear as associated production of strange particles. When the charmed particle decays leptonically there will be a di-lepton in the final state.

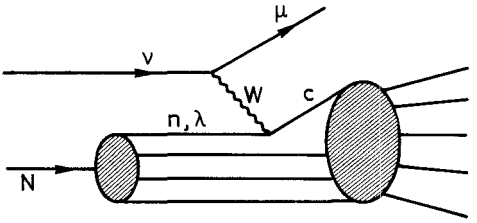

Fig. 10 Parton model picture of charmed particle production by neutrinos.

Whatever the $\lambda,\bar{\lambda}$ content of the nucleon there must be charmed particle production at a level of $\sin^2\theta_c \sim 4\%$ from the $n \to c$ transition. This process will contribute 4% to the total ν cross-section and about ½% to $\sigma^{\bar{\nu}}$. Here the signature will be apparent violation of the $\Delta S = \Delta Q$ rule if the charm decay is non-leptonic, and a di-lepton with an $S = -1$ hadronic final state ($S = +1$ for an incident $\bar{\nu}$) if the decay is leptonic.

From the above discussion we can estimate di-lepton production above charm threshold. Assuming a $\lambda,\bar{\lambda}$ parton content $\lesssim$ 5%, we have

$$\sigma^{\nu}(\text{charm}) \simeq \sin^2\theta_c \sigma_T^{\nu} + \sigma(\nu\lambda)_{\text{small x}}$$
$$\simeq 4\%\ \sigma_T^{\nu} + (\lesssim 5\%)\ \sigma_T^{\nu} .$$

The $\bar{\nu}$ charm production should all be concentrated at small x with

$$\sigma^{\bar{\nu}}(\text{charm}) \lesssim 15\%\ \sigma_T^{\bar{\nu}} .$$

Assuming further a 5% branching ratio for leptonic decay ($B_e \simeq B_\mu \simeq 0.05$), we obtain:

$$\sigma^{\nu}(\mu^+\mu^-) \simeq (2\text{-}5) \times 10^3\ \sigma^{\nu}(\mu^-)$$
$$\sigma^{\bar{\nu}}(\mu^+\mu^-) \simeq (0\text{-}7) \times 10^{-3}\ \sigma^{\bar{\nu}}(\mu^+) . \qquad (8)$$

At FermiLab, 14 di-leptons have been observed[26] with an incident beam composition

$$\bar{\nu}/\nu \simeq 0.6 .$$

The reported cross-section is

$$\sigma(\mu^+\mu^-)/\sigma(\mu) = (9 \pm 3) \times 10^{-3} , \qquad E_\nu > 40\ \text{GeV} .$$

Anomalies in the x and y distributions have also been reported by the same group[27]; such effects are expected near the threshold for new particle production. However, the calculated effects of charm production, assuming a 5% $\lambda,\bar{\lambda}$ parton sea, do not seem sufficient to account for the observed anomaly.

Direct production of high p_T leptons in nucleon-nucleon collisions has been observed[28] at a level of

$$e^{\pm}/\pi^0 \simeq \mu^{\pm}/\pi^0 \simeq 10^{-4} , \qquad 1.5 \lesssim p_T \lesssim 4 .$$

Less than 50% of this ratio can be accounted for[29] by the production and leptonic decay of ρ, ω, ϕ and $\phi_c(3.1)$. Can the remainder be due to leptonic decays of charmed particles? One remarkable feature of the ℓ/π ratio is that it is apparently independent of p_T, at least over the measured range.

Suppose the observed leptons are coming from the decay of a massive hadron H. For values $p_T >> m_H$, the transverse momentum of the lepton reflects the transverse momentum of the parent and should have a similar distribution. However, if the observed lepton has $p_T \simeq m_H/2$, the parent transverse momentum may be negligibly small. As hadron production at small p_T is favoured, one would expect a peaking of the lepton distribution around $p_T = m_H/2$. However, it turns out that[29] if high p_T ($p_T \geq 1$ GeV) hadron production is universal in the variable

$$E_T(h) = \sqrt{p_T^2 + m_h^2} ,$$

the accumulation of leptons at $p_T \simeq m_H/2$ is compensated by the extra suppression -- relative to pion production -- from the parent mass. Thus the ℓ/π ratio is reasonably flat for

$$p_T > m_H/2 \simeq 1 \text{ GeV}$$

if the parent is a charmed meson with 2 GeV mass. However, a fall-off in the ℓ/π ratio is expected for $p_T < 1$ GeV.

What is the lepton yield which might be expected from charmed particle production? Consider a qualitative picture in which high p_T hadron production arises from elementary parton scattering. We know from lepton production data that the antiparton contribution is small and that about half the momentum is carried by neutral gluons; thus the two elementary scattering processes are quark-quark scattering (Fig. 11a), from which the leading high p_T particle is expected to have S = C = 0, and gluon-gluon scattering (Fig. 11b) which should yield -- at a transverse momentum that is large

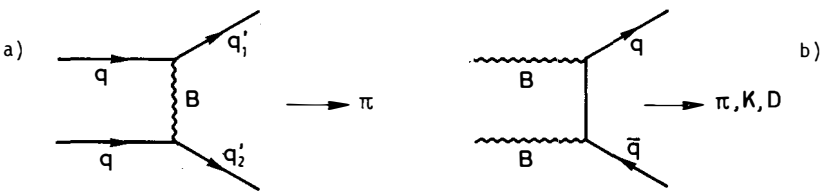

Fig. 11 Production of high p_T hadrons by (a) quark-quark and (b) gluon-gluon scattering.

compared will all hadron masses -- comparable π, K, and D distributions. If these two processes have equal weight, one expects

$$K/\pi \sim 0.5 \ ,$$

which is compatible with the data. Then assuming a production distribution of the form

$$E \frac{d\sigma(p + p \to h + X)}{d^3p} \sim (m_h^2 + p_T^2)^{-4} \ , \qquad E_T \gtrsim 1 \text{ GeV}$$

and a branching ratio of 5% for the decay $D \to K\ell\nu$, one finds[30] a contribution from D production:

$$\frac{\ell}{\pi} \simeq 2 \times 10^{-4} \lim_{p_T >> m_D} \left(\frac{D}{\pi}\right) \ ,$$

which is of the correct order of magnitude if $D/\pi \to 0.5$ for high p_T.

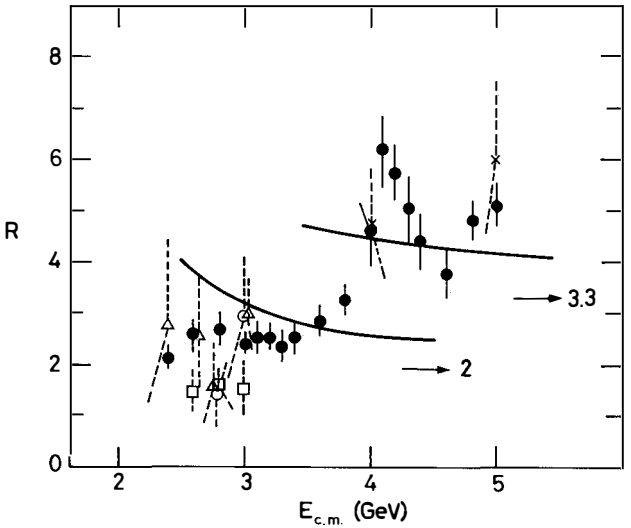

Fig. 12 The ratio $R = \sigma(e^+e^- \to h)/\sigma(e^+e^- \to \mu^+\mu^-)$. Theoretical predictions for the asymptotic behaviour compared with the data points taken from J.A. Kadyk's talk at this meeting. The 3.1 and 3.7 resonances have been omitted.

The ratio of e^+e^- annihilation cross-sections:

$$R = \frac{\sigma(e^+e^- \to \text{hadrons})}{\sigma(e^+e^- \to \text{all})}$$

is expected to approach asymptotically the value 2 for energies below the charmed particle threshold. Once the charm threshold is passed, this ratio should approach the asymptotic value of 10/3. In the asymptotically free theory mentioned in Section 1, the approach is from above[31], along logarithmic curves as indicated in Fig. 12.

5. DIRECT EVIDENCE FOR CHARM?

There is now an accumulation of indirect evidence, including the properties of the newly observed resonances, possible threshold-induced anomalies in leptoproduction (as well as the absence[23] of a large scaling violation for $x > 0.1$ in muon scattering), and direct lepton production, which tends to support the charm hypothesis. Is there any direct evidence?

The most obvious place to look for charmed particles is amongst the decay products of the ϕ_c'' (4.15). If our interpretation of the resonance widths is correct, the ϕ_c'' decays should be dominated by two-body charm-anticharm states. A systematic study of this region has not yet been performed at the e^+e^- storage rings. However, there is some data at an energy of 4.8 GeV, above the presumed charm threshold, and the results that have emerged are negative.

There is no dramatic increase in the K/π ratio[32]. As indicated in Table 2, an expected characteristic of a charmed meson decay is a kaon in the final state. However, decays are expected to be largely multibody, and although the number of events with kaons should increase, it is not clear that the K/π ratio should increase. Explicit calculations[33], based on the selection rules of Section 3, of the decays

$$0^- \to 2(0^-),\ 3(0^-),\ (0^-) + (1^-),\ 2(1^-)$$

yield the ratios

$$K_S/(\pi^+ + \pi^-) \simeq 15\%$$

$$(K^+ + K^-)/(\pi^+ + \pi^-) \simeq 23\% ,$$

which in fact do not represent a dramatic increase over the background levels ($\sim$ 10%). Furthermore, at a non-resonant energy above threshold, the two-body charm-anticharm state is no longer dominant. A more significant test is whether there is a rise in the number of events containing two or more kaons.

There is no evidence for structure in invariant mass plots in the channels[34]

$$K_S^0\pi^+, \ \pi^+\pi^-, \ K_S^0\pi^+\pi^-, \ \pi^+\pi^+\pi^- .$$

The first two final states are suppressed (see Table 2); the last two are allowed, but the branching ratio for any specific channel cannot be expected to exceed 20%. Furthermore, to the extent that multibody final states are predominant in e^+e^- annihilation, there is a large combinatorial background. A search for an invariant mass peak in events containing one lepton in the final state might provide a means of reducing the background.

Taking an optimistic point of view, the observation in Gargamelle[35] of a μe event with a strange particle in the final state, a neutrino event which apparently satisfies $\Delta S = -\Delta Q$ observed at Brookhaven[36], the apparent production of long-lived massive particles in cosmic rays[37] -- none of which might be compelling if taken alone -- may represent the beginning of an accumulation of direct evidence for charmed particle production.

The remarks collected here are largely the result of many discussions with colleagues at CERN and with the participants at the Rencontre de Moriond.

REFERENCES

1) Y. Hara, Phys. Rev. 134, B701 (1964).
D. Amati, H. Bacry, J. Nuyts and J. Prentki, Phys. Letters 11, 190 (1964).
B.J. Bjørken and S.L. Glashow, Phys. Letters 11, 255 (1964).
Z. Maki and Y. Ohnuki, Progr. Theor. Phys. 32, 144 (1964).

2) S. Weinberg, Phys. Rev. Letters 19, 1264 (1967).
A. Salam, Proc. 8th Nobel Symposium, Stockholm, 1968 (Amqvist and Wiksell, Stockholm, 1968), p. 367.

3) S.L. Glashow, J. Iliopoulos and L. Maiani, Phys. Rev. D 2, 1285 (1970).
S. Weinberg, Phys. Rev. Letters 28, 1688 (1971).
C. Bouchiat, J. Iliopoulos and Ph. Meyer, Phys. Letters 38B, 519 (1972).

4) H.I. Vainshtein and I.B. Khriplovich, Zh. Eksper. Teor. Pis'ma 18, 141 (1973) [JETP Letters 18, 83 (1973)].
E. Ma, Phys. Rev. D 9, 3103 (1974).
M.K. Gaillard and B.W. Lee, Phys. Rev. D 10, 897 (1974).
A. Gravielides, thesis, University of Minnesota (1974), unpublished.
S.D. Joglekar, K_L-K_S mass difference and rare K-decays in a phenomenological gauge model, FERMILAB Pub. 74-96 THY (1974).
D.V. Nanopoulos and G.G. Ross, Rare decay modes of the K mesons and the K_L-K_S mass difference in an asymptotically free theory, preprint CERN TH-1965, to be published in Phys. Letters.

5) S. Weinberg, Phys. Rev. D 8, 605 (1973) and Rev. Mod. Phys. 46, 255 (1974).
D. Nanopoulos, Nuovo Cimento Letters 8, 873 (1973).

6) D. Gross and F. Wilczek, Phys. Rev. D 8, 3633 (1973).
S. Weinberg, Phys. Rev. Letters 31, 494 (1973)
H. Fritsch, M. Gell-Mann and H. Leutwyler, CalTech report CALT-68-409 (1973), unpublished.

7) D. Amati et al., Nuovo Cimento 34, 1732 (1964).
H. Lipkin, Tests of unitary symmetry and possible higher symmetries, *in* Proc. 2nd Coral Gables Conf. on Symmetry Principles at High Energies, Coral Gables, 1965 (W.H. Freeman and Co., San Francisco, 1965), p. 202; and Lie groups for pedestrians, 2nd edition (North-Holland Publishing Co., Amsterdam, 1965).

8) M.K. Gaillard, B.W. Lee and J.L. Rosner, Search for charm, Rev. Mod. Phys. (to be published in April 1975).

9) J.J. Aubert et al., Phys. Rev. Letters 33, 1404 (1974).
J.E. Augustin, Phys. Rev. Letters 33, 1406 (1974).
C. Bacci et al., Phys. Rev. Letters 33, 1408 (1974).
W. Braunschweig et al., A measurement of large-angle e^+e^- scattering at the 3100 MeV resonance, DESY preprint (1974). See also the experimental talks presented at this meeting.

10) This rule is attributed to G. Zweig, largely by oral tradition; see S. Okubo, Phys. Letters 5, 165 (1963).
J.L. Rosner, Physics Reports 11C, 189 (1974).

11) T. Appelquist and D.H. Politzer, Phys. Rev. Letters 34, 43 (1975).
A. De Rujula and S.L. Glashow, Phys. Rev. Letters 34, 46 (1975).
Analogous arguments can be made in a dual model picture; see J. Ellis, Ref. 12.

12) J. Ellis, e^+e^- annihilation, the new particles, and charm, Lectures presented at the 14th Internationale Universitätswochen für Kernphysik, Schadming, 1975 (proc. to be published); CERN preprint TH-1996 (1975).

13) B.W. Lee and C. Quigg, Fermi Lab. report FERMILAB-74/110-THY (1974), unpublished.
M. Gourdin, SU(4) mass breaking, Lectures given at this meeting.
See also the addendum to Ref. 8, and S. Okubo, V.S. Mathur and S. Borchardt, Phys. Rev. Letters 34, 236 (1975).

14) CERN Theory Boson Workshop, TH-1964 (1974).

15) B. Knapp et al., Dimuon production by neutrons, Columbia preprint and Proc. Colloque International du CNRS -- Physique du Neutrino à Haute Energie, Paris, 1975 (to be published).

16) F.J. Gillman, talk presented at Coral Gables, SLAC-PUB 1537 (1975).

17) B. Knapp et al., Photoproduction of narrow resonances, Columbia preprint and Proc. Colloque International du CNRS -- Physique du Neutrino à Haute Energie, Paris, 1975 (to be published).

18) K. Berkelman, *in* Proc. 1971 Internat. Symposium on Electron and Photon Interactions at High Energies, Ithaca, 1971 (Cornell Univ., Ithaca, NY, 1971), p. 263.

19) G. Altarelli, Weak decays of charmed particles, Lectures given at this meeting.

20) M.K. Gaillard and B.W. Lee, Phys. Rev. Letters 33, 108 (1974).
G. Altarelli and L. Maiani, Phys. Letters 52B, 351 (1974).

21) G. Altarelli, N. Cabibbo and L. Maiani, Nuclear Phys. B88, 285 (1975).
R.L. Kingsley et al., Weak decays of charmed hadrons, Princeton preprint (1975).

22) Lower baryon masses are obtained in a dynamical model of A. De Rújula, H. Georgi and S. Glashow, Hadron masses in a gauge theory, Harvard preprint (1975). See also the addendum to Ref. 8.

23) D.J. Fox et al., Phys. Rev. Letters 33, 1504 (1974).
K.W. Chen, talk given at the FermiLab Muon Workshop (1975).

24) A. Dolgov and M.K. Gaillard, Can charmed particles be lighter than we think? CERN TH. internal report (1974).

25) G. Snow, Nuclear Phys. B55, 445 (1973), and Electromagnetic and weak interactions, *in* Proc. 8th Rencontre de Moriond, Méribel, 1973 (CNRS, Paris, 1973), p. 379.
A. De Rújula and S.L. Glashow, Phys. Rev. D 9, 180 (1973).
A. De Rújula, H. Georgi, S.L. Glashow and H.R. Quinn, Rev. Mod. Phys. 46, 391 (1974).
G. Altarelli, N. Cabibbo and L. Maiani, Phys. Letters 48B, 435 (1974).
M.K. Gaillard, Notes on charmed particle searches in neutrino experiments, *in* Proc. 4th Internat. Conf. on Neutrino Physics, Philadelphia, 1974 (AIP Conf. Proceedings No. 22, Particle and Fields Subseries No. 9, AIP, New York, 1974), p. 65.

26) A. Benvenuti et al., Phys. Rev. Letters 34, 419 (1975).
Further observation of di-leptons by this group and by the Caltech-FermiLab Collaboration have been reported at the Colloque International du CNRS-Physique du Neutrino à Haute Energie, Paris, 1975.

27) A. Benvenuti et al., Phys. Rev. Letters 34, 597 (1975).

28) J.P. Boymond et al., Phys. Rev. Letters 33, 112 (1974).
J.A. Appel et al., Phys. Rev. Letters 33, 722 (1974).
F.W. Büsser et al., Phys. Letters 53B, 212 (1974).

29) J.-M. Gaillard, Lepton production at high transverse momentum, talk presented at this meeting.

30) J.-M. Gaillard, private communication.

31) T. Appelquist and H. Georgi, Phys. Rev. D 8, 4000 (1973).
A. Zee, Phys. Rev. D 8, 4038 (1973).

32) F. Vannucci, private communication.

33) M.B. Einhorn and C. Quigg, FermiLab preprint, FermiLab-Pub-75/21-THY (1975).

34) H. Harari, Letters to the Weizmann Institute.

35) Gargamelle Collaboration, results presented at this meeting (see, Strange particles in Gargamelle, talk by U. Nguyen-Khac) and at the Colloque International du CNRS -- Physique du Neutrino à Haute Energie, Paris, 1975.

36) E.G. Cazzoli et al., Evidence for charmed baryon production by neutrinos, Phys. Rev. Letters (to be published); and Proc. Colloque International du CNRS -- Physique du Neutrino à Haute Energie, Paris, 1975.

37) K. Niu, E. Mikumo and Y. Maeda, Progr. Theor. Phys. 46, 1644 (1971).
K. Hoshino et al., Nagoya University preprint DPNU-3 (1975).

ON WEAK DECAYS OF CHARMED HADRONS

G. ALTARELLI
Istituto di Fisica dell'Università
Roma, Italia

Abstract : A review is presented of the expected properties of weak non leptonic decays of charmed particles.

INTRODUCTION

In this talk I shall review some work on non leptonic weak decays of charmed particles which was done in collaboration with N. CABIBBO and L. MAIANI[1,2]. It will be shown that in the SU(4) charm scheme[3] one is naturally led to expect weak non leptonic amplitudes for the decays of charmed particles to be enhanced over semileptonic or leptonic modes. Moreover the effective Hamiltonian for non leptonic charm changing transitions possesses well definite selection rules. These properties are obtained by an extension in SU(4) of the well known features of strangeness changing non leptonic transitions, such as the $\Delta T = 1/2$ rule. Phenomenological consequences for the decays of charmed particles are discussed.

A striking feature of $|\Delta S| = 1$ non leptonic decays is the $\Delta T = 1/2$ rule, or in SU(3) language the octet enhancement rule. That is, while in the product of two weak hadronic currents pieces with both $\Delta T = 1/2$ and $\Delta T = 3/2$ (8 and 27 of SU(3)) are expected to occur, it is a well established fact that $\Delta T = 1/2$ or 8 parts are the dominant terms. For example in K decays, where $K^+ \to \pi^+\pi^\circ$ is a pure $\Delta T = 3/2$ transition while $K_s \to \pi^+\pi^-$ or $K_s \to \pi^\circ\,\pi^\circ$ can occur through $\Delta T = 1/2$ amplitudes, it is experimentally found that $\Gamma(K_s \to \pi\pi)/\Gamma(K^+ \to \pi^+\,\pi^-) \simeq 660$. Moreover branching ratios are correctly reproduced to a good approximation by the $\Delta T = 1/2$ rule in $K \to \pi\pi$, $K \to 3\pi$ and hyperon decays. Although the $\Delta T = 1/2$ rule is not exact and therefore $\Delta T = 3/2$ amplitudes are certainly not zero, it is concluded from experiment that in $|\Delta S| = 1$ non leptonic decays :

$$\frac{A(\Delta T = 3/2)}{A(\Delta T = 1/2)} \lesssim 5\ \% \qquad (1)$$

A more delicate question is the following one : are $\Delta T = 1/2$ amplitudes enhanced, or are $\Delta T = 3/2$ amplitudes suppressed or both ? In order to obtain a qualitative answer to this question one may consider simple tree graph contributions to the relevant processes. For example for $K \to 2\pi$ one may consider a $K\,\pi\,W$ vertex (W is the charged intermediate vector boson) followed by a direct $W\pi$ transition. Since both couplings are known (from $K \to \pi e\nu$ and $\pi \to \mu\nu$) one can get a feeling of what should be the "natural" size for these amplitudes. The result of this sort of calculations[4] is that $\Delta T = 1/2$ amplitudes appear to be enhanced, while $\Delta T = 3/2$ amplitudes are either unaffected or suppressed by a smaller amount. Similar arguments also hold for $K \to 3\pi$ decays, as testified by the successes of PCAC in relat-

ing $K \to 3\pi$ to $K \to 2\pi$, and for hyperon decays.

THE $\Delta T = 1/2$ RULE AND SHORT DISTANCE SINGULARITIES

An appealing mechanism for explaining the $\Delta T = 1/2$ rule was first proposed by K. WILSON in 1969[5]. Neglecting Lorentz indices, leaving aside technical details, a very schematic presentation of Wilson's argument is the following one. To lowest order in the weak (and e.m.) interactions and to all orders in strong interactions the matrix element for a weak non leptonic transition is given by :

$$\langle f|H^{NL}|i\rangle \sim \int d^4x\, D(x^2, M_w^2)\, \langle f|T(J_w^+(x)\, J_w^-(o))|i\rangle \qquad (2)$$

where $D(x^2, M_w^2)$ is the W boson propagator and $J_w^{\pm}$ are the weak charged hadronic currents. The integral clearly corresponds to the emission and subsequent reabsorption of a charged W. (Contributions of weak neutral currents do not arise for $|\Delta S| = 1$ or $|\Delta C| = 1$ transitions and will not be considered here). Note that the matrix element of $T(J_w^+ J_w^-)$ between the hadronic states $|f\rangle$ and $|i\rangle$ is entirely determined by strong interactions.

Since $M_w \gg m_h$, where m_h is a typical hadronic mass scale, the leading contributions to the integral in Eq.(2) arise from short distances $x \sim 1/M_w$, where the Wilson operator expansion[5] holds :

$$T(J_w^+(x)\, J_w^-(o)) \underset{x_\mu \to o}{\simeq} \ldots + \frac{C_1(x^2)}{x^2} O_4(o) + C_2(x^2)\, O_6(o) + \ldots \qquad (3)$$

where $O_4(o)$, $O_6(o)$ ... are local operators of canonical dimension 4, 6 etc, and $C_i(x^2)$ are C-number functions that would be constant in free field theory. This is an operator expansion, that is the singularity of each term is independent of the matrix element. In general strong interaction effects renormalize the functions $C_i(x^2)$, which thus acquire singularities at short distances. It is simple to show that the terms that dominate the integral in Eq.(2) in the limit $M_w \gg m_h$ are those which correspond to the most singular terms at short distances. Thus Wilson argued that if $|\Delta S| = 1$, $\Delta T = 1/2$ operators acquire a stronger singularity at short distances than $|\Delta S| = 1$, $\Delta T = 3/2$ operators, then the $\Delta T = 1/2$ rule would follow.

On the other hand from the approximate validity of scaling in deep inelastic processes[6], which are themselves governed by short distance singularities, we know that strong interactions are free or almost free at short

distances. That is the functions $C_i(x^2)$ only acquire logarithmic or small power singularities. In particular the best approximation to scaling is provided by asymptotically free theories of strong interactions[7] where $C_i(x^2) \sim (\ell n\, x^2)^{d_i}$ where d_i are exponents which can be reliably computed in perturbation theory. In this class of theories if $C_{1/2}(x^2) \sim (\ell n\, x^2)^{d_{1/2}}$, $d_{1/2} > 0$ and $C_{3/2}(x^2) \sim (\ell n\, x^2)^{-d_{3/2}}$, $-d_{3/2} < 0$, where $C_{1/2}$ and $C_{3/2}$ are the leading terms of the coefficient functions of $|\Delta S| = 1$, $\Delta T = 1/2$ and $\Delta T = 3/2$ operators respectively, then it would follow :

$$\frac{\langle f|H^{NL}|i\rangle_{\Delta T=1/2}}{\langle f|H^{NL}|i\rangle_{\Delta T=3/2}} \sim \left(\ell n \frac{M_w^2}{m_h^2}\right)^{d_{1/2}+d_{3/2}} \frac{\langle f|O_{1/2}(o)|i\rangle}{\langle f|O_{3/2}(o)|i\rangle} \qquad (4)$$

Since $M_w \sim 100$ GeV, $m_h \sim 1$ GeV then $\ell n\, M_w^2/m_h^2 \sim 10$ and for reasonable values of $d_{1/2}$ and $d_{3/2}$ the $\Delta T = 1/2$ may be reproduced with its correct size.

Recently it has been proved[8] that this mechanism is actually realized in asymptotically free theories based on a SU(3) color group for the strong interactions and on the Weinberg-Salam theory for weak and e.m. interactions. For example in the specific model of Glashow-Iliopoulos-Maiani[3], based on three quartets of fractionally charged colored quarks, one finds $d_{1/2} = 0.48$, $-d_{3/2} = -0.24$, corresponding to an enhancement factor of $(\ell n\, M_w^2/m_h^2)^{0.72} \sim 6$ (times unknownfactors which, contrary to this one, are a priori expected to be of order 1) for $\Delta T = 1/2$ versus $\Delta T = 3/2$ amplitudes. Although the explicit factor found in this model is smaller by a factor of about 3 from what is actually observed, this computation certainly provides strong support in favour of a mechanism based on short distance singularities.

CONSEQUENCES FOR $|\Delta C| = 1$ AMPLITUDES

The assumption that octet enhancement arises from short distance singularities has general consequences for non leptonic amplitudes in a theory based on SU(4). These apply both to $\Delta S = 0$ parity violating transitions[9], and to $\Delta C \neq 0$ amplitudes[1,2]. Here we will discuss the latter and recall that these implications do not depend on the detailed dynamics of strong interactions (asymptotic freedom or else).

The concial point is that at short distances the theory is more symmetric than in general. In particular the SU(4) breaking, which only arises from mass terms in the Lagrangian, disappears. It then follows that a whole representation of SU(4) is enhanced or suppressed. Since the weak charged hadronic current transforms as a component of the 15 dimensional representation of

SU(4), the content of $T(J_w^+ J_w^-)$ in terms of irreducible representations of SU(4) is completely specified. Note that $T(J_w^+ J_w^-)$ is symmetric in the exchange of the two currents, so that only those representations in $15 \oplus 15$ which are symmetric can contribute. Thus one obtains :

$$T(J_w^+ J_w^-) \simeq 1 \oplus 15_S \oplus 20_H \oplus 84 \tag{5}$$

where 15_S is that 15 which is symmetric in the two currents while 20_H (84) is the representation spanned by a traceless tensor :

$$T^{[ab]}_{[cd]} \qquad T^{\{ab\}}_{\{cd\}}$$

with two antisymmetric (symmetric) upper and lower indices.

It is however simple to show that 1 and 15_S cannot be relevant for $\Delta S \neq 0$ or $\Delta C \neq 0$ transitions. This is obvious for 1 while for 15_S it is shown by the following argument. 15_S is uniquely determined as :

$$(15)_S \sim \left\{J_w^+ J_w^-\right\}^a_b - \frac{1}{4}\delta^a_b \left\{J_w^+ J_w^-\right\}^c_c$$

in terms of the anticommutator of the weak currents. Now recall that the motivation for charm was the need of suppressing neutral $\Delta S \neq 0$ transitions. The vanishing of $\Delta S \neq 0$ pieces in $[J_w^+ J_w^-]$ guarantees the cancellation of unwanted transitions of order G, while the vanishing of $\Delta S \neq 0$ parts of $\{J_w^+ J_w^-\}$ is necessary in order to suppress transitions of order $G\alpha$. In the Glashow-Iliopoulos-Maiani scheme 15_S is actually zero, because $\{J_w^+ J_w^-\}$ is proportional to the identity matrix in SU(4) space.

One is then left for $\Delta S \neq 0$ or $\Delta C \neq 0$ transitions only with 20_H and 84. Since 84 contains a SU(3) 27 with $|\Delta S| = 1$, $\Delta T = 3/2$ components, this is the representation to be suppressed. On the other hand 20_H has a SU(3) content : $20_H \sim 8 \oplus 6 \oplus \bar{6}$ and in the $|\Delta S| = 1$ sector behaves like an octet. Thus the enhanced effective hamiltonian for non leptonic transitions should behave like a 20_H :

$$H^{NL}_{eff} \sim 20_H \sim H^{[ab]}_{[cd]} \tag{6}$$

In order to explicitly exhibit the structure of the effective hamiltonian, we introduce the notation :

$$\sum_a \bar{p}_a \gamma_\mu (1 - \gamma_5) n_a = (\bar{p}n) \text{ etc } \ldots$$

where a is the color index (a = 1, 2, 3). We have :

$$\left(H^{N.L.}_{eff}\right)_{\substack{|\Delta S| = 1 \\ \Delta C = 0}} \simeq \cos\theta \sin\theta \left\{[(\bar{p}\lambda)(\bar{n}p) - (\bar{n}\lambda)(\bar{p}p)]\right.$$

$$\left. -[(\bar{p}'\lambda)(\bar{n}p') - (\bar{n}\lambda)(\bar{p}'p')]\right\} + \text{h.c.} \qquad (7)$$

and :

$$\left(H^{NL}_{eff}\right)_{|\Delta C| = 1} \simeq \cos^2\theta \left\{[(\bar{\lambda}p')(\bar{p}n) - (\bar{p}p')(\bar{\lambda}n)]\right\} + \text{h.c.} + \ldots \qquad (8)$$

where the dots stand for terms of order cos θ sin θ and $\sin^2\theta$, which we neglect. Note the antisymmetry of H^{NL}_{eff} in both the exchange of quark labels and of antiquark labels, corresponding to the antisymmetry of $H^{[ab]}_{[cd]}$ in both upper and lower indices. It is precisely this property that makes :

$$\left(H^{NL}_{eff}\right)_{\substack{|\Delta S| = 1 \\ \Delta C = 0}}$$

pure $\Delta T = 1/2$. In fact in $(\bar{p}\lambda)(\bar{n}p) - (\bar{n}\lambda)(\bar{p}p)$ the antiquarks $\bar{n}$ and $\bar{p}$ appear in a antisymmetric combination, hence T = 0 which combines with the quark p of T = 1/2 to make $\Delta T = 1/2$. Likewise the selection rules of :

$$\left(H^{NL}_{eff}\right)_{|\Delta C| = 1}$$

are $\underline{6 \oplus \bar{6} \text{ under SU(3)}}$, $\underline{\Delta V = 0}$, $\underline{\Delta T = 1}$, $\underline{\Delta C = \Delta S}$. V is the V-spin generator of the SU(2) subgroup of SU(3) that rotates λ and p quarks, leaving n (and μ') quarks unaffected.

We conclude this section by stressing the crucial rôle of color. Recall that V-A four fermion couplings are invariant under Fierz rearrangement. Then our effective hamiltonian would be zero if color did not exist, because $(\bar{q}_1 q_2)(\bar{q}_3 q_4)$ would be exactly the same as $(\bar{q}_3 q_2)(\bar{q}_1 q_4)$. But when color is present, in order to go from one ordering to the other, color indices should also be crossed and the equality is no more valid.

PHENOMENOLOGICAL IMPLICATIONS

Low-lying charmed particles cannot decay via strong and e.m. interactions and their lifetime is determined by weak interactions. A general consequence of the above discussion is that non leptonic amplitudes are enhanced over their "natural" size and hence over semileptonic or leptonic modes. Thus one is led to extimate [1,10] :

$$\frac{\Gamma(C \to \mu \text{ (or e)} + \text{all})}{\Gamma(C \to \text{all})} \sim \text{a few percent} \qquad (9)$$

This is an important fact to take into account if leptonic signatures are considered for charmed particle detection.

The lightest multiplet of charmed particles are the charmed pseudoscalar mesons, expected to exist in the mass range $1.8 \div 2.2$ GeV[10,11,12]. These states are made up of a p' quark and a normal antiquark, with their antiparticles. We thus have a $\bar{3}$ of SU(3) with $p'\bar{\lambda} \sim S^+$ (T = 0, S = 1) ; $(p'\bar{n}) \sim D^+$; $(p'\bar{p}) \sim D^\circ$ (T = 1/2, S = 0), with their antiparticles in a 3 of SU(3).

We have seen that, neglecting the Cabibbo angle, the effective hamiltonian is a V spin singlet. We thus have, in the limit of SU(3) symmetry :

$$\Gamma(D^\circ \to \text{non leptonic}) = \Gamma(S^+ \to \text{non leptonic})$$
$$\sum \Gamma(D^\circ \to M_{pS}\, M_{pS}) = \sum \Gamma(S^+ \to M_{pS}\, M_{pS}) \text{ etc ...} \qquad (10)$$

where the last relation refers to the sum of the partial rates into two pseudoscalar mesons and other similar relations also hold for different final states.

For two body decays we note the selection rules[1] :

$$D^+ \not\to \bar{K}^\circ \pi^+$$
$$S^+ \not\to \pi^+ \pi^\circ \qquad (11)$$

The first one follows from V-spin, the second one from isospin. Moreover the amplitudes for decays into two pseudoscalar mesons are all proportional in the SU(3) limit :

$$(D^\circ \to \pi^+ K^-) = -\sqrt{2}\,(D^\circ \to \bar{K}^\circ \pi^\circ) = -\sqrt{6}\,(D^\circ \to \bar{K}^\circ \eta) = (S^+ \to \bar{K}^\circ K^+)$$

$$= \sqrt{\frac{3}{2}}\,(S^+ \to \pi^+ \eta) \qquad (10)$$

Some relations for three body decays are also obtained[1].

We now turn to charmed baryons. Baryons with C = +1 are made up of a p' quark and two normal quarks. Among $J^P = 1/2^+$ states there are 6 baryons of the form $p'\{q_1 q_2\}$ and 3 states of the form $p'[q_1 q_2]$ with the normal quarks in a symmetric or antisymmetric combination respectively. These 9 states belong to a $6 \oplus \bar{3}$ of SU(3) contained in a 20_B of SU(4)[10,11]. This is a different 20 than 20_H, and its SU(3) content is $20_B = 8 \oplus 6 \oplus \bar{3} \oplus 3$. Note the similar situation with the Σ'S and the Λ. The Λ is made up of a λ quark together with p and n quarks in a antisymmetric combination (T = 0), while the three Σ'S are made up of a λ quark plus two pp, pn or nn quarks in a symmetric combination. Just as the Λ is lighter than the Σ'S one expects the charmed baryons of the $\bar{3}$ to be stable[12]. Thus the candidates for charmed stable baryons are $p'[pn] \sim B^+_{pn}$ (T = 0, S = 0) ; $p'[\lambda n] \sim B^\circ_{\lambda n}$ and $p'[\lambda p] \sim B^+_{\lambda p}$ (T = 1/2, S = −1). These baryons should lie in the mass range between 2 ÷ 3 GeV[11,12].

In the SU(3) limit we obtain from V spin, in analogy with Eqs. (10) :

$$\Gamma(B^+_{pn} \to \text{non leptonic}) = \Gamma(B^\circ_{\lambda n} \to \text{non leptonic})$$

$$\sum \Gamma(B^+_{pn} \to B\, M_{pS}) = \sum \Gamma(B^\circ_{\lambda n} \to B\, M_{pS}) \text{ etc ...} \qquad (12)$$

Furthermore many relations can be derived for two body decays $B_c \to B + M_{pS}$ in that, in the SU(3) limit, 14 decays are given in terms of only 3 amplitudes, as described in detail in Ref. (2).

We conclude by pointing out one further interesting consequence of the 20_H dominance in non leptonic decays. The enhancement of a given representation of SU(4) is a consequence of the symmetry of the theory at short distances. However when matrix elements of H^{NL}_{eff} are taken between hadron states the SU(4) symmetry breaking becomes effective. For this reason we restricted to relations arising from SU(3) symmetry applied to matrix elements. It would be interesting however to learn how badly SU(4) is broken. Interestingly enough this possibility is offered by normal hyperon decays. It is well known that the $\Delta T = 1/2$ rule restricts the independent amplitudes for normal hyperon

decays to four transitions which can be chosen as $\Sigma^+ \to n\,\pi^+$, $\Sigma^+ \to p\,\pi^\circ$, $\Lambda \to p\,\pi^-$, $\Xi^- \to \Lambda\,\pi^-$. If one further assumes exact SU(3) (8 dominance) and cμ invariance the Gell-Mann, Lee, Sugaware relation for s-wave amplitudes is also obtained :

$$2S(\Xi^- \to \Lambda\,\pi^-) = \sqrt{3}\; S(\Sigma^+ \to p\,\pi^\circ) + S(\Lambda \to p\,\pi^-) \qquad (13)$$

which is very well satisfied by data $(4.08 \pm 0.04) = (4.04 \pm 0.05)$.

If we now assume SU(4) symmetry and cp invariance, from $H_{eff}^{NL} \sim 20_H$, $B \sim 20_B$, $M_{pS} \sim 15$, one additional relation is obtained for s-wave amplitudes[2]. This relation can be cast in various forms either :

$$S(\Lambda \to p\,\pi^-) = \frac{1}{\sqrt{3}}\; S(\Sigma^+ \to p\,\pi^\circ) \qquad (1.48 = 0.85) \qquad (14)$$

or :

$$S(\Xi^- \to \Lambda\,\pi^-) = \frac{2}{\sqrt{3}}\; S(\Sigma^+ \to p\,\pi^\circ) \qquad (2.04 = 1.71) \qquad (15)$$

where a comparison with experiment is also shown. We see that the result is neither particularly good nor catastrophic, SU(4) being broken at the 40 % level.

REFERENCES

1) G. ALTARELLI, N. CABIBBO, L. MAIANI ; "Enhancement of Non Leptonic Decays of Charmed Particles" Orsay Preprint PTENS 74/5 (to appear on Nuclear Physics).

2) G. ALTARELLI, N. CABIBBO, L. MAIANI ; "Weak Non Leptonic Decays of Charmed Hadrons" Preprint Istituto Superiore di Sanità, Roma, 1975 (Submitted to Physics Letters).

3) S.L. GLASHOW, J. ILIOPOULOS, L. MAIANI ; Physical Review D2, 1285 (1970).

4) R.P. FEYNMAN in "Symmetries in Elementary Particle Physics" ed. by A. ZICHICHI, Acad. Press, 1965.

5) K. WILSON ; Phys. Rev., 179, 1499 (1969).

6) For a review see for example G. ALTARELLI, Rivista del Nuovo Cimento, 4, 335 (1974).

7) G.'t HOOFT ; unpublished ; D.J. GROSS, F. WILCZEK ; Phys. Rev. Lett., 30, 1343 (1973) ; Phys. Rev. D8, 3633 (1973) ; H.D. POLITZER ; Phys. Rev. Lett. 30, 1346 (1973).

8) M.K. GAIALLARD, B.W. LEE ; Phys. Rev. Letters 33, 108 (1974) ; G. ALTARELLI, L. MAIANI ; Phys. Letters 52 B, 351 (1974).

9) G. ALTARELLI, K. ELLIS, L. MAIANI, R. PETROUZIO ; Orsay Preprint PTENS 74/6 (to appear on Nuclear Physics).

10) M.K. GAILLARD, B.W. LEE, J.L. ROSNER ; to be published on Rev. of Mod. Phys.

11) S. OKUBO, V.S. MATHUR, S. BORCHARDT ; Phys. Rev. Letters 34, 236 (1975).

12) A. De RUJULA, H. GEORGI, S.L. GLASHOW ; "Hadron Masses in a Sauge Theory" ;Harvard Preprint 1975.

Pomeron Coupling to Charmed Particles

Takeo Inami*

Laboratoire de Physique Théorique et Particules Elémentaires, Orsay**

Abstract

Relations between diffractive cross-sections for processes with and without charmed particles are given in a broken SU(4) scheme of Pomeron coupling based on the conjecture of existence of f_c trajectory. Experimental consequences, in particular for photon- and neutrino-production of charmed vector mesons, are discussed.

Among the theoretical models for the recetly discovered particles of mass 3.1 and 3.7 GeV,[1] one assuming that they are $J^P = 1^-$ bound states of charmed quark (c) and anti-quark ($\bar{c}$), in an SU(4) symmetry scheme[2], seems to fit many pieces of experimental information. Hence, it is of interest to speculate how charmed particles can be incorporated into Regge model thus far developed in SU(3) framework.

In this talk* we derive relations between cross-sections for various diffractive processes including those with charmed particles in a scheme with broken Pomeron couplings. Conjecturing the existence of a $c\bar{c}$ tensor trajectory, the sixteenth member of the hexa-decimet tensor trajectories which we denote by f_c, we extend from SU(3) to SU(4) the idea of f and f' dominance of Pomeron couplings[4]. In this new picture the Pomeron couples to particles via f, f' and f_c trajectories. SU(4) breaking of Pomeron couplings given in terms of splitting of the f, f' and f_c intercepts can be used to estimate diffractive cross-section for photo- and neutrino-production of charmed vector mesons ϕ_c, D^* and F^*.

To estimate numerically the Pomeron coupling to charmed particles we propose a model of exchange degenerate (EXD) linear ϕ_c-f_c trajectory with daughters spaced by two units of angular momentum and incorporating the new particles. The low intercept of our ϕ_c-f_c trajectory leads to a large SU(4) breaking of Pomeron couplings, which tends to suppress strongly ϕ_c, D^* and F^* production compared with what is expected from exchange of SU(4) singlet Pomeron[5].

Let us consider elastic scattering

$$a(p_1) + b(p_2) \to a(p_1') + b(p_2') \,. \qquad (1)$$

We will ignore unessential complication of spin effect. At sufficiently high energies elastic scattering is governed by the exchange of Pomeron singularity with intercept

---

* Most of the content of this talk has already appeared in preprint[3].

close to unity. In this approximation the elastic amplitude is written in the form

$$F_{ab\to ab}(\nu,t) = -A_{ab}^{P}(t)\, e^{-i\pi\alpha_P(t)/2}\, \nu^{\alpha_P(t)-1} \qquad (2)$$

where $\nu = -2p_1\cdot p_2$, $t = -(p_1 - p_1')^2$ and α_P is the Pomeron trajectory. Possible logarithmic energy dependence is ignored.

In the s-channel picture Pomeron exchange is generated by the shadow of all inelastic processes. It has been found that various Regge aproaches to calculate the Pomeron in this picture, when supplemented with the notion of duality, lead to a general form of Pomeron coupling. Namely, Carlitz, Green and Zee[4] have shown that in a variety of models the Pomeron residue is related to other vacuum trajectories by the formula

$$A_{ab}^{P}(t) = \sum_{ij} \beta_{iaa}(t)\,[\alpha_P(t)-\alpha_i(t)]^{-1}\, B_{ij}^{P}(t)\,[\alpha_P(t)-\alpha_j(t)]^{-1}\, \beta_{jbb}(t) \qquad (3)$$

valid for small t. The sum runs over all vacuum trajectories and α's and β's denote Regge trajectories and residues, respectively. B_{ij}^{P} is the Pomeron "bubble". Thus one is led to a picture that in the SU(3) scheme the Pomeron couples to particles via f and f' *, the ratio of the Pomeron residue to the f and f' residues being independent of the nature of particles and related to the f and f' intercepts. This picture explains quantitatively the difference between π N and KN total cross-sections[4]. It has been tested in inclusive reactions as well and a satisfactory agreement with experiment has been found.[7]

We consider SU(4) penta-decimet-meson nucleon scattering

---

* The models considered in Ref.(4) are too simplified to be realistic approximations to production amplitudes. Recently, Chan et al. proposed a more realistic method of calculating the Pomeron based on duality and EXD[6]. Their approach also leads to the f dominance of Pomeron couplings.

$$M_i + N \to M_i + N \qquad (4)$$

and apply the s-channel picture for generating the Pomeron. We extend to an SU(4) scheme the earlier calculations using two-cluster,[8] multiperipheral or dual models[9] which lead to eq.(2). This can be done by introducing charmed particles in the intermediate states and then exchange of charmed Regge trajectories. The only modification in the final expression will be tnat the sum now includes the f_c and its possible daughters in addition to the f,f and their daughters. As an example, figures below depict the leading f, f' and f_c contributions to Pomeron couplings in $D^- N$ and $F^- N$ diffractive scattering using quark diagrams and the one-loop approximation for the Pomeron "bubble" B_{ij}^{P}. Wavy lines represent reggeon propagators. Crosses indicate twisted propagators.

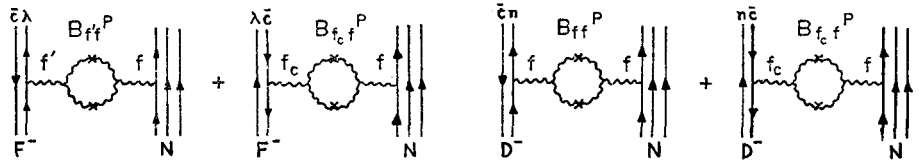

In addition to the basic notions such as Regge behaviour and duality we will introduce a few extra assumptions.

(1) The leading f,f', and f_c contributions dominate the sum over vacuum trajectories.

(2) All coupling preserve SU(4) symmetry. The tensor mesons f, f' and f_c are ideally mixed. The Pomeron "bubble" B_{ij}^{P} couples to the f,f' and f_c like an SU(4) singlet,

$$B_{ff}^{P}/\sqrt{2} = B_{f'f}^{P} = B_{f_c f}^{P} \qquad (5)$$

In these approximations we get for small t

$$A_{M_i N}^{P}(t) \simeq \{ \beta_{f M_i M_i}(t)[1-\alpha_f(t)]^{-1} B_{ff}^{P}(t) + \beta_{f' M_i M_i}(t)[1-\alpha_{f'}(t)]^{-1} B_{f'f}^{P}(t) + \beta_{f_c M_i M_i}(t)[1-\alpha_{f_c}(t)]^{-1} B_{f_c f}^{P}(t) \}[1-\alpha_f(t)]^{-1} \beta_{f NN}(t) \quad . \qquad (6)$$

When the f,f' and f_c intercepts are split, as they are experimentally, an effective SU(4) breaking of the Pomeron couplings is induced. This breaking is parametrized by the two ratios

$$r_1(t) = [1-\alpha_f(t)][1-\alpha_{f'}(t)]^{-1}, \qquad r_2(t) = [1-\alpha_f(t)][1-\alpha_{f_c}(t)]^{-1} \tag{7}$$

In terms of these two parameters we predict the following ratios between diffractive amplitudes*

$$F_{\rho N} : F_{\omega N} : F_{K^*N} : F_{\phi N} : F_{D^*N} : F_{F^*N} : F_{\phi_c N}$$
$$= 1 : 1 : \frac{1}{2}(1+r_1) : r_1 : \frac{1}{2}(1+r_2) : \frac{1}{2}(r_1+r_2) : r_2 \tag{8}$$

where vector mesons ω, ϕ, ϕ_c are assumed to be ideally mixed. Eq.(7) also applies to pseudo-scalar nucleon scattering with a slight modification depending on how η, η' and η_c are mixed.

The above predictions (8) can possibly be checked by charmed meson production experiment using nucleus targets. This requires, however, a great deal of effort from experimentalists on one hand, and a satisfactory theory of particle interaction in nuclei on the other. Our aim is to apply the present model to the diffractive photo- and neutrino-production of vector mesons at $t \simeq 0$, usnig the vector meson dominance (VMD) idea.

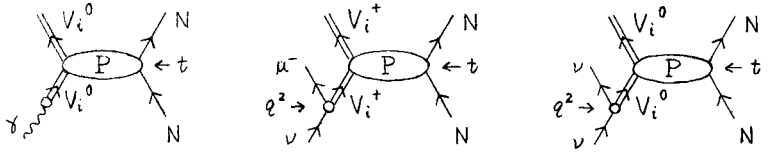

Let us first consider photo-production of ρ, ω, ϕ and ϕ_c. According to the VMD prescription, we have

$$\frac{d\sigma}{dt}(\gamma N \to V_i N) = e^2 g_i^{-2} \frac{d\sigma}{dt}(V_i N \to V_i N) \tag{9}$$

$$= e^2 g_i^{-2} |F_{V_i N \to V_i N}|^2 \tag{10}$$

where γ-V_i coupling constants g_i are defined by $\langle 0|J_\mu^{em}|V_i\rangle = \epsilon_\mu m_{V_i}^2 / g_i$. To write eq.(9) we have ignored possible contributions from other vector mesons V_i', V_i'', $\cdots$ with the same quantum number as V_i. The ratios (8) then imply the following

* We use notations in Ref.(5) of charmed particles ; D^{*+}, D^{*o}, F^{*+} and ϕ_c are $c\bar{n}$, $c\bar{p}$, $c\bar{\lambda}$ and $c\bar{c}$ members of the hexa-decimet vector mesons.

relations betaween diffractive cross-sections,

$$\frac{d\sigma}{dt}(\gamma N\to\rho N):\frac{d\sigma}{dt}(\gamma N\to\omega N):\frac{d\sigma}{dt}(\gamma N\to\phi N):\frac{d\sigma}{dt}(\gamma N\to\phi_c N)$$
$$=g_\rho^{-2}:g_\omega^{-2}:g_\phi^{-2}r_1^2:g_{\phi_c}^{-2}r_2^2\ . \tag{11}$$

We can also estimate how copiously strange and charmed vector mesons will be diffractively produced in high energy neutrino reactions

$$\nu(p_1)+N(p_2)\to\mu^-(p_1')+V_i^+(k)+N(p_2') \tag{12}$$

taking the hadronic weak current suggested by Glashow, Iloipoulos and Maiani;[10]

$$J_\mu^{W+}=J_\mu^+(\Delta S=0,\ \Delta C=0)\cos\theta_c+J_\mu^+(\Delta S=1,\ \Delta C=0)\sin\theta_c$$
$$-J_\mu^+(\Delta S=0,\ \Delta C=1)\sin\theta_c+J_\mu^+(\Delta S=1,\ \Delta C=1)\cos\theta_c \tag{13}$$

where S and C represent strangeness and charm, and θ_c is Cabbibo angle. For small q^2 $(=-(p_1-p_1')^2)$, i.e. outside deep inelastic region, and small t, we have

$$\sigma(\nu N\to\mu^-\rho^+N):\sigma(\nu N\to\mu^-K^{*+}N):\sigma(\nu N\to\mu^-D^{*+}N):\sigma(\nu N\to\mu^-F^{*+}N)$$
$$=g_\rho^{-2}\cos^2\theta_c|F_{\rho N\to\rho N}|^2:g_{K^*}^{-2}\sin^2\theta_c|F_{K^*N\to K^*N}|^2$$
$$:g_{D^*}^{-2}\sin^2\theta_c|F_{D^*N\to D^*N}|^2:g_{F^*}^{-2}\cos^2\theta_c|F_{F^*N\to F^*N}|^2 \tag{14}$$
$$=g_\rho^{-2}\cos^2\theta_c:g_{K^*}^{-2}\sin^2\theta_c\left(\frac{1+r_1}{2}\right)^2:g_{D^*}^{-2}\sin^2\theta_c\left(\frac{1+r_2}{2}\right)^2$$
$$:g_{F^*}^{-2}\cos^2\theta_c\left(\frac{r_1+r_2}{2}\right)^2 \tag{15}$$

where the weak-current vector-meson coupling constants g_i are defined by

$$\langle 0|J_\mu^+(i)|V_i\rangle=\epsilon_\mu m_{V_i}^2/g_i\ .$$

Similarly we can derive relations between ρ^0, ω, ϕ, and ϕ_c production cross-sections in reactions $\nu+N\to\nu+V_i^0+N$ for small q^2 and t and at large ν, if we take a particular model for neutral weak current. For Weinberg-Salam current[11], we get

$$\sigma(\nu N\to\nu\rho^0N):\sigma(\nu N\to\nu\omega N):\sigma(\nu N\to\nu\phi N):\sigma(\nu N\to\nu\phi_c N)$$
$$=g_\rho^{-2}(1-2\sin^2\theta_w)^2:g_\omega^{-2}(2\sin^2\theta_w)^2:g_\phi^{-2}(2\sin^2\theta_w)^2r_1^2:g_{\phi_c}^{-2}(2\sin^2\theta_w)^2r_2^2 \tag{16}$$

where θ_w is the Weinberg angle.

To estimate numerically the Pomeron coupling ratios we assume EXD liner hexa-

decimet 1^{-}-2^{+} trajectories. Data on meson resonances give for f and f'

$$\alpha_f(0) \simeq 0.5, \quad \alpha_{f'}(0) \simeq 0.15 \tag{17}$$

As for f_c we assume a liner ϕ_c-f_c trajectory with daughters spaced by two units of angular momentum, based on the original notion of daughters[12, 13] and in analogy with the case of ρ'[14], and incorporating the new particles(see ref.(3) for detail). The 3.1GeV resonance can be identified with ϕ_c. We suggest the interpretation that the 3.7 GeV resonance (ϕ_c')iis the daughter of $\phi_c(3^{-})$ (see fig.1). Then we get

$$\alpha_{f_c}(0) \simeq -3.8 \tag{18}$$

The f, f', f_c intercepts (17, 18) give*

$$r_1(0) = 0.5 - 0.7, \qquad r_2(0) = 0.085 - 0.13 \tag{19}$$

where we have allowed the following uncertainties of intercepts : $\Delta\alpha_f(0) = \Delta\alpha_{f'}(0) = 0.05$, $\Delta\alpha_{f_c}(0) = 0.5$. Predictions for the ratios between vector meson production cross-sections at t = 0 and at sufficiently high energies are given in table 1. For photo-production γ-V_i coupling constants determined from $e^{+}e^{-}$ experiments** are used. For neutrino reaction the quark model ratios for $J^{W}(i)$-V_i coupling constants g_i are used but they should be replaced by experimental values as soon as they are known from weak decay measurements.

We take experimental values of $(d\sigma/dt)_{t=0}$ for $\gamma N \to \rho N$ at 9-16 GeV/c[16] as input in order to calculate $(d\sigma/dt)_{t=0}$ for $\gamma N \to \omega N$, ϕN and $\phi_c N$. The meson (f and A_2) exchange contributions in $\gamma N \to \rho N$ and ωN reactions can easily be taken care of using the approximate relation

$$d\sigma_{\gamma N \to \rho N}(p_L)/dt = [\sigma_{\pi N}(p_L)/\sigma_{\pi N}(p_L = \infty)]^2 \, d\sigma_{\gamma N \to \rho N}(p_L = \infty)/dt . \tag{20}$$

---

* If we take the universal slope $\alpha' \simeq 1.0$ for the EXD ϕ_c-f_c trajectory instead, we get $r_2(0) \simeq 0.050$.

** We have taken $g_\rho^2/4\pi = 2.3$, $g_\omega^2/4\pi = 18.4$, $g_\phi^2/4\pi = 14.4$[15] and $g_{\phi_c}^2/4\pi = 9.2$ ($\Gamma(\phi_c \to e^+e^-) = 6.0$ keV).

We ignore possible weak variation of diffractive cross-sections as $p_L \to \infty$ and estimate $[\sigma_{\pi N}(p_L)/\sigma_{\pi N}(\infty)]^2 = 1.3 - 1.4$ for $p_L \simeq 10$ GeV/c. Table 1a gives predictions for $(d\sigma/dt)_{t=0}$ for ω, ϕ and ϕ_c production at $E_\gamma \simeq 10$ GeV, i.e. SLAC energy, as well as at $E_\gamma = \infty$, where $E_\gamma \doteq p_L$. ϕ_c production cross-section is taken to be negligible for $p_L \lesssim 20$ GeV/c due to a large kinematical effect. Comparison of vector meson dominance calculations with experiment has already been done by many authors[17] and will not be repeatted here.

The most important experimental consequence of our speculation is that a large deviation of r_2 from unity implies that ϕ_c and F^{*+} production will be suppressed considerably, i.e. by two orders of magnitude or a bit more for ϕ_c production and one order for F^{*+} production. Note that one would expect ϕ_c and F^{*+} to be produced as copiously as ρ in a model of SU(4) singlet Pomeron exchange[5].

Calculation of the slope B of $d\sigma/dt$ involves too many assumptions to be reliable quantitatively. One may, however, guess that the slope of ϕ_c production is a little flatter than that of ϕ production ($B_{\gamma p \to \phi p} = 4 - 5$ GeV^{-2} [16] at $E_\gamma \simeq 10$ GeV). If we suppose $B_{\gamma p \to \phi_c p} \simeq 3$ GeV^{-2} at NAL energy, we get a crude estimate $\sigma(\gamma p \to \phi_c p) \simeq 0.05 - 0.10$ μ b .

The author is greatly indebted to Professor D. Geffen for his valuable suggestions at various stages of this work. He is also grateful to Professor A. Krzywicki for a careful reading of the manuscript and to Dr. L. Oliver, H. Yoshida, and Professors A. Capella, Chan Hong-Mo and Tran Thanh Van for helpful discussions. He also thanks Dr. S.Kitakado for informative discussions.

Referrences

(1) J.J.Aubert et al., Phys.Rev.Letters 33(1974) 1406 ; J.E.Augustin et al., Phys. Rev.Letters 33(1974) 1406 ; C.Bacci et al., Phys.Rev.Letters 33(1974) 1408 ; J.E.Augustin et al., Phys.Rev.Letters 33 (1974) 1453.

(2) Z. Maki, Prog. Theor. Phy. 31 (1964) 331 and 333 ; Y.Hara, Phys.Rev. 134 (1964) B701 ; J.D.Bjorken and S.L.Glashow, Phys.Letters 11(1964) 255 ; D.Amati, H.Bacry, J.Nuyts and J.Prentki, Phys.Letters 11(1964) 190.

(3) T.Inami, Orsay preprint LPTPE 75/5, February, 1975.

(4) R.Carlitz, M.B.Green and A.Zee, Phys.Rev.D4 (1971) 3439 and references therein.

(5) M.K. Gaillard, B.W.Lee and J.L.Rosner, Fermilab preprint (1974).

(6) Chan Hong-Mo, J.E.Paton and Tsou Sheung Tsou, Rutherford preprint (1974).

(7) Chan Hong-Mo, T.Inami and R.G.Roberts, in preparation ; S.Yazaki, Phys.Letters 43B (1973) 225.

(8) R.C.Hwa, Phys.Rev.Letters 25 (1970) 1728.

(9) C.Lovelace, Phys.Letters 34B (1971) 500.

(10) S.L.Glashow, J.Iliopoulos and L.Maiani, Phys.Rev. D2 (1970) 1285.

(11) S.Weiberg, Phys.Rev.Letters 27 (1971) 1688; A.Salam, Elementary Particle Physics (Ed. N.Svartholm, Almqvist and Wiksells, Stockholm, 1968), p.367

(12) D.Z.Freedman and J.M.Wang, Phys.Rev.160 (1967) 1560 ; M.Toller, Nuovo Cimento 53A (1968) 671.

(13) H.R.Rubinstein, A.Schwimmer, G.Veneziano and M.Virasoro, Phys.Rev.Letters 21 (1968) 481 ; T.Eguchi and K.Igi, Phys.Rev.Letters 27 (1971) 1319.

(14) See, for example, F.Wagner, Proceedings of London Conference, 1974.

(15) D.Benkasas et al., Phys.Letters 42B (1972) 507 ; G.Cosme et al., Phys.Letters 48B (1974) 155.

(16) Quoted by K.C.Moffeit, Proceedings of Bonn Syposium, 1973.

(17) See, for example, R.P.Feynman, Lectures 15-21, Photon-Hadron Interactions, W.A.Benjamin, INC.

(18) J.Ballam et al., Phys.Rev.D7 (1943) 3150.

Table 1a

Predictions for $(d\sigma/dt)_{t=0}$ for vector meson photo-production. To calculate the ratios we have used $r_1 \approx 0.55$ and $r_2 = 0.09 - 0.14$ Predictions are given at $E_\gamma = p_L \approx 10$ GeV as well as at $E_\gamma = \infty$ in order that comparison with experiment [17, 19] at SLAC energy may be done. ρ production cross-section has been used as input.

Reactions	Theory				Experiment $(d\sigma/dt)_{t=0}$ μb/GeV^2 $E_\gamma \approx 10$ GeV
	Ratios		$(d\sigma/dt)_{t=0}$ μb/GeV^2		
			$E = \infty$	$E_\gamma \approx 10$ GeV	
$\gamma N \to \rho N$	g_ρ^{-2}	1	75–80	105	105 ± 5
$\gamma N \to \omega N$	g_ω^{-2}	0.124	9–10	13	12.5 ± 2
$\gamma N \to \phi N$	$g_\phi^{-2} r_1^2$	~0.05	~4	~4	2± 1
$\gamma N \to \phi_c N$	$g_{\phi_c}^{-2} r_2^2$	$(2-4)\times 10^{-3}$	0.15 – 0.3	0	

Table 1b

Predictions for cross-section ratios between vector meson neutrino-production at large ν, small q^2 and $t = 0$. The quark model values of g_i have been used to calculate the ratio numerically.

Reactions	Ratios	
$\nu N \to \mu^- \rho^+ N$	$g^{-2} \cos^2\theta_C$	1
$\nu N \to \mu^- K^{*+} N$	$g_K^{-2} * \sin^2\theta_C \frac{1}{4}(1+r_1)^2$	~ 0.03
$\nu N \to \mu^- D^{*+} N$	$g_D^{-2} * \sin^2\theta_C \frac{1}{4}(1+r_2)^2$	~ 0.02
$\nu N \to \mu^- F^{*+} N$	$g_F^{-2} * \cos^2\theta_C \frac{1}{4}(r_1+r_2)^2$	0.1 – 0.2

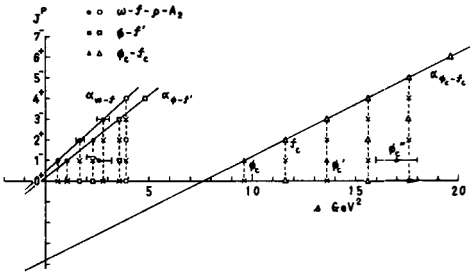

Fig. 1. Chew–Frantschi plot of EXD linear ϕ_C-f_C trajectory proposed in the present paper together with ω-f-ρ-A_2 and ϕ-f' trajectories. Predicted and observed states are denoted by an open and a full circle, square or triangle. Crosses represent odd daughter points where one does not expect resonances.

THE SU(4) CHARACTER OF THE POMERON: A CALCULATION OF THE ψp (AND πp, Kp, ηp, ETC.) TOTAL CROSS-SECTION.*

M. Teper
Institute of Theoretical Science
University of Oregon
Eugene, Oregon 97403 (USA)

Abstract : We calculate the ratios of πp, Kp, ... , ψp total cross-sections utilising a phenomenologically motivated peripheral-type model for production processes, supplemented with SU(4) symmetry for the couplings. Kinematic effects arising from mass splittings are crucial. We obtain $\sigma_{\psi p} \approx \frac{1}{2}$ mb.

Résumé : Nous calculons les rapports des sections efficaces totales πp, Kp, ..., Ψp en utilisant un modèle du type périphérique d'origine phénoménologique pour les processus de production - avec la symétrie SU(4) pour les couplages. Les effets cinématiques provenant des écarts de masse sont cruciaux. Nous obtenons $\sigma_{\psi p} \approx \frac{1}{2}$ mb.

* Work done in collaboration with J.W. Dash and M. S. K. Razmi.

Supported in part by U.S. Atomic Energy Commission contract AT(45-1) - 2230.

THE SU(4) CHARACTER OF THE POMERON

A particularly interesting interpretation of the ψ is that it is the charmed analogue of the ϕ i.e. its quark content is a charmed, c, and an anti-charmed, $\bar{c}$, quark. Within the context of this picture we shall calculate the ψp total cross-section, $\sigma_{\psi p}$, and compare it to the experimental estimate presented at this meeting.[1]

We certainly expect $\sigma_{\psi p} \neq \sigma_{\pi p}$ since we know that $\sigma_{\pi p} \neq \sigma_{Kp}$ i.e. the Pomeron is not an SU(3) singlet. This is no surprise: we usually think of the Pomeron as having vacuum quantum numbers, and the vacuum is clearly not an SU(3) (or SU(4)) singlet. Thus if we take a picture of the vacuum, some of the time it will look like a 2π pair, and sometimes like a 2K pair. By the uncertainty principle, however, it will look like 2π more often than 2K, because the mass of a K is greater than that of a π. It will look like 2D even less often (D,F,η_c are the extra particles in the 15 multiplet of pseudoscalars that contains π, K etc.).

More directly if we look at collisions in impact parameter, we expect 2π exchange to extend further than 2K exchange and much further than 2D exchange. Correspondingly one expects $\sigma_{\pi p} > \sigma_{Kp} >> \sigma_{Dp}$.

Clearly we have no rigorous prescription as to how to set about calculating these -- or any other -- strong interaction cross-sections. We must choose both our approach and model. Our approach is to have a model for inelastic processes, and to sum over such processes to give the required total cross-section. Our model will be a slightly generalised version of the multiperipheral model.

We shall calculate $\sigma_{\pi p} : \sigma_{KP} : \sigma_{\eta p}$ first since we have experimental results for these quantities -- and a comparison between our results and experiment here will be indicative of the reliance we should place on our later results for $\sigma_{\psi p}$. Results on these ratios are, of course, of interest in themselves.

Our model for ap collisions is as in Fig. la -- leading to a contribution to the total cross-section as shown in Fig. lb

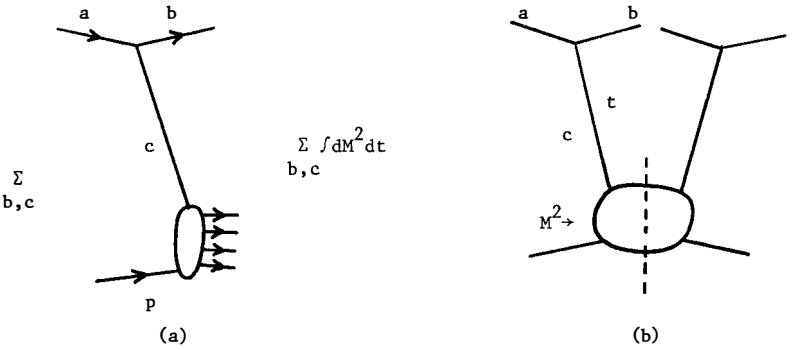

Fig. 1

In general a belongs to the pseudoscalar octet and we take b,c to be the vector, pseudoscalar, octets respectively. Thus our equations are

$$\frac{\sigma_{\pi p}}{\sigma_{Kp}} = \frac{\pi\ \rho \;+\; \pi\ K^*}{K\ K^* \;+\; K\ \rho,\phi,\omega} \qquad (1)$$

$$\frac{\sigma_{\eta p}}{\sigma_{\pi p}} =$$

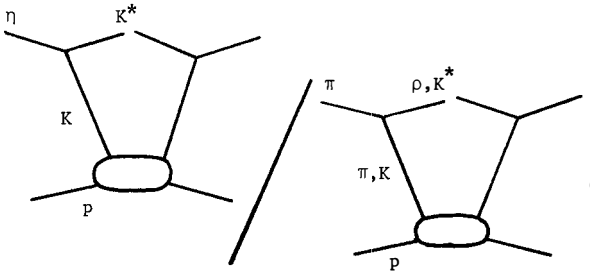

(2)

If we iterate Fig. 1a we obtain a multiperipheral model which has received detailed comparison[2] against multiparticle data: hence we are confident that it provides a reasonable representation of a substantial fraction of the total cross-section. In the present context Fig. 1a is in fact better than the derived multiperipheral model. Thus, suppose for example that our choice for the exchanges c is just half right. Then the derived multiperipheral model will be only $(1/2)^{n-1}$ right (n is the final multiplicity) which can be a very small number. In using the model directly as shown in Fig. 1a,b we simply do one loop integral and use the physical σ_{cp} for the lower blob: hence in the case where the exchange is half right, our final answer is also likely to be at least half right (taking ratios improves things in any case). The results reported here are calculated assuming the only t dependence in the loop integral to come from the propagators, $1/(t - m_c^2)$. The same model results if we use the form factors employed in Ref. (2).

The size of $\sigma_{\pi p}/\sigma_{Kp}$ will be determined primarily by the fact that strange mesons are more massive than non-strange mesons. Hence one may anticipate that even if we were to allow b and c in Fig. 1a to belong to SU(3) multiplets with various spins, etc., in taking the ratios (1) and (2) the final results would remain largely unaltered.

With pure SU(3) couplings we obtain

$$\frac{\sigma_{\pi p}}{\sigma_{Kp}} \approx 1{\cdot}74 \qquad \frac{\sigma_{\eta p}}{\sigma_{\pi p}} \approx 0{\cdot}4$$

With conventionally broken (~4%) couplings we obtain

$$\frac{\sigma_{\pi p}}{\sigma_{Kp}} \approx 1{\cdot}45 \qquad \frac{\sigma_{\eta p}}{\sigma_{\pi p}} \approx 0{\cdot}5$$

The experimental values are

$$\frac{\sigma_{\pi p}}{\sigma_{Kp}} \approx 1{\cdot}3 \qquad \frac{\sigma_{\eta p}}{\sigma_{\pi p}} \overset{?}{\approx} \frac{3}{2}\frac{\sigma_{\phi p}}{\sigma_{\rho p}} \approx 0{\cdot}6 - 0{\cdot}7$$

Clearly the comparison is good enough to motivate an extension from SU(3) to SU(4).

Extending this procedure to the full 15 multiplets of pseudoscalars and vectors, we obtain a larger set of coupled equations. The solutions are

$$\frac{\sigma_{Dp}}{\sigma_{\pi p}} \approx 0{\cdot}2 \qquad \frac{\sigma_{Fp}}{\sigma_{\pi p}} \approx 0{\cdot}1 \qquad \frac{\sigma_{\eta cp}}{\sigma_{\pi p}} \approx 0{\cdot}02$$

where D, F are non-strange and strange charmed pseudoscalar mesons, while ηc is the spin zero analogue of the ψ. Hence our final result is

$$\sigma_{\psi p} \approx \sigma_{\eta cp} \approx \tfrac{1}{2}\text{mb} \qquad (3)$$

which compares reasonably well with the value obtained in ψ-photoproduction, $\sigma_{\psi p} \overset{\sim}{} 1\text{mb}$, as reported at this meeting. In this calculation pure SU(4) couplings were used -- on the assumption that to a first approximation, just as in SU(3), the mass-breaking is more significant than coupling breaking.

The result (3) would appear to provide additional evidence for the $c\bar{c}$ interpretation of the ψ. However some caution is necessary. The fact that the decay $\psi'(3{\cdot}7) \to \psi(3{\cdot}1) + 2\pi$ goes, means that there is a contribution to the ψp cross-section where (in Fig. 1a) a = ψ, b = ψ', c = ordinary meson. Our estimate of the couplings on the basis of the known decay width (a highly non-unique procedure) suggests that this type of contribution could perhaps be as high as $\frac{1}{2}$ mb. So at this stage it is

perhaps too early to conclude that the ψ is a $c\bar{c}$ pair: however the fact that the calculated $\sigma_{\psi p}$ is not too large retains its significance.

We thank Gordon Aubrecht and Robert Mazo for help with the computing.

References

1. J. Peoples : Talk at this Meeting.

2. J. Dash, J. Huskins, S. Jones : Phys. Rev. D9 (1974) 1404.

EXTENDED PARTICLE MODEL WITH QUARK CONFINEMENT AND CHARMONIUM SPECTROSCOPY

Peter Hasenfratz and Julius Kuti

Central Research Institute for Physics, Budapest, Hungary

High Energy Physics Department

Alexander S. Szalay

Eötvös University, Budapest, Hungary

1. QUALITATIVE DESCRIPTION OF THE MODEL

In recent years there has been increasing evidence that hadrons are composite objects with fractionally charged quark constituents. However, there are strong indications that hadrons are very difficult, if not impossible, to break into their quark constituents:

The hadron spectrum is strongly reminiscent of an infinite tower excitation spectrum of extended objects without any indication for an "ionization point" into constituents. Further, no quark constituents have been seen in deep inelastic or other high energy collision processes. As a radical response to this situation quark confinement and the study of extended objects has became an attractive theoretical approach to hadron physics in the last two years.

In 1962 Dirac[1] made a proposal for an extended particle model of the electron. As far as we know his Lagrangian model has served as the first prototype of an extended object described in a four-dimensional relativistic picture abandoning conventional nonlinear field theory.

The electron is assumed to have a charged surface. Outside the surface Maxwell's equations hold. Inside the surface there is no field. The electron is stabilized against the Coulomb repulsion of its surface charge by a non-Maxwellian force of the type of a surface tension. So the electron may be pictured as a bubble whose energy in addition to the electromagnetic field energy contains a positive term proportional to the surface of the particle.

In Dirac's theory the spherical excitation /radial vibration/ of the electron is conjectured to correspond to a massive particle vaguely interpreted as the muon.

There is a different way of stabilizing an extended object if a special force of the type of a volume tension is introduced which correspons to some positive energy proportional to the volume of the extended particle. Volume tension serves as the confining mechanism for quarks in the MIT bag model.[2]

Recently, we have proposed a minimal extended particle model[3] for the quark confinement mechanism abandoning conventional nonlinear field theory. Here we will present the main features of the model together with some applications to charmonium spectroscopy.

As the most important element of the model first we introduce extended particle-like vector gluon bubbles /bags/ which are stabilized against free expansion by a surface tension or volume tension. Since quarks are coupled to the gluon field they are confined to the inside of the gluon bag without any further mechanism.

Only color singlet gluon bags are allowed in our model. Gauss's theorem as applied to the gluon field will assure that all hadrons are necessarily color singlets. However, in the limit when the quark-gluon coupling vanishes quarks become free particles since they are decoupled from the color singlet gluon bags in that limit. This feature makes the model distinctive from bag type theories[4] where quarks are confined without utilizing the vector gluon field and the quark-gluon coupling is introduced only at a later stage to arrange for color singlet hadron states.

Since nonlinear boundary conditions are not imposed on the quark fields in our model, we hope to avoid some peculiar problems (as the construction of local currents, to mention one) which are related to the quantum field theory of extended particle models.

Surface tension seems to us to be the most straightforward application of Dirac's idea to the quark confinement problem abandoning conventional nonlinear field theory. Somewhat more reminiscent of the MIT bag model, volume tension may also be applied for stabilizing the gluon bag and we will further elaborate on both possibilities at several points of our discussion.

We have no deep physical interpretation for the rather mysterious surface tension or volume tension. Perhaps the model is internally consistent even on the quantum field theoretic level so that we can work with it phenomenologically, at least. If, however, we will run into inconsistences then we will be forced to understand to what extent the tension type force is only an artifact of some hitherto undiscovered quark confinement mechanism.

A conventional solution may be offered by an underlying relativistic field theory where the vector gluon field is trapped somehow via a nonlinear scalar field[5] which is non-vanishing inside the gluon bubble and vanishes outside (or vice versa). The gradient of the scalar field across the smooth surface of the bubble would generate some surface

tension whereas the approximately constant potential energy of the scalar field inside the bubble acts like a volume tension. The relative weight of the two types of tensions would be determined by the detailed behaviour of the nonlinear system.

Or, more probably, some hitherto not known mechanism may be phenomenologically well approximated by a tension type confinement force.

Though in the most sophisticated version of our model the classical field equations inside the bag are identical with those of an asymptotically free non-abelian gauge theory, the differences are relevant. In the Yang-Mills theory higher order quantum effects from the infrared region are conjectured to lead to quark confinement. In our case the finite size of the gluon bag balanced by a tension type force represents an effective infrared cutoff so that we don't expect infrared divergences here. That is consistent with the main features of the model since the gluon field is already confined by the tension force and we must not impose another confinement mechanism on the quarks. (Is the gluon bag with quarks inside perhaps an artifact of the quantum field theory of Yang-Mills fields coupled to quarks?)

The coupling of the gluon field to quarks is sufficiently weak in our model so that vacuum polarization effects are expected to be small for the lowest meson and baryon states. The "fine structure constant" α_s of the quark-gluon interaction is approximately $\frac{1}{5}$ in what follows here.[6] Even though we would certainly feel uneasy with a much larger value, $\alpha_s = \frac{1}{5}$ is not necessarily a best choice in hadron spectroscopy. We have chosen this number for a first orientation in our calculations.

Since vacuum polarization is expected to be fairly weak, we attempt to calculate bound states with a fixed number of point-like quarks (valence quark). The quark-constituent picture is valid then and valence quarks dominate the structure of hadrons.

The lowest meson states would be represented by relativistic "positronium-like" $q\bar{q}$ -bound states whereas baryons are conjectured to be $3q$ -bound states. A relatively weak Coulomb-like force will dominate the quark- anti-quark interactions at small distances and the valence quarks will be confined to the inside of the gluon bag by a linear confinement potential.

The gluon bubble carries vacuum polarization $q\bar{q}$ -pairs

(sea-quarks) whose feeble presence should be calculated from the gluon bag-valence quark bound states. This approach may open the way to a dynamical foundation of the quark-parton model of the nucleon.

Radially excited mesons with large excitation from their "bag-like" ground state become rather similar to rotating strings with linear confinement potential between the quark constituents. Excited mesons and baryons may split into lower mass states via the presence of vacuum polarization pairs. A better understanding of this decay mode would provide us with a dynamical explanation of Zweig's rule for some decay properties of hadrons.

Multiparticle production is associated with the creation of $q\bar{q}$ -pairs from the vacuum polarization of the strong gluon field which represents the quark confinement force to balance large disturbances in the high energy collision process. The asymptotic behaviour of strong interaction cross sections is related to this mechanism.

2. GAUGE FIELD BAGS WITH QUARKS INSIDE

First we consider a massless abelian gauge field (like the electromagnetic field) confined by surface tension. We will work in a four-dimensional relativistic picture in which the surface of the gauge field bubble appears as a tube with a three dimensional surface.

The classical action W consists of two terms, a four--dimensional integral W_0 extended over the space inside the tube and a three-dimensional integral W_S extended over the surface of the tube. The space outside the tube contributes no action. We take W_0 to be the usual action for the Maxwell field

$$W_0 = -\frac{1}{16\pi}\int F_{\mu\nu}F^{\mu\nu}\,d^4x\,, \qquad /2.1/$$

$$F_{\mu\nu} = \partial_\mu A_\nu - \partial_\nu A_\mu \,.$$

We choose W_S to be a constant times the three-dimensional area of the tube.

To avoid certain difficulties in working with the action principle we must introduce curvilinear coordinates . The surface of the tube is defined to be $f(x)=0$ in terms of these curvilinear coordinates, with $f(x)>0$ for the region outside the bag. $f(x)$ is not changed in the variation process

and an arbitrary variation of the surface is produced by varying the coordinate system. For convenience, the curvilinear coordinate system and its variations are described in a fixed system with rectilinear and orthogonal coordinates y^λ. The metric for the x system is

$$g_{\mu\nu} = \partial_\mu y_\lambda \partial_\nu y^\lambda \qquad /2.2/$$

If there is one gauge field bag, the most convenient choice for $f(x)$ is

$$f(x) = x^1, \qquad /2.3/$$

which can be fitted in with a deformed system of polar coordinates. With the choice /2.3/ for $f(x)$, the action is

$$W_0 = -\frac{1}{16\pi} \int_{x^1<0} J\, g^{\mu\rho} g^{\nu\sigma} F_{\mu\nu} F_{\rho\sigma}\, d^4x, \qquad /2.4/$$

$$W_S = -\frac{\omega}{4\pi} \int_{x^1=0} M\, dx^0 dx^2 dx^3 \qquad /2.5/$$

where $-J^2$ is the determinant of $g_{\mu\nu}$ and M^2 is the determinant of g_{ab}, where a, b take on the values $0, 2, 3$, so that

$$M = J(-g^{11})^{1/2}$$

ω is a positive constant that determines the strength of the surface tension introduced by /2.5/.

The variation of $A_\mu(x)$ and $y_\lambda(x)$ which describes the curvilinear coordinate system leads to the Maxwell equations inside and two boundary conditions on the surface

$$F^{\rho\mu} n_\mu = 0, \qquad /2.6/$$

$$-\frac{1}{4} F_{\mu\nu} F^{\mu\nu} = -\omega J^{-1} \partial_\mu (J n^\mu) \qquad /2.7/$$

where n_μ is a unit normal vector to the surface

$$n_\mu = -\partial_\mu f(x) (\partial_\mu f(x) \partial^\mu f(x))^{-1}$$

We have derived the boundary conditions /2.6/ and /2.7/ by varying $A_\mu(x)$ on the surface. An alternative choice in the variational principle is to keep $A_\mu(x)$ vanishing on the surface with $\delta A_\mu(x) = 0$. This leads to a complementary set of boundary conditions:

$$\tilde{F}^{\rho\mu}\, n_\mu = 0 \quad , \qquad /2.6a/$$

$$\frac{1}{4} F_{\mu\nu} F^{\mu\nu} = -\omega J^{-1} \partial_\mu (J n^\mu) \qquad /2.7a/$$

where $\tilde{F}^{\mu\nu} = \varepsilon^{\mu\nu\rho\sigma} F_{\rho\sigma}$ is the dual tensor.

The second set of boundary conditions /2.6a/, and /2.7a/ would be applied if our quarks carried magnetic monopole charges /magnetic bag/[8]. Since we study here quarks with color charges /electric bag/ we will use the boundary conditions /2.6/ and /2.7/. The right-hand side of /2.7/ has a simple geometrical meaning. It is proportional to the mean curvature in the case of a static surface.

A similar analysis can be repeated with volume tension if W_s in /2.5/ is replaced by

$$W_v = -\frac{\beta}{4\pi} \int_{x^4<0} J \, d^4x \qquad /2.8/$$

where β is a positive constant that determines the strength of the volume tension. The Maxwell equations are valid inside the surface, the linear condition /2.6/ remains the same, only the nonlinear boundary condition /2.7/ will change:

$$-\frac{1}{4} F_{\mu\nu} F^{\mu\nu} = \beta \qquad /2.9/$$

where the left-hand side is now constant on the surface.

The Yang-Mills theory is a straightforward generalization of the abelian case. We define

$$F_{i\mu\nu} = \partial_\mu A_{i\nu} - \partial_\nu A_{i\mu} + g f_{ijk} A_{j\mu} A_{k\nu}$$

with a coupling constant g in the nonlinear term. W_0 becomes

$$W_0 = -\frac{1}{16\pi} \int_{x^4<0} J \, g^{\mu\rho} g^{\nu\sigma} F_{i\mu\nu} F_{i\rho\sigma} \, d^4x$$

and /2.5/ or /2.8/ remain the same. Introducing the gauge covariant derivative

$$D_{ij\mu} = \delta_{ij} \partial_\mu - g f_{ijk} A_{k\mu} \, ,$$

we have the Yang-Mills field equations inside the gluon bag

$$D_{ij\mu} (J F_j^{\mu\nu}) = 0$$

The boundary conditions are:

surface tension	volume tension	
$F_i^{\rho\mu} n_\mu = 0$	$F_i^{\rho\mu} n_\mu = 0$	/2.10/
$-\frac{1}{4} F_{i\mu\nu} F_i^{\mu\nu} = -\omega \int^{-1} \partial_\mu (J n^\mu)$	$-\frac{1}{4} F_{i\mu\nu} F_i^{\mu\nu} = \beta$	/2.11/

Finally, we introduce quark fields $q_{i\alpha}(x)$ where the first index refers to the $SU(3)$ of color and the second to the hadronic $SU(4)$. The quark fields are coupled to the Yang--Mills fields through a conserved current as if they were massless, whereas the quark mass term is put in additionally. Since quarks are also coupled to the electromagnetic and weak gauge fields, the quark mass term is perhaps generated by the Higgs field in a unified theory. The bag is, of course, transparent against electromagnetism and weak interactions.

Now we have the complete classical field theory. Inside, we have the field equations of a Yang-Mills theory of quark--gluon interaction. They are derived from W_0 which now includes the quark fields and the quark-gluon coupling. On the surface /2.10/ and /2.11/ remain the same since there is no change in W_s and W_v . In addition, we introduce a linear boundary condition for the quark field

$$q_{i\alpha}(x) = 0 \qquad /2.12/$$

on the surface of the bag.

The field equations for the gauge fields and quarks, together with the boundary condition /2.10/ eliminate all the extended particles with non-zero color charges.

3. BORN-OPPENHEIMER /ADIABATIC/ APPROXIMATION

As a first application of the model we will study a simple approach to bound states of heavy charmed quarks.

Similar to the Born-Oppenheimer approximation in molecular physics heavy charmed quarks will be treated as nonrelativistic in their motion whereas the gluon bag and light quarks (u, d, s) will be treated in adiabatic approximation.[7] Under special circumstances the interaction between a charmed quark antiquark will be described by a nonrelativistic potential $V(r)$.

It is worth of recalling that in molecular approximations due to the large ratio of nuclear mass to electron mass the

nuclear periods are much longer than the electronic periods. It is then a good approximation to regard the nuclei as fixed calculating the electronic motion. Moreover, the nuclear motion can be calculated under the assumption that the electrons have their steady motion for each instantaneous arrangement of the nuclei /adiabatic approximation in molecular physics/.

The analogy is suggestive. The charmonium bound state is like a quark molecule whose heavy charmed quarks correspond to the heavy nuclei whereas the gluon oscillations and light $q\bar{q}$ -pairs from vacuum polarization are analogous to light electrons in molecules.

We imagine a pair of static sources (charmed quark and charmed antiquark) of the gluon field $A_{i,a}(x)$. The gluon field is coupled also to the light quark fields. The position vectors $\vec{r}_1$ and $\vec{r}_2$ of the static sources are parameters in the static Hamiltonian $H_s(\vec{r}_1, \vec{r}_2)$ whose dynamical variables are associated with the gluon bag and the light quark fields. Now we assume, that in adiabatic approximation for slowly moving charmed quarks when the c -quark is found at $\vec{r}_1$ and the $\bar{c}$ -quark at $\vec{r}_2$ the other dynamical degrees of freedom representing the gluon bag and the light quarks are described by the static Hamiltonian $H_s(\vec{r}_1, \vec{r}_2)$. Physically we assume that the gluon bag and light quarks inside can instantenously readjust themselves to the slowly moving sources ignoring retardation effects.

In adiabatic approximation we identify the nonrelativistic potential energy of the charmed quark and charmed antiquark with the energy stored in the gluon bag including the light $q\bar{q}$ -pairs from vacuum polarization. This energy is calculable from the static Hamiltonian

According to our assumption the gluon coupling to quarks is rather weak so that in first approximation we will calculate the contribution of the gluon bag to the potential energy of the c -quark and $\bar{c}$ -quark sources and ignore the light $q\bar{q}$ -pairs from vacuum polarization.

Since the $c\bar{c}$ -bound state must be a color singlet, the color spins of the static sources are antiparallel. In that case the non-abelian field equations decouple and effectively we have to work with an abelian gluon field coupled to opposite color charges.

The ordinary spins and the associated "color magnetic moments" of the sources are ignored for the moment.

After this reduction of the problem we have to solve now a rather peculiar exercise from electrostatics: given two fixed color charges at positions $\vec{r}_1$ and $\vec{r}_2$ with opposite signs for their charges find the shape of a domain (gluon bag) inside which the Maxwell equations are valid for the gluon field $(\vec{E}, \vec{H})$

$$\operatorname{curl} \vec{E} = \operatorname{curl} \vec{H} = 0$$

$$\operatorname{div} \vec{H} = 0$$

$$\operatorname{div} \vec{E} = 4\pi e_c \left[\delta(\vec{r}-\vec{r}_1) - \delta(\vec{r}-\vec{r}_2)\right] \qquad /3.1/$$

where e_c is the color charge of the C-quark. On the static surface of the gluon bag we have the following boundary conditions :

surface tension	volume tension	
$\vec{E}\cdot\vec{n} = 0$	$\vec{E}\cdot\vec{n} = 0$	/3.2/
$\vec{H}\times\vec{n} = 0$	$\vec{H}\times\vec{n} = 0$	
$\frac{1}{2}\vec{E}^2 = \omega\left(\frac{1}{R_1}+\frac{1}{R_2}\right)$	$\frac{1}{2}\vec{E}^2 = \beta$	/3.3/

where $\vec{n}$ is a normal vector to the surface, $\frac{1}{R_1}$ and $\frac{1}{R_2}$ are the principal curvatures in two orthogonal directions at a given point of the surface. $\frac{1}{2}\left(\frac{1}{R_1}+\frac{1}{R_2}\right)$ is the mean curvature of the surface.

When the distance $r = |\vec{r}_1 - \vec{r}_2|$ between the C-quark and $\bar{C}$-quark is small we expect a dominant Coulomb interaction. However, for large r an electric vortex develops between the color charges and the interaction energy becomes proportional to r.

In fact, there is an infinite electric vortex solution to the boundary conditions which is exact. The electric field is homogenous inside the vortex and $\vec{E}^2$ is determined by the nonlinear boundary conditions /3.3/. The radius R of the vortex tube is given then by the total flux of the vortex which is specified through the color charge e_c

$$4\pi e_c = R^2 \pi |\vec{E}|$$

With surface tension we find

$$R_s = \left(\frac{8 e_c^2}{\omega}\right)^{1/3} \qquad /3.4/$$

whereas the radius of the electric vortex with volume tension is

$$R_v = \left(\frac{8 e_c^2}{\beta}\right)^{1/4} \qquad /3.5/$$

R_s and R_v are expressed in terms of e_c and ω (or β) which are the fundamental constants of the theory. e_c is a positive dimensionless coupling constant (color charge) and the dimensional parameter ω (or β) sets the fundamental scale in the theory.

The energy stored in a vortex of length r is λr with $\lambda = \lambda_e + \lambda_b$, where we have

surface tension	volume tension	
$\lambda_e = \frac{1}{2}(\omega e_c)^{\frac{2}{3}}$	$\lambda_e = \frac{1}{\sqrt{12}}(\beta e_c^2)^{1/2}$	/3.6/
$\lambda_b = (\omega e_c)^{\frac{2}{3}}$	$\lambda_b = \frac{1}{\sqrt{12}}(\beta e_c^2)^{1/2}$	/3.7/

The electric field energy stored in the vortex of length r is $\lambda_e r$ and surface tension (or volume tension) contributes $\lambda_b r$ to the vortex energy.

For a first orientation the value $\frac{1}{5}$ was chosen for $\alpha_s = e_c^2$ which approximately satisfies several considerations. The values of ω and β are given then in terms of λ from /3.6/ and /3.7/. The value $\lambda = 0.2\ \mathrm{GeV}^2$ is suggested from a qualitative description of the charmonium spectrum.

Whith these values of α_s and ω (or β) we have solved the static bag problem on a computer. The method we used was based on the observation that we can study the principle of least action on the computer.

With the two color charges fixed the problem has cylindrical symmetry. The surface of the bag was expanded in terms of a series of Legendre polinomials with variable coefficients. Similarly, the electric field inside was given as the sum of an electric dipole field and a remainder field expressed in terms of a series of Legendre polynomials with another set of variable coefficients.

The Maxwell equations were satisfied inside by the Legendre expansion of the electric field. The computer has calculated the action W as a function of the variable parameters and searched for the stationary point of the parameter space monitoring the action W. This nonlinear approach to the problem gave rapid convergence and satisfactory results.

For numerical work we have used our CDC 3300 computer facility. The results for the potential energy $V(r)$ of the $c\bar{c}$-system are shown in Fig.1 and Fig.2. $V(r)$ is approximately $-\frac{\alpha_s}{r}$ at small distances and λr at large distances, in excellent agreement with our qualitative expectations.

It is interesting to see that the electric vortex solution with linearly rising potential energy sets in at rather small distances. In Fig.1 and Fig.2 the bag energy stored in the form of surface tension or volume tension is also shown. It goes linearly with the distance and confirms our conjecture for an electric vortex between the two color charges. In the vortex region, according to /3.6/ and /3.7/ , twice as much energy is stored in the form of surface tension than in the form of electric field energy. For volume tension the two terms are equal in the vortex energy. The slope of $V(r)$ in the vortex region compared with the slope of the bag energy from surface tension or volume tension nicely agrees with this picture.

The shape of the bag with surface tension is shown in Fig.3 for several values of r . The position of the charge is also indicated there. The value of the vortex radius R_s is calculated from /3.4/ to be $2.45\,GeV^{-1}$ with our numbers for e_c and ω . One can see from Fig.3 the rapid convergence to this value of R_s with increasing r .

4. CHARMONIUM SPECTROSCOPY

Recently two narrow resonances have been discovered [9] at 3.1 and 3.7 GeV. The most plausible explanation of this phenomenon is that of Appelquist and Politzer [10] who suggested that the new particles are $c\bar{c}$ -bound states of charmed quarks. The new particles would lie then below the threshold M_c for the production of a pair of charmed hadrons. The bound state system has been called charmonium.

Since our potential $V(r)$ is fairly well approximated by the sum of a Coulomb term and a linear confinement part

$$V(r) \simeq -\frac{\alpha_s}{r} + \lambda r \quad , \qquad /4.1/$$

the predictions of the charmonium spectrum qualitatively agree with those of some recent papers which appeared during the preparation of our work. The authors of Ref. 11 have used intuitively a potential of the form /4.1/ and we are close in our predictions to their results.

The potential $V(r)$ is used in the nonrelativistic Schrödinger equation for massive charmed quarks in the spirit of the Born-Oppenheimer approximation.

With $m_c = 1.2\,GeV$ the level spacing is shown in Fig.4 for the low-lying S, P and D -states. Spin effects and the "fine-structure" of the level scheme are not indicated here. For example, three levels of a multiplet are lumped together in the lowest P -state.

The calculated level spacing and the electronic widths into e^+e^- - pairs of the particles $\psi(3.1)$ and $\psi'(3.7)$ can be adjusted to the experimental data by the fundamental constants of the theory. Other decay modes are open for discussions. For example, the hadronic widths of ψ and ψ', which eventually violate Zweig's rule, may be explained as annihilation of the $c\bar{c}$ -system into three gluons.

One of the most important consequences of the potential $V(r)$ with a linear confinement term is monochromatic photon decays between S and P -states. The partial decay widths associated with $E1$ transitions are rather large:

The $\psi'(3.7)$ state can decay into the lowest P -multiplet by the emission of a monochromatic $E1$ -photon with a partial decay width of the order of $100-200\,keV$. The states of the P -multiplet can decay into the $\psi(3.1)$ state via the emission of an $E1$ photon with similar decay widths.

It is a challenge for theorists to establish to what extent the location of the lowest P -multiplet between the $\psi(3.1)$ and $\psi(3.7)$ states is model-independent and it is a challenge for experimentalists to search for monochromatic photons.

The $3S$ state at $4.1\,GeV$ in our model must be above the threshold M_c for charm production and perhaps part of the impressive bump at $4.1\,GeV$ in the total cross section for $e^+e^- \to$ hadrons is associated with the $3S$ - state. It may happen that other resonant states in this energy region are not resolved experimentally and a more complicated structure

will be found there. We will come back to this point at the discussion of the small oscillations of the gluon bag.

It is interesting to observe that the lowest D -state is fairly close to the $\psi'(3.7)$ $2S$ -state. The level separation with linear confinement potential is perhaps less than $100\ MeV$. In the presence of tensor forces there is a possibility for level mixing. If that happened then the D - -state could be produced in e^+e^- -annihilation via its $2S$ -component in the wave function.

5. FURTHER DEVELOPMENTS

Our work in the framework of the Born-Oppenheimer approximation is far from complete. Even neglecting vacuum polarization, the gluon bag may oscillate with new dynamical degrees of freedom. The gluon oscillations are difficult to calculate except for a particular case: the radial oscillations of the vortex with volume tension in linear approximation.

When the flux of the vortex is kept constant in time ($\phi = 4\pi e_c$) we can find the eigenfrequencies of the radial vibrations of the vortex. The infinite series of eigen frequencies is given by

$$\omega_n = \frac{\lambda_n}{R_v} \quad , \quad n = 1, 2, 3, \cdots \qquad /5.1/$$

where R_v is calculated to be $2\ GeV^{-1}$ from /3.5/ with our choice of the parameters e_c and β . λ_n is the n^{th} zero of the Bessel function of zero order.

So we conclude from /5.1/ that the first quantum excitation of an infinite electric vortex with volume tension is separated from the ground state by an excitation energy of about $1.2\ GeV$.

This calculation is not an empty exercise. We believe it is the first step toward the quantum field theory of our gluon bag model. Also, when the $c\bar{c}$ -system is radially excited the electric vortex is dominant and perhaps the small oscillations of the bag are well approximated by /5.1/.

In the general case we have to calculate the eigen-frequencies $\omega_n(r)$ as a function of the distance between the color charges. We expect that $\omega_n(r) \to \frac{\lambda_n}{R_v}$ for large r in the case of cylindrically symmetric vibrations. When r is small the eigenfrequencies are larger. We are working on the complete theory of small gluon oscillations along the line of the adiabatic Born-Oppenheimer approximation.

It is likely that gluon oscillations correspond to a level separation of $\sim 1.2\,GeV$ (or even larger) above the static ground state. The gluon variables are more strongly coupled with the quark variables for smaller values of r and they become decoupled in the infinite vortex limit.

Gluon oscillations carry angular momentum and more generally, we have to understand serious theoretical questions there. It is not impossible that there are gluon excitations of the $\psi(3.1)$ in the $4\text{-}5\,GeV$ region which are new states in addition to ordinary radial excitations.

When the meson is radially excited, the probability of vacuum polarization $q\bar{q}$ -pairs increases. Then the meson may split into two lower-lying meson states. This mechanism offers a dynamical understanding of Zweig's rule for meson decay With the inclusion of vacuum polarization the Born-Oppenheimer approximation becomes complete and we may understand decay processes like the decay of the $3S$ $c\bar{c}$ -state at $4.1\,GeV$ into charmed hadrons.

If we wish to go beyond the nonrelativistic and adiabatic approximation we have to respect relativity. Already the first question is rather provocative: what happens with the Klein--paradox in the case of linear confinement potential in the Dirac equation?

It is instructive to see a fairly simple solution to this problem. The term $\lambda_e r$ from the field energy of the electric vortex is represented as the fourth component of a vector potential in the Dirac equation. The bag energy $\lambda_b r$ comes from a scalar term in the Lagrangian and it is represented by a scalar potential in the Dirac equation. Due to the balance of the two types of potentials we face no Klein-paradox here. Detailed solutions for the Dirac equation will be given elsewhere.

The Dirac equation corresponds to a situation where one particle is fixed and the other moves around in the given potential $V(r)$. That is not enough for the calculation of light relativistic meson states. We have to develop our Bethe--Salpeter equation for the relativistic case. Work is in progress in this direction.

Relativistic invariance is not separable from the question of spin dependence. The spin dependence of the quark-antiquark interaction is an interesting question in itself. It is rather dramatic if we wish to interpret the $\mathcal{K}$-ρ mass difference as spin-spin interaction.

We have qualitative arguments that due to gluon confinement the spin dependent part of the $q\bar{q}$- interaction is large in our model. This spin-dependence is associated with gluon confinement and the color magnetic moments of quarks. It is presumably much stronger than ordinary hyper-fine interactions. SU(6) is badly broken then in a rather natural, built in way. Our results on this problem will be published elsewhere.

The problem of baryons and the description of strong interaction phenomena remains entirely open in the model. It is a long way before we can say something definite about the baryon spectrum or the nature of the Pomeron[12] and other exciting problems which go beyond the Born-Oppenheimer approximation.

Nevertheless the model is promising and incorporates many important features of hadron physics in a desirable manner.

ACKNOWLEDGEMENTS

The authors are deeply indebted to Peter Gnädig for his most valuable help during the preparation of this work. Interesting conversations with the members of the Particle Theory Group in Budapest are also acknowledged. One of us /J. K./ benefited from discussions with Carleton de Tar.

We were educated on the Breit equation and the Bethe-Salpeter equation by T.Nagy and K.Ladányi. P. Boschan provided us with his numerical assistance.

We are indebted to professor A. Szalay who kindly arranged for us access to the CDC 3300 computer facility.

FOOTNOTES AND REFERENCES

1. P.A.M. Dirac, Proc. Roy. Soc. 268A, 57 /1962/
2. A. Chodos, R.L. Jaffe, K. Johnson, C.B. Thorn and V.F. Weisskopf, Phys. Rev. D9, 3471 /1974/
3. J. Kuti, talk presented at the Regional Triangle Meeting, November 5-7, 1974 Visegrad
4. W.A. Bardeen, M. Chanowitz, S.D. Drell, M. Weinstein and T.M. Yan to be published. This paper contains further references.
5. G. t'Hooft, CERN preprint, TH. 1902
   R.F. Dashen, B.Hasslacher, A. Neveu, Princeton preprint, COO-2220-30, A.M.Polyakov, preprints from the Landau Inst.
6. $\hbar = c = 1$ in our calculations here. The metric is $(+---)$, the fine structure constant $\alpha = e^2$
7. We are grateful to Carleton de Tar who has pointed out to us this analogy in our approach.
8. For a magnetic bag, see A. Patkos, ITP preprint # 348, Budapest. The paper contains further references to quark confinement with magnetic monopoles.
9. For a reference, see this Proceedings
10. T. Appelquist and H.D.Politzer, Phys. Rev. Letters 34, 43 /1975/
11. E. Eichten etal., Phys. Rev. Letters, 34, 369 /1975/ This paper contains further references
12. For a recent model of the Pomeron with quark confinement, see F.E. Low, MIT-preprint, CTP-438 /1975/

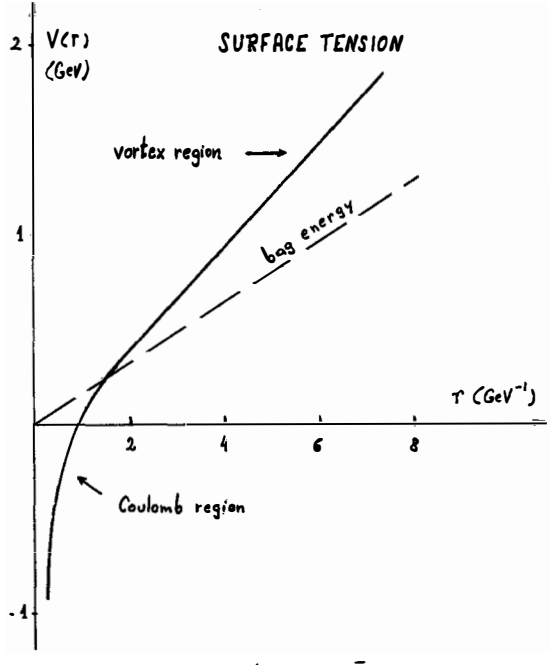

Fig.1 The potential energy $V(r)$ of $C\text{-}\bar{C}$ for gluon bag with surface tension is represented by the solid line. Dashed line denotes the bag energy associated with surface tension.

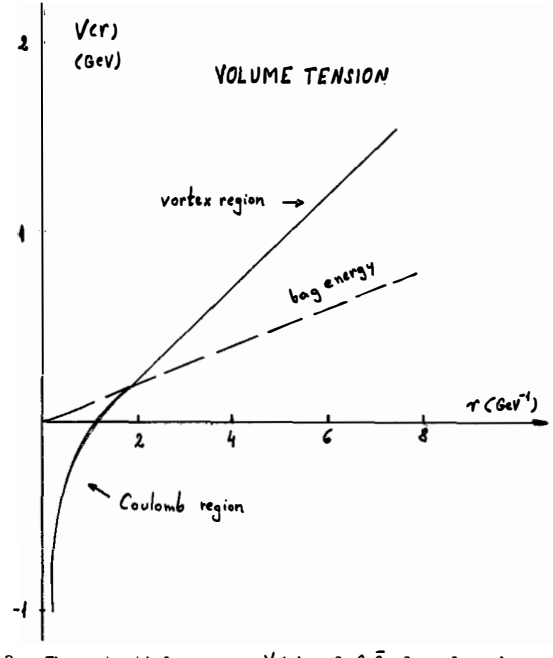

Fig.2 The potential energy $V(r)$ of $C\text{-}\bar{C}$ for gluon bag with volume tension is represented by the solid line. Dashed line denotes the bag energy associated with volume tension

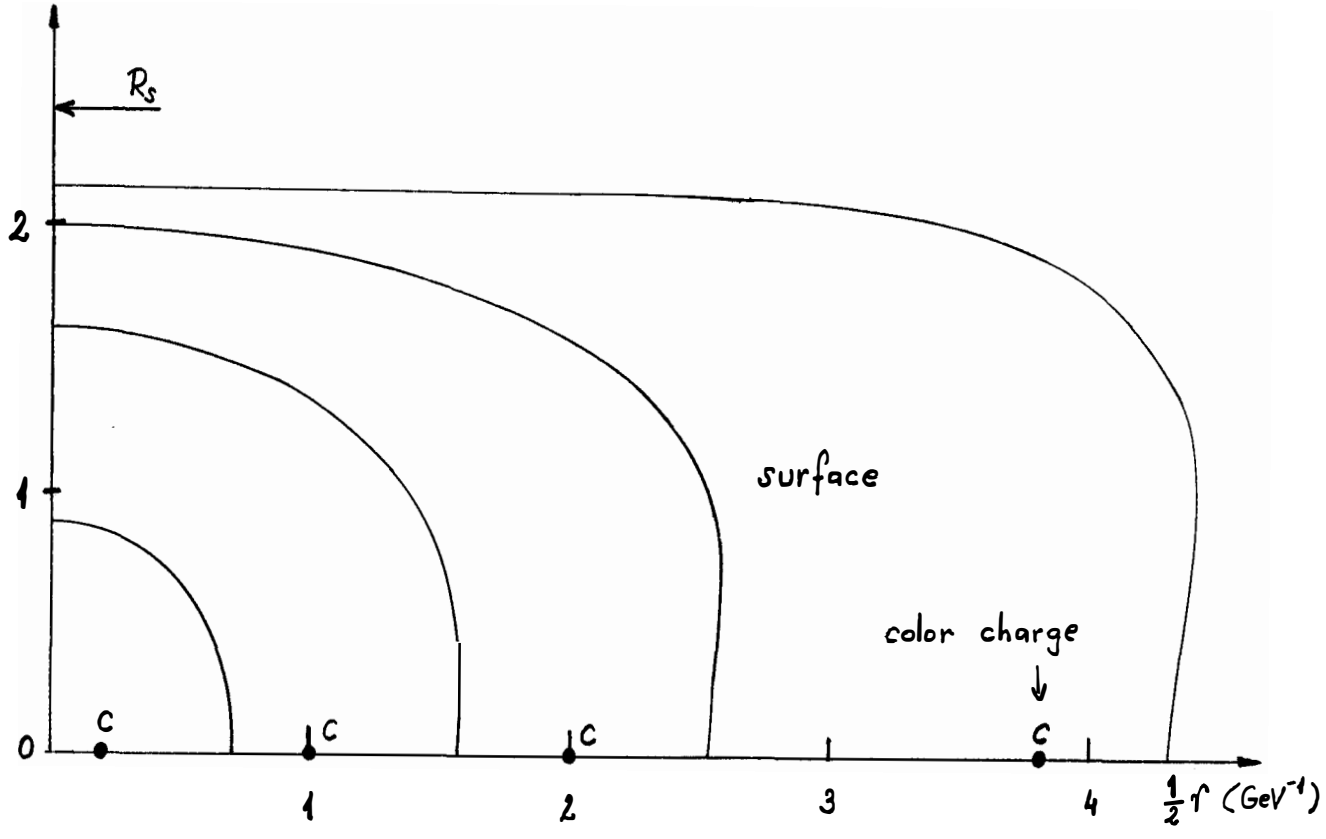

Fig.3 The surface of the bag as a function of the distance between C and $\bar{C}$. Only the first quadrant of the surface is shown. R_s is the radius of the electric vortex asymptotically when r goes to infinity

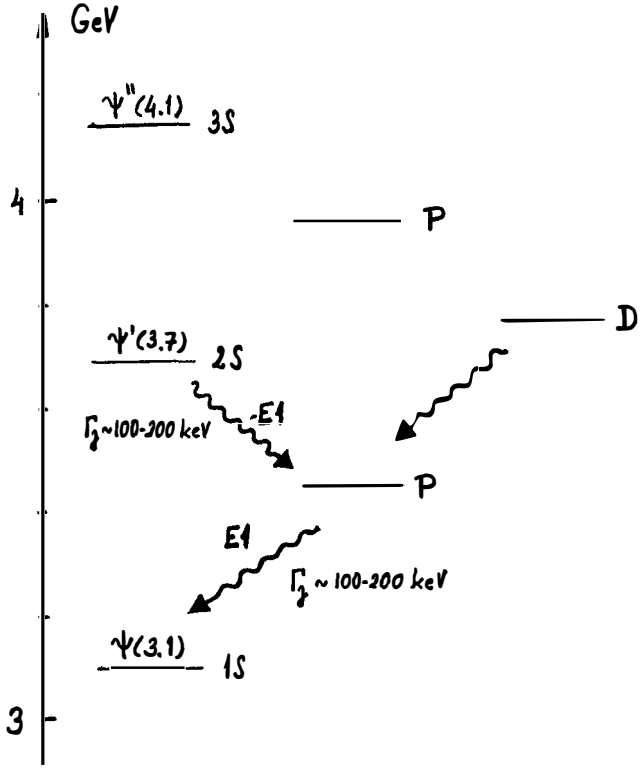

Fig.4 The charmonium spectrum with low-lying states. Some E1 transitions are indicated.

MASS FORMULAE AND MIXING IN SU(4) SYMMETRY

M. GOURDIN
Laboratoire de Physique Théorique et Hautes Energies
Univ. P. et M. Curie, T.16, 4 pl. Jussieu 75005 Paris
(France)

Warning : These notes do not form an organized and systematic paper on the subject and they must be considered as an illustrative appendix to M.K. Gaillard's talk at the same meeting. The SU(4) symmetry and its mass breaking are regarded in a very naive way. Dynamics is not included, only Clebsch-Gordan coefficient calculations have been done. Criticism is not given because the calculations are in progress.

Avertissement : Ces notes ne constituent pas un article structuré et systématique sur le sujet. Elles doivent être considérées comme une illustration de l'exposé de M.K. Gaillard, à cette même rencontre. La symétrie SU(4) et sa brisure de masse sont traitées de façon très naive. La dynamique a été exclue et seuls les coefficients de Clebsch-Gordan ont été calculés. Les calculs étant en cours, aucune critique n'est présentée.

A - SU(4) MASS BREAKING

I. ASSUMPTION

We proceed as for the breaking of SU(3) symmetry and we assume that the physical masses can be computed in a perturbative way, the first order calculation being sufficient. The underlying problem of the dynamics is disregarded here.

The medium strong interaction Hamiltonian has the quantum numbers

$$I = 0 \qquad S = 0 \qquad C = 0 \qquad Q = 0 \qquad B = 0$$

We assume that the non singlet part H_{MASS} of such a Hamiltonian transforms like a component of the adjoint representation of the SU(4) algebra. It follows that, a priori, H_{MASS} may be associated to any direction in the two-dimensional subspace of the Cartan algebra orthogonal to I_3. In other terms H_{MASS} transforms like any linear combination of the SU(4) traceless operators $\tilde{S}$ and $\tilde{C}$ associated to strangeness and charm

$$\tilde{S} = S + \frac{3}{4} B \qquad\qquad \tilde{C} = C - \frac{3}{4} B$$

and the mass formula is written

$$m = m_0 + m_1(\tilde{C} - \tilde{S}) + m_2(\tilde{C}) + m_3 \ \Omega^{SYM}_{\tilde{C}-\tilde{S}} + m_4 \ \Omega^{SYM}_{\tilde{C}}$$

The symmetric isometries Ω^{SYM} are computed in the enveloping algebra and the result is

$$\Omega^{SYM}_{\tilde{C}-\tilde{S}} = 2\,\bar{I}(\bar{I}+1) - 2\,I(I+1)$$

$$\Omega^{SYM}_{\tilde{C}} = \frac{1}{2}\,x_4 - x_3 + \frac{2}{3}\,\tilde{C}^2$$

The $\bar{I}$ spin is associated to the SU(2) subgroup of SU(4) commuting with isospin. The non-strange or charmed quarks are $\bar{I}$ spin singulet and the system λ , p' is a $\bar{I}$ doublet.

x_3 and x_4 are respectively the SU(3) and SU(4) quadratic Casimir operators.

1) Baryons $J^P = 1/2^+$ in $D^{20}(1,1,0)$

5(4) parameters

2) Baryons $J^P = 3/2^+$ in $D^{20}(3,0,0)$

$$\Omega^{SYM}_{\tilde{C}-\tilde{S}} = 4(\tilde{C} - \tilde{S}) \qquad \Omega^{SYM}_{\tilde{C}} = 4\tilde{C}$$

We only have 3 parameters and a generalized equal spacing rule with two scales, one for strangeness and one for charm.

3) Mesons $J^P = 0^-, 1^-$ in $D^{15}(1,0,1)$

Because of TCP invariance $m_1 = m_2 = 0$ and we remain with three parameters.

III. MIXING FOR MESONS

1) Mesons constructed as quark-antiquark states will form a 16-plet, the sum of an irreducible 15-plet and of a singulet. We then expect, as in the ω-ϕ case, a mixing of I = 0, S = 0, C = 0 mesons as a consequence of the SU(4) breaking.

2) We first have a 3 × 3 mass matrix M_0 in the basis of representation SU(4) ⊃ SU(3). The physical states are the eigenvectors of M_0 and the diagonalization is achieved by introducing a 3 × 3 orthogonal rotation matrix depending on three parameters R. After rotation, we get a diagonal mass matrix M whose elements are the physical masses. The relation between these three matrices is

$$M = R\, M_0\, R^{-1}$$

3) When M is known, the mixing constraint determines all the parameters. This procedure can be applied to vector mesons when the ψ (3100) is identified as the third isoscalar, S = C= 0 vector meson.

IV. SU(4) VERSUS SU(3) BREAKING

1) The mass splitting due to strangeness is typically of order 150 MeV, e.g. an effect of 15%. The splitting due to charm is expected to be larger probably by an order of magnitude. Therefore a perturbation idea is perhaps totally crazy. Nevertheless let us be naive.

2) The ratio $m_2/m_1 = m_4/m_3$ is associated to the direction of H_{MASS} in the $\tilde{S}$, $\tilde{C}$ plane. From group theory there is no a priori reason for this ratio to be the same for all supermultiplets, except in particular dynamical models based on quarks.

V. LINEAR OR QUADRATIC MASS FORMULAE ?

1) It is usual to write linear mass formulae for baryons and quadratic mass formulae for mesons. In the SU(3) framework the Gell-Mann-Okubo relation for the $J^P = 1/2^+$ octuplet and the equal spacing rule for the $J^P = 3/2^+$ decuplet work so nicely that we are very reluctant to abandon linear mass formulae for baryons.

The situation concerning mesons is more obscure because of the occurrence of mixing in the nonets. For vector mesons, the mixing angles associated to linear and quadratic mass formulae differ only by a few degrees. For pseudoscalar mesons the difference is more important but, to our knowledge, there is no unquestionable argument for choosing one form.

2) In the SU(4) framework the use of universality

$$\frac{m_2}{m_1} = \frac{m_4}{m_3} = \text{CONSTANT} \simeq 20$$

where the last number is obtained from vector mesons with quadratic mass formulae, will lead, with a linear mass formula for baryons, to very heavy charmed states in the 5-8 GeV range. That situation looks physically unreasonable and it was a reason to propose quadratic mass formulae also for baryons. We do not like this solution for the reasons previously given.

Therefore, if quadratic mass formulae for mesons and linear mass formulae for baryons is the correct assignment, we have to abandon universality and to work with a breaking ratio of order 20 for mesons and 10 for baryons.

3) A possible way to restore, at least partially, universality is to use linear mass formulae for all the particles. The general properties for vector mesons are unchanged but the effect is more important in the case of pseudoscalar mesons. The breaking ratio is now less than 10 but even in this case it is not obvious that universality for m_4/m_3 could be a reasonable assumption. Nevertheless, by itself, the use of linear mass formula for mesons might be an interesting assumption.

B - VECTOR MESON ROTATION MATRIX

I. INPUT MASSES

m_ω = 782.7 MeV $\quad m_\phi$ = 1019.7 MeV $\quad m_\psi$ = 3095 MeV

The neutral value has been used for the K^* mass : $m_{K^{o*}}$ = 898 MeV and because of the experimental uncertainties of the ρ meson mass the matrix is computed for the three cases

$$m_\rho = \left| \begin{matrix} 775 \\ 770 \\ 765 \end{matrix} \right| \text{ MeV}$$

II. ROTATION MATRIX : QUADRATIC MASS FORMULA

	$\phi_{NS} = \frac{p\bar{p} + n\bar{n}}{\sqrt{2}}$	$\phi_S = \lambda\bar{\lambda}$	$\phi_C = p'\bar{p}'$
ω	0.9979 0.9987 0.9991	-0.0551 -0.0485 -0.0423	-0.0341 -0.0153 +0.0019
ϕ	0.0541 0.0483 0.0423	0.9981 0.9987 0.9991	-0.0296 -0.0131 +0.0017
ψ	0.0357 0.0160 -0.0020	0.0277 0.0124 -0.0017	0.9990 0.9998 0.9999

III. PREDICTIONS

The ratio m_4/m_3 is computed by the same calculation to be

$$\frac{m_4}{m_3} = \begin{vmatrix} 19.71 \\ 19.59 \\ 19.42 \end{vmatrix}$$

and we make predictions for the D^* and F^* charmed vector meson masses

$$m_{D^*} = \begin{vmatrix} 2205 \\ 2234 \\ 2259 \end{vmatrix} \text{ MeV} \qquad m_{F^*} = \begin{vmatrix} 2251 \\ 2281 \\ 2307 \end{vmatrix} \text{ MeV}$$

IV. ROTATION MATRIX - LINEAR MASS FORMULA

	ϕ_{NS}	ϕ_S	ϕ_C
ω	0.9999 0.9995 0.9988	-0.0076 -0.0005 +0.0066	0.0124 0.0308 0.0477
ϕ	0.0075 -0.0004 -0.0086	0.9999 0.9996 0.9991	0.0112 0.0272 0.0415
ψ	-0.0125 -0.0308 -0.0473	-0.0111 -0.0272 -0.0419	0.9999 0.9992 0.9980

V. PREDICTIONS

The ratio m_4/m_3 takes smaller values

$$\frac{m_4}{m_3} = \begin{vmatrix} 8.61 \\ 8.49 \\ 8.35 \end{vmatrix}$$

and the predictions for the D^* and F^* charmed vector meson masses become

$$m_{D^*} = \begin{vmatrix} 1957 \\ 1985 \\ 2009 \end{vmatrix} \text{ MeV} \qquad m_{F^*} = \begin{vmatrix} 2080 \\ 2113 \\ 2142 \end{vmatrix} \text{ MeV}$$

VI. REMARKS

1) The physical situation is very close to an ideal mixing where

$$\omega = \phi_{NS} \qquad \phi = \phi_S \qquad \psi = \phi_C$$

2) The ω-ϕ mixing parameter is practically unaffected by the presence of the heavy ϕ meson and it is the same as in SU(3) symmetry.

3) The non diagonal matrix elements are very sensitive to the input masses and they cannot be accurately determined by such a calculation. More can be learned on these quantities from ψ meson decay .

4) The prediction for the D^* and F^* masses are also very sensitive to the input masses whereas the ratio m_4/m_3 is not.

5) The predicted masses for D^* and F^* are lower with linear formula than with quadratic ones. The shift is 250 MeV for D^* and 170 MeV for F^* .

C - DECAY V $e^+ + e^-$

I. The photon in SU(4) symmetry is a linear superposition of 15-plet and singulet weights. We then have TWO coupling constants g_{15} and g_1 for the photon-vector meson junction.

II. SUM RULE

The ρ meson constant determines g_{15}

$$g_\rho = \frac{3}{\sqrt{2}} g_{15}$$

For the three other quantities we can derive a sum rule independent of the mixing parameters

$$g_\omega^2 + g_\phi^2 + g_\psi^2 = g_\rho^2 + g_1^2$$

The constant g_1 is not known and by positivity we get an inequality

$$g_\psi^2 \geq g_\rho^2 - (g_\omega^2 + g_\phi^2)$$

The unitary symmetry being broken, we do not have a definite prescription on what quantity the symmetry relations must be applied. In the SU(3) framework with ρ, ω, ϕ data two possibilities are equally compatible

$$g_V = \frac{1}{f_V} \qquad g_V = \frac{\sqrt{m_V}}{f_V}$$

In the first case we obtain $\Gamma(\psi \to e^+e^-) > 14.4$ keV. In the second case we obtain $\Gamma(\psi \to e^+e^-) > 3.2$ keV.

The first assumption is obviously inconsistent with the ψ data.

III. PREDICTIONS

We retain the second assumption $g_V^2 \propto \Gamma(V \to e^+e^-)$ and we use the quadratic mixing parameters in order to compute the $\Gamma(\psi \to e^+e^-)$ widths. With the ACO data as experimental inputs, the predictions are :

$$\Gamma(\psi \to e^+e^-) = \left| \begin{array}{l} (5.54 \pm 0.68) \text{ keV} \\ (5.41 \pm 0.66) \text{ keV} \\ (5.30 \pm 0.65) \text{ keV} \end{array} \right|$$

for the three cases previously considered of the ρ meson mass. These values are compared with the SLAC result

$$\Gamma(\psi \to e^+e^-) = (5.2 \pm 1.3) \text{ keV}$$

IV. UNIVERSALITY

The same calculation determines g_1 and the result turns out to be compatible with a universality relation

$$g_{15} = g_1$$

If the universality relation is assumed the previous sum rule with our phase space assumption becomes

$$\Gamma(\omega \to e^+e^-) + \Gamma(\phi \to e^+e^-) + \Gamma(\psi \to e^+e^-) = \frac{11}{9}\Gamma(\rho \to e^+e^-)$$

Using again the ACO data for ρ, ω, ϕ, we make a prediction for the ψ radiative width independent of the mixing parameters

$$\Gamma(\psi \to e^+e^-) = (5.30 \pm 0.88) \text{ keV}$$

in very good agreement with experiment.

D - DECAY V → P + P

I. PHASE SPACE

We apply the unitary symmetry on the dimensionless coupling constant f_{VPP} , the phase space factor being taken as

$$\frac{K_{CM}^3}{m_V^2}$$

II. INPUT DATA

The most accurately known results concerns the K meson and the experimental value of the K^* width is

$$\Gamma(K^* \to K\pi) = (49.8 \pm 1.1) \text{ MeV}$$

III. PREDICTIONS

In exact SU(3) symmetry $f^2_{\rho MM} = 4/3\ f^2_{K^*KM}$ and the ρ width is computed to be

$$\Gamma(\rho \to \pi\pi) = (172 \pm 10) \text{ MeV}$$

whereas the average of experimental data is

$$\Gamma(\rho \to \pi\pi)_{aV} = (150 \pm 10) \text{ MeV}$$

For the $\phi \to K\bar{K}$ and $\psi \to K\bar{K}$ decays the coupling constants are proportional to the matrix elements $< \phi_8 \mid \phi >$ and $< \phi_8 \mid \psi >$, where ϕ_8 is the SU(3) octet weight.

Using the previous quadratic rotation matrix, we predict :

	$\Gamma(\phi \to K\bar{K})$ (MeV)	$\Gamma(\psi \to K\bar{K})$ (eV)
$m_\rho = \begin{vmatrix} 775 \\ 770 \\ 765 \end{vmatrix}$ MeV	3.27 ± 0.14 3.30 ± 0.15 3.34 ± 0.15	2287 ± 101 173 ± 8 7.45 ± 0.33
EXPERIMENT	3.41 ± 0.18	< 130

IV. REMARK

With the input masses used the coefficient $< \phi_8 \mid \psi >$ vanishes and changes of sign in the investigated range

$$< \phi_8 \mid \psi > = \begin{vmatrix} -0.002047 \\ -0.000888 \\ +0.000185 \end{vmatrix}$$

Therefore there is no difficulty in understanding an extremely small $\Gamma(\psi \to K\bar{K})$ width.

E - DECAY $V \to \pi^\circ + \gamma$

I. PHASE SPACE

We apply the unitary symmetry on the coupling constant $g_{VP\gamma}$ having the dimension of the inverse of a mass. The phase space factor is taken as K_{CM}^3.

II. INPUT DATA

The experimental value for the partial decay width $\omega \to \pi^\circ + \gamma$ is

$$\Gamma(\omega \to \pi^\circ + \gamma) = (0.87 \pm 0.09) \text{ MeV}$$

III. PREDICTIONS

The three decay widths $\Gamma(\rho \to \pi^\circ + \gamma)$, $\Gamma(\phi \to \pi^\circ + \gamma)$, $\Gamma(\psi \to \pi^\circ + \gamma)$

are all proportional to the width $\Gamma(\omega \to \pi^\circ + \gamma)$ and the proportionality factors are given by the quadratic rotation matrix. The predictions are

	$\Gamma(\rho^\circ \to \pi^\circ + \gamma)$ (keV)	$\Gamma(\phi \to \pi^\circ + \gamma)$ (keV)	$\Gamma(\psi \to \pi^\circ + \gamma)$ (keV)
$m_\rho =$ 775 MeV	94.1 ± 9.7	(5.86 ± 0.61)	(74.88 ± 7.75)
$m_\rho =$ 770 MeV	92.0 ± 9.5	(4.68 ± 0.48)	(14.95 ± 1.55)
$m_\rho =$ 765 MeV	90.0 ± 9.3	(3.58 ± 0.37)	(0.24 ± 0.03)
EXPERIMENT	< 750	(7.6 ± 3.2)	< 0.7

IV. REMARKS

1) With the input masses used the coefficient $\langle \phi_{NS} \mid \psi \rangle$ which governs the $\psi \to \pi^\circ \gamma$ decay amplitude vanishes and changes sign in the investigated range. Therefore there is no difficulty in understanding an extremely small $\Gamma(\psi \to \pi^\circ\gamma)$ width despite the enormous phase space available.

2) The other decays $\psi \to P^\circ + \gamma$ of the same type are also experimentally suppressed. In order to evaluate the corresponding matrix elements we need information on the pseudo-scalar meson mixing. The calculations are in progress.

F - PSEUDOSCALAR MESON ROTATION MATRIX

I. INPUT MASSES

$m_{\pi^\circ} = 134.96$ MeV $\qquad m_{K^\circ} = 497.7$ MeV $\qquad m_\eta = 548.8$ MeV

Two assumptions for η'

1.- $\eta' \equiv X^\circ \qquad m_{\eta'} = 957.6$ MeV

2.- $\eta' \equiv E^\circ \qquad m_{\eta'} = 1416$ MeV

II. SYMMETRY BREAKING RATIO

The calculations are made for two values of the ratio m_4/m_3.

1.- The value deduced from the vector meson analysis (universality assumption)

2.- A value such that $2m_D$ is above the ψ' mass and below the 4-1 GeV enhancement observed at SLAC. The value chosen is 1.980 MeV for m_D.

Numerically we use

$$\frac{m_4}{m_3} = \left| \begin{matrix} 19.3 \\ 16 \end{matrix} \right| \quad \text{for quadratic mass formulae}$$

$$\frac{m_4}{m_3} = \left| \begin{matrix} 8.46 \\ 4.09 \end{matrix} \right| \quad \text{for linear mass formulae}$$

III. CASE $\eta' \equiv X^\circ$ QUADRATIC MASS FORMULA

	$\eta_{NS} = \frac{p\bar{p} + n\bar{n}}{\sqrt{2}}$	$\eta_S = \lambda\bar{\lambda}$	$\eta_C = p'\bar{p}'$
$\eta(549)$	0.7222 0.7226	-0.6908 -0.6906	0.0351 0.0324
$X^\circ(958)$	0.6669 0.6676	0.7089 0.7093	0.2297 0.2262
η''	-0.1835 -0.1792	-0.1425 -0.1418	0.9726 0.9735

PREDICTIONS

$$m_D = \left| \begin{matrix} 2164 \\ 1980 \end{matrix} \right| \text{MeV} \qquad m_F = \left| \begin{matrix} 2217 \\ 2037 \end{matrix} \right| \text{MeV}$$

$$m_{\eta''} = \left| \begin{matrix} 2720 \\ 2516 \end{matrix} \right| \text{MeV}$$

IV. CASE $\eta' \equiv X^\circ$ LINEAR MASS FORMULA

	η_{NS}	η_S	η_C
$\eta(549)$	0.8543 0.8579	-0.5038 -0.5081	0.0943 0.0675
$X^\circ(958)$	0.4714 0.4701	0.8383 0.8331	0.2741 0.2913
η''	-0.2355 -0.2043	-0.1897 -0.2184	0.9571 0.9542

PREDICTIONS

$$m_D = \left| \begin{matrix} 3567 \\ 1980 \end{matrix} \right| \text{ MeV} \qquad m_F = \left| \begin{matrix} 4066 \\ 2342 \end{matrix} \right| \text{ MeV}$$

$$m_{\eta''} = \left| \begin{matrix} 5578 \\ 3049 \end{matrix} \right| \text{ MeV}$$

V. CASE $\eta' \equiv E^\circ$ QUADRATIC MASS FORMULA

	η_{NS}	η_S	η_C
$\eta(549)$	0.6682 0.6682	-0.7437 -0.7439	-0.0089 -0.0120
$E^\circ(1416)$	0.7409 0.7383	0.6668 0.6650	-0.0795 -0.1127
η''	0.0650 0.0918	0.0465 0.0664	0.9935 0.9968

PREDICTIONS

$$m_D = \left| \begin{matrix} 2164 \\ 1980 \end{matrix} \right| \text{ MeV} \qquad m_F = \left| \begin{matrix} 2217 \\ 2037 \end{matrix} \right| \text{ MeV}$$

$$m_{\eta''} = \left| \begin{matrix} 3073 \\ 2843 \end{matrix} \right| \text{ MeV}$$

VI. CASE $\eta' \equiv E^\circ$ LINEAR MASS FORMULA

	η_{NS}	η_S	η_C
$\eta(549)$	0.7848 0.7850	-0.6195 -0.6193	0.0181 -0.0131
$E^\circ(1416)$	0.6136 0.6191	0.7809 0.7838	0.1170 0.0484
η''	-0.0853 -0.0197	-0.0798 -0.0461	0.9916 0.9987

PREDICTIONS

$$m_D = \left| \begin{matrix} 3567 \\ 1980 \end{matrix} \right| \text{MeV} \qquad m_F = \left| \begin{matrix} 4066 \\ 2342 \end{matrix} \right| \text{MeV}$$

$$m_{\eta''} = \left| \begin{matrix} 6079 \\ 3402 \end{matrix} \right| \text{MeV}$$

VII. REMARKS

1.- If we insist on the condition $m_D < 2050$ MeV, the universality for the ratio m_4/m_3 between vector mesons and pseudoscalar mesons cannot be maintained.

2.- In the quark model approach the orthocharmonium-paracharmonium mass difference $m_\psi - m_{\eta''}$ is expected to be positive and small. This feature is realized in our examples

for $\eta' \equiv X^\circ$ with a linear mass formula

for $\eta' \equiv E^\circ$ with a quadratic mass formula

Only the first of these two cases satisfies also the previous requirement.

3.- The pseudoscalar meson mixing is far to be of the ideal type as for vector mesons and the non diagonal matrix elements in the considered basis are important. In particular the quantity $< \eta_C \mid \eta' >$ is very crucial for the partial decay width $\psi \to \eta' + \gamma$. In this respect the case $\eta' \equiv E^\circ$ is certainly more favourable.

REFERENCES

M.K. Gaillard, B.W. Lee and J.L. Rosner, preprint (1974) + addendum (1975).

S. Borchardt, V.S. Mathur and S. Okubo, Phys. Rev. Letters 34, 38 (1973) and Phys. Rev. Letters 34, 236 (1973).

K. Kajantie, C. Montonen, M. Roos and N. Törnqvist, preprint 1975.

Experimental papers on new particles.

Particle Data Table, April 1974

M. Gourdin, "Unitary Symmetries" (North-Holland, Amsterdam 1967).

PRELIMINARY RESULTS OF OUR CHARM SEARCH

presented by M.M. Nussbaum

Authors: L. Baum, M. Block, J. Crawford, B. Couchman, A. Derevshchikov, I. Golutvin, H. Hilsher, J. Irion, A. Kernan, V. Kukhtin, J. Layter, W. Marsh, F. Muller, P. McIntire, B. Naroska, M. Nussbaum, A. Orkin-Lecourtois, L. Rossi, C. Rubbia, D. Schinzel, B. Shen, A. Staude, G. Tarnopolski, V. Telegdi, R. Voss

ABSTRACT

As part of our experiment we measure the electron to pion ratio at 30° from pp collisions at the ISR (26 GeV on 26 GeV). Preliminary results are presented.

We began an experiment, last november, at the ISR, designed to study the production and decays of charmed particles. The scheme is to trigger on electrons at 30^{o} and to look for correlations with oppositely charged muons and/or strange particles, including the possibility of hadronic decays of charmed particles.

Fig. 1 shows the set-up briefly, arm 2 is used to signal either an inclusive or a diffractive event. Arm 1 is used for detection of muons and/or hadrons. The electron arm is designed to detect electrons with a rejection power for hadrons of approximately 10^{5}.

The preliminary results, I will report today, will be concerned exclusively with our findings from the electron arm. Therefore, I will describe it in more detail.

Fig. 2 is an enlarged view of the electron arm. Each of the scintillation counters shown, is in fact, subdivided into two vertical sections (i,e, four dE/dx counters near the interaction region and two in front of a block of fifteen lead glass counters). The positions of the six X and six Y planes of drift chambers are as shown. The magnet has a 0.6 tesla-meter field, and houses a one meter atmospheric pressure CO_2 Cerenkov counter. The lead glass blocks are twelve radiation lengths long and are arranged in a 5 x 3 matrix that covers the geometrical acceptance of the magnet.

The trigger conditions were: (1) a signal in arm 2, (2) at least two particles in spectrometer arm 1, (3) in the electron arm counts in both front and back scintillation counters, greater than one half photoelectron pulse from the gas Cerenkov counter, and more than 0.4 GeV energy deposition in the lead glass. Pulse heights from all counters in the electron arm were recorded.

In eighty hours of running we recorded approximately five million events. In addition, about 10% of the time was devoted to various calibration runs. The data analysis, so far, has been directed to extracting a clean electron signal. In order to guard against conversion pairs, we require that only one particle enters the electron arm. This is accomplished

by requiring: (1) that the pulse heights in each of the front counters be compatible with minimum ionization, (2) that the counters hit have an appropriate pattern, (3) that there be evidence of only one track in the drift chambers and (4) that there be only one hit cluster in the lead glass. From these we extract our electron candidates by requiring that the gas Cerenkov has a signal greater than two photoelectrons.

A subsample (first 20% of the total) is displayed in fig. 3. Here we plot, for the residual events, the momentum of the candidate (vertical scale) as measured by the magnetic bending, versus the energy deposited in the lead glass (horizontal scale). The dense population along the line of unit scope is a clear indication of our electron signal. An e/π ratio is obtained by relating these results to runs where no Cerenkov nor lead glass signals were required in the trigger. In order to extract the ratio of "prumpt" electrons to pions two main sources of background must be subtracted. First, there are Dalitz pairs which contribute only one electron to our detector. This background is calculated by a "Monte Carlo" method, and contributed $(1. \pm .5) \times 10^{-4}$ to above ratio. Second, there are electron pairs (produced mainly in the vacuum chamber wall, from π^o gammas) which are not rejected by our pulse height cut, where subsequently one of the pair is swept out by the magnet. This background was measured by using variable absorbers inserted between the vacuum tank and the electron arm, as well as the variable thickness of the vacuum tank by extrapolating to zero thickness of material. After these corrections, we tentatively conclude that our integrated electron to pion ratios above 0.4 GeV are $e^-/\pi^- = e^+/\ ^+ = (7. \pm 2.) \times 10^{-4}$.

In order to have a better empirical determination of our corrections we have now installed numerous "guard" counters, designed to capture both larger angle Dalitz pairs, as well as electrons swept out by the magnet. In addition, we have inserted a third dE/dx counter at the front of electron arm.

In conclusion, let me stress again that these are very preliminary results. We shall be running for the rest of this year, and I hope, before long, we will have a lot more to say on this subject, including the report of our findings in the main spectrometer arm.

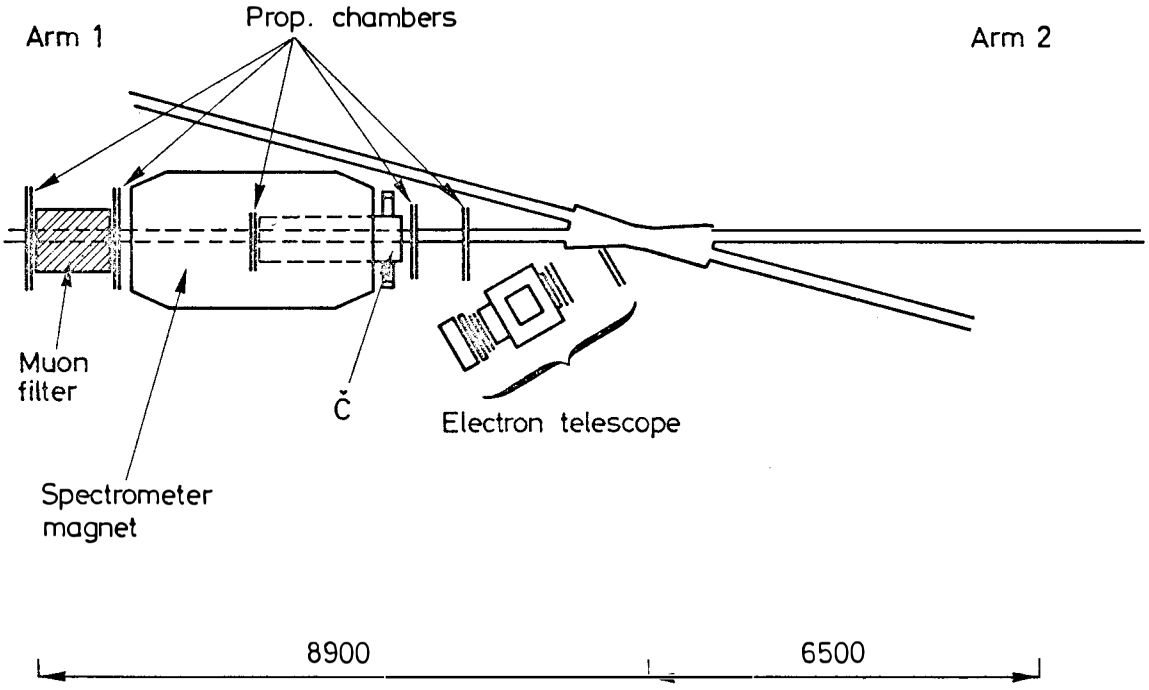
Arm 1
Prop. chambers
Arm 2
Muon filter
Č
Electron telescope
Spectrometer magnet
8900
6500

FIG. 1

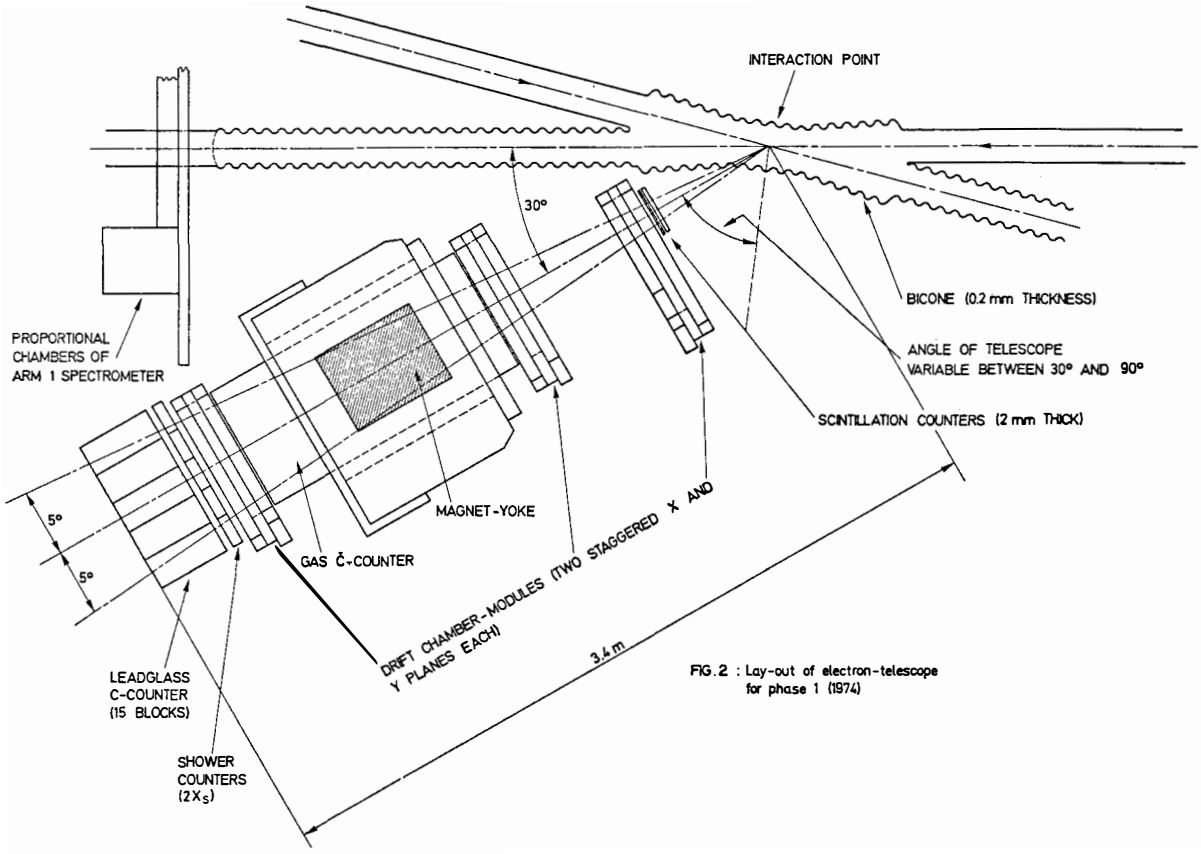

FIG. 2 : Lay-out of electron-telescope for phase 1 (1974)

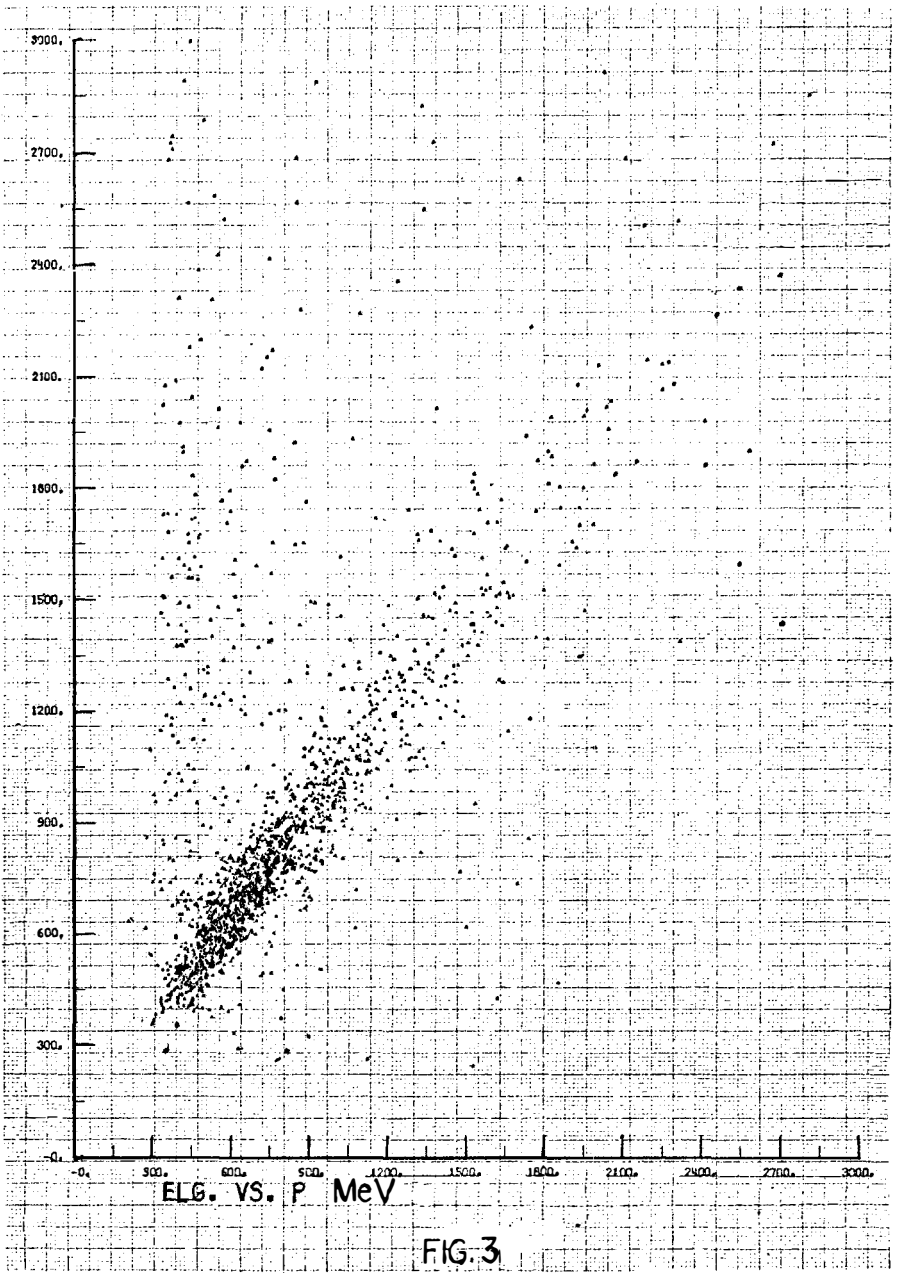
3000.
2700.
2400.
2100.
1800.
1500.
1200.
900.
600.
300.
-0.
-0.
900.
600.
900.
1200.
1500.
1800.
2100.
2400.
2700.
3000.
EL0. VS. P MeV

FIG. 3

THE EXPERIMENTAL SEARCH FOR CHARMED HADRONS

Clemens A. Heusch*)
CERN, Geneva, Switzerland
and
Sektion Physik, University of München, Germany

Abstract : We give a review of the motivation, scope, methodology, and promise of experimental projects that look for the postulated new additive quantum number, charm.

Résumé : Nous discutons les investigations expérimentales à la poursuite du nouveau nombre quantique postulé pour les hadrons: le charme, sa motivation, son étendue, les méthodes employées et l'information à obtenir.

*) Permanent address: University of California, Santa Cruz, California.

For a number of years, the existence of a new, simply additive, quantum number has been postulated for the hadrons[1]. This postulate was motivated originally by the observation of relatively subtle phenomena in the weak interaction of hadrons: the $K_L - K_S$ mass difference, the small decay mode $K_L \to 2\mu$, the recent observation of neutral $\Delta S = 0$ weak currents; and by a desire to put leptons and hadrons on a similar logical level by juxtaposing *four* basic hadronic building blocks (e.g. quarks) to the four leptons μ, ν_μ, e, ν_e. The fourth (new) quark would carry the new quantum number; all previously known hadrons would carry a zero eigenvalue of the new charge, the new quark would have an eigenvalue of one.

Only recently has this new quantum number been called upon to do the yeoman's work usually assigned the hadronic "charges" B, Q, (or I_3), S (or Y): to help explain the gross features of the observed hadron spectrum. The emergence of narrow mesonic states with masses much superior to those of all previously known hadronic states, and widths considerably inferior to those of all well-established strongly decaying hadrons, gives a new impetus to ask whether a law implying the conservation of a new charge, CHARM, can be established to be at the basis of these phenomena.

Charm has to date not been explicitly observed. If the narrow heavy meson states are due to bound pairs of quarks and antiquarks carrying the charm quantum number, we may find ourselves in the position of the experimenter who knows all about positronium but is in search of electric charge; or of the observer of ϕ mesons who is not sure whether there is such a thing as strangeness. Is this a likely conjecture? Theories abound, and will permit any variation of the basic charm theme to be considered. We will here avoid all prejudice in this matter and simply review the experimental evidence.

I will quickly focus on some utilitarian topics that will later on permit me to discuss the most incisive experimental efforts that have been undertaken or, at last, are close to yielding data. These topics are:

1) Summary of parameters: *What*, if any, observables do we look for?

2) Production mechanisms: *Where* do we look?

3) Detection strategy and techniques: What experimental effects do we expect, and *how* do we isolate a signal?

We will then discuss individual efforts chosen both for the promise they offer, and for representative illustration of the various approaches. Finally, a *status quo* of our knowledge as to the existence or non-existence of charmed hadrons will be given, with an outlook on the foreseeable future.

1. SUMMARY OF PARAMETERS

What hadronic states are expected? For each quark in the qqq baryon and $q\bar{q}$ meson states, we now have four possible choices. Using the properties of the new quark, p′ (or c)

$$\begin{aligned} I &= 0 \qquad Q = {}^{2}/_{3} \\ S &= 0 \qquad B = {}^{1}/_{3} \end{aligned} \tag{1}$$

we span a three-dimensional lattice for the spectroscopy of hadrons. Figure 1a shows the fundamental quartet. The weak interaction connects states of different eigenvalues of C (as of S) according to the favoured mode (by $\cos\theta_c$) C

$$\Delta S = \Delta C \ , \tag{2}$$

and we assume that all the known selection rules of the weak interaction remain valid. This simple picture then gives charm-changing interactions which (Fig. 1b) predominantly change strangeness simultaneously according to (2), with $\Delta S/\Delta Q = 1$. We will be looking for the weak decays of the lowest-mass charmed hadrons, whose *narrow width* and *largely strange* final-state will be the most telling features.

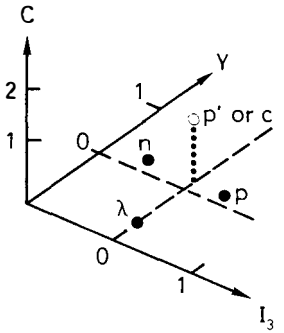

Fig. 1a

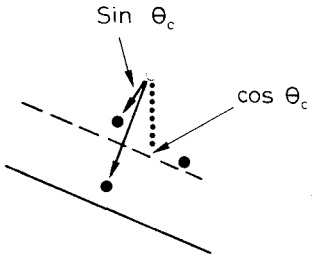

Fig. 1b

What are the lowest-mass charmed hadrons? For baryons, we have the qqq states

$$\underset{\sim}{4} \times \underset{\sim}{4} \times \underset{\sim}{4}$$

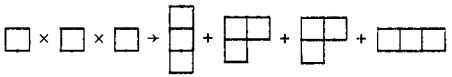

$$\underset{\sim}{4} \qquad \underset{\sim}{20} \qquad \underset{\sim}{20} \qquad \underset{\sim}{20}$$

The symmetric $\underset{\sim}{20}$  is identified as

$$\underset{\sim}{20}\ (J^P = 3/2^+) = \underset{\sim}{10} + \underset{\sim}{6} + \underset{\sim}{3} + \underset{\sim}{1}$$

$$\text{(with charm} \quad 0 \quad 1 \quad 2 \quad 3) \ .$$

$\underset{\sim}{10}$ contains the Δ's and their strange partners, the $\underset{\sim}{6}$ gives charm-one Δ-type states. For mixed-symmetry, we have

$$\underset{\sim}{20}\ (J^P = 1/2^+) = \underset{\sim}{8} + \underset{\sim}{6} + \underset{\sim}{\bar{3}} + \underset{\sim}{3}$$

$$\text{(with charm} \quad 0 \quad 1 \quad 1 \quad 2) \ .$$

$\underset{\sim}{8}$ is the usual nucleon octet; we have a $\underset{\sim}{6}$ and $\underset{\sim}{\bar{3}}$ of singly charmed $\frac{1}{2}^+$ states, the non-strange members of which would decay principally (by $\Delta I = 0$) into $\Sigma^{\pm 0}$ and Λ^0. If we make the reasonable assumption that the S = 0, C = 1 baryons are the charmed baryon "ground states" that can decay only weakly, there should be sharply defined narrow states decaying into Σ^+ pions from an I = 1 multiplet containing a *doubly charged* state, and into Λ^+ pions from a singlet that has Q = 1.

For the mesons, we have the basic

$$\underset{\sim}{4} \times \underset{\sim}{\bar{4}} \rightarrow \underset{\sim}{15} + \underset{\sim}{1} \ ,$$

where

$$\underset{\sim}{15}\ (J^P = 0^-, 1^-) = \underset{\sim}{8} + \underset{\sim}{3} + \underset{\sim}{\bar{3}} + \underset{\sim}{1}$$

$$\text{(with charm} \quad 0 \quad -1 \quad +1 \quad 0)$$

yields back the pseudoscalar and vector octets, plus positively and negatively charmed triplets that decay characteristically into K and π combinations.

The current structure of the weak interaction imposes certain selection rules on these decays, as has been worked out in detail in Ref. 2; most noticeably, the lowest-mass pseudoscalar meson would not decay into Kπ in its charged state, which couples to K$\pi\pi$, but its neutral partner would decay into $K^{\mp}\pi^{\pm}$.

So, we will be looking for narrow $K\pi$, $K\pi\pi$, $\Lambda\pi\ldots$, $\Sigma\pi\ldots$ peaks, including a $\Sigma^+\pi^+$ state; but at what masses and lifetimes?

The range of possible masses for the charmed "ground states" is highly model-dependent, but the analogy between c and p quarks which effects the cancellation of the $\Delta S = 1$ weak neutral currents sets limits. A reasonable range might be for baryons, B^c, and mesons, M^c,

$$2.5 \lesssim m(B^c) \lesssim 5 \quad \text{GeV}$$

$$1.5 \lesssim m(M^c) \lesssim 3.5 \text{ GeV} .$$

If, however, we assume that the observed narrow mesonic state at 3.1 GeV is to be interpreted as a bound $(c\bar{c})$ state ϕ^c, a mass scale gets established that allows us to narrow our range of interest. This could lead, for the mesons, to masses of order

$$m(M^c) \simeq \frac{1}{\sqrt{2}}\, m(\phi^c) \simeq 2.2 \text{ GeV}$$

for the 0^-, 1^- triplets of $C = \pm 1$. If the $\psi(3.1)$ is the charm analogy to the $\phi = (\lambda\bar{\lambda})$, we also expect an η analogy,

$$\eta^c = (p\bar{p} + n\bar{n} + \lambda\bar{\lambda} - 3c\bar{c})\, \frac{1}{\sqrt{12}}$$

where the mass is

$$m(\eta^c) \simeq \frac{\sqrt{3}}{2}\, m(\phi^c) \simeq 2.7 .$$

For the baryons, masses depend on our choice as to the use of a linear or quadratic mass formula. If we choose the linear formula, the $J^P = \frac{1}{2}^+$ states will have masses

$$m(\underset{\sim}{\bar{3}}) \simeq 4.5 \text{ GeV} ,$$

$$m(\underset{\sim}{6}) \simeq 6 \quad \text{GeV} .$$

With the use of a quadratic mass formula, we find

$$m(\underset{\sim}{\bar{3}}) \simeq 2.7 \text{ GeV} ,$$

$$m(\underset{\sim}{6}) \simeq 3.3 \text{ GeV} .$$

These numbers will set an approximate scale for minimum total-energy requirements in charm search experiments.

The lifetimes follow from simple dimensional considerations in a strangeness charm analogy. They yield[2)]

$$\tau \lesssim 10^{-13} \text{ sec}$$

$$c\tau \lesssim 10^{-3} \text{ cm} .$$

2. PRODUCTION MECHANISMS

2.1 Weak production

This will be principally observable from

$$\nu N \text{ (or } \nu A) \to C^{\pm} + \ldots + \text{lepton}$$

according to

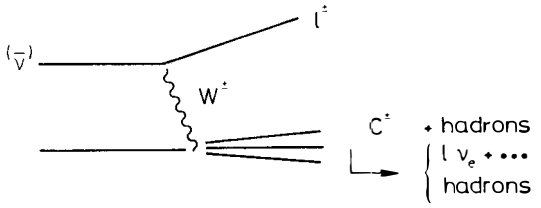

The principal difficulties are these: the small cross-section of the weak production process; the suppression of the production of $(c\bar{n},c\bar{p})$ states from non-strange nucleon constituents, by $\sin^2 \theta_c$ ($\sim 1/20$); the small amount of $\lambda\bar{\lambda}$ pairs inside the nucleon, to make $\Delta C = \Delta S$ transition to $(c\bar{p},c\bar{n})$ states without suppression.

2.2 Electromagnetic production

This can occur from lepton or photon beams: first, in electron-positron collisions

$$e^+e^- \to \gamma \to C^+C^- + \ldots .$$

Below threshold for $C^+ + C^-$ production, there may be the production of the "hidden-charm" bound state analogous to the hidden-strangeness $\phi = (\lambda\bar{\lambda})$:

$$e^+e^- \to \gamma \to (c\bar{c}) \quad (\psi, \psi', \ldots ?) .$$

If this were the correct interpretation of ψ,ψ' production, then we would almost certainly have to see

$$(c\bar{c})_{ortho} \rightarrow (c\bar{c})_{para} + \gamma \ ,$$

with $(c\bar{c})_{ortho}$ to be identified with either $\psi(3.1)$ or $\psi'(3.7)$, and the monoenergetic photon giving the process away.

For the production of meson pairs $C^+ + C^-$, all the characteristics of the weak C decays would be useful. There should be an enhancement in the K/π ratio, the reconstructibility of sharp mass peaks, semi-leptonic decays giving direct leptons, and more.

Furthermore, a promising route of investigation would be the photoproduction or electroproduction processes

$$\gamma p \text{ (or } \gamma A) \rightarrow C^+C^- + \ldots$$
$$\rightarrow (c\bar{c}) + \ldots$$

If, again, we believe the $(c\bar{c})$ interpretation of $\psi(3.1)$, then the ψ photoproduction cross-section observed at FNAL[3] can give a rough idea of what C^+C^- cross-section to expect:

$$\frac{\sigma(C^+C^-)}{\sigma_{tot}(\gamma p)} \lesssim 10^{-3} \ .$$

A particularly telling experiment may be feasible at high energies, using the Primakoff production graph to observe the pseudoscalar η^c state,

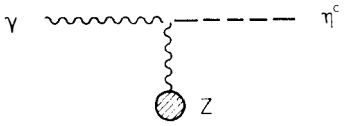

and its expected subsequent 2γ decay mode. The characteristic energy and Z-dependence of this sharply forward-peaked process open it up to very selective observation; note, however, that this meson still has no *manifest* charm even if its quark composition is correctly estimated.

2.3 Production by strong interaction processes

This will proceed largely in analogy with the strong production of strange hadrons: charm conservation leads to "associated production":

$$NN \text{ (or } \pi N) \rightarrow C^+C^- + \ldots \ ,$$

where C^+ and C^- are baryons or mesons carrying opposite charm number. What hadron states will be visible? Close to threshold, the most economical quark graphs in πN interactions will be

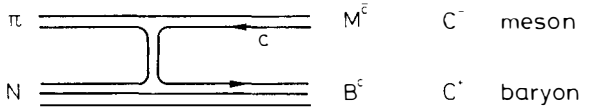

and, if $M^{\bar{c}}$ and B^c are the charmed "ground states", their characteristic weak decay properties should be noticeable. Alternatively,

will lead to the observation of two mesonic "ground states". If $m(B^c) > m(N) + m(M^c)$, these two graphs may not be experimentally distinguishable. As the available energy increases, more channels open up, but most likely there will be strong cascading to C^-, C^+ ground states, so that the basic observation of narrow states of relatively low mass remains a promising tactic.

One specific stratagem that, if valid, would lead to a particularly telling signature for associated charmed hadron production is predicated on the assumption that $\psi(3.1) = (c\bar{c})$, and on the empirical rule that will not permit quark lines to meet inside a bound system (= hadron)[4]: if, in a high-energy pp collision, a $\psi(3.1)$ can be identified, say, by its $\mu^+\mu^-$ decay mode, C^+C^- production is indicated by means of diagrams of the type

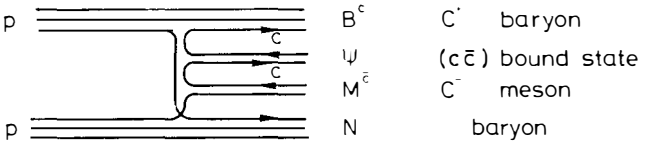

Since the $\psi \to \mu\mu$ events should stand out clearly, these assumptions and an acceptable cross-section for ψ production would lead to the clearest C^+C^- trigger imaginable. Unfortunately, it is not quite clear whether in the parallel case of $pp \to \phi\ (= \lambda\bar{\lambda}) + S^+S^-$, such a mechanism is manifest. Irrespective of the precise process occurring, strong production should ultimately yield, by SU(4) symmetry, plentiful C^+C^- events.

3. DETECTION STRATEGIES

In the above-discussed production processes, what will be the most promising stratagems for detecting the charmed states? We will quickly pass review, then go over to the experimental methods by which we can most profitably follow these courses of attack.

3.1 Weak interaction

The production of *single* charmed states according to

$$\overset{(-)}{\nu}N \to C^{\pm} + \ell + \ldots$$

(with ℓ the appropriate final-state lepton) is most easily indicated by a "dilepton signature": *if* $C^{\pm}$ has an appreciable (semi-)leptonic decay mode, then lepton pairs $\ell^+\ell^-$ (with $\ell = \mu$ or e) would be a telling feature. Thus neutrino interactions yielding lepton pairs of *opposite charge* should be closely studied. While the interpretation of dilepton signals[5], in the absence of detailed additional information, remains an open question, their charm connotation is certainly a probability.

If detailed observation of a neutrino event is possible, there is also the observation of an apparent violation of the $\Delta S = \Delta Q$ rule, as in an event recently reported by a BNL group[6]. However, precise reconstruction of kinematics and correct particle identification, with satisfactory statistics, are hard tasks in neutrino interactions (see below).

Other, less direct, implications of charmed hadron production would reflect in inclusive features of neutrino interactions[7]: the kinematical distributions (in the y variable) would change; sum rules would change their saturation values; apparent charge asymmetries may show up in the final

state; and the scaling of the structure functions describing neutrino-nucleon scattering would exhibit a new threshold. None of these features, while indicative, will give information sufficiently concise to establish or rule out any specific type of charm scheme.

3.2 Electromagnetic interaction

The production processes discussed under Section 2.2 are open to a variety of conclusive experimental checks: $e^+e^- \to C^+C^-$ will most clearly give rise to observables: there should be a discernible threshold in $R \equiv \sigma(e^+e^- \to \text{hadrons})/\sigma(e^+e^- \to \mu^+\mu^-)$; mass reconstruction should be possible for C^+,C^- decaying into charged hadrons; a threshold should show up for lepton yields from the weak C^+,C^- decays; the mean charged multiplicity should change abruptly at C^+C^- threshold, as should the ratio of neutral to charged particle energy, owing to the sudden occurrence of neutrinos.

Many of these features should equally be observable in photoproduction and in electroproduction. There, the use of higher-Z targets may also allow the coherent diffractive production of $J^P = 1^-$ systems, with characteristic angular dependence. The same holds for the process $\gamma Z \to \eta_c Z + \ldots$, as mentioned before.

3.3 Strong interaction

We start from the basic scheme

$$h + h \to C^+C^- + \ldots$$
$$\qquad\qquad \downarrow \quad \begin{cases} \ell\bar{\nu}_e \text{ (+ hadrons)} \\ \text{hadrons} \end{cases}$$

We assume C^+,C^- to be "ground states" that decay weakly and have a sharply defined mass. The principal stratagems then are the following:

i) C^+ and/or C^- → charged hadrons: look for any sharp mass peak among final-state hadron combinations, particularly those involving strange particles (favoured by $\sim \cos\theta_c$).

ii) $C^+ \to \ell\nu + \ldots$, $C^- \to \ell\nu + \ldots$: look for dileptons of opposite charge, in particular for $\mu^{\mp}e^{\pm}$. Also, invariant mass distributions of lepton + + hadron(s) should exhibit limiting values:

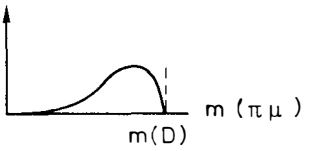

iii) $C^{\pm} \to K$ (or π) $\ell\nu$, $C^{\mp} \to$ hadrons: use "direct" lepton ℓ for trigger; then reconstruct invariant masses of hadron combinations, $\pi\mu$, πK, as above.

iv) $C^{\pm} \to K\pi$, $C^{\mp} \to K\pi\pi$: trigger on large p_T kaon, use fully reconstructed 4C events to determine invariant masses of $K\pi$, $K\pi\pi$ systems. Plot $m(K\pi)$ versus $m(K\pi\pi)$: an enrichment along the bisector $m_1 = m_2$ would indicate pair production C^+C^-.

3.4 All interactions

Direct observation of a charged-particle track of very short range, with characteristic subsequent decay, will be an extremely potent indicator. However, the expected short lifetimes of $\tau \lesssim 10^{-13}$ make this method suitable only for techniques resolving on the 10^{-4} cm level.

4. DETECTION TECHNIQUES

In order to make use of the stratagems reviewed above, what are the most appropriate detection methods in the particle physicist's arsenal?

4.1 Visual techniques

For the reconstruction of charged-particle decays, all visual techniques, depending on their time and space resolution, are useful.

Nuclear emulsions have by far the most precise spatial resolution, to a level of $\sim$ 1 micron. Disadvantages are obvious: the recording of an event cannot be triggered; the emulsion contains high-Z nuclei rather than free nucleons; feedback to the experimenter is extremely slow.

Bubble chambers: reconstruction is good for all charged tracks; selective triggering of the camera system permits the experimenter to use hybrid systems for, say, muon identification outside the chamber. Disadvantages are

its virtual lack of particle identification, its limited total mass for neutrino exposures, and its slow thermodynamics, which combine to disallow searches for very small cross-section processes.

Streamer chambers do not share these disadvantages: selective triggering of chamber and recording gear allow small cross-sections to be tackled. The low-density gas volume permits accurate kinematical reconstruction. High-intensity beams (up to several hundred particles per chamber memory time) can be tolerated, liquid or heavy targets can be inserted. On the negative side, particle identification remains a problem, and the interaction vertex is not directly visible in most cases.

4.2 Electronic techniques

In addition to the visual techniques, which allow for a full reconstruction of multiparticle final states, as well as visualization of decay vertices, all electronic detection techniques come into the game: precision spectrometers have the advantage of separating charged-particle rest masses as well as their momenta and charges. Double-arm or wide-acceptance spectrometers are able to give a fairly precise determination of two-particle masses at high counting rates. Large solid-angle devices such as the Omega spectrometer at CERN or LASS at SLAC are capable of combining many of the useful features of visual and electronic techniques, although their performance still has to be established in rigorous tests.

5. SOME CHARM SEARCHES DONE OR IN PROGRESS

I will now mention a number of experimental projects that have been undertaken or, at least, started charm searches. Before the unexpected discovery of the ψ (or J) particles[8] last fall, only one such experiment was completed[9]. Subsequently, a flood of projects has been entered upon; some have published results. While a connection between ψ's and the charm quantum number may or may not turn out to be existent, the current vogue of charm searches has certainly been largely motivated by their advent on the scene of particle physics.

Since completeness is not a meaningful criterion under the circumstances, I have chosen projects that best illustrate the stratagems and techniques described in the previous sections, and that show the highest promise of yielding telling results, confirming or refuting the charm hypothesis (in the simple form assumed in Section 1).

5.1 Neutrino experiments

Exposures of hydrogen bubble chambers have looked for narrow peaks involving many-particle mass combinations. No sharp peaks have emerged. Direct charmed-particle tracks do not appear, even at FNAL energies, just as expected from the lifetime estimates. One event has been reported from BNL[6], with an apparent $\Delta S = -\Delta Q$ implication in the fit

$$\nu_\mu p \to \mu^- \Lambda^0 \pi^+ \pi^+ \pi^+ \pi^- \ .$$

A charm interpretation would imply the existence of a fairly low-mass (2.4 GeV) C = 1 baryon. We would hope to see more results from that (low-energy) experiment before forming an opinion in this connection.

The counter experiments in the FNAL Neutrino Laboratory have produced suggestive results on dimuon production[10]: experiment 1A sees some 30 $\mu^+\mu^-$ pairs, with reconstructed masses between 2 and 4 GeV. There is no dimuon signal of equal sign. A charm connection is possible, but can hardly be expanded upon in the absence of all detailed information on vertex, full final-state, precise momenta, etc.

An interesting project has just moved past the approval stage[11]: Some of the calorimeter and muon identification apparatus of the FNAL neutrino counter experiments will be used to give fast external information on where a vertex may be found inside a set of 5.6 cm thick emulsion stacks. Direct charmed-particle tracks can be resolved for lifetimes of $\gamma^{-1} \times 3 \times 10^{-15}$ sec. The idea is simply to let the external muon track guide the experimenter to a νZ vertex inside the stack; then follow the hadron tracks from this vertex to see whether there is a charmed-particle decay vertex at a distance of more than 1 μm (Fig. 2). For all its statistical limitation, we believe this to be a very promising effort.

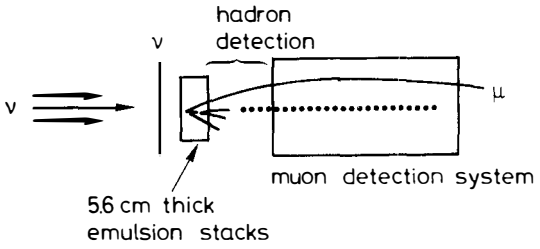

Fig. 2

5.2 Electromagnetic interaction experiments

The well-known experimental set-ups at SPEAR (Stanford) and DORIS (Hamburg) are training their sights on all possible signals for charmed-particle production. While both magnetic detection systems can tell charges and momenta of particles emerging from e^+e^- collisions, there are the problems of incomplete solid-angle coverage; of limited π/K separation, and of electron, photon, and muon detection and identification. Still, within these limitations, some very important features have emerged.

Suppose that $\psi(3.1)$ is the $(c\bar{c})$ state analogous to the $(\lambda\bar{\lambda})$ state $\phi(1.02)$. Then the naïve charm picture demands that there be charmed O^- mesons of masses not much above 2.2 GeV each; in other words, at a total energy of 4.8 GeV (2.4 GeV per beam), SPEAR should find itself above the threshold for charmed meson pair production. We might also identify the reported broader "resonance" $\psi''(4.15)$ and the accompanying increase in $R \equiv \sigma(\text{hadrons})/\sigma(\mu^+\mu^-)$ as denoting the onset of C^+C^- production. Then the strategies discussed under Section 3.2 above should apply.

In fact, data collected at those energies give no indication that any of the criteria discussed would indicate C^+C^- emergence[12]. The K/π ratio does not increase within errors, the ratio of neutral to charged energy has no noticeable step, neither does the charged hadron multiplicity. A reconstruction of invariant masses for various mesonic systems shows no sign of a meaningful enhancement[13], to a level of cross-section X branching ratio of nanobarn order. These observations, if anything, *rule out the simple charm scheme with*

the mass scale set by the $(c\bar{c})$ identification of $\psi(3.1)$. Improved and more detailed results may have to await another generation of detectors to become really restrictive.

In photoproduction, the recent commissioning of the FNAL Tagged Photon Laboratory should allow an early result on the conjectured production of η^c and its 2γ decay. Approved experiments[14] should set clean limits within a year's time.

5.3 Strong interaction experiments

A number of experiments have been performed; we will mention them according to the stratagems discussed in Section 3.3.

i) Looking for mass peaks (inclusively)

The MIT-BNL experiment that discovered the $\psi(3.1)$ in $pp \to e^+e^- + \ldots$ [8], can use its precise double spectrometer to look for properly defined and identified *pairs* of charged hadrons. In a recent six-week run, no meaningful signal was found in the $K^{\pm}\pi^{\mp}$, $\pi^{\pm}p^{(-)}$, $K^{\pm}p^{\mp}$, $\pi^+\pi^-$ or K^+K^- channels in the mass range expected by the simple charm scheme[15]; this experiment was performed at BNL, where the total hadronic energy available is of order 8 GeV. Note that this project is limited to all-charged, all-hadronic two-body decays.

ii) Looking for dileptons from C^+C^- decays

At the CERN Intersecting Storage Rings, an experiment is in progress[16] to study (semi-)leptonic decays of charmed hadron pairs by means of precisely identifying leptons in the final state. The experiment banks on a diffractive production process

$$pp \to pp^* \quad \hookrightarrow B^c + \bar{M}^c \ (\text{or } p + M^c + \bar{M}^c) \to \begin{cases} \ell^{\pm}\mu^{\mp} + \ldots \\ \ell^{\pm} + \ldots \\ \mu^{\pm} + \ldots \end{cases}$$

where both the charmed meson and the charmed baryon will essentially follow the excited proton:

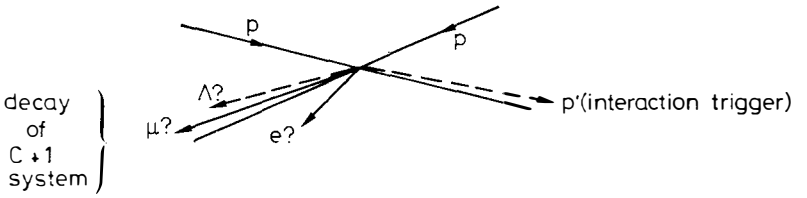

A very efficient electron spectrometer (Fig. 3) is seen to be set at ∿ 30° to the beam; a forward large-aperture spectrometer incorporating Čerenkov counters and large wire-chamber planes as well as a steel shield for muon identification should make it possible to probe for B^c, $\bar{M}^c$ decays into leptons and (strange) hadrons, with the $e^{\pm}$ arm giving a precisely defined trigger. The high centre-of-mass energy of the ISR should make this project definitive in the framework of the production model employed. It is at present in the running stage. A result on μ - e coincidences should soon be emerging.

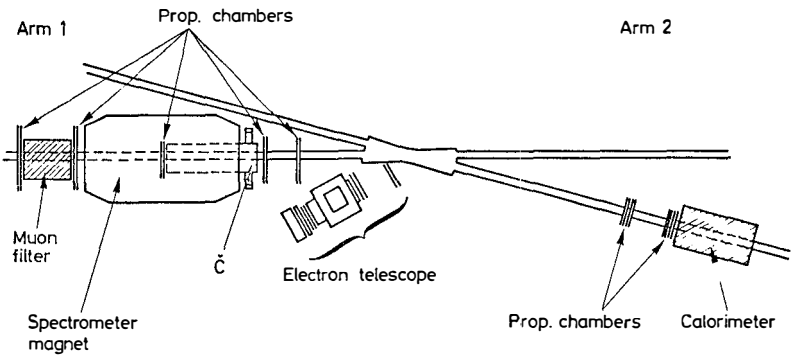

Fig. 3

iii) $C^{\pm} \to \ell\nu_e + \ldots$ *yields trigger,* $C^{\mp}$ *gives (strange) hadrons for sharp mass reconstruction*

One such project is in final preparation at the ISR[17]. While the previous experiment assumed peripheral C^+C^- production, this one starts from the notion that a *central* collision is most likely to give rise to the production of new particle types. In terms of quark diagrams, Figs. 4a and 4b show the approach of the R-605 experiment versus that of the R-702 ISR experiment in

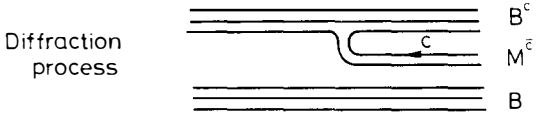

Fig. 4a

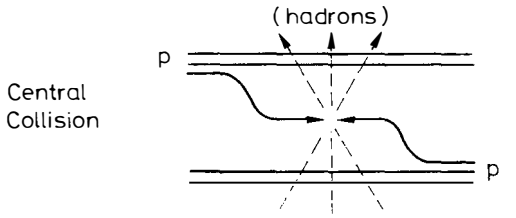

Fig. 4b

preparation by the CERN-Saclay Collaboration. Their method is illustrated in Fig. 5: since a central collision leads to isotropic emission of secondaries, large-angle detection of leptons and (strange) hadrons will be most clearly promising. Two large solid-angle magnets combined with hodoscopes and wire chambers, with Čerenkov counters inserted in their aperture, determine production and decay vertices of processes "tagged" by the emission of a large p_T electron. These electrons are momentum-analysed in the magnets *and* energy-analysed in a bank of lead-glass total absorption counters that provide the trigger for event read-out. Detection of γ and π^0 will therefore also be possible over a limited solid angle.

One lower-energy experiment using this same stratagem -- trigger on direct lepton, reconstruct hadron masses -- was completed in June of last year at SLAC by a Santa Cruz-SLAC Collaboration[9]. It made use largely of detection apparatus that had been tuned for a very selective muon trigger from muon inelastic scattering. The apparatus is schematically shown in Fig. 6. A 15 GeV pion beam of small phase space interacts with nucleons in a number of discretely positioned polyethylene targets inside a 2 m long streamer chamber. All charged particles emerging from the interaction are momentum-analysed in

the chamber. If there is a muon from $C^{\pm} \rightarrow \mu + \nu + \ldots$, it will, over a large solid angle, be identified by penetration of a 1.5 cm Pb wall. The trigger for streamer chamber firing and event read-out is thus simply a muon of energy $\gtrsim$ 2 GeV in the final state.

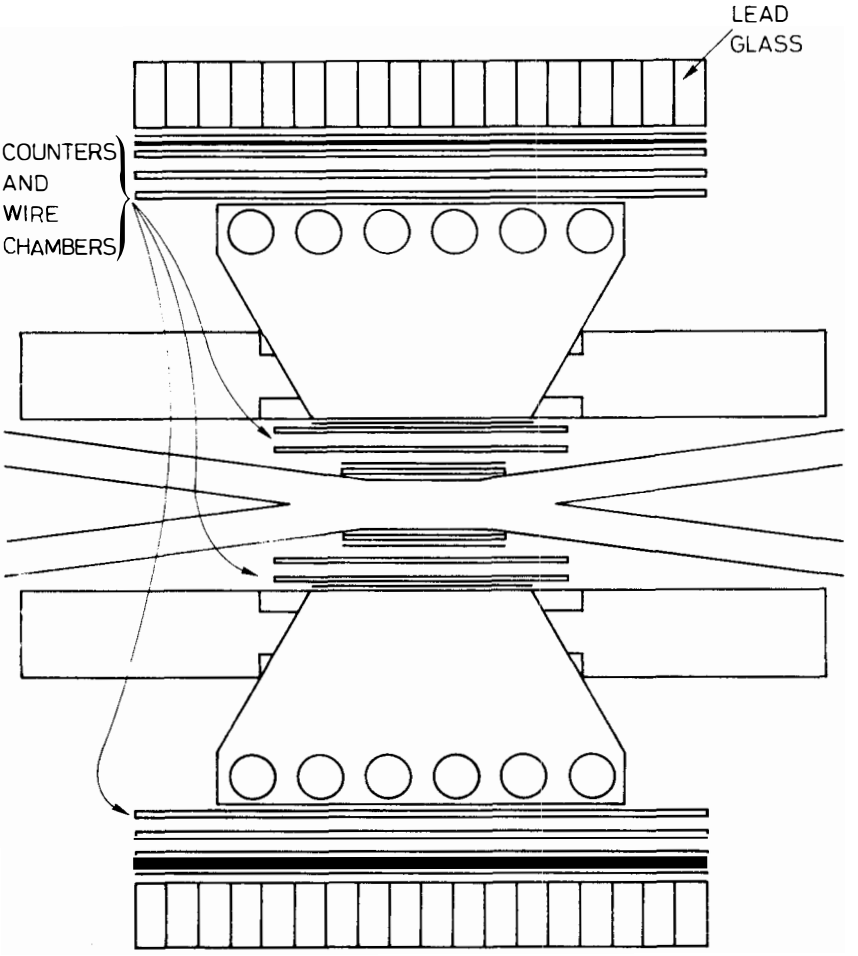

Fig. 5

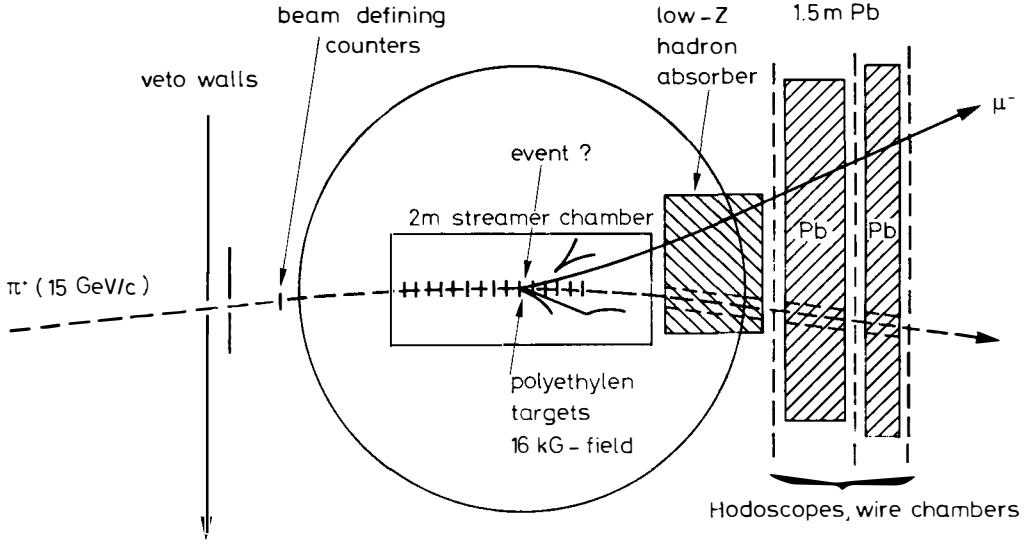
beam defining
counters
low - Z
hadron
absorber
1.5 m Pb
veto walls
μ⁻
event ?
2m streamer chamber
Pb
Pb
π⁺ (15 GeV/c)
polyethylen
targets
16 kG - field
Hodoscopes, wire chambers

Fig. 6

The strategy for first analysis was straightforward: look for obvious strange-particle events (vees from Λ^0, K^0 decay in the chamber) triggered by the "prompt" muon. Then reconstruct hadron tracks, calculate invariant masses of all charged-particle combinations as well as K^0, Λ^0 plus charged particles. A total of 16,000 pictures were taken: it became immediately obvious that a first look at these data did *not* show a strange-particle yield much superior to that seen in normal hadron-hadron collisions. A much more sophisticated analysis then became necessary: measure all events; calculate all invariant mass distributions ($K\pi$ ..., $\Lambda\pi$ ..., KK, Kp, $\pi\pi$ ...) for any 2, 3, 4 ... charged tracks and K^0's, Λ^0's. Cuts can then be introduced to clean up the sample, which will have a considerable combinational background: on the p_T of trigger muon or (strange) hadron, on location of the vertex in the chamber (the further downstream the event occurred, the less the chance that a secondary π decayed before hitting the absorbers, thus simulating a "direct" muon), and others. The Collaboration has to date not seen any conclusive evidence for a narrow peak; bear in mind, however, that the hadronic mass W in that experiment is about 5.6 GeV, just enough to make a pair of charmed mesons in addition to the proton, according to our above mass estimates, or possibly a $B^C\bar{M}^{\bar{C}}$ pair. One would have to bank on a threshold enhancement to expect a large yield.

The sensitivity of the experiment is defined by its $\sim$ 1000 events/μb exposure, but may be heavily modified by systematic effects.

iv) C^+, C^- → *hadrons: try for charmed meson-antimeson production*

A Collaboration[18] using the Omega Spectrometer Facility at CERN has proposed to use full kinematic reconstruction of an all-charged final state in the reaction

$$\pi^- p \to M^C \bar{M}^{\bar{C}} p \ (+ \ldots)$$

M^C → $K\pi\pi$, $K\pi$ } all charged

to search for the occurrence of sharp mass peaks associated with kaons, for *two* simultaneously occurring particle combinations. The set-up is sketched in Fig. 7: salient points are the K^- trigger at high p_T, the requirement of ≥ 5

charged particles in the final state, identification of K versus π and p by a large-aperture Čerenkov counter, and the capability of multiparticle momentum analysis.

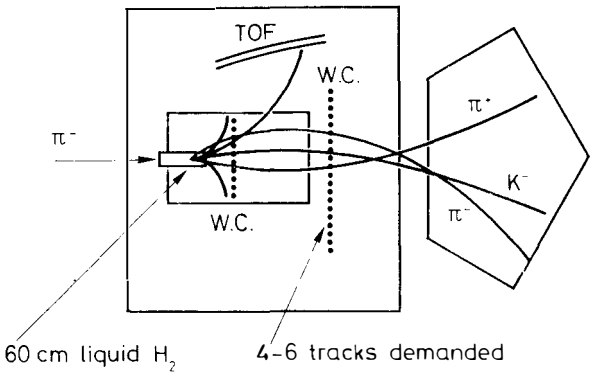

Fig. 7

The experiment is quoted to be sensitive to $M^c\bar{M}^{\bar{c}}$ pair production on the 50 - 100 nb level; preliminary results looking for an event enrichment along the m(Kπ) = m(Kππ) (where K's and π's are all different particles) line

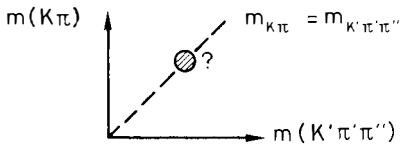

have not produced any suggestive evidence[19].

v) $pp \to \psi(3.1) + B^c + (\ldots)^{\bar{c}}$: *use* $\psi \to 2\mu$ *decay to tag an event containing charmed hadrons*

This scheme, highly model-dependent though it is, is sufficiently attractive to motivate serious efforts at the ISR. Appropriate detection apparatus will consist of a large magnetic detector including a muon identifier -- with reconstruction power sufficient to pin down narrow states such as ψ(3.1). A dimuon experiment performed recently in the Split-Field Magnet[20] using the iron of that structure for hadron/muon rejection, may be able to

give first limits. There is another approved project looking for dimuons, together with hadron track reconstruction close to the vertex, that will do the same thing in a much more ambitious way[21].

6. SUMMARY AND OUTLOOK

Throughout this discussion, we have centred our attention on the observation of clear signals for the existence of charmed hadrons in the framework of the straightforward SU(4) charm scheme as suggested by the non-observation of $\Delta S = 1$ neutral weak currents. We have discussed the nature of the observables that we might hope to experimentally detect, specifically leaving out estimates of production cross-sections, which are of necessity based on assumed, un-understood dynamical models, and therefore vary by large amounts.

Next, we reviewed the most promising ways in which the experimenter may be able to convince himself of the existence of these observables. We then followed active (or, in some cases, merely approved) experimental efforts at various accelerator laboratories, trying to illustrate the different lines of attack by our choice. There are many efforts, particularly approved FNAL experiments, that we left out since they either follow similar lines, or, as in the case of the various hh → dimuon experiments, will not lead to results that are restrictive enough to decide between C^+C^- or other mechanisms.

At the time of the writing of this lecture (May 1975), there are these inferences outstanding:

- the simple charm scheme with its scale set by the subsidiary assumption that $\psi(3.1) = \phi^c(c\bar{c})$ does not work;
- no statistically meaningful indication has been seen of sharp mass peaks, implying the existence of weakly decaying charmed hadron "ground states", either mesonic or baryonic.
- sufficiently many experimental efforts are presently active that, within the foreseeable future, the framework of this review should be experimentally exhausted.

REFERENCES

1) Y. Hara, Phys. Rev. 134, B701 (1964).
J.D. Bjorken and S.L. Glashow, Phys. Letters 11, 255 (1964).

2) M.K. Gaillard, B.W. Lee and J.L. Rosner, FNAL preprints 74/86 THY and 75/14 THY, to be published in Rev. Mod. Phys.

3) B. Knapp et al., Phys. Rev. Letters 34, 1040 (1975).

4) G. Zweig, CERN Report Th-402 (1964), unpublished.

5) A. Benvenuti et al., Phys. Rev. Letters 34, 416 (1975).

6) E.G. Cazzoli et al., BNL preprint NG-308 (1975).

7) M.K. Gaillard, Proc. of 1974 AIP Conference "Neutrinos" (C. Baltay, ed., 1974) p. 65.

8) J.J. Aubert et al., Phys. Rev. Letters 33, 1404 (1974).
J.E. Augustin et al., Phys. Rev. Letters 33, 1406 (1974).

9) UC Santa Cruz/SLAC Group D: SLAC Proposal 110, May 1974.
C.A. Heusch, Proc. Erice Summer School (1974).

10) C. Rubbia, C.R. Conf. "Physique du neutrino à hautes énergies", Paris 1975, p. 91.
B. Barish, same conference as above, p. 131.
(See also Ref. 5).

11) Brussels-Dublin-London-Rome-Strasbourg Collaboration, NAL proposal 247, (1974).

12) Various members of SLAC-LBL Collaboration, private communications.

13) A.M. Boyarski et al., SLAC-PUB-1583 (1975), to be published.

14) UC Santa Barbara-NAL-Toronto Collaboration, FNAL Experiment 25.
UC Santa Cruz, FNAL Experiment 152.

15) S.C.C. Ting, data presented at CERN Seminar, May 1975.

16) CERN-Harvard-Munich Univ.-Northwestern-Riverside Collaboration, ISR Proposal R-605 (1974).

17) CERN-Saclay Collaboration, ISR Proposal R-702 (1975).

18) R. Hubbard et al., CERN (Omega)-Saclay Collaboration, CERN EEC 15-6 (1975).

19) R. Hubbard, private communication.

20) CERN-Hamburg-Orsay-Vienna Collaboration, ISR Experiment R-401.
K. Winter, private communication.

21) Genova-Harvard-MIT-Pisa Collaboration, ISR Proposal R-804.

INCLUSIVE HADRON PRODUCTION AT HIGH MOMENTUM AT SPEAR I

G. GOGGI
Istituto di Fisica Nucleare, Università di Pavia
Istituto Nazionale di Fisica Nucleare, Pavia, Italy

Abstract: Recent results of the Maryland-Pavia-Princeton collaboration on inclusive hadron production in $e^+ e^-$ annihilation at $\sqrt{s}$ = 4.8 GeV are presented. The results are discussed in the framework of other results obtained at SPEAR I and of the implications at the higher energies attainable at SPEAR II.

Résumé : Nous présentons les résultats récents de la collaboration Maryland-Pavia-Princeton sur la production inclusive des hadrons dans l'annihilation e^+e^- à $\sqrt{s}$ = 4.8 GeV. Nous comparons ces résultats avec d'autres obtenus à SPEAR I et discutons les implications pour les energies plus hautes comme celles de SPEAR II.

INCLUSIVE HADRON PRODUCTION AT HIGH MOMENTUM AT SPEAR I

I would like to present some of the preliminary results of an experiment on inclusive hadron production in e^+e^- annihilation, that was performed at SPEAR by a collaboration of the Universities of Maryland, Pavia and Princeton.(*)

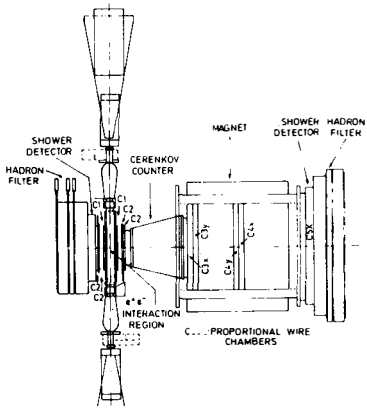

Fig. 1 - Plan view of the apparatus.

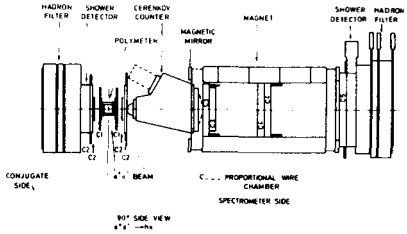

Fig. 2 - Elevation view of the apparatus.

The main characteristics of the experiment are the following (see Figs. 1 and 2):

1. The apparatus consisted essentially of a single-arm spectrometer, equipped with proportional chambers; it was placed at 90° to the colliding beams, and it subtended about 1% of the solid angle. The trigger required one charged particle in the spectrometer.
2. Every particle detected by the spectrometer was identified as an e, μ, π, K or p by means of a gas Cerenkov counter, shower counters, hadron absorbers, and time of flight.

(*) MP^2 Collaboration: T. Atwood, B.A. Barnett, M. Cavalli-Sforza, D.G. Coyne, G. Goggi, G.C. Mantovani, G.K. O' Neill, A. Piazzoli, B. Rossini, H.F.W. Sadrozinski, D. Scannicchio, L. Trasatti, G. Zorn.

3. Particles travelling in the direction roughly opposite to the spectrometer were also detected by shower counters and hadron absorbers.
4. A proportional chamber central detector subtending 99% of the solid angle measured the charged particle multiplicity associated to every trigger, and the φ azimuthal angle of every track.
5. Chambers and shower counters at small angle tagged events produced in "2 γ" processes by detecting the associated electrons or positrons.

The experiment was set up and debugged in late '73 and data were taken in the first half or '74, prior to the discovery of the narrow resonances. The experiment was optimized to identify particles with momentum greater than .8 GeV/c. At the energies of SPEAR I (up to 2.5 GeV/beam) this correspons to the upper part of the range of the x variable. Due to the E^4 dependence of the luminosity at SPEAR, most of our data come from the higher energy runs (2.4 GeV/beam). The results presented here come from the analysis of about 60% of the data at the latter energy, and are for momenta higher than 1 GeV/c.

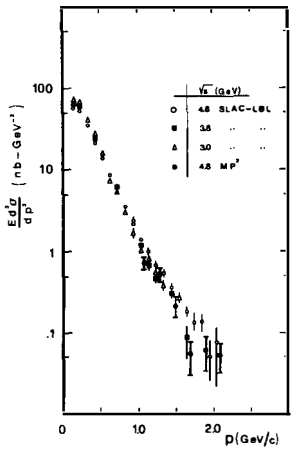

Fig. 3 - Invariant hadronic cross sections from the SLAC-LBL and MP^2 experiments.

The hadronic inclusive cross sections were obtained by normalizing to the $\mu^+\mu^-$ rates, ad assuming the $\mu^+\mu^-$ cross section from QED. Fig. 3 shows the invariant cross section at 4.8 GeV CMS, plotted together with the SLAC-LBL results[1] at different energies. The agreement is good. It should be pointed out, in this respect, that the one particle trigger we used (due to the small solid angle of the spectrometer)

makes the efficiency calculations direct and especially model independent.

The cross section above was obtained merging together all events identified as hadrons. Turning to K/π separation, Fig. 4 shows how this was achieved by means of the Cerenkov counter.

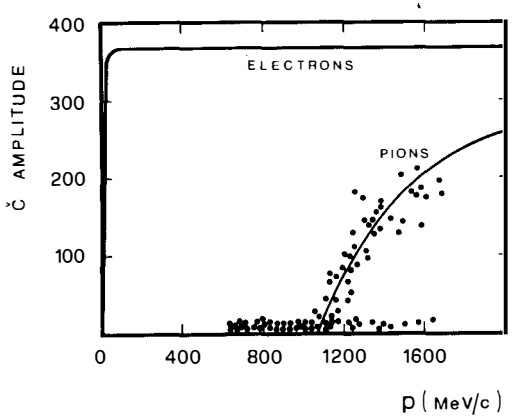

Fig. 4 - Behaviour of the Cerenkov counter for pions of kaons. Points represent pulse amplitude (in arbitrary units) for part of the sample. Calculated curves for electrons and pions are shown. The arrow indicates the practical lower limit of the acceptance of the spectrometer.

The threshold for pions is at p = 1.05 GeV/c and above 1.2 GeV/c there is a clear separation of pions from kaons and protons. The pulse height expected for pions as a function of momentum is indicated.

We get 53 pions and 13 kaons or protons with momentum greater than 1.2 GeV/c. Of the latter, three could not be analyzed by time of flight; the other ten were identified by time of flight as kaons. Considering all of them as K's, since we have no evidence of protons, we get a K/π ratio of $.33 \pm .10$ for hadrons with $P_{had} > 1.2$ GeV/c. If we split the sample at 1.6 GeV/c, we get:

$$K/\pi = .28 \pm .09 \quad \text{for} \quad 1.2 < P_{had} < 1.6 \text{ GeV/c}$$
$$K/\pi = .64 \pm .32 \quad \text{for} \quad 1.6 < P_{had} < 2.4 \text{ GeV/c}$$

Fig. 5 shows the results of this experiment and of the SLAC-LBL experiment[1], together with the results on K/π ratios obtained in p-p interactions at FNAL by Cronin et al.[2] and at the ISR by Alpert et al.[3]. The e^+e^- and p-p results look similar at the lower momenta, but as momentum increases

there seem to be relatively more kaons produced in the e^+e^- interaction. If we attach weight to our high momentum point, that is based presently on only 5 K's, the ratio could still be rising.

Particle separation also allows to check on the behaviour of thermodynamic scaling models and the universality of particle distributions at large energies compared to the rest masses of the particles. Invariant cross sections for kaons and pions are plotted versus total energy of the particle in Fig. 6, together with the data of SLAC-LBL. The exponential thermodynamic-like distribution that holds very well under 1 GeV breaks down

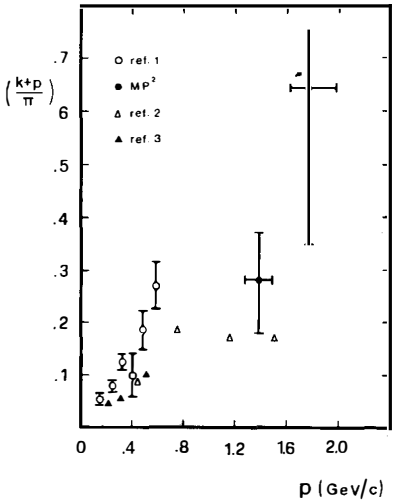

Fig. 5 - K/π ratios from the SLAC-LBL and MP^2 experiments and in p-p experiments at FNAL and ISR.

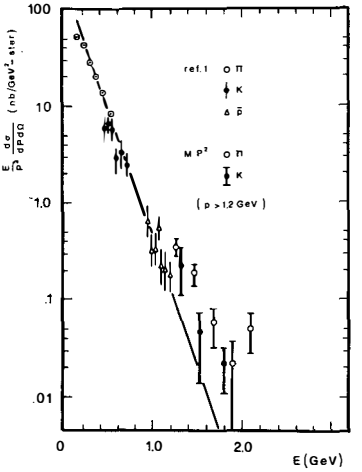

Fig. 6 - Particle energy distributions from the SLAC-LBL and the MP^2 experiments at 4.8 GeV in the CMS.

for higher energies. Also, whereas under 1 GeV the energy distributions of different particles seem to belong to the same universal distribution, this is not true for pions and kaons above 1 GeV. It is perhaps worth to point out that although deviations from the exponential are more evident for energies approaching the beam energy, one cannot use only phase space arguments to explain the breakdown of this scaling behaviour, since pion and

kaon invariant cross sections are already above the exponential and well separated from the antiproton cross section for energies just above 1 GeV.

The charged particle multiplicity measured for each event by the central detector is shown in Fig. 7 against the momentum of the hadron detected in the spectrometer. The multiplicity decreases as the momentum of one particle increases, as one might expect from phase space arguments. A few events have (unphysical) odd multiplicities; this can be attributed to γ -ray conversion in the vacuum chamber, or, to a lesser extent, to inefficiencies in the chambers near the support wires.

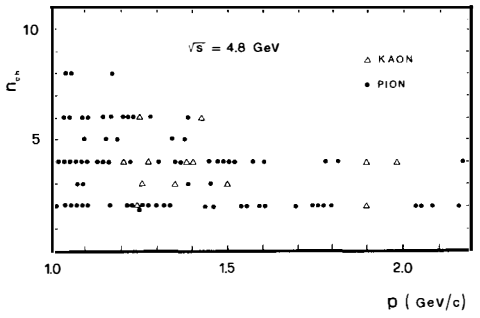

Fig. 7 - Charged multiplicity vs. momentum of the particle detected in the spectrometer at 4.8 GeV in the CMS.

The average multiplicity measured in the central detector is 3.7 ± .3, a value somewhat lower than the SLAC-LBL number, that is 4.2 ± .4 at 4.8 GeV in the CMS. This is not surprising, given the momentum-multiplicity correlation shown in Fig. 7 and the 1 GeV/c momentum cut of this part of our analysis.

It should be pointed out that this experiment is approved to run again at SPEAR II at CMS energies of 7 ÷ 8 GeV. At these energies particle separation at high x with large solid angle detectors gets more difficult, and the unique range of our system in identifying particles will expand.

Some points which this experiment should contribute to clarify in the next round are the following:

1. Bjorken scaling - Fig. 8 shows the well-known SLAC-LBL result: with increasing s, the range of x in which a Bjorken kind of scaling holds increases. More specifically, $s\, d\sigma/dx$ seems to approach quite rapidly a pure exponential. If this is

the case, some dramatic changes in the present trends should be rather near at hand:

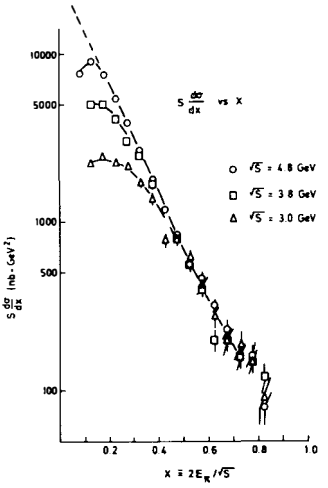

Fig. 8 - s dσ/dx from the SLAC-LBL experiment at three energies. The dotted line is hand-drawn through the exponential part of the curves.

(a) $\int_0^1 s \frac{d\sigma}{dx} dx = s \langle n \rangle \sigma_h$ would tend to a constant value; the product $\langle n \rangle \sigma_h$ would then decrease like s^{-1}; in other words, in the approximation of a constant or very slowly rising $\langle n \rangle$, σ_h would begin to decrease like 1/s.

(b) in this approsimation, $R = (\frac{\sigma_h}{\sigma_{\mu\mu}})$ would also become asymptotic. Integrating s dσ/dx with the parametrization shown in Fig. 8[4], and making an educated guess at $\langle n \rangle$; one obtains $R_{asympt.} \approx 10$ if $\langle n \rangle \doteq 5$

(c) from the above relationship, and with $\sigma_h \approx 20$ nb, $\langle n \rangle \doteq 5$, one gets for the onset of these phenomena

$$s \approx 42 \text{ GeV}^2, \text{ i.e. } E \approx 3.25 \text{ GeV/beam}$$

that is within the SPEAR II energy range.

2. Particle inclusive cross sections - Should the trend forwards full Bjorken scaling be confirmed at higher energies, it might be reasonable to expect each individual particle inclusive cross section to scale. This would imply an asymptotic K/π ratio, and an s-independent curve for its dependence on the x variable.

We must keep in mind, however, that up to now the e^+e^- interaction has sistematically given surprises to theoreticians and experimenters alike. We should not be too surprised, therefore, if more new features should arise in the SPEAR II energy range.

REFERENCES AND FOOTNOTES

1. B. Richter, XVII International Conference on High Energy Physics, London, 1974

2. B. Alper, H. Boggild, P. Booth, F. Bulos, L.J. Carroll, G. Von Dardel, G. Damgaard, B. Duff, F. Heymann, J.N. Jackson, G. Jarlskog, L. Jonsson, A. Klovning, L. Leistam, E. Lillethun, G. Lynch, M. Prentice, D. Quarrie, and J.M. Weiss, Phys. Lett. 47 B, 275 (1973).

3. J.W. Cronin, H.J. Frisch, M.J. Shochet, J.P. Boymond, P.A. Piroue, and R.L. Sumner, P.R.L. 31, 1426 (1973).

4. Drawing a straight line through the exponential part of the three curves, we get $s\, d\sigma/dx \triangleq 30{,}000 \exp(-x/.139)$. On then has:

$$\int_0^1 s \frac{d\sigma}{dx} dx \doteq 4170 \text{ nb.GeV}^2$$

THEORETICAL STUDIES FOR LEPTONS PRODUCTION IN HADRONIC COLLISIONS

F.M. RENARD
Département de Physique Mathématique
U. S. T. L., 34060 MONTPELLIER CEDEX, France

Abstract : Predictions are given for the leptons pairs production taking into account the new informations about the quark partons (antipartons distributions from ν datas, charm, colour) and about the vector mesons (heavy vector mesons and ψ particles). Applications are given for various hadronic beams and energies in the cases where one detects either the pair of leptons or a single lepton. Modifications of the partons model and additional contributions are noticed.

Résumé : Nous donnons des prédictions pour la production de paires de leptons tenant compte des informations nouvelles obtenues sur les quark partons (distributions d'antipartons à partir des expériences neutrinos, charme, couleur) et sur les mésons vecteurs (mésons lourds et particules ψ).Nous faisons des applications pour divers faisceaux hadroniques et diverses énergies dans les cas où l'on détecte soit la paire soit un seul lepton. Nous signalons la possibilité de modifications du modèle à partons ainsi que de contributions supplémentaires.

We reconsider globally the effects of a set of new informations[7,8,9] which modify our expectations about the leptons production in hadronic collisions, i.e. constraints on antipartons distributions inside the nucleon from DIS of neutrinos, existence of charmed and coloured states, higher vector mesons and new ψ particles. We give new predictions for cross-sections with various hadronic beams in a large energy range. In the first part we use the parton model with the Drell-Yan mechanism[1,2,3] in which a $q\bar{q}$ pair annihilates into one photon which gives then the leptons pair. In the 2nd part we consider the vector meson production (ρ, ω, ϕ, $\psi_{3.1}$) and their series of higher masses) ; this production is described by two processes, annihilation diagrams (A) and Bremstrahlung of vector mesons by the initial hadrons (B). In both parts we give applications for collisions of p, $\bar{p}$, π^+, π^-, K^+, K^-, K°, $\bar{K}^\circ$ on protons at various energies and with measurements of $\frac{d\sigma}{dQ^2}$, $\frac{d\sigma}{dQ^2 d\xi}$ and $\frac{\ell^\circ d\sigma}{d_3\ell}$ for a single lepton.

Detailed results can be found in

"Leptons production in hadronic collisions, partons, vector mesons and new particles", Preprint Montpellier PM/75/3, to be published in Il Nuovo Cimento A.

Let us just notice some discussions :

We believe that the contributions of the process (A) to the vector meson production is in a sense "dual" to the point-like Drell-Yann mechanism but that the process (B) is an additionnal term which may also have a dual counter part in a Bremstrahlung process of a $q\bar{q}$ pair by a single initial hadron. Those connections between partons and vector mesons have already been discussed[4] in the case of deep inelastic scattering and e^+e^- annihilation[5]. We observe then that the sum of (A) and (B) approaches the famous 10^{-4} ratio for ℓ/π in the range $1. < \ell_T < 7$ GeV/c for p + p collisions. Of course for $\bar{N}$ and π beams the cross-sections are much larger.

Additional contributions can be imagined.

First a modification of the Drell-Yan mechanism due to gluons effects is possible[6]. For example for vector meson production and more generally time-like photons one can require the extraction from the initial hadrons of more partons than the valence pair, i.e. the complete set of configurations with other pairs and gluons which constitute the sea of any hadronic state. Knowing[7] from DIS that in a nucleon state there are in average 49 % of gluons the effect can be important. In a very simple model with Poissonian

distributions of pairs and gluons in the sea ($P^h(n) = e^{-g}\frac{g^n}{n!}$ in h and $P(n) = e^{-g'}\frac{g'^n}{n!}$ in the vector meson or photon) one gets the correction factor to the Drell-Yan formulas :

$$K = (1 + gg')\, e^{g'(g-1)} \qquad (11)$$

If the sea of gluons is sharply x dependant (like some power of (1-x)) one may have a τ dependance in eq (11) through $g(\tau) \equiv g(1-\tau)^k$; g' is related to the hadrons produced in e^+e^- annihilation: $g' \simeq \frac{<n(n-1)>}{<n>}$; here also the shape of $q^2\frac{d\sigma}{dx}$ and its scaling violations[8] (apart from threshold effects for example of charmed particles) can be related to the opening of the sea configurations of the time-like photon (notice the similarity of the regions in x : $x < 0.5$ for scaling violations in $q^2\frac{d\sigma}{dx}$ and for the sea contributions to F(x)). For reasonable values of g and g' one can get from eq (11) an enhancement factor for small τ and ℓ_T and a flatening or depression factor for large τ and ℓ_T ; exactly what seems to be required by experiments[9].

In addition new vector meson states (non singlet colour representations, Han-Nambu's) can still appear with high masses and contribute to large $\ell_T \simeq \frac{m_V}{2}$. Finally single charged lepton production due to weak decays of new pairs of (charmed) particles is also possible but difficult to evaluate[10].

REFERENCES :

(1) S.D. Drell and T.M. Yan, Ann. of Phys. 66 (1971) 578

(2) S.M. Berman, J.D. Bjorken and J.B. Kogut, Phys. Rev. D4 (1971) 3388

(3) R.Mc Elhancy and S.F. Tuan, Phys. Rev. D8 (1973) 2267
S. Pakvasa, D. Parashar and S.F. Tuan, Preprint Univ. of Hawaii (1974)

(4) J.J. Sakuraï and D. Schildknecht, Phys. Lett. 40B (1972) 121, 41B (1972) 489 and 42B (1972) 216
A. Bramon, E. Etim and M. Greco, Phys. Lett. 41B (1972) 609
F.M. Renard, Nucl. Phys. B82 (1974) 1

(5) T. Goldman and P. Vinciarelli, Slac-Pub 1414 (1974)
F.M. Renard, Phys. Lett. 53B (1974) 70

(6) J. Layssac and F.M. Renard, Phys. Lett. 56B (1975) 364

(7) D.C. Cundy, proc. XVII Int. Conf. London (1974) IV - 131
P.V. Landshoff, proc. Cern School of Phys. (1974), Cern 74-22
G. Altarelli, proc. Gif-sur-Yvette Summer School, IN2P3, (1974)
(8) B. Richter, proc. XVII Int. Conf. London (1974) IV - 37
(9) L.M. Lederman, proc. XVII Int. Conf. London (1974) V - 55
J. Christenson et al, Phys. Rev. Lett. 25 (1970) 1523
J.J. Aubert et al, Phys. Rev. Lett. 33 (1974) 1404
(10) J.D. Bjorken, Journ. de Phys., Suppl. n° 10, 34 (1973) C1-385.

JET STRUCTURE AND APPROACH TO SCALING IN e^+e^- ANNIHILATION

K. Schilling
University of Wuppertal
56 Wuppertal (Germany)

I report on a detailed analysis [+] about the plausible onset of scaling for normalized inclusive pion spectra $\frac{1}{\sigma_{tot}}\frac{d\sigma}{dx}$, $x = \frac{2p_0}{\sqrt{s}}$, in the reaction

$$e+e- \to \pi(p_0) + \text{any pions.}$$

Since, as a surprise to many, at least to theorists, Bjorken scaling was not confirmed by data in the energy range $\sqrt{Q^2} < 5$ GeV, it seemed worthwhile to us to calculate nonasymptotic effects in a scaling model, for which we chose as the simplest prototype an uncorrelated jet model (UJM) with randomly oriented jet axis. The two inherent parameters, the jet width, λ, and the slope, κ, of the asymptotic logarithmic increase of the average particle number were chosen to be equal to the hadronic jet dimensions observed in proton-proton collisions at the ISR, i.e. from fits of type

$$\bar{N}_{tot} \underset{s\to\infty}{\simeq} \kappa \ln Q^2 + \ldots$$

$$\frac{2p_0}{\sigma_{tot}}\frac{d^3\sigma}{d^3p}\Big|_{\substack{p_L = 0 \\ p_t \text{ small}}} = \exp(-\lambda p_t)$$

With the values $\lambda = 6.2\ \text{GeV}^{-1}$, $\kappa = 3$, we evaluated the predictions of the model by Monte Carlo methods by use of the formulas

$$\frac{2p_0}{\sigma_{tot}}\frac{d^3\sigma}{d^3p} = \frac{\int d^2\hat{e}\cdot\exp\{\lambda|\vec{p}\times\hat{e}|\}\cdot\Omega(\hat{e},Q-p)}{\int d^2\hat{e}\,\Omega(\hat{e},Q)}$$

with

$$\Omega(\hat{e},Q) = \sum \frac{1}{N!}\left(\frac{\kappa\lambda}{\pi}\right)^N \Omega_N(\hat{e},Q)$$

[+] work done in collaboration with R. Baier, J. Engels and H. Satz, to be published in Nuovo Cimento B

and $$\Omega_N(e,Q) = \int \prod_{i=1}^{N} \left\{ \frac{d^3 p_i}{2p_i^0} e^{-\lambda |\hat{e}\vec{x}\vec{p}_i|} \right\} \delta^4 \left(\sum_{i=1}^{N} p_i - Q \right)$$

The main result is shown in the figure which demonstrates the deviations from the scaling curve at 3 GeV (dash-dotted), 3.8 GeV (broken), 4.8 GeV (full line) and 20 GeV (points). Conclusion: one would not expect scaling to occur before 20 GeV.

UJM differs from Fermi phase space and Statistical Bootstrap Model predictions mainly at $p_0 > 1$ GeV. Conclusive comparison of models to present data is not yet possible because of lacking particle separation and the unknown secondary distribution of neutrals. As the observed unseparated invariant particle spectrum deviates from $\exp(-p_0/kT)$, a jet type picture has a good chance to be confirmed at the next generation storage rings.

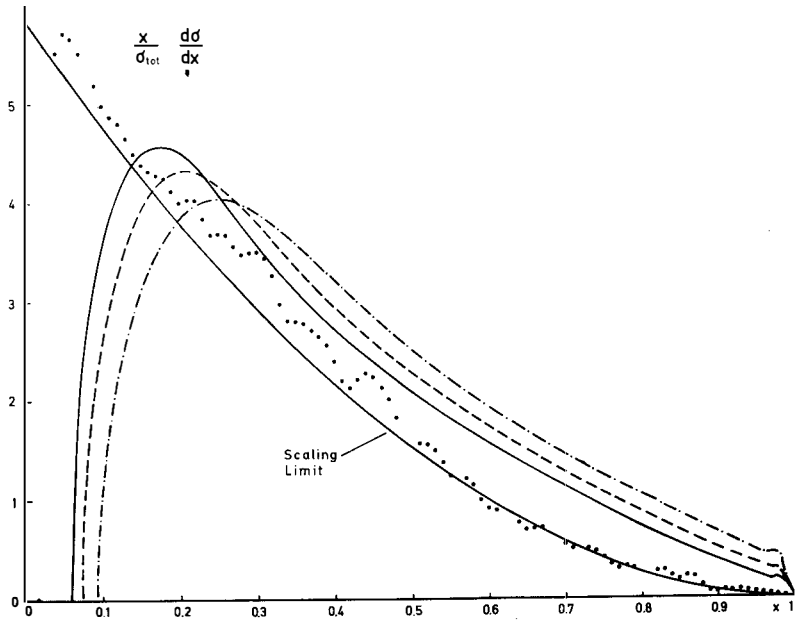

COMMENT CONCERNING THE CONSERVATION OF LEPTON NUMBER

G.W. LONDON

LPNHE - Université Pierre et Marie Curie

Abstract : We make a short and off the beaten track comment concerning the additive and "multiplicative" schemes for the conservation of lepton number. First we recall the two schemes. Then we discuss the use of μ decay to distinguish between the two schemes, noting the theoretical complications in interpreting the published experimental results. We conclude that the only practical experiment which can clearly distinguish between the two schemes is the search for $e^-e^- \to \mu^-\mu^-$ events in the DORIS (DESY) or DCI (Orsay) colliding electron machines.

Résumé : Nous faisons un commentaire court et insolite sur la conservation du nombre leptonique additif ou "multiplicatif". D'abord nous faisons un rappel des deux schémas. Ensuite, nous discutons l'utilisation de la désintégration du μ pour distinguer les deux schémas, tout en notant les complications théoriques dans l'interprétation des résultats expérimentaux publiés. Nous concluons que la seule expérience pratique pour distinguer clairement les deux schémas est la recherche des événements $e^-e^- \to \mu^-\mu^-$ dans les anneaux de collision DORIS ou DCI.

The ordinary scheme for lepton conservation requires the conservation separately and additively of electron and muon number. The e^- and its neutrino (μ^- and its neutrino) have electron (muon) numbers, $L_e(L_\mu) = +1$ while their antiparticles are assigned $L_e(L_\mu) = -1$. The "multiplicative" scheme [1] for lepton conservation requires the conservation of the additive lepton number (L=+1 for e^-, μ^- and their neutrinos and L=-1 for the antileptons) and the conservation of the multiplicative lepton parity (L_p=+ for $e^\pm$ and their neutrinos, and L_p=- for $\mu^\pm$ and their neutrinos).

In the intermediate boson picture, the $W^\pm$ which mediate ordinary μ decay, $\mu^- \to e^- \bar{\nu}_e \nu_\mu$, and the Z^o which mediates $\nu_\mu e^- \to \nu_\mu e^-$ have lepton numbers in the two schemes : $L_\mu = L_e = 0$ and $L = 0$, $L_p = +$.

The multiplicative scheme allows a second μ decay, $\mu^- \to e^- \nu_e \bar{\nu}_\mu$. Assuming L = 0 for the intermediate bosons which mediate this decay, there are <u>two</u> diagrams which contribute, one with $W^\pm$ with L_p=- and one with a Z^o with L_p=-. <u>Thus these intermediate bosons are not the same as those in ordinary weak interactions.</u>

The Gargamelle [2] experiment has attempted to measure the fraction of "wrong" μ decay by looking for events from the "wrong" e^- neutrino. Their result is that this fraction is <1/4 with 90% confidence. But what should it be in the multiplicative scheme ? Since the intermediate bosons are not the same, their coupling constants to leptons, G', are unknown. Since there are two competing diagrams for the "wrong" μ decay, cancellations are possible. Therefore the expected fraction of "wrong" μ decay can be anywhere from 0 to 1. Thus the Gargamelle experiment does not give a limit on the coupling constants for the "wrong" decay, providing a poor test of the multiplicative scheme. A related analysis [3] of $\nu_\mu A \to e^- \mu^+ \nu_e A'$ suffers from the same theoretical ambiguity.

A better test of this scheme is the reaction $e^- e^- \to \mu^- \mu^-$ since this involves only the Z bosons with L=0 and L_p=-. The only published result [4] gives $G' < 610\ G_{Fermi}$, hardly meaningful. The new storage rings, DORIS (DESY) and DCI (Orsay), can be used to get a much better limit. With $G' = G_{Fermi}$ and $S = (4 \times 4)\ GeV^2$, the cross section, $G^2S/4\pi$, is about $3 \times 10^{-37} cm^2$.

(1) G. Feinberg and S. Weinberg, Phys. Rev. Letters 6, 38 (1966)

(2) T. Eichten et al, Phys. Letters 46B, 281 (1973)

(3) C.Y. Chang, Phys. Rev. Letters 24, 79 (1970)

(4) W.G. Barber et al, Phys. Rev. Letters 22, 902 (1969)

SU(6)-STRONG BREAKING, STRUCTURE FUNCTIONS AND STATIC PROPERTIES OF THE NUCLEON

A. Le Yaouanc, L. Oliver, O. Pène and J.C Raynal

Laboratoire de Physique Théorique et Hautes Energies
Université de Paris-Sud
91405 ORSAY - France

Abstract : The breaking of SU(6)-strong in the harmonic oscillator quark model : implications for the ratio F_2^{en}/F_2^{ep}, the static properties μ_p^{tot}/μ_n^{tot}, $(F/D)_{axial}$ and the slope of the neutron electric form factor.

Résumé : La brisure de SU(6) dans le modèle des quarks de l'oscillator harmonique : conséquences pour le rapport des fonctions de structure du nucléon F_2^{en}/F_2^{ep}, les quantités statiques μ_p^{tot}/μ_n^{tot}, $(F/D)_{axial}$, et le facteur de forme électrique du neutron.

In order to explain the experimental x-behaviour of the ratio of deep inelastic scattering structure functions F_2^{en}/F_2^{ep}, which is a manifestation of SU(6)-breaking, we propose to introduce, in the harmonic oscillator quark model, the following inter-band mixing for the nucleon wave function at rest : $\cos\varphi(\underline{56},0^+)_{N=0} + \sin\varphi(\underline{70},0^+)_{N=1}$. The effect on the x-behaviour of the ratio

F_2^{en}/F_2^{ep} is linear in $\mathrm{tg}\,\varphi$; the angle is found to be $\varphi \simeq -20°$. It turns out that the famous successes of unbroken SU(6) for the low-lying octet static porperties are not broken significantly,
$\mu_p^{tot}/\mu_n^{tot} \simeq -\frac{3}{2}(1 + 0.03)$, $(F/D)_{axial} \simeq \frac{2}{3}(1 + 0.02)$, since the breaking effect is proportional to $\mathrm{tg}^2\,\varphi$ with reducing coefficients. Moreover, the mixing implies a slope for the neutron electric form factor, which is a linear effect in $\mathrm{tg}\,\varphi$, of the right sign and order of magnitude.

$|G_A/G_V|$ is correctly predicted to 1.25.

The chiral configuration mixing describing the nucleon wave function at $P_z = \infty$ is shown to come from the intercombination of two effects :

i) introduction of small components in the quark Dirac spinors to account for the highly relativistic internal quark velocities as described in our previous papers, which preserves the 56 assignment of the nucleon wave function at rest, .

ii) the new effect of SU(6) mixing for the nucleon wave function at rest.

In a first step, we compute the structure functions in the approximation of three valence quarks, whose momentum and spin distributions are described by the wave function boosted at $P_z = \infty$. This wave function exhibits automatically the scaling as a consequence of the Lorentz contraction. We predict correctly the ratio F_2^{en}/F_2^{ep} for $x \geq 0.2$. The proton and neutron asymmetries are positive and close to each other at $x \simeq 1$.

Introducing a structure for the quarks which parallels the need for quark structure in the leptoproduction of hadrons, we end with a good description of the unpolarized structure functions in deep inelastic electro- and neutrino-production.

Further predictions are made of the yet unmeasured asymmetries in deep inelastic polarized electro-production.

Careful comparison is made with previous works by Alterelli et al. and Close, which have adopted different approaches.

REVIEW OF THE EXPERIMENTAL STATUS OF NEUTRAL CURRENTS REACTIONS IN GARGAMELLE

P. Musset
European Organization for Nuclear Research
1211 Geneva 23 (Switzerland)

Abstract : We present the status of the experimental study of neutral current reactions ($\Delta Q = 0$) of neutrinos and antineutrinos on nuclei in the inclusive channel and on electrons in the elastic channel.

Résumé : Nous présentons l'état de l'étude expérimentale des réactions de courant neutre ($\Delta Q = 0$) des neutrinos et des antineutrinos sur les noyaux dans le canal inclusif et sur les électrons dans le canal élastique.

The neutral currents reactions have been detected and studied in Gargamelle by the collaboration of Aachen, Brussels, Cern, Ecole Polytechnique, Milan, Orsay, University College of London laboratories.

Three channels have been explored

(1) $\nu_\mu\ (\bar{\nu}_\mu) + N \rightarrow \nu_\mu\ (\bar{\nu}_\mu) + \text{hadrons}$ (inclusive)

(2) $\nu_\mu\ (\bar{\nu}_\mu) + N \rightarrow \nu_\mu\ (\bar{\nu}_\mu) + N' + \pi$ (one pion)

(3) $\nu_\mu + e^- \rightarrow \bar{\nu}_\mu + e^-$ (leptonique)

The experimental observations were that there are neutral penetrating particles (i.e. not hadrons) producing events without muon or electron. The hadrons produced in reaction (1) behave similarly to the hadrons produced in the charged current reaction

(4) $\nu_\mu\ (\bar{\nu}_\mu) + N \rightarrow \mu^-\ (\mu^+) + \text{hadrons}.$

Also a few electrons at small angle from the beam are observed as expected from reaction (3). Reaction (2) is treated separately in the present Rencontres.

These observations were subjected to interpretation following the three steps. Firstly, it may be assumed that the unobserved primary particles are neutrinos, and more specifically neutrinos of the muon type. Secondly because of our current ideas about the conservation of leptonic numbers, it may be assumed that secondary neutrinos, also of the muon type, are emitted in the reactions. Finally, one can also speculate about the possibility that these reactions are described by a current-current type lagrangian, as the usual charged current reactions are.

The chamber has been described elsewhere, and we only remind the dimensions : length 4.8 m, diameter 1.9 m which are large compared to radiation length 0.1 m, and collision length 0.6 m. The chamber is surrounded by the yoke and the coils of the magnet, i.e. 1.5 m of iron or copper everywhere except at the two ends when only ~ 0.6 m of copper shields the chamber (fig. 1).

I. THE INCLUSIVE CHANNEL

This channel gave first positive evidences for neutral currents. At the time this search was engaged no specific prediction existed for reaction (1) $\nu_\mu\ (\bar{\nu}_\mu) + N \rightarrow \nu_\mu\ (\bar{\nu}_\mu) + \text{hadrons}$. The study of this possible reaction together with reaction (4) $\nu_\mu\ (\bar{\nu}_\mu) + N \rightarrow \mu^-\ (\mu^+) + \text{hadrons}$ was hence attacked with the following principles. The hadronic

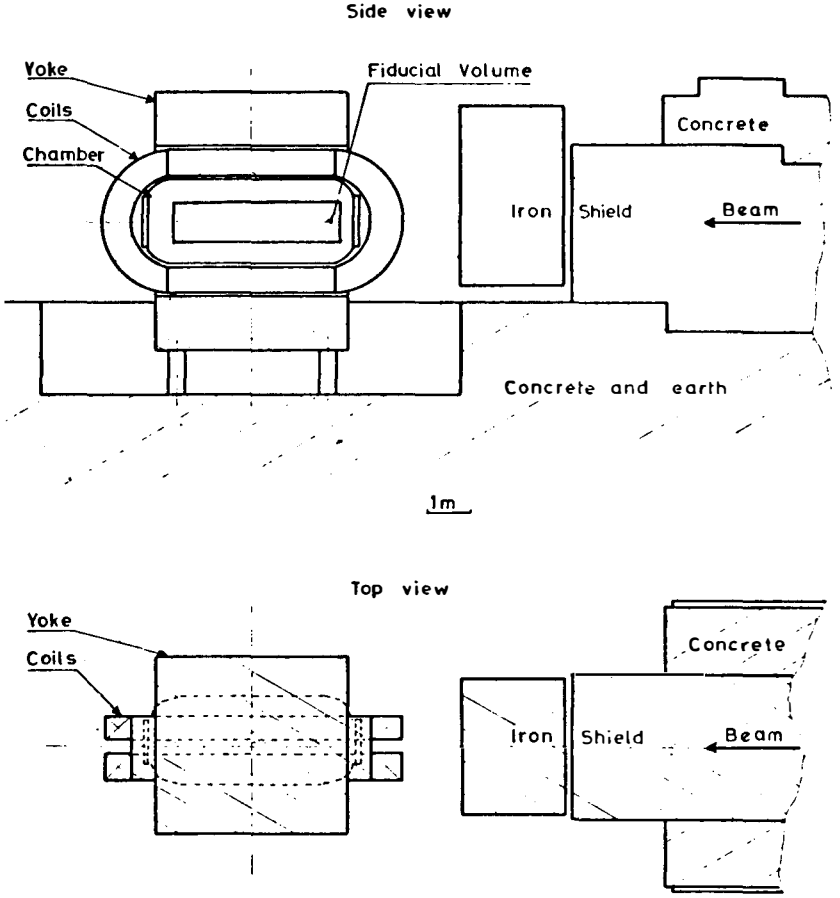
Side view
Yoke
Coils
Chamber
Fiducial Volume
Concrete
Iron
Shield
Beam
Concrete and earth
1m
Top view
Yoke
Coils
Concrete
Iron
Shield
Beam

Fig.1

parts in (1) and (4) were assumed to be similar, or at least not very different. This assumption has proven to be adequate since the hadronic distributions are indeed much more dominated by the shape of the energy spectrum than by the inelasticity distribution. This channel was believed to be less sensitive than (2) to possible nuclear effects, and these effects were believed to lead to similar results in (1) and (4). Then, criteria were searched for in order to minimize the biases.

METHOD

It was aimed to completely separate (1) from (4). All the hadrons were identified in reactions (1), and a subsequent analysis proved that reaction (4) contamination into reaction (1) is indeed at the level of the percent. Hadrons are identified in exactly the same way in (1) and (4), so that the bias is minimum. The analysis proved that reaction (1) contamination into reaction (4) was at the level of the percent too. In order to reduce the background coming from neutrons which simulates reactions (1) a cut in hadronic energy is applied ($E_H > 1$ GeV).

Before events are classified, the tracks are identified according to the following rules. A possible muon is a track which leaves or stops, or,if positive, decays into a positron. No kink > 30° has to be observed and if any < 30° the transverse momentum at the kink has to be less than 100 MeV/c. The hadrons are all unambiguously identified by interaction (π, p), stop (p), decays (π^o, K, Λ).

The events are then classified into the two categories, NC consists of hadrons with no muon, CC consists of hadrons plus one and only one possible muon. In order to study the background of neutrons produced in neutrino interactions outside the visible volume, we use as a reference background sample the neutron stars produced by neutrinos inside the fiducial volume. These consist of neutrons simulating an NC event downstream a primary ordinary neutrino interaction. For all these categories we require that no further interaction existed in the picture, in order to minimize the background.

On the other hand, the observable properties of the neutron interactions in the chamber have been thoroughly studied in a special run with primary protons of different energies. We call the neutron star simulating NC events in this run the NS events.

RESULTS

The number of events is given by the table (1).

TABLE 1

	events	films
CC	218	60
NC	189	209
AS	42	268
NS	78	

We remind briefly the first observations. All the spatial and kinematical distributions of the NC events are comparable and compatible with those of the hadronic parts of the CC events (distribution along the beam direction, radial distribution, total energy and resulting momentum direction distributions). Only the distributions obtained in the new improved statistics for neutrinos are shown (fig.2).

The background was calculated from a Monte Carlo method, in which the neutrino interactions are generated through the whole apparatus. The neutrons produced are then followed through the cascade inside the shielding. The neutron cross sections were first taken from measurements of neutron and proton reactions on nuclei.

A special study of the absorption length was made in the proton run and the measured value was found to be in agreement with the calculation at various neutron energies.

The number of background events B in the NC sample is calculated in the Monte Carlo to be such that $\frac{B}{AS} = 0.6 \pm 0.3$ where the error includes systematics. After all corrections for contaminations, the ratios of the two types of events are :

$$\left(\frac{NC}{CC}\right)_{\nu} = 0.217 \pm 0.026$$

$$\left(\frac{NC}{CC}\right)_{\bar{\nu}} = 0.43 \pm 0.12$$

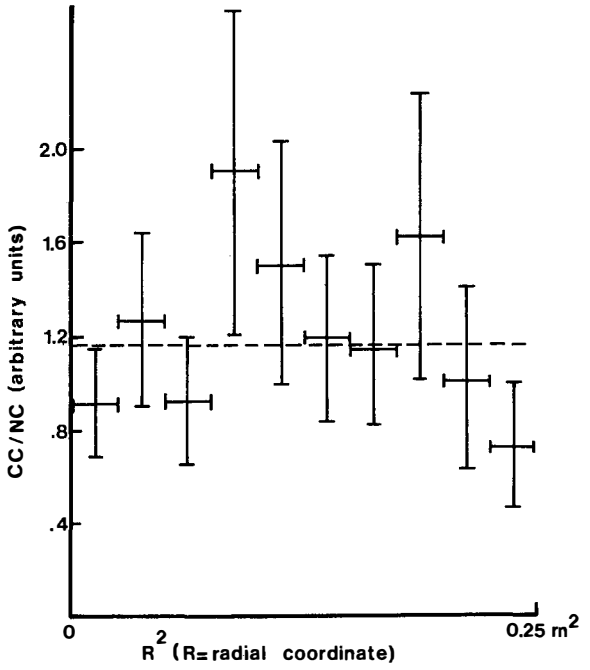
2.0
1.6
1.2
.8
.4
CC/NC (arbitrary units)
0
0.25 m²
R² (R= radial coordinate)

Fig.2 (a)

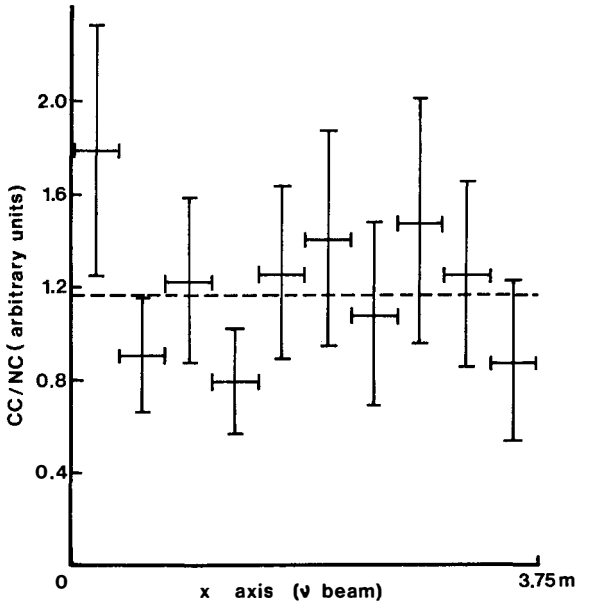
2.0
1.6
1.2
0.8
0.4
CC/NC (arbitrary units)
0
3.75m
x axis (ν beam)

Fig.2 (b)

FURTHER TESTS ON THE NATURE OF NC EVENTS

We will report here on further tests of the nature of the NC events. In these new tests the hypothesis of the neutrino nature of the NC events was reinforced by two observations. The first one is that the charge distributions of the secondary pions are not the same for NC and AS (NS) events, as it should be if NC events were due to neutrons. The second one is a more precise study of the spatial distributions of the NC events. This distribution is found much closer to that of CC events than that of neutrons. The spatial distribution is able to produce information on the fraction of neutron background in the NC sample.

CHARGE DISTRIBUTIONS

Since the energy spectrum of NS, AS, and NC events are not the same (fig. 3) the comparison has been done within energy bins of 1 GeV.

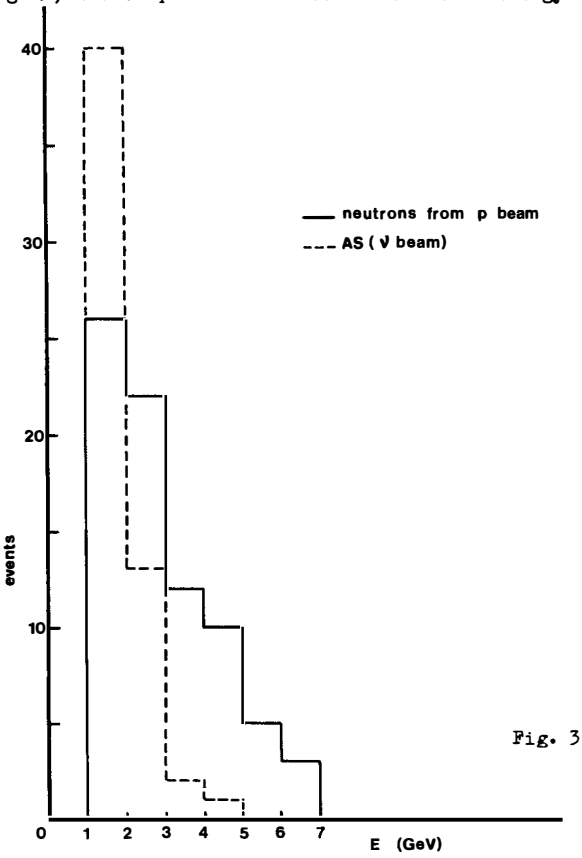

Fig. 3

The ratio $r = \frac{\text{number of } \pi^o}{\text{number of } \pi^+ + \text{number of } \pi^-}$ is calculated for each type of events. All the information on neutrons (AS and NS events) was combined into only one r, called r combined. This quantity was compared with the same quantity for NC events (table 2), called r_{NC}.

TABLE 2

ΔE	r(AS)	r(NS)	$r_{combined}$	r_{NC}
1 - 2 GeV	0.24 ± 0.08	0.38 ± 0.12	0.30 ± 0.07	0.75 ± 0.09
2 - 3 GeV	0.10 ± 0.07	0.23 ± 0.09	0.18 ± 0.06	0.53 ± 0.11
3 - 5 GeV	0.20 ± 0.20	0.31 ± 0.10	0.30 ± 0.08	0.37 ± 0.08
5 - 7 GeV	...	0.31 ± 0.16	0.31 ± 0.16	0.48 ± 0.16

It is clear from the table that r_{NC} is generally greater than $r_{combined}$. The probability that the NC events are all due to neutrons, so that the differences between r_{NC} and $r_{combined}$ have to be attributed to statistical fluctuations is $\sim 10^{-4}$.

SPATIAL ANALYSIS

The spatial analysis of the NC events has been done with the use of the variable $v = (1 - e^{-\ell/\lambda})/(1 - e^{-L/\lambda})$ where ℓ, L are respectively the interactions length and the potential length of the events calculated along the total momentum direction. λ is the interaction length. The v distribution has to be uniform for hadron interactions. It is not so for NC events (fig. 4) and a χ^2 gives the following estimate of the apparent interaction length λ

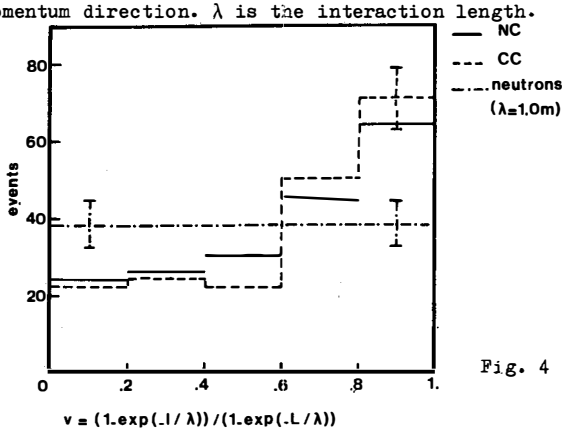

Fig. 4

ν	$\bar{\nu}$
$(1/\lambda)_{NC} = 0.16 \pm 0.12$	$(1/\lambda)_{NC} = 0.39 \pm 0.21$
$(1/\lambda)_{CC} = 0.15 \pm 0.10$	$(1/\lambda)_{CC} = 0.15 \pm 0.14$

These results also favour the neutrino character of the NC events. Note that the value of the apparent interaction length was tested by measurements in the proton run with proton and neutron (NS) reactions (fig. 5).

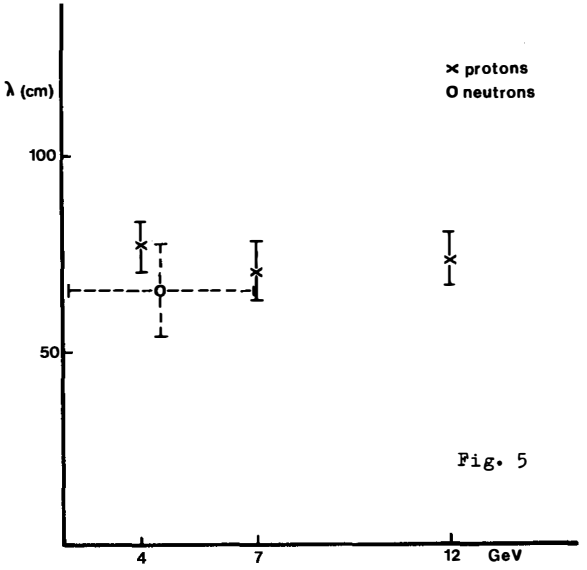

Fig. 5

CORRECTED VALUES FOR THE RATIO OF NEUTRAL-TO-CHARGED REACTIONS

The experimental conditions slightly affect the ratios NC/CC. The corrections have been sometimes evaluated by using only the energy criteria. These corrections are then largely overestimated. It seems more adequate to use the CC neutrino and antineutrino events to evaluate the effects of all the experimental conditions. This has been done, assuming that vector and axial contributions to CC reactions are equal. Comparison of the results can be made with the Weinberg-Salam model elaborated by C. Albright, R. Palmer or L. Sehgal. These three last models give similar results. Taking into account the relative number of protons and neutrons in CF_3Br, the selection criteria, and applying a

correction to charged current reactions (0 for ν, $tg^2\theta_c$ for $\bar{\nu}$), assuming no $\Delta S = 1$ NC reactions, the following numbers are obtained :

$$(NC/CC)_{\nu}^{corr} = 0.224 \pm 0.026 \qquad (NC/CC)_{\bar{\nu}}^{corr} = 0.39 \pm 0.11$$

$$\frac{(NC)_{\bar{\nu}}^{corr}}{(NC)_{\nu}} = 0.67 \pm 0.18$$

If the presence of only V or only A is assumed for NC reactions, as in the Sakuraï model, then the corrections lead to :

$$\frac{(NC)_{\bar{\nu}}^{corr}}{(NC)_{\nu}} = 0.62 \pm 0.17$$ while the theoretical value 1 is predicted.

Note the excellent agreement obtained for the test of consistency in the Sehgal model

$$0.38 \pm 0.07 = 0.37 \begin{matrix} + 0.10 \\ - 0.15 \end{matrix}$$

The mixing parameter is finally estimated to be $\sin^2\theta_W = 0.38 \begin{matrix} + 0.06 \\ - 0.05 \end{matrix}$.

At the present stage of the analysis, the relative "probability" of the Weinberg-Salam model against the Sakuraï model, deduced from the measurement of $(NC)_{\nu}/(NC)_{\bar{\nu}}$ is ~ 10.

II. LEPTONIC NEUTRAL CURRENT

We recall our previous search for the reaction

$$\nu_{\mu} + e^- \rightarrow \nu_{\mu} + e^- \qquad (1)$$

in which no candidate was found.

The experiment is presently concentrated on the reaction

$$\bar{\nu}_{\mu} + e^- \rightarrow \bar{\nu}_{\mu} + e^- \qquad (2)$$

for which the background is the lowest.

The availability of the booster with which the intensity is increased by a factor 3 has made this experiment feasible.

The signature of such a reaction is the emission of an isolated electron in the liquid of the bubble chamber at a small angle with respect to the neutrino beam. Indeed at sufficiently high energy, the angle is less than $\sqrt{\frac{2me}{E}}$.

The electron is identified with an ~ 100 % probability by spiralization in the magnetic field. This spiralization is the result of the energy losses at the Bremsstrahlung processes.

The cross sections are predicted in a definite way in the W-S model as a function of the mixing parameter $\sin^2\theta_W$ (fig. 6).

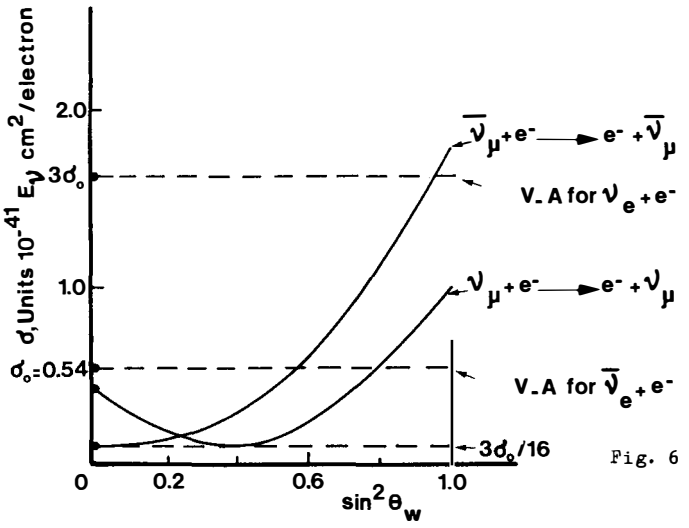

Fig. 6

There are two main sources of background which might simulate reaction (5).

Firstly, the elastic scattering of electronic neutrinos with an invisible secondary proton

$$\nu_e + n \rightarrow e^- + p$$

in the case the proton is of very small energy.

This background can be evaluated by assuming the e-μ universality and using the observed reactions with a muon and without any visible proton.

$$\nu_\mu + n \rightarrow \mu^- + p.$$

This amounts to a background of 0,22 event in the film presently scanned.

Secondly, the presence of a certain number of isolated γ-rays coming mainly from the NC semi leptonic events is a source of background. They may be mistaken as electron if they produce a compton electron (~ 0,5 % probability) or if the electron pair is asymetric (~ 3,5 % probability, as measured in observed pairs). From the number of

observed pairs, this amounts to a background of 0,24 events in the film presently scanned. Hence 0,46 event is expected from the background.

Three unambiguous events are observed with the following characteristics :

	1	2	3
Energy of the electron	385	412	800
Angle to the beam	1.5 ± 1.5	2 ± 2	1 ± 1
Liquid upstream along the beam	0.6 m	2.6 m	3.7 m
Position transverse to the beam	0.16 m	0.40 m	0.35 m

Another ambiguous event at 2 GeV has been observed in which two low-energy electrons and one low-energy positron at the beginning of the track might come from a low-energy Bremsstrahlung γ-ray. The probability of this configuration ranges from 5 % at low energy up to 25 % at higher energy. Nevertheless instead of keeping this event as a candidate it is possible to restrict the sample to the three unambiguous events and to evaluate the loss due to this process. The effect of this loss will depend on the model since it depends upon the energy of the electron. In the W-S model, the losses due to cuts, to scanning efficiency and to this last effect are ~ 50 % together. From these preliminary numbers, the cross section is then calculated to be :

$$\sigma \sim 0.17\ 10^{-41}\ E\ cm^2/GeV.$$

COMPARISON OF THE LEPTONIC CHANNEL WITH THE SEMI LEPTONIC CHANNEL

If the mixing parameter $\sin^2\theta_W$ is 0.38 as calculated from the observations in the semi leptonic channel, four to five electron events are expected. The three observed events are to be considered in good agreement with this expectation.

CONCLUSIONS

Firstly we have observed events that we interpret as due to neutral currents in the semi leptonic channel.

Secondly, a few isolated electron events can also be interpreted as due to elastic neutral current on electron.

Thirdly, the rates in the two semi-leptonic channels, neutrino and antineutrino and the rate of the electron events are all compatible with one value of the mixing parameter $\sin^2\theta_W \sim 0.38^{+0.06}_{-0.05}$ of the Weinberg-Salam model as explicited by C.Albright, R.Palmer and L.Sehgal.

Nevertheless, many properties of the $\Delta Q = 0$ reactions remain to be investigated. The spatial VASTP structure and the isotopic properties of the neutral current can be studied at the P.S. energy in the one pion channel (in freon and propane), and in the elastic semi-leptonic channel. At the SPS energy, the study of the differential cross-section in the ν-Q^2 plane will be possible in a narrow band beam, and more statistics on the elastic leptonic channel will be accumulated. Finally, let us mention the attractive properties of the diffractive reactions of neutrino which are due to neutral currents. In these reactions the quantum numbers of the neutral current are directly observable. For example, the diffractive production of ω and ϕ, ρ, A_1, π... would be due respectively to respective components of the neutral current : vector isoscalar, vector isovector, axial vector isovector, pseudo-scalar isovector, ... At sufficiently high energy, these reactions would constitute a unique tool for the study of the neutral current.

"Je remarquais, touchant les expériences, qu'elles sont d'autant plus nécessaires qu'on est plus avancé en connaissance". R. Descartes.

Latest results on the subject and references can be found in :

- Further investigation on the events without muons in the neutrino experiment in Gargamelle, presented by A. Pullia, London Conference 1974.
- A search for the reaction $\bar{\nu}_\mu + e^- \rightarrow \bar{\nu}_\mu + e^-$, presented by J. Sacton, London Conference 1974.
- Neutrino Physics Plenary Report, D.C. Cundy, London Conference 1974.
- Neutrino interactions at ANL, BNL and CERN, P. Musset, Ecole d'Eté, Gif-sur-Yvette, Sept. 74.

NEUTRINO AND ANTINEUTRINO INTERACTIONS IN GARGAMELLE

U. NGUYEN-KHAC

Laboratoire de Physique Nucléaire des Hautes Energies
Ecole Polytechnique, Paris
France

Résumé : On passe d'abord en revue les résultats importants obtenus dans l'analyse des interactions ν_μ et $\bar{\nu}_\mu$ produisant des leptons μ^- et μ^+. On étudie ensuite les interactions ν_μ et $\bar{\nu}_\mu$ donnant 1 ou 2 particules étranges dans l'état final. L'analyse des réactions à "courant neutre" et "courant chargé" donne $R = (SNC/SCC) = 0.29 \pm 0.14$ pour les deux contributions $\Delta S = 0$ et $\Delta S = 1$. Des limites de sections efficaces de production des particules charmées ont été estimées pour la bande d'énergie 2-10 GeV.

Abstract : We briefly review the most important results obtained from ν_μ and $\bar{\nu}_\mu$ interactions involving charged leptons μ^- and μ^+. Then, the study of the ν_μ and $\bar{\nu}_\mu$ interactions providing 1 or 2 strange particles in the final state are discussed. The analysis of "charged" and "neutral" processes gives $R = (SNC/SCC) = 0.29 \pm 0.14$ for both contributions $\Delta S = 0$ and $\Delta S = 1$. Limits for production cross sections of "charmed particles" have been estimed for the 2-10 GeV energy range.

This paper is divided in 2 parts. The first part refers only to charged current interaction (CC) without strange particle production in the final state (strangeness S = 0) and the second one refers to charged current and neutral current interactions (SCC and SNC) with strange particle production (strangeness S ≠ 0). Since the results on charged current events have been already published (ref. 1, 2, 3, 4) only important data related to ν_μ, $\bar{\nu}_\mu$ total and differential cross sections as well as the sum rules will be reviewed. On the other hand, the charged and neutral current events associated to strange particles will be discussed in details.

1. Introduction

Neutrino reactions can be represented by the following graph :

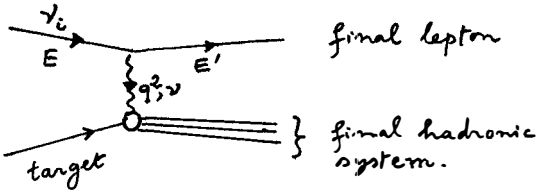

where $\nu_i = \nu_\mu, \bar{\nu}_\mu, \nu_e, \bar{\nu}_e$

target = p, n or e^-

E incident neutrino energy

E' final lepton energy

θ angle of the final lepton with the incident neutrino direction.

$q^2 = 2EE'(1-\cos\theta)$

$\nu = E - E'$

ν_μ and $\bar{\nu}_\mu$ come from the decays $K \to \mu\nu$ and $\pi \to \mu\nu$ whereas ν_e and $\bar{\nu}_e$ come mainly from the $K \to \pi e\nu$ decays. The final lepton may be a neutral lepton (ν_μ, $\bar{\nu}_\mu$, ν_e, $\bar{\nu}_e$) or a charged lepton (μ^-, μ^+, e^-, e^+). According to the charge of the final lepton, there are 2 types of interactions

- charged current interaction
- neutral current interaction

only CC, SCC and SNC processes corresponding to these configurations

$$\nu_i = \nu_\mu, \bar{\nu}_\mu$$
$$\text{target} = p, n$$

will be discussed. (NC process and purely leptonic process will be reviewed in a separate report). Reactions induced by electronic neutrino ν_e, $\bar{\nu}_e$ have been purposely omitted since the ν_e, $\bar{\nu}_e$ fluxes coming from Ke3 decays are very low, of the order of 10^{-2} to 10^{-3} compared to ν_μ, $\bar{\nu}_\mu$ fluxes).

The final state may be defined by 2 variables :

- quantities which are measured directly in the laboratory system : θ and E'
- quantities which are invariant

$$q^2 = (p_\nu - p_\mu)^2$$
$$\nu = -pq/M \quad (\text{or } W^2 = -q^2 + M^2 + 2M\nu), \text{ M=Nucleon mass}$$

- dimensionless quantities

$$\begin{cases} x = q^2/2M \\ y = \nu/E \quad (\text{or } \rho = E'/E) \end{cases}$$

$$\text{or} \quad \begin{cases} x' = q^2/(2M + M^2) \\ y = \nu/E \quad (\text{or } \rho = E'/E) \end{cases}$$

Total and differential cross sections will be discussed in terms of of (x, y) variables or (x', y) variables.

Experimental conditions

The experimental conditions of Gargamelle neutrino experiment are summarized below :

i) Gargamelle

- . cylindrical chamber : length L = 4,8 m
  diameter ϕ = 1,85 m
- . Magnetic field B = 20 KG
- . Liquid : freon CF_3Br (radiation length X_o = 11 cm)
- . visible volume 7 m^3
- . fiducial volume 3 m^3

ii) Beam

- . Focussed wide band ν_μ and $\bar{\nu}_\mu$ beam at the CERN proton-synchrotron

iii) Energy resolution

$(\Delta E_\mu / E_\mu) = 8\%$

$(\Delta \nu / \nu) = 15\%$

2. "Charged current" interactions (CC) (Strangeness S = 0)

2.1 - Total cross sections

Reactions

$$\nu_\mu + N \rightarrow \mu^- + \text{hadrons}$$
$$\bar{\nu}_\mu + N \rightarrow \mu^+ + \text{hadrons}$$

where N is a nucleon (neutron or proton) have been studied.

The analysis of total and differential cross sections for charged current interactions have been made on the basis of 2656 ν events and 1062 $\bar{\nu}$ events with total energy larger than 1 GeV ($E_{\nu, \bar{\nu}} > 1$ GeV) and longitudinal momentum larger than 0.6 GeV/c ($P_L > 0.6$ GeV/c)

Results on ν_μ and $\bar{\nu}_\mu$ total cross sections and their ratio (Ref. 2, 3, 5) have been summarized in table 1.

Table 1

Total cross sections σ^ν, $\sigma^{\bar{\nu}}$ =	
$\sigma^\nu = (0.76 \pm 0.02)\ E\ 10^{-38}$ cm^2/nucleon	(E > 1 GeV)
$\sigma^{\nu\pi} = (0.74 \pm 0.03)\ E\ 10^{-38}$ cm^2/nucleon	(E < 5 GeV)
$\sigma^{\nu K} = (0.77 \pm 0.10)\ E\ 10^{-38}$ cm^2/nucleon	(E > 8 GeV)
$\sigma^{\bar{\nu}} = (0.28 \pm 0.01)\ E\ 10^{-38}$ cm^2/nucleon	(E > 1 GeV)
Ratio $\sigma^{\bar{\nu}} / \sigma^\nu$ =	
$\sigma^{\bar{\nu}}/\sigma^\nu = 0.38 \pm 0.02$	(E > 2 GeV)

These data lead to the following conclusions :

i) the ν_μ and $\bar{\nu}_\mu$ total cross sections in the energy range 1-10 GeV are compatible with the Bjorken scaling prediction (the scale invariance for structure functions implies $\sigma^{\nu,\bar{\nu}} \underset{E \rightarrow \infty}{=} a_{\nu,\bar{\nu}} E_{\nu,\bar{\nu}}$ where a is a constant)

ii) As we know, ν from π decays and ν from K decays correspond respectively to $E_\nu < 5$ GeV and $E_\nu > 8$ GeV. The two slopes of $\sigma^\nu\pi$ and $\sigma^\nu K$ are compatible and we thus conclude than we do not observe any difference between ν from π and ν from K total cross sections.

iii) The ratio of total cross sections $\sigma^{\bar{\nu}}/\sigma^\nu$ is near the physical boundary, 1/3, implying that the left helicity is dominant in the neutrino process and longitudinal contribution to the cross section is negligible as compared with the transverse contribution. This result is compatible with the parton model with a spin 1/2 for point-like constituent. (if we assume $\Delta S = 1$ contribution is negligible and charge symmetry for weak hadronic process, one can show $1/3 < \sigma^{\bar{\nu}}/\sigma^\nu \leqslant 3$)

2.2. Structure functions

i) Differential cross sections in the scaling region

The double differential cross sections in the scaling region, neglecting the $\Delta S = 1$ contribution is given by .

$$\frac{d^2\sigma^{\nu,\bar{\nu}}}{dxdy} = \frac{G^2ME}{\pi}\left\{(1 - y)\, F_2(x) + \frac{y^2}{2} 2x F_1(x) \pm y\left(1 - \frac{y}{2}\right) x F_3(x)\right\}$$

By assuming the Callan-Gross relation $2x F_1(x) = F_2(x)$ (relation which is supported by electron and neutrino scattering data), the structure functions $F_2(x)$ and $xF_3(x)$ are calculated and shown in figure 1a. Fig. 1b shows the y distributions.

Our data are in agreement with the SLAC results and compatible with the scaling hypothesis in inelastic neutrino reactions within errors of order of 10-20%.

ii) Differential cross sections without scaling cuts

Since the scaling behaviour seems to hold down to low values of E and q^2, distributions in terms of $x' = q^2/(2M\nu + M^2)$ and $y = \nu/E$ have also been calculated. Consequently, new structure functions $\overline{F_1}(x')$, $\overline{F_2}(x')$, $\overline{F_3}(x')$ were arbitrarily defined. Fig. 2 gives $\overline{F_2}(x', E)$ and Fig. 3 shows $\overline{F_2}(x')$ and $x'\overline{F_3}(x')$. The shape and magnitude of $\overline{F_2}(x')$ is independent of E and is in agreement with the SLAC data. $x'\overline{F_3}(x')$ is compared to calculations based on fits of quark parton models to the electron scattering data.

Distributions in y for ν and $\bar{\nu}$ events are shown in figure 4 for different energies. At low energy, the main contribution is due to elastic events, but as the energy increases, the ν distribution becomes flat whereas the $\bar{\nu}$ one varies rougly as $(1-y)^2$.

2.3. Sum rules

Results obtained from electron and neutrino experiments required spin 1/2 for point-like constituents, allowing a direct comparison of the experimental data with the quark parton model. In terms of the Bloom-Gilman variable $x' = q^2/(2M\nu + M^2)$, structure functions $F_2^{\nu N}(x')$ and $F_3^{\nu N}(x')$ have been calculated (Ref. 4) and if we assume that they represent the high energy asymptotic region, we find the following results :

Sum rules per nucleon in freon CF_3Br	Experiment	Theory
$\int \bar{F}_2^{\nu N} dx' \Big/ \int F_2^{eN} dx'$ (Llewellyn-Smith)	3.6 ± 0.3	3.6 (quark model)
$\int \bar{F}_3^{\nu N}(x') dx'$ (Gross/Llewellyn-Smith)	3.2 ± 0.6	2.94 (SU3)
$\frac{\pi}{G^2}\left(\frac{d\sigma^{\nu N} - d\sigma^{\bar{\nu} N}}{dq^2}\right)$ (Adler)	< 0.3	0.08 (SU3)

We conclude that our data are in good agreement with the Llewellyn-Smith and Gross/Llewellyn-Smith sum rules and we find no detectable deviations from the Adler sum rule for the 1-10 GeV energy range.

3. Charged current and neutral current interactions (SCC, SNC) (strangeness. $S \neq 0$)

The usual quark model constructed on the basis of a triplet (λ,n,p) of SU3 can not at the present time be reconcilled with any gauge theory. In particular, it would induce a changing strangeness neutral hadronic current with a rate of the same order as charged current incompatible with the experimental data. Following Glashow, Iliopoulos and Maiani (Ref. 6) it should be necessary to add a fourth quark C

with a new quantum number called "charm" introducing thus a new current

$$\bar{c}(-n\sin\theta + \lambda\cos\theta)$$

This current is the orthogonal combination of the one in the Cabbibo charged current

$$\bar{p}\ (n\cos\theta + \lambda\sin\theta)$$

where θ is the Cabbibo angle. Therefore, charmed particles, if they do exist, could be produced for example by ν, $\bar{\nu}$ reactions and could decay predominantly into strange particles via hadronic or semi-leptonic modes (Ref. 7). In order to search for charmed particles, we have made on the one hand a study of "strange particle" production and on the other hand an analysis of "muon-electron" pairs observed and associated to strange particles in the ν, $\bar{\nu}$ reactions.

3.1. Strange Particle Production

We present here a study of the reactions

(SCC) $\nu\ (\bar{\nu}) + N \rightarrow \bar{\mu}(\mu^+) + \text{hadrons} + \text{"S"}$ (1)

(SNC) $\nu\ (\bar{\nu}) + N \rightarrow \bar{\nu}(\bar{\nu}) + \text{hadrons} + \text{"S"}$ (2)

where "S" represents one or two strange particles. Reactions (1) and (2) are called SCC and SNC referring respectively to strange particle production in charged current and neutral current events. Charged current events are signed by the presence of at least one muon candidate and neutral current events by the absence of any possible muon.

In a $\Delta S = 0$ reaction a $K\bar{K}$ pair or a KY pair should be observed. According to the $\Delta S = \Delta Q$ rule single production of K is allowed in ν reaction ($\Delta S = +1$) and single production of $\bar{K}$ or Y is allowed in $\bar{\nu}$ reaction ($\Delta S = -1$) :

$\Delta S = 0$ associated production (ν and $\bar{\nu}$ reactions)	$\Delta S = 1$ (ν reactions)	$\Delta S = -1$ ($\bar{\nu}$ reactions)
K^+K^-, $K^+\bar{K}^\circ$	K^+	K^-
$K^\circ K^-$, $K^\circ\bar{K}^\circ$	K°	Λ°
$K^+\Lambda^\circ$, $K^+\Sigma^{\circ,-,+}$		$\Sigma^{\circ,-,+}$
$K^\circ\Lambda^\circ$, $K^\circ\Sigma^{\circ,-,+}$		

Due to the experimental conditions, the probability of detecting and identifying K^-, $\Sigma^\pm$ and Σ° is very small, so the event selection has been performed only on the reactions involving a K^+, K°_S or Λ°. Furthermore to ensure a good detection efficiency, K°_S and Λ° have been selected by charged decay modes ($K^\circ_S \to \pi^+\pi^-$, $\Lambda^\circ \to p\pi^-$) and K^+ have been identified by the $K_{\pi 2}$ and $K_{\mu 2}$ decays at rest. The numbers of the selected events are displayed in table 2 using a fiducial volume of 3 m^3 and after applying the following criteria :

i) K° and Λ° time of flight smaller than three lifetimes,

ii) total visible energy $E_{\nu\,\bar{\nu}} \geq 1$ GeV,

iii) longitudinal momentum along the ν beam $P_L > 0.6$ GeV/c (only for strange charged current events).

TABLE 2

		INCIDENT FLUX (E>1GeV)	Λ°	$K^\circ(\bar{K}^\circ)$	K^+	$\Lambda^\circ K^\circ$	$\Lambda^\circ K^+$	$K^+\bar{K}^\circ$	$K^\circ\bar{K}^\circ$	TOTAL
ν (6129 events)	SCC	8.677 x 10^{14}	28	13	15	1	11	0	0	68
	SNC		7	3	3	0	2	0	1	16
$\bar{\nu}$ (2430 events)	SCC	9.134 x 10^{14}	22	6	2	3	3	0	0	36
	SNC		1	0	1	1	0	0	0	3

In most of the cases the V° are classified easily as a K°_S or a Λ° by identifying the positive track. Nevertheless there remain 13 ambiguous K°/Λ° in ν sample and 6 in $\bar{\nu}$ sample. 13 of them are classified as Λ° and 6 as K° by choosing the best mass fit. In figure 5 are shown the energy distributions of both ν and $\bar{\nu}$ events.

In order to calculate production cross-sections we have to take into account the corrections for

i) loss of Λ° and K° neutral decays,

ii) nuclear absorption effects,

iii) Λ°, K° and K^+ detection probability.

The probability of Λ° absorption inside the nucleus is estimated to be (5 ± 5)% using a Monte-Carlo calculation, whereas the K° absorption has been neglected.

The main loss of K° or Λ° is essentially due to very short decay lengths. From the observed life-time distributions, the Λ° and K° detection probabilities are respectively estimated to be $P_{\Lambda^\circ \to p\pi^-}$ = (85 ± 3)% and $P_{K^\circ_S \to \pi^+\pi^-}$ = (75 ± 8)%.

From the observed number of Λ°, $\Lambda^\circ K^+$ and $\Lambda^\circ K^\circ$ assuming no $\Delta S = -1$ in ν reactions, the K^+ observation probability is estimated to be 0.31 ± 0.09. This value is in good agreement with the one deduced from the comparison of the observed K° and K^+ momentum spectra.

We also calculated the background of associated production by hadrons interacting inside the nucleus using the same Monte Carlo technique. This gives a maximum of 15% of events in ν reactions and 8% of events in $\bar{\nu}$ reactions which have to be subtracted from the observed numbers of events corrected for detection efficiency.

Due to the lack of K^- and Σ detection, this experiment gives only a lower limit for $\Delta S = 0$ production and an upper limit for $\Delta S = 1$ production in ν reaction :

$$R_0^\nu = \sigma^\nu_{SCC}(\Delta S = 0)/\sigma^\nu_{CC} \geq 0.6\% \text{ at } 90\% \text{ CL}$$

$$R_1^\nu = \sigma^\nu_{SCC}(\Delta S = 1)/\sigma^\nu_{CC} \leq 2.4\% \text{ at } 90\% \text{ CL}$$

In addition, the values of R_0 and R_1 for the ratio (SCC/CC) in ν, $\bar{\nu}$ reactions and their correlations have been given in figures 6 and 7, calculated by a maximum likelihood method. In ν reactions, "$\Delta S = 0$" refers to observed associated production ($K^\circ Y^\circ$, $K^+ Y^\circ$, $K^\circ \bar{K}^\circ$, $K^+ K^\circ$) and "$|\Delta S| = 1$" refers to the upper limit corresponding to single K^+ or K° production. On the other hand, in $\bar{\nu}$ reactions "$\Delta S = 0$" refers to observed associated production ($K^\circ Y^\circ$, $K^+ Y^\circ$, $K^\circ \bar{K}^\circ$, $K^+ \bar{K}^\circ$) and possible associated production (K^+ or K° associated to non observed K^- or $Y^\pm$) whereas " $|\Delta S| = 1$" refers only to single Λ° and Σ° production.

In order to estimate the ratio SNC/SCC, we required that a SCC event contain one and only one muon candidate. After subtracting events with a hadronic energy less than 1 GeV and events having more than one muon candidate, there remain 48 events in ν and 11 events in $\bar{\nu}$ for the normalization :

	SNC events	SCC events
ν	16	48
$\bar{\nu}$	3	11

The background of SNC events in ν sample due to neutron or K_L° is estimated to be 3 events. Since the $\Delta S = 0$ contribution can not be separated correctly from the $\Delta S = 1$, we give only the result (SNC/SCC) for both contributions :

$$\left(\frac{SNC}{SCC}\right)_{\nu}^{\Delta S = 0 + \Delta S = 1} = 0.29 \pm 0.14$$

3.2 Search for "charmed" particles

Reactions

$$\nu_\mu + N \rightarrow \mu^- + \text{hadrons} + C \quad \hookrightarrow e^+ \nu_e + (S = -1 \text{ state})$$

$$\bar{\nu}_\mu + N \rightarrow \mu^+ + \text{hadrons} + \bar{C} \quad \hookrightarrow e^- \bar{\nu}_e + (S = +1 \text{ state})$$

have been studied.

As pointed out in our previous paper (2) electrons in Gargamelle are unambiguously distinguished from other tracks and very well identified, the decay modes (charmed particles are expected to obey a $\Delta C = \Delta Q$ rule)

$$C \rightarrow e^+ + \nu_e + (S = -1 \text{ state})$$

$$\bar{C} \rightarrow e^- + \bar{\nu}_e + (S = +1 \text{ state})$$

should be efficiently picked up at the scanning stage.

A special scan was carried out and charged current events (signed by the presence of a muon) with an identified electron (negative, positive or ambiguous charge) were selected.

The results are summarized in the table below :

	Photographs	Charged current events ($E > 1$ GeV)	"Charmed" Candidate
ν	$2{,}22.10^5$	6108	1
$\bar{\nu}$	$6{,}5\ .10^5$	8700	0

The "Charmed" candidate found in ν sample is of type $\mu^- e^+ (K^\circ/\Lambda^\circ)$ $\pi^- 3p2n$ with a visible energy of 3.15 GeV.

The probability that the candidate found in the ν film is due to an asymmetric Dalitz pair or a $\bar{\nu}_e$ events is estimated to be respectively 2.10^{-3} and $0.5.10^{-3}$.

As the threshold for charmed particle production is unknown, the upper limit with 90% of confidence to the charged current cross section is given (figure 8) as a function of energy E and hadronic invariant mass squared W^2.

The $\Lambda\pi$ invariant mass in the ν film has been calculated and is shown in figure 9. There is no evidence for an enhancement below a mass of 2.5 GeV/c^2 which is about the maximum mass which can be produced in the experiment.

I am indebted to Dr M. Haguenauer for very useful discussions.

REFERENCES

(1) Gargamelle Collaboration : T. Eichten et al, Physics Letters 40B, 593 (1972)

(2) Gargamelle Collaboration : T. Eichten et al, Physics Letters, 46B, 281 (1973)

(3) Gargamelle Collaboration : T. Eichten et al, Physics Letters, 46B, 274 (1973)

(4) Gargamelle Collaboration : H. Deden et al, Nuclear Physics, B85, 269 (1975)

(5) Gargamelle Collaboration : M. Haguenauer, Proceedings of the XVII International Conference on High Energy Physics (London), IV-95 (1974)

(6) S.L. Glashow, J. Iliopoulos and L. Maiani, Phys. Rev. D2, 1285 (1970).

(7) M.K. Gaillard, B.W. Lee and J.L. Rosner, National Accelerator Laboratory, Fermilab. Pub 74/34 - THY.

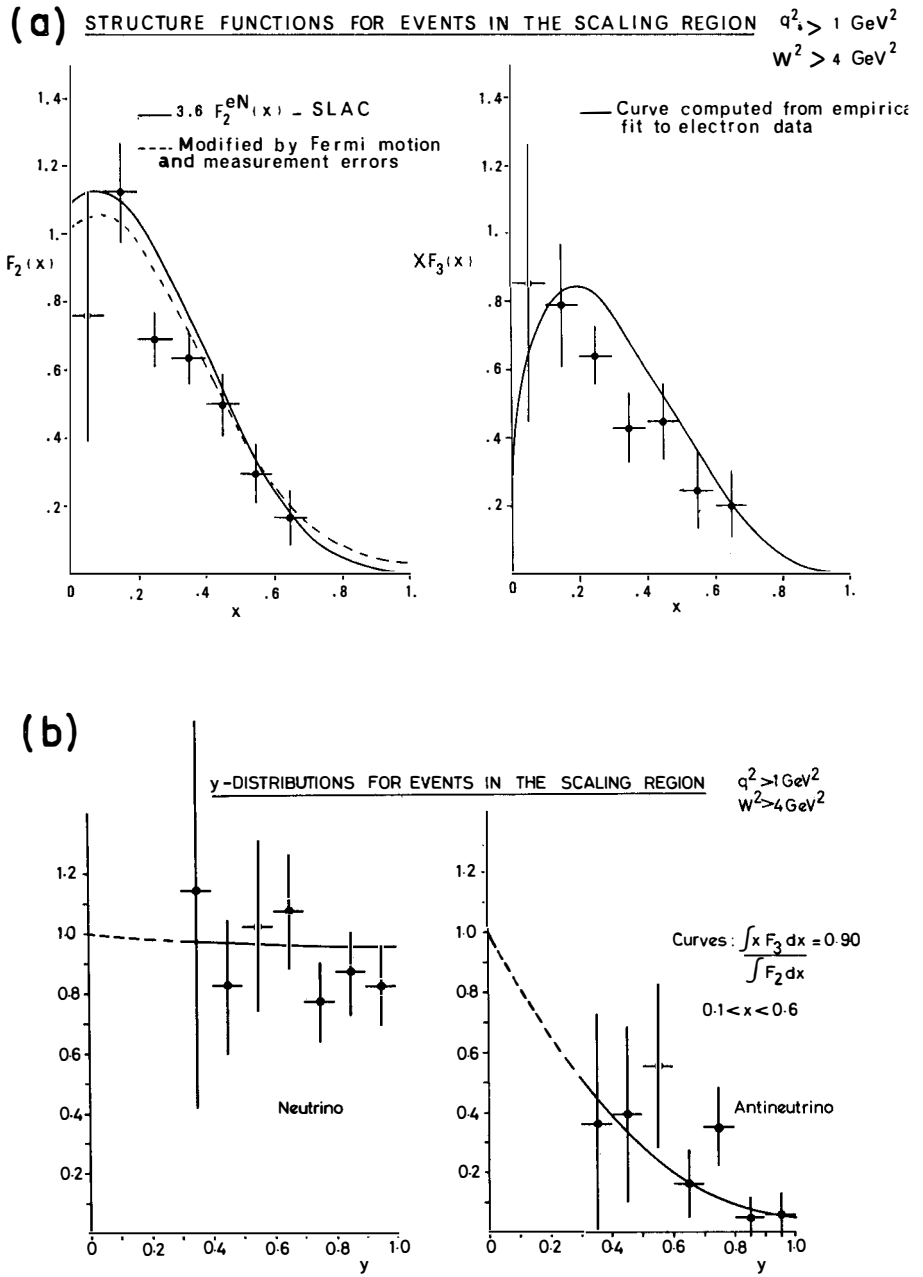
(a)
STRUCTURE FUNCTIONS FOR EVENTS IN THE SCALING REGION
$q^2 > 1$ GeV^2
$W^2 > 4$ GeV^2
3.6 $F_2^{eN}(x)$ - SLAC
Modified by Fermi motion and measurement errors
$F_2(x)$
Curve computed from empirical fit to electron data
$XF_3(x)$
x
x
(b)
y-DISTRIBUTIONS FOR EVENTS IN THE SCALING REGION
$q^2 > 1$GeV^2
$W^2 > 4$GeV^2
Neutrino
Antineutrino
Curves: $\frac{\int x F_3 dx}{\int F_2 dx} = 0.90$
$0.1 < x < 0.6$
y
y

Figure 1

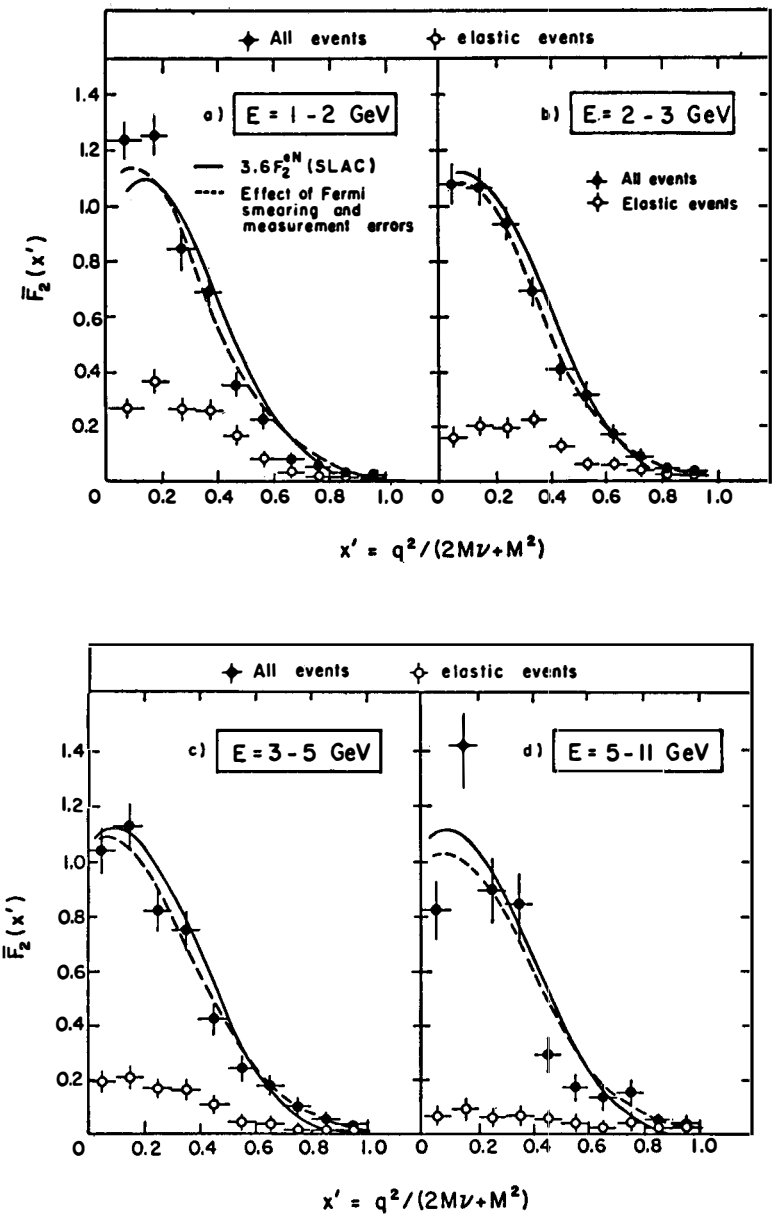
All events
elastic events
a) E = 1 - 2 GeV
b) E = 2 - 3 GeV
c) E = 3 - 5 GeV
d) E = 5 - 11 GeV
3.6 F_2^{eN} (SLAC)
Effect of Fermi smearing and measurement errors
All events
Elastic events
$\bar{F}_2(x')$
$x' = q^2/(2M\nu+M^2)$

Figure 2

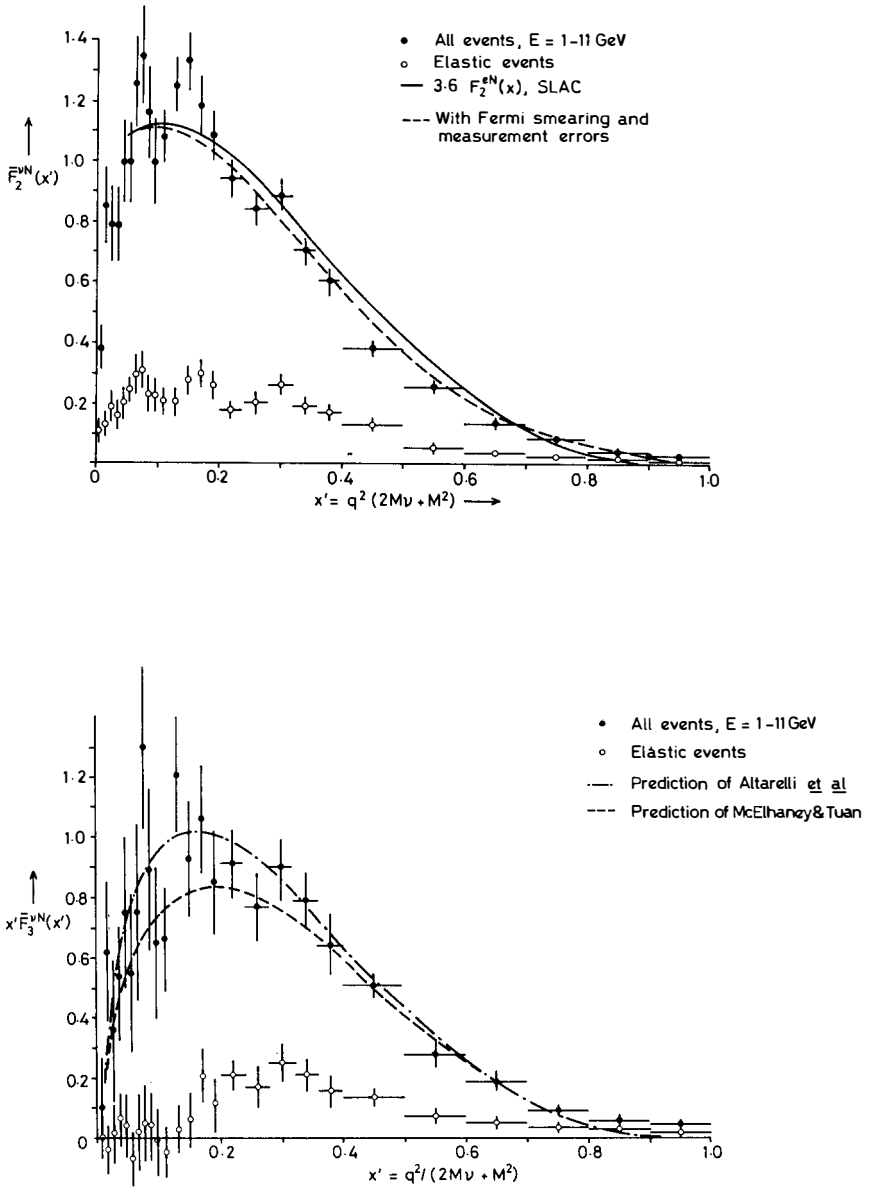
All events, E = 1-11 GeV
Elastic events
3·6 $F_2^{eN}(x)$, SLAC
With Fermi smearing and measurement errors
$\bar{F}_2^{\nu N}(x')$
$x' = q^2/(2M\nu + M^2)$
All events, E = 1-11 GeV
Elastic events
Prediction of Altarelli et al
Prediction of McElhaney & Tuan
$x'\bar{F}_3^{\nu N}(x')$
$x' = q^2/(2M\nu + M^2)$

Figure 3

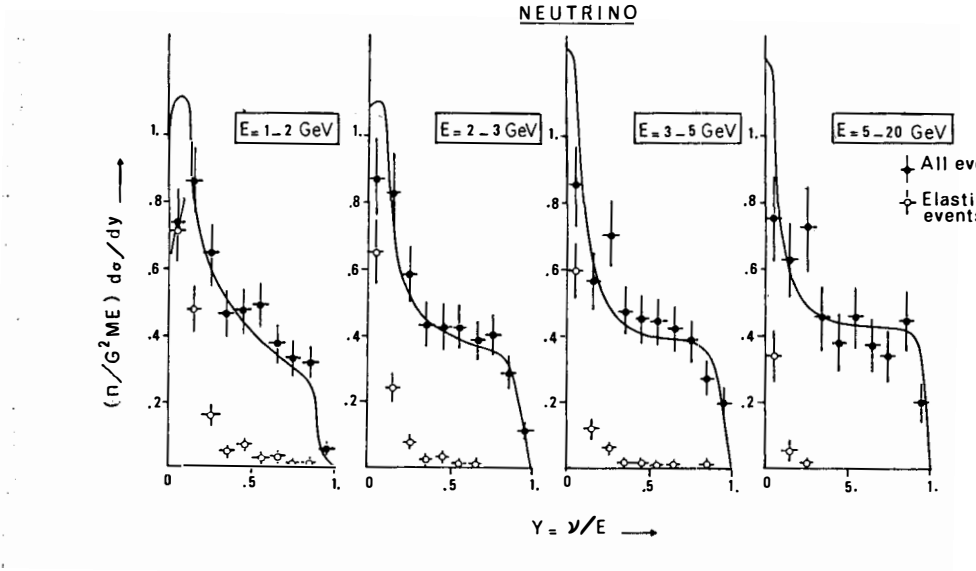
NEUTRINO
E = 1_2 GeV
E = 2_3 GeV
E = 3_5 GeV
E = 5_20 GeV
All events
Elastic events
(n/G²ME) dσ/dy
Y = ν/E

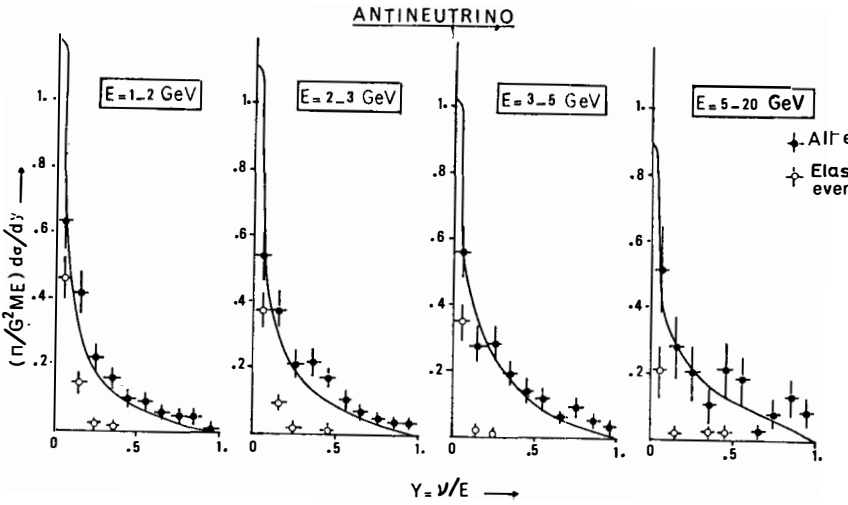
ANTINEUTRINO
E = 1_2 GeV
E = 2_3 GeV
E = 3_5 GeV
E = 5_20 GeV
All events
Elastic events
(n/G²ME) dσ/dy
Y = ν/E

Figure 4

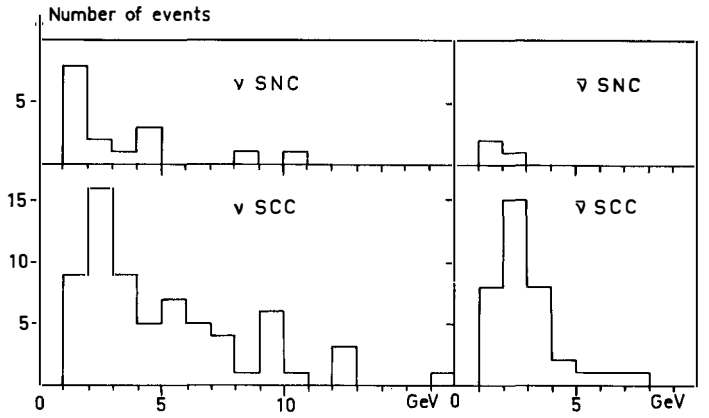

Figure 5 VISIBLE ENERGY DISTRIBUTION

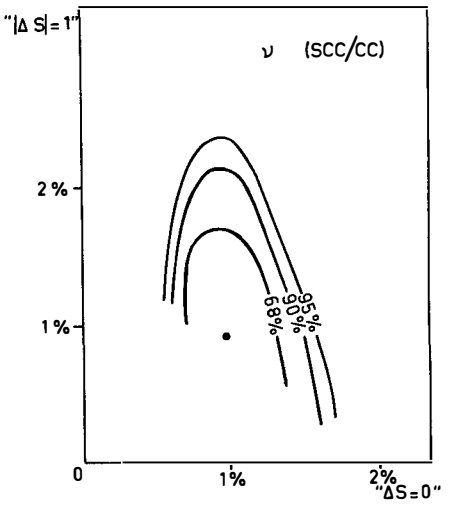

Figure 6

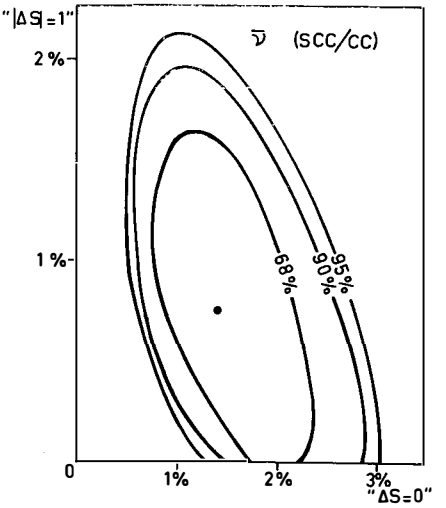

Figure 7

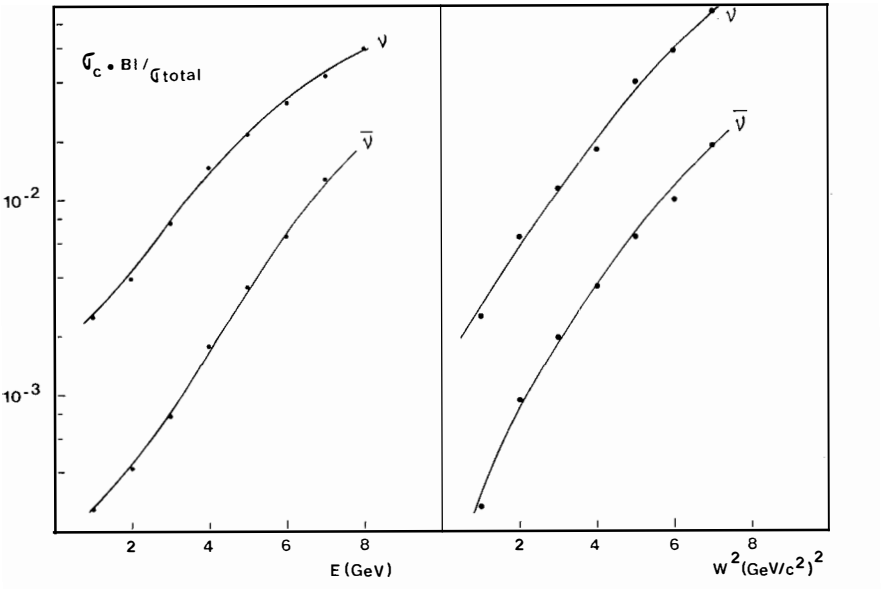

Figure 8 _ LIMITS FOR CHARMED PARTICLE PRODUCTION

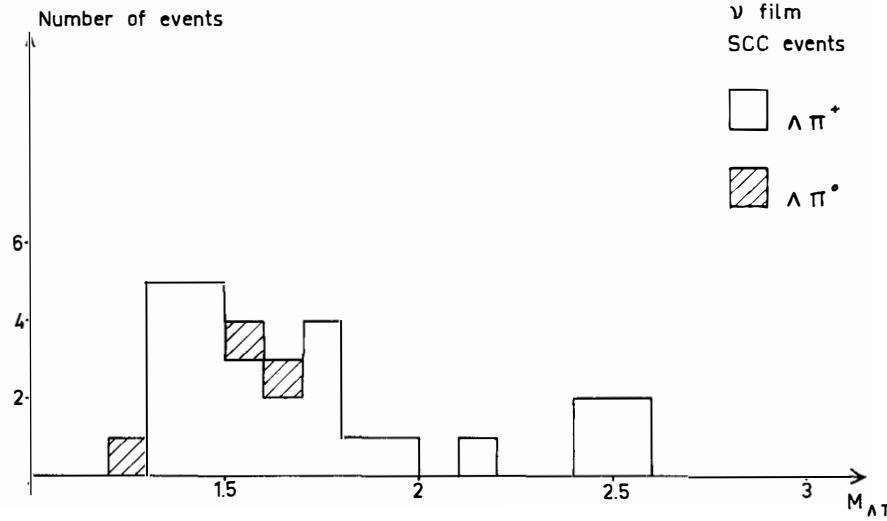

Figure 9 _ $\Lambda\pi^+$ and $\Lambda\pi^0$ mass distribution

RECENT NEUTRAL CURRENT EXPERIMENTS IN THE FERMILAB NARROW BAND BEAM

FRANK S. MERRITT
California Institute of Technology
Pasadena, California 91125 (USA)

Abstract: Neutral current measurements obtained by the Caltech-Fermilab neutrino experiment during the past year are reviewed. Preliminary results are presented from the most recent experiment, in which hadron energy distributions of neutral current events were measured in both ν and $\bar{\nu}$ narrow band beams. The measured distributions are compared to the distributions expected from V-A, V+A, and scalar or pseudoscalar couplings. Dominant S and P couplings are inconsistent with the data, as is dominant V+A. Very preliminary comparisons show no inconsistency with some combination of V-A and V+A couplings.

Résumé: On passe en revue les mesures de courants neutres obtenues l'an dernier au cours de l'expérience sur les neutrinos du Caltech-Fermilab. On présente les résultats préliminaires de l'expérience la plus récente au cours de laquelle la distribution en énergie des hadrons dans les évènements correspondant à des courants neutres a été mesurée à partir de faisceaux à bandes ètroites de neutrinos et d'antineutrinos. Les distributions mesurées sont comparées aux distributions prèvues par la thèorie des interactions scalaire, pseudoscalaire, V-A et V+A. Les couplages dominants S ou P sont incompatibles avec l'expèrience, de même que V+A. Des comparaisons très préliminaires ne montrent aucune incompatibilité dans le cas d'un mélange déterminé de couplages V+A et V-A.

Until about two years ago, the Fermi theory accounted for all the major experimental features of the weak interaction. It was known that the theory would have to be modified at high energy, but the first radical experimental disagreement with the theory came with the discovery of neutral current neutrino events.[1]

Gauge theories (in particular, the Weinberg theory[2]) have predicted that neutral current (NC) events of the kind

$$\nu(\bar{\nu}) + N \rightarrow \nu(\bar{\nu}) + \text{hadrons} \qquad (1)$$

exist in addition to the charged current (CC) interactions

$$\nu(\bar{\nu}) + N \rightarrow \mu^-(\mu^+) + \text{hadrons}. \qquad (2)$$

Both kinds of interaction are expected to show scaling behavior at high energy, and are described in terms of the scaling variables defined in Figure 1. The observed level of NC events is consistent with gauge theory predictions. However, there have been some preliminary experimental

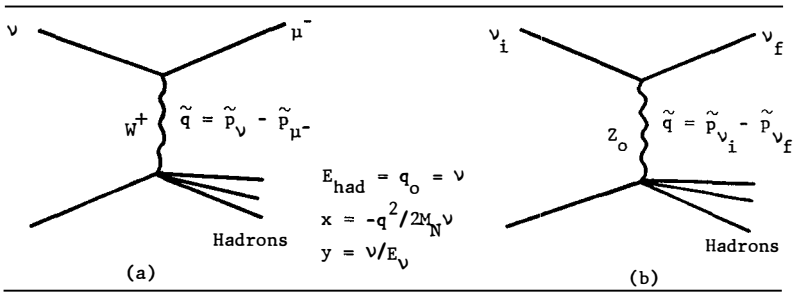

Figure 1

indications that neutral current events may not conform in detail to theoretical predictions based on V and A couplings[3], and there has been theoretical speculation[4] that neutral currents might couple through the helicity-flipping couplings scalar(S), pseudoscaler (P), and tensor (T) rather than through the helicity-conserving V and A. Such couplings would imply that the neutral current phenomenon is unrelated to the usual gauge models. Although experiments are difficult to perform and to analyze since neither the incident nor final-state lepton is directly observable, more

experimental information is clearly needed to determine the structure, as well as the magnitude, of the coupling.

The Caltech-Fermilab experiment has carried out two major runs to investigate neutral currents. The first, in February 1974, was exploratory in nature and aimed at confirming the existence of neutral currents. The results of that run have recently been published[5] and I will review it only briefly. The second run was carried out last September to measure the hadron energy distributions of NC events and to extract constraints of the possible types of coupling. The analysis of this data is still in an early stage, and I will only be presenting preliminary results.

In the first experiment, the Fermilab narrow band beam was tuned to 140 Gev to produce a neutrino spectrum composed of two energy bands centered at 45 and 125 Gev. Data was taken with both neutrino and anti-neutrino beams. A wide-band background component, coming from decays occuring before the beam was momentum selected, was separately measured by running the experiment with the momentum slit closed.

Neutrino interactions were observed in a target-calorimeter approximately 50 feet in length and 5 x 5 feet in transverse dimensions. It consisted mainly of steel plates with a liquid scintillation counter after every 10 cm of steel (1 collision length); altogether, there were 70 counters and 140 tons of steel. When a neutrino interacted in the steel, the resulting hadron shower typically penetrated through 4 to 14 counters, depending on the energy of the shower. The signals from the counters were summed to measure the total energy of the shower. The resolution in hadron energy varied approximately as $1/\sqrt{E_{had}}$, and ranged from $\sim 10\%$ at 150 Gev to $\sim 35\%$ at 12 Gev. A spark chamber was placed after every second counter to measure the transverse position of the interaction and to track the final-state muon produced in CC events.

The apparatus was triggered by a total measured energy deposition in the calorimeter of $\gtrsim$ 6 Gev, in coincidence with a penetration of charged particles through at least 2 - 4 counters. All good events were further

required to have a vertex at least five inches from the edges of the apparatus.

Charged current events are characterized by the presence of a very penetrating particle (the muon) in the final state. NC events were distinguished from CC events, then, by their penetration P, defined as the number of collision lengths of steel (measured by the counters) traversed by the most penetrating charged particle produced in the interaction. Since the final-state neutrinos in NC events give no signal, the penetration for such events is just the range of the hadron shower and was generally $\leq$ 10-12 counters. For CC events, P was generally the distance travelled by the muon before it left the apparatus through the sides or end (relatively few muons actually ranged out in the apparatus).

Neutral currents, therefore, should appear as an excess of events in the short-penetration region $P < 14$. Figures (2a) and (2b) are the experimental distributions in penetration for ν and $\bar{\nu}$ events, respectively[6]. The smooth curves, normalized to all events with $P \geq 14$, represent the distributions expected from CC events alone. The excess of the data over the curve in the large peaks centered at $P = 9$ is interpreted as a neutral current signal.

Backgrounds due to cosmic rays, electron neutrinos, and neutrons were small[5]. The only major background source was from CC events with wide-angle muons (and hence short penetration). The extrapolation of the penetration curves for CC events shown in Figure 2 is based on a Monte-Carlo which uses the measured narrow band spectrum and assumes Bjorken scaling, the SLAC nucleon structure functions, and a V-A coupling with negligible antiquark component in the nucleon. These assumptions are consistent with previous measurements of CC data[6]. The extrapolation from large P to small P is not sensitive to deviations from these assumptions, so long as the deviations don't violate existing CC data.

In fact, conservation of energy and momentum requires that wide-

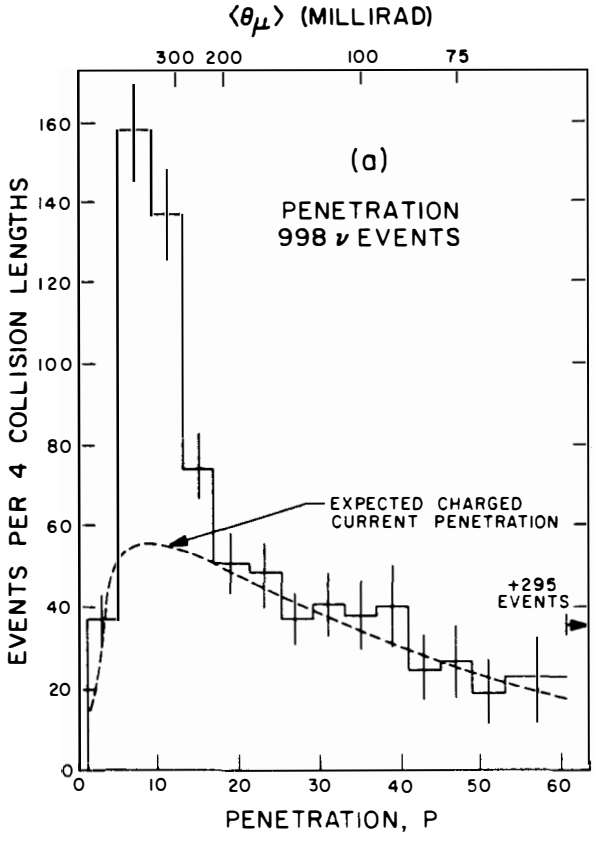
⟨θμ⟩ (MILLIRAD)
300 200 100 75
(a)
PENETRATION
998 ν EVENTS
EXPECTED CHARGED
CURRENT PENETRATION
+295
EVENTS
EVENTS PER 4 COLLISION LENGTHS
PENETRATION, P

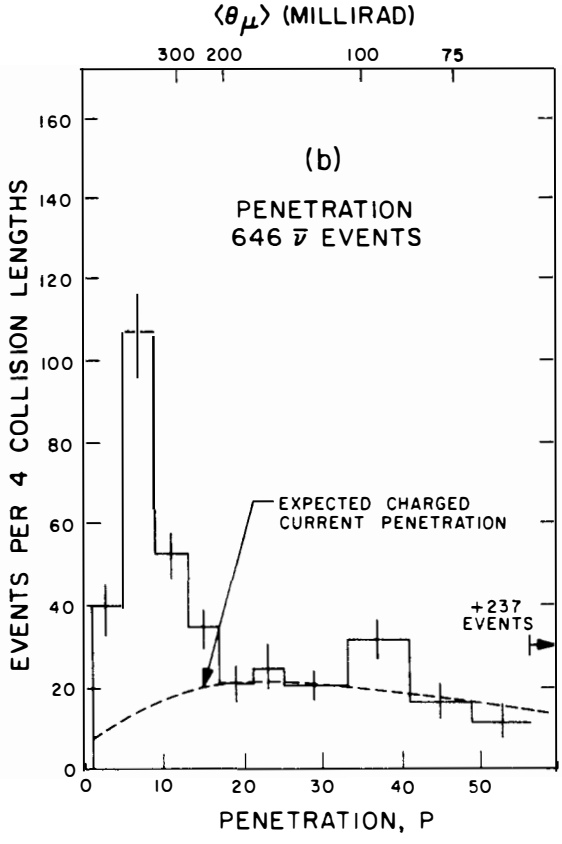
⟨θμ⟩ (MILLIRAD)
300 200 100 75
(b)
PENETRATION
646 ν̄ EVENTS
EXPECTED CHARGED
CURRENT PENETRATION
+237
EVENTS
EVENTS PER 4 COLLISION LENGTHS
PENETRATION, P

FIGURE (3)

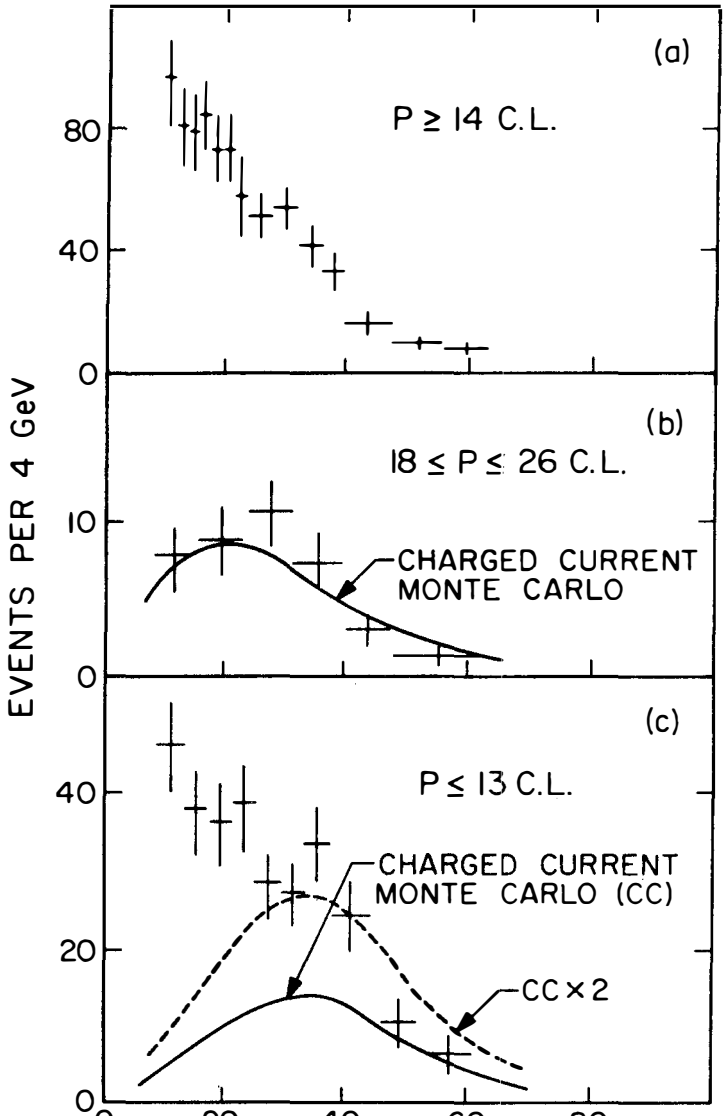

(DATA FROM FEBRUARY, 1974)

angle muons cannot have very high energy, since the hadron shower must have enough energy to balance transverse and longitudinal momentum. For example, a 50 Gev interaction with $\theta_\mu \geq 200$ mrad must have $E_{had} \geq 25$ Gev. This means that $\langle E_{had} \rangle$ should increase as we move from the large P region (small θ) to the small P region (large θ), as illustrated by the E_{had} distributions of CC events in Figures (3a) and (3b). As we move down from the intermediate P region of Figure (3b) to the short-penetration region of Figure (3c), the E_{had} distribution should continue to shift upward in energy as indicated by the Monte-Carlo curve. But the hadron energy distribution of the data, in fact, looks similar to the CC data of Figure (3a), and not at all like the CC background curve in Figure (3c).

The low-energy events in the short-P region cannot be due to high-energy CC events, therefore, and since the experiment was performed in a narrow band beam the number of low-energy neutrinos is much too small to account for them. They also, of course, can't be $\nu + N \rightarrow$ hadrons, since the hadron energy would then have to equal the beam energy. In fact, the existence of these low-energy, short-length events shows that unobserved energy is being transported out of the steel apparatus, and strongly indicates the presence of a non-interacting neutral particle in the final state, as expected from interaction (1).

To obtain the ratios $\sigma_{NC}^{\nu,\bar{\nu}}/\sigma_{CC}^{\nu,\bar{\nu}}$, it is necessary to extrapolate the measured NC hadron energy distributions to $E_{had} = 0$. However, the shape of the $\frac{d\sigma}{\sigma y}$ distribution strongly affects the result of this extrapolation. The unextrapolated ratios we obtained were .22 for ν and .33 for $\bar{\nu}$, but the extrapolated ratios could differ by nearly a factor of 2 depending on the $d\sigma/dy$ shape assumed.

But of equal importance with the actual magnitude of the neutral current cross-section is the question of the structure of the neutral current coupling. If we assume scaling of the hadron vertex and for the moment ignore possible propagator effects due to a low mass Z_0, then the most general form for the NC differential cross-section is

$$\left(\frac{d\sigma}{dy}\right)^{\nu}_{NC} = \frac{G^2 M E}{\pi}\left[\alpha + \beta(1-y)^2 + \gamma y^2\right]$$

$$\left(\frac{d\sigma}{dy}\right)^{\bar{\nu}}_{NC} = \frac{G^2 M E}{\pi}\left[\beta + \alpha(1-y)^2 + \gamma y^2\right] \quad . \tag{4}$$

(This relation between ν and $\bar{\nu}$ cross-sections does not depend on charge symmetry arguments, but only on the hermiticity of the neutral current.) If the coupling is V-A (as for CC interactions), then the α term will dominate for both ν and $\bar{\nu}$ interactions, with perhaps a small admixture of β. If the coupling is V+A, then the β term will dominate, with perhaps a small admixture of α (in the parton model, these small admixtures correspond to scattering off antipartons). On the other hand, a dominant S or P coupling would produce a γ, or y^2, distribution for both ν and $\bar{\nu}$.[4,7] In general, it is not possible to determine the coupling uniquely from the y-distribution alone. In fact, a combination of the helicity flipping couplings P,S, and T can conspire in such a way as to mimic any combination of V and A. However, it is possible to see if the y distributions are consistent with the α and β distributions expected from V and A; if any positive γ component is observed the helicity-flipping components P,S, or T are involved.

Since $E_{had} = y \cdot E_{\nu}$, these different y distributions will produce correspondingly different E_{had} distributions in a narrow band beam. In order to exploit the advantages of this beam, we carried out the second run in September to measure the E_{had} distributions of NC events, and so to obtain constraints on NC coupling schemes and to better measure the $\sigma_{NC}^{\nu,\bar{\nu}}/\sigma_{CC}^{\nu,\bar{\nu}}$ ratios.

In preparation for this run, we made several changes in the apparatus and beam. Since E_{had} is the only kinematical variable measured in NC interactions, we made extensive studies of the calibration and resolution of the target-calorimeter using a scaled-down test calorimeter. An improved monitoring system was set up to systematically monitor the

counters during the run. To reduce the possibility of bias against very low-penetration NC events, the trigger was altered to require a minimal penetration of only 2 counters (this necessitated a slight increase in the trigger threshold to avoid increasing the cosmic ray trigger rate).

To better measure the wide-band background component in the beam, we ran for a considerable time with the momentum slit closed. The distributions measured during this closed-slit running were normalized to the open-slit running and subtracted from the open-slit distributions. This eliminated low-energy events (both CC and NC), so the resulting distributions reflect a pure narrow band spectrum.

The efficiency for detecting the muon produced in CC events is better for high-energy events, and the relative resolution in measured hadron energy is also better. We therefore ran the hadron beam at 170 Gev, somewhat higher than in the preceeding run. To further enhance the relative number of high-energy events, we steered the beam away from the center of the apparatus during part of the running. Since the pion neutrinos (~ 50 Gev) are much more collimated than the kaon neutrinos (~ 150 Gev), this decreased the size of the low-energy band without substantially affecting the high-energy band.

In analyzing the data, we have applied a fiducial cut on the vertex of all interactions and only used events with a total energy deposition in the calorimeter of $E_{had} \geq 12$ Gev. Cosmic ray and wide-band backgrounds were measured during the run and have already been substracted from all distributions.

Figure 4 shows the penetration curve obtained for neutrino events (both CC and NC), and again the NC peak is evident. To extract the hadron energy distribution of the NC events we have divided the data into two penetration regions, $P \leq 14$ counters and $P > 14$, and have plotted the E_{had} distributions in Figures (5a) and (5b). The high-penetration region (Figure (5a)) contains most of the CC events, while the low-P region

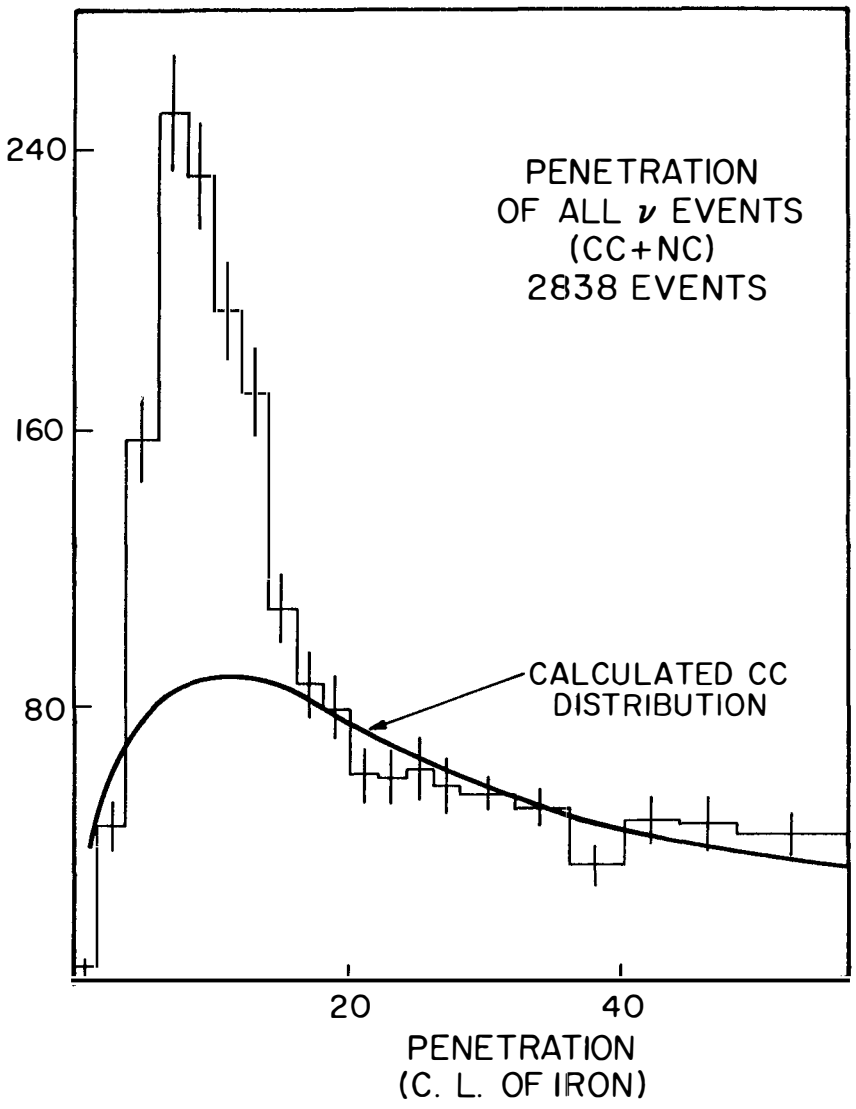
240
160
80
PENETRATION
OF ALL ν EVENTS
(CC+NC)
2838 EVENTS
CALCULATED CC
DISTRIBUTION
20
40
PENETRATION
(C. L. OF IRON)

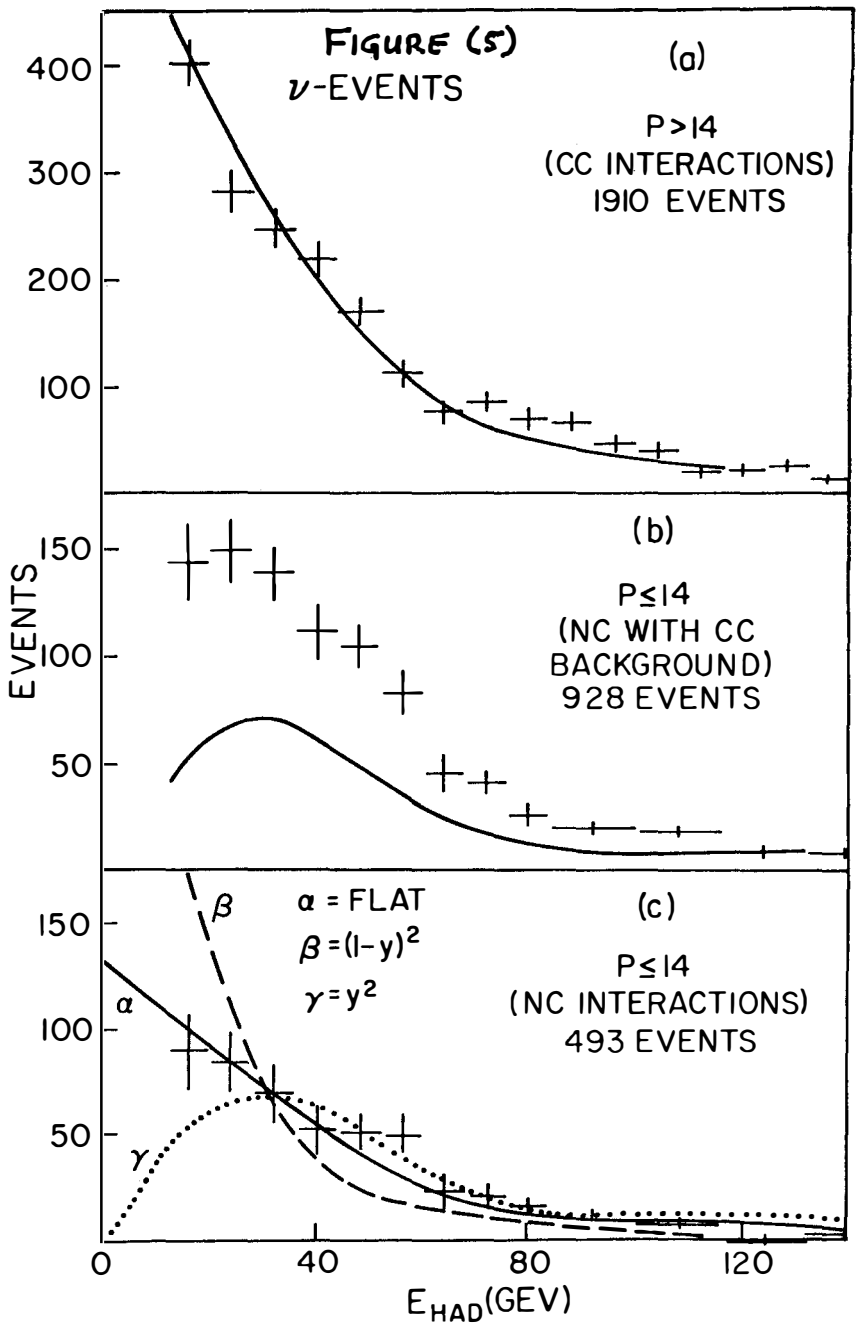
FIGURE (5)
ν-EVENTS
(a)
P>14
(CC INTERACTIONS)
1910 EVENTS
(b)
P≤14
(NC WITH CC
BACKGROUND)
928 EVENTS
(c)
P≤14
(NC INTERACTIONS)
493 EVENTS
α = FLAT
β = (1-y)²
γ = y²
α
β
γ
EVENTS
400
300
200
100
150
100
50
150
100
50
0
40
80
120
E_HAD(GEV)

(Figure (5b)) contains essentially all the NC events plus CC events with wide-angle muons. The smooth curves in both figures are the calculated distributions expected from CC events.

In Figure (5c) we have subtracted the calculated CC curve in Figure (5b) from the short-P data in that figure to obtain the NC hadron energy distribution. The three curves shown are the distributions calculated for $\frac{d\sigma}{dy}$ = flat, $(1-y)^2$, and y^2, corresponding to the α, β, and γ components for neutrinos in Equation (3). All three curves are normalized to the data above E_{had} = 12 Gev. The flat y distribution (α) looks most like the data.

The types of coupling can more easily be distinguished when correlations in magnitude, as well as shape, of the neutrino and antineutrino NC signals are considered. Equation (3) allows us to predict both the shape and magnitude of the $\bar{\nu}$ NC distributions corresponding to the shape and magnitude of the three curves fitted to the ν data in Figure (5c). For example, if an α distribution is assumed, Equation (3) integrated over y shows that the total number of $\bar{\nu}$ NC events should be 1/3 the number of ν NC events (for equal ν and $\bar{\nu}$ fluxes). But if a β distribution is assumed, there should be 3 times as many $\bar{\nu}$ as ν NC events. The measured number of CC events recorded in the ν and $\bar{\nu}$ runs, together with the previously measured CC total cross-sections,[6] gives the relative normalization of the ν and $\bar{\nu}$ fluxes.

The three curves predicted in this manner from the α, β, γ curves of Figure (5c) are compared to the E_{had} distributions of $\bar{\nu}$ NC events in Figure (6). A dominant γ distribution is clearly inconsistent with the data, as is dominant β; a combination of α and β (with more α than β) will fit the data. We cannot, of course, rule out the presence of some γ component. We can conclude at this point, however, that we are not consistent with dominant scalar and pseudoscalar couplings, but are consistent with a combination of V and A.

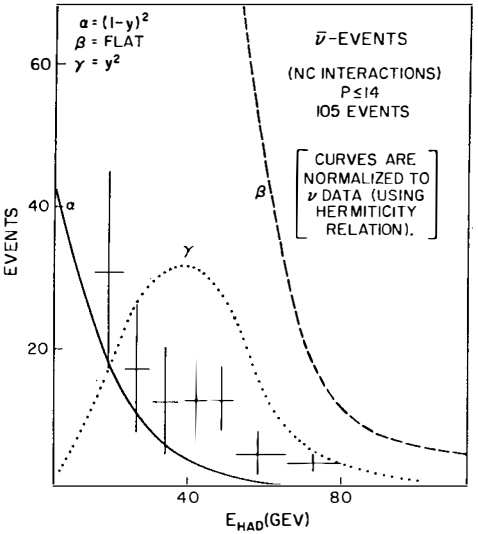

FIGURE 6

The calculation of the total cross-section ratios $R_{\nu,\bar{\nu}} = \sigma_{NC}^{\nu,\bar{\nu}}/\sigma_{CC}^{\nu,\bar{\nu}}$ depends strongly on the shape assumed for the E_{had} distributions, since the fitted curves must be extrapolated below the cut at E_{had} = 12 Gev. The table below lists the "raw" unextrapolated ratios obtained by assuming each of the three shapes considered. The top line uses the α, β, γ distributions normalized to the ν NC data to obtain extrapolated values of R_ν; the second line gives the corresponding ratios for $\bar{\nu}$ (normalized to the $\bar{\nu}$ data), and the third line gives, for comparison, the values predicted from the corresponding R_ν and equation (3). The predicted value is low if pure α is assumed and very high

	"Raw"	Extrapolated		
	$E_{had} \geq 12$	Pure α	Pure β	Pure γ
R_ν	.21	.23	.37	.18
$R_{\bar{\nu}}$	.43	.50	.31	.24
$R_{\bar{\nu}}$ (predicted)		.23	3.33	.54

if pure β is assumed. If the coupling is in fact a combination of V-A and V+A, the actual values of $R_{\nu,\bar{\nu}}$ should lie between the limits of pure α and pure β given in the table (probably closer to α than to β). This range of values is in general agreement with the Gargamelle ratios of $R_\nu = .22 \pm .03$ and $R_{\bar{\nu}} = .43 \pm .12$,[8] and is also consistent with the predictions of the Weinberg model.

Our conclusions at this stage are more qualitative than

quantitative, however, and several sources of possible error must be studied before a meaningful fit can be made to the values of α, β, and γ that best represent the data. For example, we have assumed in the calculation that CC events couple through pure V-A with no antiquark component in the nucleon. If this assumption is relaxed, both the subtraction of CC events in the low-penetration region and the extrapolation of the E_{had} distributions to low hadron energy are altered, and the $R_{\bar{\nu}}$ ratios can be increased by as much as 20% of the values listed above (the effect on R_{ν} is much smaller). The CC interactions must be studied in greater detail to determine how much antiquark component can be tolerated and to check the extrapolation in E_{had}.

Another effect that must be investigated is the possible energy dependence of the NC total cross-section. This analysis has assumed a linearly rising cross-section for neutral currents, and the agreement between the $R_{\nu,\bar{\nu}}$ range indicated by the table and the Gargamelle measurements provides some support for this assumption. To make an independent measurement of the energy dependence, we have steered the beam at different angles relative to the apparatus, thereby varying the relative sizes of the low-energy and high-energy bands. By comparing the NC/CC ratios at different steering angles and by studying how the E_{had} distributions change as a function of angle, we hope to obtain a better measure of the E_{ν} dependence and perhaps to better measure the shape of the y distributions.

The analysis is still in a fairly early stage, then, and several corrections will need to be made. Our most important conclusion at this point is that strongly dominant scalar and pseudoscalar (and also V+A) couplings do not agree with the data. This effect is too large to be substantially affected by future corrections.

References

1. J. F. Hasert, et.al., Phys. Lett. 46B, 138 (1973);
   A. Benueneuti, et.al., Phys. Rev. Lett. 32, 800 (1974);
   B. Aubert, et.al., Phys. Rev. Lett. 32, 1454 and 1457 (1974);
   S. J. Barish, et.al., Phys. Rev. Lett. 33, 448 (1974).
2. S. Weinberg, Phys. Rev. Lett. 19, 1264 (1967) and 27, 1683 (1972).
   A. Salam and J. C. Ward, Phys. Lett. 13, 168 (1964).
3. In particular, preliminary data on threshold pion production by neutral currents (P. Schreiner, XVII Int'l. Conf. on High Energy Physics, London 1974, IV-123) has resulted in speculations that neutral currents may have S, P, or T couplings (S. L. Adler, Phys. Rev. Lett. 33, 1511 (1974)). Very recent results reported by that experiment seem to conform more to V, A expectations.
4. B. Kayser, et.al., Phys. Lett. 52B, 385 (1974); R. L. Kingsley, F. Wilczek, A. Zee, Phys. Rev. D10, 2216 (1974).
5. B. C. Barish, et.al., Phys. Rev. Lett. 34, 538 (1975).
6. F. Sciulli, XVII Int'l. Conf. on High Energy Physics, London, 1974, IV-105.
7. T. Curtright, private communication.
8. A. Pullia, XVII Int;1. Conf. on High Energy Physics, London, 1974, IV-114.

Neutral Currents in Semileptonic Reactions

Emmanuel A. Paschos

Brookhaven National Laboratory, Upton, New York 11973

ABSTRACT

The evidence for weak neutral currents is analysed in semileptonic reactions with special emphasis in their Lorentz and internal symmetry structure. It is found that present observations are consistent with the expectations of gauge theories, but other possibilities can not be ruled out. Of particular interest in this respect is the presence of a large isoscalar component. The excitation of the Δ-resonance by neutral currents is analysed and pion-nucleon mass distributions are presented. Charge asymmetries sensitive to isoscalar-isovector interferences are discussed.

RESUME

L'évidence pour des courants neutres faibles est analysé dans des réactions semi-leptoniques en soulignant leur structure de Lorentz et en symétrie interne. On trouve que les observations actuelles sont compatibles avec ce qu'on attend des théories de gauge, mais on ne peut éliminer d'autres possibilités. La présence d'une grande composante isoscalaire est d'un intérêt particulier à ce propos. L'excitation de la résonance Δ par des courants neutres est analysée et on présente des distributions de masse pion-nucléon. On discute des asymétries de charge sensibles aux interférences isoscalaire-isovecteur.

INTRODUCTION

The revived interest in neutral currents arose with the possibility of constructing a renormalizable theory[1] of weak interactions. This interest was further enhanced by their discovery[2,3] and subsequent confirmation in numerous neutrino experiments.[4-7] The present activity is partly motivated by the implications that this discovery has for other problems of high energy physics. It is believed that neutral currents play a crucial role in developing a finite and unified gauge theory of weak and electromagnetic interactions. It is also believed that they are intimately connected with the existence of new quantum numbers and consequently new hadronic states. The arguments leading to such conclusions have been discussed elsewhere and we review them very briefly.

In gauge theories the bad high energy behavior of tree graphs must be cancelled by other graphs. For example, to lowest order in perturbation theory the cross section for the production of zero helicity W's in processes like

$$\nu + \bar{\nu} \rightarrow W^+ + W^-$$

$$e + \bar{e} \rightarrow W^+ + W^-$$

grows with the square of the c.m. energy and violates unitarity. Unitarity is restored by introducing other graphs whose role is to cancel the bad high energy behavior. The new graphs have either s-channel poles, which require neutral currents, or t-channel poles, which require heavy leptons.

The extension of these arguments to semileptonic reactions must satisfy additional constraints. It is observed that

$$\frac{K^+ \rightarrow \pi^+ e^+ e^-}{K^+ \rightarrow \mu^+ \nu} = (5 \pm 2) \times 10^{-6} \qquad (1)$$

$$\frac{K_L \rightarrow \mu^+ \mu^-}{K^+ \rightarrow \mu^+ \nu} \leq 8 \cdot 10^{-9} \qquad (2)$$

which imply that strangness changing neutral currents are greatly suppressed[8] (at least at low energies). To account for this suppression, but still

allow for $\Delta S = 0$ neutral currents, several schemes have been devised which invariably introduce new quantum numbers. They, in turn, require a new stratum of hadronic states carrying new quantum numbers. An elegant solution by Glashow, Iliopoulos and Maiani[9] introduces a fourth quark carrying charm. In this scheme, there are two left handed multiplets

$$\psi_1 = \begin{pmatrix} p \\ n_c \end{pmatrix} \quad , \quad \psi_2 = \begin{pmatrix} p' \\ \lambda_c \end{pmatrix} \tag{3}$$

where $n_c = n\cos\theta_c + \lambda\sin\theta_c$, $\lambda_c = -n\sin\theta_c + \lambda\cos\theta_c$, p, n, λ are the conventional quarks and p' is a new quark carrying charm. The neutral current operator is

$$J_\mu = \text{const.}\ \bar{\psi}_L\ \gamma_\mu(T_3 - Q\sin^2\theta_W)\psi_L \tag{4}$$

with T_3 being the third component of the isospin operator, Q the charge operator and $\sin\theta_W$ a mixing parameter. To lowest order the scheme gives only $\Delta S = 0$ neutral currents. In higher orders it suppresses induced $\Delta S = 1$ and 2 neutral current effects. The model also leads to a rich phenomenology which is now enjoying a good deal of attention since experiment is close to providing decisive tests.

Of basic importance to the above topics is the existence and nature of neutral currents. The first issue, concerning their existence, has been settled by the overwhelming evidence shown in Tables I and II. The next issue concerns their nature. To be precise, we would like to know

(α) The Lorentz structure of neutral currents. Are they vector and axial or scalar, pseudoscalar and/or tensor?

(β) The internal symmetry structure. Do they have components which can be classified within SU(3) or are there also new components?

In dealing with these issues we are fortunate because there are two separate kinematic regions where we know a good deal about the charged-weak and electromagnetic matrix elements. In the deep inelastic region we have a scaling law and an explicit parton model both of which have been success-

ful in interpreting experiments. This region provides information concerning the Lorentz structure. In the low energy region, on the other hand, there is the $\Delta(1236)$ resonance, whose excitation by conventional currents is well understood. Consequently, a detailed study of its excitation by neutral currents might provide relevant information concerning their isospin structure.

In the next few sections we study properties of the neutral currents with emphasis on their space-time and isospin structure.

SPACE-TIME STRUCTURE OF CURRENTS

The general local neutral current interaction between neutrinos and hadrons assuming T-invariance and left-handed incident neutrinos has the form

$$\mathcal{L} = \frac{G}{(2)^{\frac{1}{2}}} \left\{ \bar{\nu}\gamma_\mu(1-\gamma_5)\nu(V^\mu+A^\mu) + \bar{\nu}(1-\gamma_5)\nu\, S + i\bar{\nu}\gamma_5(1-\gamma_5)\nu P \right.$$
$$\left. + \bar{\nu}\,\sigma_{\mu\lambda}(1-\gamma_5)\nu T^{\mu\lambda} \right\} \qquad (5)$$

where $S,P,V^\mu,A^\mu,T^{\mu\lambda}$ are scalar, pseudoscalar, vector, axial-vector and tensor hadronic currents. They are hermitean and have a general internal symmetry structure which is not shown explicitly. G is the Fermi coupling constant. In calculating cross sections we observe that there are no interference terms between the (V,A) and (S,P,T) interactions because the former do not flip the neutrino helicities, while (S,P,T) couplings do so. We can thus discuss separately the contributions from the two classes and look for differences which can distinguish between them. One obviously can discuss specific channels, but the inclusive reactions on matter

$$\nu(\bar{\nu}) + N \rightarrow \nu(\bar{\nu}) + X \qquad (6)$$

are the easiest to be measured and we concentrate on them. It is also convenient to extend the Bjorken scaling phenomenon to the (S,P,T) currents and obtain the double differential cross section in the scaling limit

$$\frac{d\sigma^{\nu,\bar{\nu}}}{dxdy} = \frac{G^2 ME}{\pi}\left\{xy^2[F_{ss}+F_{pp}] \pm 4xy(2-y)[F_{ST}+F_{PT}]\right.$$
$$\left. + 4[x(2-y)^2 F_{TT}^{1} + 4(1-y)F_{TT}^{2} - 2x^2y^2F_{TT}^{3} + 2xy^2F_{TT}^{4}]\right\} \qquad (7)$$

Here $x = Q^2/2M\nu$, $y = \nu/E$ and $F_{ij}^{\alpha} = F_{ij}^{\alpha}(x)$ are the scaling limits of the structure functions bilinear in the currents i and j and the superscipt α is used in order to distinguish the different contributions of the tensor terms. For comparison we give the corresponding cross section for the (V,A) combination

$$\frac{d\sigma^{\nu,\bar{\nu}}}{dxdy} = \frac{G^2 ME}{\pi}\left\{(1-y)\bar{F}_2 + \frac{1}{2}y^2[2x\bar{F}_1] \mp y(1-\tfrac{1}{2}y)[x\bar{F}_3]\right\} \qquad (8)$$

where the superscript bar emphasizes that we allow for an arbitrary admixture of V and A currents.

Remarks: 1) In the absence of T-couplings and for any admixture of S- and P-couplings[11,12]

$$\frac{d\sigma^{\nu}}{dy} = \frac{d\sigma^{\bar{\nu}}}{dy} = \frac{G^2 ME}{\pi} y^2 \int_0^1 x\,[F_{SS}(x) + F_{pp}(x)]dx \qquad (9)$$

The rise of the cross sections with y^2 is a unique signature of S and P interactions. The results presented by the CIT-FNAL group[13] indicate that this possibility is already ruled out. The equality of the two cross sections is another testable property. Table I gives the world's compilation of data on inclusive neutral current reactions.[14] The Gargamelle data give

$$\frac{\sigma_{NC}^{\nu}}{\sigma_{CC}^{\nu}} = 0.22 \pm 0.03 \quad \text{and} \quad \frac{\sigma_{NC}^{\bar{\nu}}}{\sigma_{CC}^{\nu}} = 0.14 \pm 0.04 \qquad (10)$$

which within two standard deviations are consistent to being equal. The ratios from the HPWF-collaboration are also consistent with equal ν and $\bar{\nu}$ neutral current cross sections. It is important to determine this number precisely, because it is also relevant to the presence of a V-A interference term.

Table I - Neutral Current Measurements for Total Cross-Sections

Ratio	Experiment	Energy Range	Group
$\frac{\sigma(\nu N \to \nu x')}{\sigma(\nu N \to \mu^- x'')}$	0.217 ± 0.026	1-10 GeV	Gargamelle[2]
	0.11 ± 0.05	5-150 GeV	HPW-FNAL[3]
	$0.22 \pm$	$E_\pi \approx 38$ GeV $E_K \approx 108$ GeV	CIT-FNAL[5]
	0.20 ± 0.06	1-10 GeV	BNL[7]
$\frac{\sigma(\bar{\nu} N \to \bar{\nu} x)}{\sigma(\bar{\nu} N \to \mu^+ x')}$	0.43 ± 0.12	1-10 GeV	Gargamelle[2]
	0.32 ± 0.09	5-150 GeV	HPW-FNAL[3]
	$0.33 \pm$	$E_\pi \approx 38$ GeV $E_K \approx 108$ GeV	CIT-FNAL[5]

2) $$\frac{1}{E}\left(\frac{d\sigma^{\nu}}{dy} - \frac{d\sigma^{\bar{\nu}}}{dy}\right) \propto y(1-\tfrac{1}{2}y) \qquad (11)$$

the y dependence is identical for the two classes of couplings.

3) Theorem[11]: For any admixture of V and A there is a corresponding admixture of S, P and/or T which yields the same y-distributions for reactions (6).

The proof follows by looking at Eqs. (7) and (8), because (V,A) gives at most a quadratic distribution in y. From (7) we see that we obtain again at most quadratic terms with enough arbitrary coefficients to imitate the (V,A) y-distribution (remark (2) is also relevant). The theorem implies that it is difficult to distinguish (S,P,T) and (V,A). Extensive studies of this issue indicate that in order to separate the interactions one needs precise and difficult experiments of exclusive channels or the observation of neutral currents in electron-positron experiments.

I have gone into some detail in discussing the presence of S,P,T couplings for neutrinos because their existence will have some important consequences. Their existence means that there are two new states: a

right-handed neutrino and a left-handed antineutrino; that the multiplet structure is more complicated and that gauge Yang-Mills theories do not provide a complete picture. Keeping all this in mind, it is still useful to proceed and analyze the data in terms of the (V,A) possibility[14] looking for deviations which can reveal new components or confirm the theoretical expectations and thus provide additional support for the gauge theories.

ISOVECTOR COMPONENTS

In analogy with the effective current-current interaction for charged currents, we write an effective neutral current interaction

$$\mathcal{L} = \frac{G}{(2)^{\frac{1}{2}}} \; J_\lambda J^\lambda \tag{12}$$

where J_λ is a hermitean neutral current of the form

$$J_\lambda = \bar{\nu}_e \gamma_\lambda (1-\gamma_5)\nu_e + \bar{e}\gamma_\lambda(v_e + a_e\gamma_5)e + \{^{e \to \mu}_{\nu_e \to \nu_\mu}\}$$

$$+ v_3 V_\lambda^{\,3} + a_3 A_\lambda^{\,3} + v_0 V_\lambda^{\,0} + a_0 A_\lambda^{\,0} + \sin\theta_c [v_6 V_\lambda^{\,6} + a_6 A_\lambda^{\,6} + v_7 V_\lambda^{\,7} + a_7 A_\lambda^{\,7}] \tag{13}$$

The underlying assumption is that the hadronic neutral current components transform like an octet representation of SU(3) plus an SU(3) singlet. The superscripts indicate the particular SU(3) assignments. In general, the couplings $V_\lambda^{\,7}$ and $A_\lambda^{\,7}$ to other currents lead to CP violation[8] and will be omitted. The suppression of K decays in Eq. (1) and (2) suggest that v_6 and a_6 are very small so we set them equal to zero. The remaining currents are representative of a large number of the possibilities discussed in the literature. We mention three distinct examples. (1) In the Weinberg-Salam model[15] $a_3 = 1$, $v_3 = 1-2\sin^2\theta_w$. Both $v_0 \neq 0$ and $a_0 \neq 0$ in the extension of the model that incorporates strange particles.
(2) In the model of Beg and Zee[16] the neutral current is proportional to the electromagnetic current ($a_3 = a_0 = 0$).

(3) In Sakurai's[17] model $a_3 = v_3 = 0$. The current is an SU(3) singlet with the vector part identified as the baryonic current and it may also have a chiral (axial) partner ($v_0 \neq 0$, maybe $a_0 \neq 0$). There are numerous other models but their enumeration is beyond the scope of these lectures.

Concerning the isovector components the problem is now reduced to the determination of the parameters v_3 and a_3. There are two general theorems[18] which are helpful in this respect.

Theorem II. Consider the cross sections

$$\Sigma^0 = \sigma(\nu p \to \nu x_1) + \sigma(\nu n \to \nu x_2)$$
$$\Sigma^+ = \sigma(\nu p \to \mu^- x_3) + \sigma(\nu n \to \mu^- x_4) \qquad (14)$$

with the corresponding cross sections for antineutrinos denoted by $\bar{\Sigma}^0$ and Σ^-. Let x_i refer to the sum of all final states or a subset of states, subject only to the requirement that a sum over all possible charge configurations has been performed,

THEN $$R_I = \frac{\Sigma^0+\bar{\Sigma}^0}{\Sigma^++\Sigma^-} \geq \frac{1}{2}\,\frac{v_3^2 V + a_3^2 A}{V+A} \qquad (15)$$

where V(A) is the contribution of V_λ^3 (A_λ^3) alone to the cross section.

In applying the results to the total cross sections we can appeal to the experimental observation that

$$V \approx A$$

and obtain

$$R_I \geq \tfrac{1}{4}(v_3^2 + a_3^2) \qquad (16)$$

R_I can be evaluated from Table 1 giving

$$0.27 \pm 0.09 \geq R_I \text{ to 90\% confidence level.} \qquad (17)$$

The main conclusion is that the V_λ^3 on A_λ^3 couplings cannot be maximal ($|v_3| = |a_3| = 1$). This is shown graphically in Fig. 1 where the interior of the large circle is the allowed physical region.

Theorem III[19] : Under the same assumptions of theorem II

$$R_{II} = \frac{\Sigma^0 - \bar{\Sigma}^0}{\Sigma^+ - \Sigma^-} = \frac{1}{2} v_3 a_3 + \frac{1}{2} v_0 a_0 \frac{\sigma_I^0}{\sigma_I^+} \qquad (18)$$

where σ_I^0 (σ_I^+) is the contribution to the cross section arising from the V-A interference term of the isoscalar (charged) current.

We could calculate R_{II} from Table 1, but the errors are so large that Eq. (18) is not very restrictive. To demonstrate the restrictions implied by the theorem we consider the central values given by the experiments. Neglecting the isoscalar term, the Gargamelle results give the hyperbola H shown in Fig. 1. For the HPWF experiment the hyperbola degenerates into the two axes and implies that neutral currents are only vector or only axial.

Further restrictions are obtained by appealing to Schwartz's inequalities for the isovector and isoscalar currents. For the Gargamelle data the physical region is constrained to lie within the octagon ABCD, which looks very much like a rectangle.[20] The HPWF experiment gives a different region but it too premature to take two standard deviations very seriously, because the experimental values require further refinements.

To sum up, for any arbitrary isoscalar current v_3 and a_3 cannot be maximal. For a multi-parameter theory the latitude of physical possibilities is shown in Fig. 1. This is a natural extension of the model independent bounds[21,18] often discussed in the literature and could be realized within the gauge theories.

The conditions become more restrictive, if one assumes that the isoscalar contribution is much smaller than the isovector. This is a reasonable assumption, because in parton model calculations[22] they couple to strange and charm-quark distributions which make them small. For zero isoscalar current contributions the allowed physical region from Eq. (15) is a circular ring indicated in Fig. 1. Its overlap with the region within the octagon is indicated by the shaded areas. The fact that one of them contains the point $a_3 = 1$ and $v_3 = 0.28$ is consistent with the

Weinberg-Salam theory. It is evident that estimates of the isoscalar components are very important and we analyze them in the next section.

ISOSCALAR COMPONENTS

Most of the studies concerning the internal symmetry structure of neutral currents deal with low energy reactions where the number of final state particles is limited. In this case both the initial and final states have precise quantum numbers and it is possible to infer the internal symmetry structure of the current. A clear example is provided by single pion production, where one expects to see evidence for the excitation of the Δ-resonance. The absence of the Δ will imply the absence of an $I = 1$ component, belonging to the same multiplet with the charged currents. The analysis of such reactions is greatly facilitated by earlier calculations in isobar models [23] which account for electromagnetic and weak pion production. A relativistic generalization of the static model, developed by Adler, [24] has been applied extensively to charged current reactions and seems to be successful. Theoretical interpretations are easiest in experiments with hydrogen and deuterium targets. Experimental considerations, however, neccessitate the use of complex nuclear targets and in the latter part of this section we address the question of nuclear corrections involved in the interpretation of the experiments.

Reactions in hydrogen and deuterium

The following charged current reactions have been observed [25]

$$\nu p \to \mu^- p \pi^+ \tag{19}$$

$$\nu n \to \mu^- p \pi^0 \tag{20}$$

$$\nu n \to \mu^- n \pi^+ \tag{21}$$

The rates and pion-nucleon mass distributions are within the expectations of the model. Figure 2 shows the data for reaction (19) together with the theoretical calculation [25]. The theoretical curve is normalized to the integrated experimental cross section. In the same Fig. I plotted the pre-

diction of the model for the reaction

$$\bar{\nu}n \to \mu^+ n\pi^- \tag{22}$$

We note that the ratio of $\bar{\nu}/\nu$ is in the vicinity of 0.38 over an extensive range of pion-nucleon masses. Measurement of this reaction provides a specific test for the I = 3/2 amplitude of the model. The striking feature in reactions (19) and (22) is the dominant Δ-resonance. A smaller enhancement in the Δ-region has also been observed[25] for reactions (20) and (21), but the statistics are more limited. The data are again consistent with the model calculations.

In discussing neutral currents one encounters the matrix elements of new operators and it is desirable to discuss them independent of specific dynamic models. Results of this general nature are available in the form of lower bounds.[26] For the Weinberg-Salam theory they are listed in Table II together with the experimental observations. The bounds are consistent with the experimental values, but they still allow substantial isoscalar contributions. It is therefore desirable to go beyond the bounds and attempt detailed comparisons between theory and experiment. Estimates of the pion-nucleon mass distributions are along these lines.

I describe here one general approach.

1) Reaction (19) determines the I = 3/2 amplitude. The relative vector and axial contributions can be inferred from reactions (19) and (21), provided that the two terms are relatively real.

2) The magnitude of the I = 1/2 amplitude can be obtained from the sum

$$\sigma(\nu n \to \mu^- n\pi^+) + \sigma(\nu n \to \mu^- p\pi^0) \tag{23}$$

where the interference term between the two isospin amplitudes is absent. The relative contributions of vector and axial matrix elements is also determined by comparing them with corresponding electroproduction data.

Table II. Neutral Current Measurements for Single Pion Production

Reaction	Experiment	Theory	Ref	Target
$R_0 = \frac{\sigma(\nu p \to \nu p\pi^0)}{\sigma(\nu p \to \mu^- p\pi^+)}$	$= 0.40 \pm 0.22$	≥ 0.10	4, 24	H_2
$R_+ = \frac{\sigma(\nu p \to \nu n\pi^+)}{\sigma(\nu p \to \mu^- p\pi^+)}$	$= 0.13 \pm 0.06$	≥ 0.08	4, 24	H_2
$R_- = \frac{\sigma(\nu n \to \nu p\pi^-)}{\sigma(\nu p \to \mu^- p\pi^+)}$	$= 0.07 \pm 0.03$		4	D_2
$R_{0+} = R_0 + R_+$	$= 0.53 \pm 0.23$	≥ 0.10	4, 26	H_2, D_2
$R = \frac{\sigma(\nu N \to \nu N'\pi^0)}{\sigma(\nu N \to \mu^- N'\pi^0)}$	$= 0.17 \pm 0.06$	≥ 0.03	6, 26	75% Al 25% C
	≤ 0.21		27	Freon

3) The phase of the I = 3/2 amplitude relative to the I = 1/2 amplitude is assumed to be given by the phase of the Breit-Wigner denominator. In general this is the phase of a resonance relative to a non-resonant background.

The calculation indicates that the I = 1/2 amplitude is important and it is most important away from the peak of the resonance. The phases of the amplitudes are also important. Figure 3 shows the pion-nucleon mass distribution for the reaction

$$\nu p \to \nu p\pi^0 \qquad (24)$$

at an incident neutrino energy of 1 GeV. Curve (a) shows the expectation of models with destructive interference below the resonance and constructive above the resonance. Curve (b) corresponds to constructive interference below the resonance. Curve (c) shows the incoherent sum of the two amplitudes. Figure 4 shows the results of a similar calculation but for

the sum of the cross sections

$$d\sigma(\nu p \to \nu p\pi^0) + d\sigma(\nu p \to \nu n\pi^+) \qquad (25)$$

In this case the interference term between the two isospin amplitudes cancels out. A prominent feature of Figs. 3 and 4 is their similarity to corresponding mass distributions in electroproduction.[28]

Nuclear Targets

The cross sections on heavy nuclear targets are considerably different because of multiple scattering and charge exchange corrections within the nuclei. There are two types of calculations available at this time. In the first approach,[26] one considers the scattering from an isospin zero nucleus and describes the final states in terms of the isospin of the resulting nucleus and a pion. The lower bounds derived are also included in Table II and are again consistent with experiment.[29] In the second approach, one calculates the cross sections on free protons and neutrons and then folds in the nuclear corrections. The main aspects of the nuclear-corrections-model could be tested in electromagnetic and charged current experiments but this has not been done as yet. To indicate the importance of the I = 1/2 amplitude[24] and of the nuclear corrections we discuss the ratio

$$R = \frac{\sigma(\nu''p'' \to \nu p\pi^0)+\sigma(\nu''n'' \to \nu n\pi^0)}{2\sigma(\nu''n'' \to \mu^- p\pi^0)} \qquad (26)$$

which has been measured in $_{13}Al^{27}$. Table III shows the different contributions to R in the Weinberg-Salam theory. The model also indicates that

$\sin^2\theta_W$	Δ-only	$\Delta_{1/2}$+(I = 1/2)	Δ+(I = 1/2) + charge exchange correction
0.3	0.56	0.40	0.23
0.4	0.46	0.33	0.18

Table III

the charge exchange correction for the reactions in the numerator is ~10% while the corresponding correction for the denominator is ~50%. The origin of this disparity lies in the presence of a large correction from reaction (19).

Other calculations on single pion reactions by the Princeton group were reported at this meeting by Colglazier.[30] The low energy theorem derived for $\nu n \to \nu p\pi^-$ is still untested, because the new Argonne data[31] are not sensitive to such small cross sections.[4]

The main conclusion from all the studies so far is the following: There is no statistically significant evidence which indicates a discrepancy between the expectations of gauge theories and experiment. However, as was already mentioned, the comparisons made so far are not very sensitive to isoscalar contributions. Detailed pion-nucleon mass distributions are sensitive to large isoscalar terms, but because one encounters many corrections their sensitivity is also limited. Additional tests are needed.

There are measurements which are sensitive to the presence of an isoscalar-isovector interference term. For isoscalar targets the interference term shows up in the charge asymmetry of inclusive pion production[26]

$$A_\pi(\nu) = \sigma(\nu+N \to \nu+\pi^+ +x) - \sigma(\nu+N \to \nu+\pi^- +x) \qquad (27)$$

$$A_\pi(\bar{\nu}) = \sigma(\bar{\nu}+N \to \bar{\nu}+\pi^+ +x) - \sigma(\bar{\nu}+N \to \bar{\nu}+\pi^- +x) \qquad (28)$$

Similarly for experiments on protons and neutron targets there are interference terms in the expressions[8]

$$A(\nu) = \sigma(\nu+p \to \nu+Y^+) - \sigma(\nu+n \to \nu+Y^0) \qquad (29)$$

$$A(\bar{\nu}) = \sigma(\bar{\nu}+p \to \bar{\nu}+Y^+) - \sigma(\bar{\nu}+n \to \bar{\nu}+Y^0) \qquad (30)$$

where the Y's stand for any final states summed over all possible charges. For bubble chamber experiments[7] the study of the difference

$$A_{2\pi}(\nu) = \sigma(\nu+p \rightarrow \nu+p+\pi^+ +\pi^-) - \sigma(\nu+n \rightarrow \nu+n+\pi^+ +\pi^-) \qquad (31)$$

is relatively simple and does not depend critically on the neutron background. In all these cases $[A(\nu)+A(\bar{\nu})]$ is sensitive to v_0v_3 and a_0a_3 while $[A(\nu)-A(\bar{\nu})]$ is sensitive to v_0a_3 and a_0v_3. $A_{2\pi}$ is proportional to the isoscalar-isovector interference and a large non-zero value will be evidence for substantial isoscalar components.

The study of η^0 meson production by charged and neutral currents is more demanding experimentally, but it is worth the effort, since it has a simple isospin structure. The general methods developed for single pion production are applicable and give additional constraints.

CONCLUSIONS AND OUTLOOK

The existence of muonless events in neutrino induced reactions is well established and their interpretation in terms of neutral currents seems natural.[32] The general picture so far is consistent with the existence of vector and axial currents, which have both isovector and isoscalar components. However, one can not rule out other possibilities, nor can one determine yet the importance and magnitude of the different components. In this respect, there are several issues, whose resolution is relevant to future theoretical and experimental developments.

The absence of $\Delta S = 1$ neutral currents is inferred from low energy experiments. The absence of such components has never been tested at higher energies. In almost all theoretical models the absence of $\Delta S = 1$ components is taken for granted.

A dominant isoscalar component is not expected in gauge theories. This issue can be settled by studies on the excitation of the Δ-resonance, by determination of the charge asymmetries in Eqs. (27)-(31) and by the production of η^0 mesons. The existence of such a component is of importance not only to the internal structure of the models but it also has far-reaching applications providing a candidate[33] for the explanation

supernovae explosions in massive stars.

Data with antineutrino beams are very limited. In fact data on reactions with specific final states are practically non-existent. Antineutrino reactions will clarify the space-time structure of the interactions and can provide more confidence for many of the calculations.

The theory for elastic scattering has been studied[34] in detail and it is known that the magnitude and Q^2-dependence of the cross section can distinguish among several models. An experiment[35] sensitive to ν-p elastic scattering is now in progress.

Studies on the couplings of neutral currents[36] to $e\bar{e}$ and $\mu\bar{\mu}$ pairs are still in their infancy.

Looking back at the problems which were studied a few years ago, we can not fail to notice that considerable progress has been made. Most of the issues on the existence of neutral currents have been settled. The two new issues which have emerged, in the meanwhile, are concerned with the operator structure of the currents and their basic role within the framework of weak and electromagnetic interactions.

REFERENCES AND FOOTNOTES

1. See, for example: S. Abers and B.W. Lee, Phys. Reports, 9C, No. 1 (1973); J. Bernstein, Rev. Mod. Phys. 46, 7 (1974); J. Iliopoulos, Lectures at the IX Recontre de Moriond, 1974.

2. F.J. Hasert et al., Phys. Lett. 46B, 138 (1973) and Nucl. Phys. B73, 1 (1974). The groups mentioned in Refs. 2-7 have contributed up-to-date reports to "Colloque du Neutrino a Haute Energie", Paris, (1975).

3. A. Benevenuti et al., Phys. Rev. Lett. 32, 800 (1974); B. Aubert et al., Phys. Rev. Lett. 32, 1454 and 1457 (1974). This experiment is a collaboration between Harvard-Pennsylvania-Wisconsin Universities and Fermi Laboratory. It is referred to as HPWF.

4. S. Barish et al., Phys. Rev. Lett. 33, 448 (1974). The contribution to the Paris meeting contains new results and should be consulted. L. Hyman, ANL preprint (1975).

5. B.C. Barish et al., Phys. Rev. Lett. 34, 538 (1975).

6. W. Lee et al., Report at the London Conference (1974), pg. IV-127.

7. E.G. Cazzoli et al., BNL preprint NG-301 (1975).

8. A wider spectrum of topics is covered in the review by L. Wolfenstein (COO-3066-39)(1974) Carnegie-Mellon University preprint.

9. S.L. Glashow, J. Iliopoulos and L. Maiani, Phys. Rev. D2, 1285 (1970).

10. S. Pakvasa and G. Rajasekaran, University of Hawaii preprint UH-511-183-74 (1974).

11. B. Kayser, G.T. Garvey, E. Fischbach and S.P. Rosen, Phys. Lett. 52B, 385 (1974).

12. R.L. Kingsley, F. Wilzeck and A. Zee, Phys. Rev. D10, 2216 (1974).

13. See article by F. Merrit to this meeting.

14. The (V,A) character of the charged currents has not been tested in high energy neutrino experiments yet.

15. S. Weinberg, Phys. Rev. Lett. 19, 1264 (1967); A. Salam in Elementary Particle Physics (N. Svartholm, ed.) Stockholm (1968) p. 367.

16. M.A.B. Beg and A. Zee, Phys. Rev. Lett. 30, 675 (1973); Y. Achiman, Nucl. Phys. B56, 635 (1973).

17. J.J. Sakurai, Phys. Rev. D9, 250 (1974).

18. The theorems are generalizations of the results by E.A. Paschos and L. Wolfenstein, Phys. Rev. D7, 91 (1973); Eqs. (15) and (17) and their proofs are omitted.

19. The isoscalar term in Eq. (18) was omitted in the original article of Ref. 18. Different neutrino and antineutrino spectra must be included in the evaluation of the ratio and have been discussed by D.H. Perkins, Lectures at the Fifth Hawaii Topical Conference in Particle Physics, August 1973, p. 563.

20. The constraints on the coupling constants are similar to those of G. Rajasekaran and K.V.L. Sarma, Tata Institute preprint TIFR/TH/74-23 (1974) and M. Gourdin, Lectures at the Internationale Universitäts-Wochen für Kernphysik Schladming (Austria), PAR/LPTHE 75.3 (1975).

21. A. Pais and S.B. Treiman, Phys. Rev. D6, 2700 (1972); D9, 1459 (1974).

22. L.M. Sehgal, Nucl. Phys. B65, 141 (1973); C.H. Albright, Nucl. Phys. B70, 486 (1974); R. Palmer, Phys. Lett. 46B, 240 (1973). The dialectic approach to the subject is found in the work of A. DeRujula, H. Georgi, S. Glashow and H. Quinn, Rev. Mod. Phys. 46, 391 (1974).

23. A summary of dynamical calculations is given by C.H. Llewellyn Smith, Phys. Reports 3C, No. 5 (1972).

24. S.L. Adler, Ann. Phys. (N.Y.) 50, 189 (1968); the model has also been adopted for the analysis of neutral current reactions, Phys. Rev. D9, 229 (1974) and FNAL-Conf-74/34-THY (1974).

25. A.F. Garfinkel, "Single-Pion Production in Charged-Current Neutrino Reactions at ANL", submitted to "Colloque du Neutrino à Haute Energie", Paris (1975). The theoretical curve at E_ν = 0.5 GeV is according to P.A. Schreiner and F. Von Hippel, Nucl. Phys. B58, 33 (1974); effects

arising from the neutrino spectrum have not been included. Calculations for reactions (20) and (21) were made according to Ref. 24.

26. C.H. Albright, B.W. Lee, E.A. Paschos and L. Wolfenstein, Phys. Rev. D7, 2220 (1973).

27. The bound is from the Gargamelle Group (private communication). See contribution to this meeting by P. Musset,

28. S. Galster et al., Phys. Rev. D5, 519 (1972). I was informed that mass distributions have also been calculated by S.L. Adler in the model of Ref. 24.

29. S.L. Adler, S. Nussinov and E.A. Paschos, Phys. Rev. D9, 2125 (1974); S.L. Adler, Phys. Rev. D9, 2144 (1974).

30. E.W. Colglazier at this meeting; see also S.L. Adler, E.W. Colglazier, Jr., J.B. Healy, I. Karliner, J. Lieberman, Y.J. Ng and H.S. Tsao, Phys. Rev. D (to be published).

31. S.L. Adler, Phys. Rev. Lett. 33, 1511 (1974).

32. Alternative interpretations are summarized by D.H. Perkins, in Ref. 19, p. 559.

33. D.Z. Freedman, Phys. Rev. D9, 1389 (1974); J.R. Wilson, Phys. Rev. Lett. 32, 849 (1974).

34. S. Weinberg, Phys. Rev. D5, 1412 (1972); J.J. Sakurai and L.F. Urrutia, Phys. Rev. D11, 159 (1975).

35. BNL, Exp-613 "Search for Weak Neutral Currents".

36. For a recent summary see C.H. Llewellyn Smith and D.V. Nanopoulos, Nucl. Phys. 78B, 205 (1974).

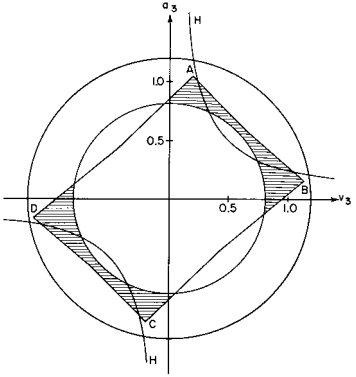

Fig. 1 Physical ranges for the isovector coupling constants.

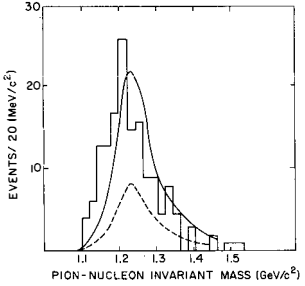

Fig. 2 Pion-nucleon mass distribution. Data are from Ref. 24. Solid curve corresponds to reaction (19); dashed curve to reaction (22).

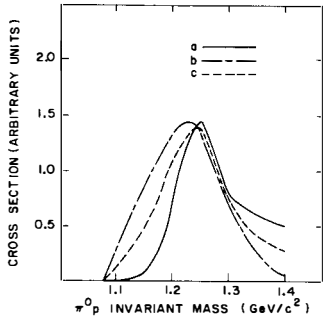

Fig. 3 Pion-nucleon mass distributions for reaction (24).

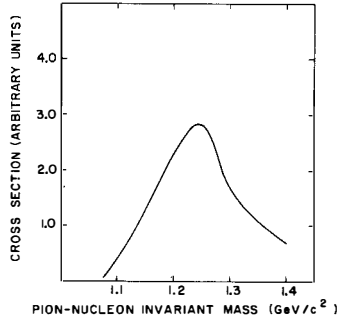

Fig. 4 Pion-nucleus mass distribution for the sum of reactions (25).

C O N C L U S I O N

Julius Kuti

Central Research Institute for Physics

Budapest

It is difficult to conclude at the end of an exciting conference where so many interesting experimental data became available to us. I think the long waited breakthrough is somehow in the air but it can hardly happen before a convincing unification scheme will be found for all what we know in these stormy days.

I will try to summarize the conference in a rather evasive way. I will briefly go through the important parts of my introductory talk I gave at the beginning of this conference where I summarized what was known to us when we came here. Then I will make comments on what we have learned during the conference about our outstanding problems.

1. NEUTRAL CURRENTS

The discovery of the neutral currents has given a large boost to Unified Gauge Theories though it is not the only scheme which can accomodate neutral currents.

Still, I think the Unified Gauge Theory represents the most attractive possibility and we are waiting for the concrete model in which its beauty will be materialized.

We learned at this conference that experimentalists are working to establish the Lorentz structure of neutral currents in neutrino induced hadronic reactions. It seems likely that the neutral currents are some combination of V and A and the relative weight with sign will be available in the near future.

That is great progress and will help to narrow down the roads in searching for THE MODEL.

It is perhaps even more interesting for a theorist that no strangeness changing neutral currents have been

found so far in first order in the Fermi coupling G_w . If we accept the assumption that quarks are the building blocks of hadronic matter it is rather hard in an attractive theory to arrange for the absence of strangeness changing neutral currents without the hypothesis of the fourth /charmed/ quark.

An easy way out of this dilemma may be overlooked somehow by the theorists, but as we stand now the fourth quark seems to be a nearly necessity.

2. THE QUARK MODEL

The conventional Gell-Mann - Zweig quark model with three color triplets works remarkably well for the nucleon. The accumulation of charged neutrino and antineutrino data in the deep inelastic region when combined with the SLAC- M.I.T. data strongly suggest that the nucleon consists mainly of three valence quarks in the region $0.1 < x < 1$ in the scaled momentum variable x . Further, about 50 % of the nucleon's momentum is carried by neutrals usually associated with gluons.

There are some problems with the constituent model. SU(6) must be badly broken in the constituent quark model, at least in some kinematic regions. It is rather dramatic in deep inelastic electron-nucleon scattering where the ratio $\frac{\sigma_{en}}{\sigma_{ep}} \underset{x\to 1}{\sim} \frac{1}{4}$ is extracted from proton and deuteron data. With SU(6) -symmetric wave functions a ratio $\frac{2}{3}$ is expected here. A better understanding of the connection between constituents and partons is badly needed.

The relatively small weight of $q\bar{q}$ -pairs indicates that vacuum polarization via the gluon force field is rather ineffective inside the nucleon. However, the gluon

field carries 50 % of the nucleon's momentum what we would naively associate with a strong gluon field and sizable vacuum polarization.

The question is further sharpened if we accept quark confinement at least as a temporary solution for the absence of free light quarks. The confinement force is expected to be strong enough to make vacuum polarization dramatic.

A partial answer is offered in quark confinement theories. The fundamental quark-gluon interaction is fairly weak and the force acting between the constituent quarks inside mesons and nucleons is similar to the Coulomb force and governed by the small fundamental coupling constant. Vacuum polarization is weak then. When quarks become separated via large disturbances or excitations, a confinement potential proportional to the distance between quarks appears and vacuum polarization from the confinement force is responsible for particle production.

The explanation for the 50 % momentum is still missing!

3. THE NEW PARTICLES

Recently, there has been a deep worry about the cross section $\sigma_{e^+e^- \to \text{hadrons}}$. The ratio

$$R = \frac{\sigma_{e^+e^- \to h}}{\sigma_{e^+e^- \to \mu^+\mu^-}}$$

was large and rising, totally unexpected.

Also there was an uneasy feeling about the Lederman experiment $p + U \to \mu^+\mu^- + \cdots$ where there was a famous shoulder in the differential cross section, an excess of

$\mu^+\mu^-$ -pairs around 3 GeV in invariant mass over parton model predictions.

Further, a large ratio $\frac{e}{\pi} \geq 10^{-4}$ was observed in single-arm experiments at large transverse momenta in strong interaction collisions.

Then it came the tremendous discovery of the new particles at 3.1 GeV and 3.7 GeV in the e^+e^- -channel at SPEAR and in the reaction $p + Be \to e^+e^- + \cdots$ at Brookhaven.

Our conference was the first one about the new particles. There were many exciting experimental talks and interesting theoretical discussions. Right after the discoveries four possibilities were widely discussed by theorists

weak boson

color

charm /onium/

something else

The possibility of the weak boson is practically eliminated by the angular distribution measurements.

The photoproduction experiment from FNAL has confirmed that the ψ /3.1/ strongly interacts with matter. That was the final blow against the W-boson hypothesis.

Han-Nambu color is a running model with severe difficulties.

Charm with the fourth quark seems to be the most attractive interpretation. The new particles are interpreted as c -quark - $\bar{c}$ -quark bound states. This hypothesis can be confirmed or killed in the near future.

The most direct evidence would be the direct production of charmed mesons and baryons. We have heard many talks

about planning experiments on this line. Nonetheless, we already have some data in which some surprises may be hidden.

The accumulating number of energetic dimuon events in high energy neutrino reactions at FNAL may imply the production of charmed baryons.

There is then the famous bubble chamber picture from Brookhaven where a neutrino induced reaction with $\Delta S = -\Delta Q$ is observed.

Finally, there is the large ratio $\frac{e}{\pi} \geq 10^{-4}$ in hadron collisions. We have heard here that it is very difficult to explain this large number of energetic electrons even allowing for decays from parent ψ-particles. Something else may be produced there which decays into energetic leptons.

If the charmonium hypothesis is correct then monochromatic photons are expected from $E1$ transitions between S-states and P-states. It is a challenge for experimentalists to search for monochromatic photons and it would be a headache for theorists who believe in charm if they are not found. It will be exciting to wait for answers to these questions in the near future.

Finally it is my most pleasant commission to thank Professor Tran Thanh Van and his staff in the name of all participants of this tremendously enjoyable conference for the organization, hospitality and pleasant stay at the Hotel Le Lac Bleu.

MORIOND PROCEEDINGS

N° 1	First Rencontre de Moriond : 2 vol.	(1966)
N° 2	Second Rencontre de Moriond : 2 vol.	(1967)
N° 3	Third Rencontre de Moriond : 2 vol.	(1968)
N° 4	Fourth Rencontre de Moriond : 1 vol.	(1969)
N° 5	Fifth Rencontre de Moriond : 1 vol.	(1970)
N° 6	Electromagnetic and Weak Interactions	(1971)
N° 7	High-Energy Phenomenology	(1971)
N° 8	Two Body Collisions	(1972)
N° 9	Multiparticle phenomena and inclusive reactions	(1972)
N° 10	Electromagnetic and Weak Interactions	(1973)
N° 11	The Pomeron	(1973)
N° 12	High energy hadronic physics	(1974)
N° 13	High energy leptonic physics	(1974)
N° 14	Phenomenology of Hadronic Structure	(1975)
N° 15	Charm, Color and the $\mathcal{J}\!\!\!\!\!\!\mathcal{J}$	(1975)

All orders should be sent to.

Rencontre de Moriond
Laboratoire de Physique Théorique et Particules Élémentaires
Bâtiment 211 - Université de Paris-Sud
91405 ORSAY (France)
Tél. 928.59.87

12 HIGH ENERGY HADRONIC INTERACTIONS

CONTENTS

13 HIGH ENERGY LEPTONIC INTERACTIONS

Proceedings of the second session of the Ninth Rencontre de Moriond
3-15 March 1974

CONTENTS

14 PHENOMENOLOGY OF HADRONIC STRUCTURE

CONTENTS

First Session

15 CHARM, COLOR AND THE $\mathcal{J}$

Proceedings of the second session of the Tenth Rencontre de Moriond
2-14 March 1975

CONTENTS

Achevé d'imprimer le 14 juillet 1975
sur les presses de l'Imprimerie Laboureur et Cie - Paris
113, rue Oberkampf, 75011 Paris
Dépôt légal n° 8183